ELSEVIER

Biochimica et Biophysica Acta 1357 (1997) 297–305

BIOCHIMICA ET BIOPHYSICA ACTA
BBA

G1 accumulation caused by iron deprivation with deferoxamine does not accompany change of pRB status in ML-1 cells

Kunihiko Fukuchi [a,*], Shigeru Tomoyasu [b], Hiroyuki Watanabe [a], Nobuyoshi Tsuruoka [b], Kunihide Gomi [a]

[a] *Department of Clinical Pathology, School of Medicine, Showa University, 1-5-8 Hatanodai, Shinagawaku, Tokyo Japan*
[b] *Department of Hematology, School of Medicine, Showa University, 1-5-8 Hatanodai, Shinagawaku, Tokyo Japan*

Received 18 July 1996; revised 23 December 1996; accepted 26 February 1997

Abstract

We analyzed G1 accumulation induced by the iron chelator deferoxamine B mesylate (DFO) compared it with that caused by etoposide and cytosine arabinoside (AraC). The results showed that p53 protein increased with all three treatments without an increase in p53 mRNA. After treatment for 3 or 6 h, p21 mRNA increased with 10^{-4} DFO to 159% or 556% of pretreatment levels, to 509% or 391% with 10^{-5} etoposide, and to 263% or 304% with 10^{-5} AraC. Induction of p21 protein was not observed with fluorescence activated cell sorting and Western blot analysis after treatment with DFO or AraC. Treatment with DFO did not cause any change in levels of CDK4 mRNA or protein, whereas etoposide or AraC treatment did diminish CDK4 protein. Enzyme linked immunosorbent assay for pRB and its phosphorylation, which reflects CDK4 activity, revealed that treatment with DFO did not change the amount of pRB or the phosphorylation status. Results of this investigation show that the mechanism of G1 accumulation induced by DFO involves a p53-independent pathway and that expression of p21 protein may be regulated posttranscriptionally. © 1997 Elsevier Science B.V.

Keywords: Deferoxamine B mesylate; ELISA; p53; p21; pRB

1. Introduction

The iron chelator deferoxamine B mesylate (DFO) is known to inhibit DNA synthesis and cell proliferation both in vitro and in vivo [1–3]. DFO is generally thought to inhibit the iron-requiring enzyme ribonucleotide reductase, thereby altering the supply of deoxyribonucleotides and decreasing DNA synthesis [1]. Growth inhibition by DFO has been reported at different points of the cell cycle, as shown by accumulation at the G1-S [4–6] and the G2M phases [7,8]. Cellular responses differ with cell type and DFO concentration. These observations suggest that more than one point of the cell cycle is sensitive to DFO.

We have reported that treatment with DFO causes growth inhibition, as reflected by G1 accumulation and apoptosis, in the human myelocytic leukemia cell lines HL-60 and ML-1 [9,10]. In ML-1 cells, G1 accumulation and accumulation of the tumor suppressor gene product p53, are observed 6 h after DFO treatment [10]. The increased levels of p53 protein enhances expression of p21 mRNA, a target for p53 [10]. Growth is inhibited by DFO immediately after treatment, as with such DNA-damaging agents as gamma irradiation and antitumor agents [10–15]. Ac-

* Corresponding author. Fax: (81-3) 3788-4927; E-mail: kfukuchi@med.showa-u.ac.jp

PII S0167-4889(97)00040-2

cordingly, the growth inhibition by DFO may involve regulation of cell-cycle checkpoints, as with DNA-damaging agents, but is unlikely to be due to a decrease in DNA synthesis [12–15].

Progression through the G1-S checkpoints requires phosphorylation of Rb protein (pRB) by D-type cyclin-cyclin-dependent kinase 4 (CDK4) and cyclin E-CDK2 complexes [16–18]. Several CDK inhibitors (CDKIs), such as p21, $p16^{INK4a}$, and $p15^{INK4b}$, have been shown to bind to this complex and inhibit its kinase activity [19]. p53 protein accumulates in response to DNA damage and plays an important role in cell growth inhibition by inducing p21 transcription, inhibiting activity of proliferating-cell nuclear antigen, and blocking translation of CDK4 [19,20].

Analysis of the mechanism by which DFO inhibits growth is important for the further use of DFO as an antiproliferative agent. In this investigation, we analyzed the p53 sequential cascade by examining expression of p21 and CDK4 mRNA and protein and the phosphorylation status of pRB after DFO treatment in ML-1 cells. We then compared these results with those after treatment with a typical DNA-damaging agent etoposide, and with those of the antimetabolite cytosine arabinoside (AraC).

2. Materials and methods

2.1. Cell culture

ML-1 cells, supplied by the Health Science Research Resource Bank (HSRRB), were cultured in RPMI 1640 containing 10% fetal calf serum. Deferoxamine B mesylate (M_r 656.8) was obtained from Ciba-Geigy, Basel, Switzerland. Etoposide and AraC were purchased from Sigma (St. Louis, MO, USA).

2.2. Flow cytometric assay

Cells were fixed with 4% paraformaldehyde for 20 min, washed, then incubated with 1 μg/ml of anti-p53 monoclonal antibody (DO-7, DAKO, Glostrup, Denmark), anti-p21 monoclonal antibody (2G12, PharMingen, San Diego, CA, USA) or anti-CDK4 polyclonal antibody (4802, PharMingen) for 1 h on ice. After washing, cells were incubated with fluorescein isothiocyanate-conjugated goat anti-mouse Ig (for monoclonal antibodies) or anti-rabbit Ig (for polyclonal antibody) for 30 min on ice, washed, stained with 50 μg/ml propidium iodide, then analyzed with a FACScan flow cytometer (Becton Dickinson, Sunnyvale, CA, USA).

2.3. RNA extraction and Northern blot analysis

RNA extraction and Northern blot hybridization were performed as described previously [10]. p53 cDNA (supplied by HSRRB), p21 cDNA (provided by Dr. Noda, Meiji Cell Technology Center, Japan), CDK4 cDNA, and β-actin DNA were labeled with digoxigenin by the random primer method [21]. CDK4 cDNA was generated by a reverse transcription polymerase chain reaction using total RNA from the normal human fibroblast cell line WI38 (supplied by HSRRB) as a template and the following primers: forward primer, 5'TCTGAGAATGGCTACCTCTC-G3'; reverse primer, 5'AGCCAACACTCCACATGT-CC3'. A PCR product of 611 bp was cloned into pT7Blue (Novagen, Madison, WI, USA). The cloned DNA was then confirmed as representing a partial CDK4 cDNA for comparison with its expected size of 611 bp and its sequencing analysis. The level of expression was normalized by comparison with β-actin mRNA levels. Experiments were repeated three times independently, and similar results were obtained.

2.4. Western blot and ELISA

Cells (1×10^7) were lysed in 1 ml of lyse buffer (0.05 M Tris-HCl, pH 8.0, 0.15 M NaCl, 0.1% Nonidet P-40, 0.01 M EDTA, 0.05 M NaF, 0.01 M sodium orthovanadate, 2 μg/ml aprotinin, 2 μg/ml leupeptin, and 5 μg/ml PMSF). After incubation on ice for 30 min, the lysate was clarified by ultracentrifugation at 30 000 rpm for 30 min at 4°C. The cell lysate was immunoprecipitated with a specific antibody, after which the precipitate was separated by SDS polyacrylamide gel electrophoresis and blotted to an Hybond N+ membrane (Amersham, Amersham, UK), and then subjected to Western blot analysis using anti-p53 monoclonal antibody (DO-7, DAKO), anti-p21 monoclonal antibody (2G12, PharMingen), anti-CDK4 polyclonal antibody (4802, PharMingen), anti-pRB monoclonal antibody (G99-

73, PharMingen), or anti-phosphorylated serine and anti-phosphorylated threonine polyclonal antibodies (Zymed Laboratories, San Francisco, CA, USA). Enzyme-linked immunosorbent assay (ELISA) to quantify pRB and the phosphorylation status of pRB was performed as follows. Polystyrene beads were coated with an anti-pRB monoclonal antibody that recognizes an epitope between amino acids 240–384 of human pRB (G99-73, PharMingen) in 0.1 M phosphate (pH 7.0). Antibody-coated beads were incubated with 50 μg of cell lysate in 0.1 M phosphate (pH 7.0), 0.1 M NaCl, and 1% BSA at 4°C for 8 h. After washing with wash buffer (0.1 M phosphate (pH 7.0) and 0.1 M NaCl), the beads were incubated with a rabbit anti-pRB polyclonal antibody that recognizes an epitope between amino acids 914-928 of human pRB (Ab-2, Oncogene Science, Uniondale, NY, USA) or rabbit anti-phosphorylated serine and anti-phosphorylated threonine polyclonal antibodies (Zymed Laboratories) in 0.1 M phosphate (pH 7.0), 0.5 M NaCl and 1% BSA for 1 h on ice. After washing with wash buffer, the beads were incubated with horseradish peroxidase-conjugated anti-rabbit IgG in 0.1 M phosphate (pH 7.0), 0.1 M NaCl and 1% BSA for 1 h on ice. For chemiluminescent detection, 200 μl of substrate, ECL solution (Amersham) was added to each bead, after which chemiluminescence was measured with Luminescence Reader (Aloka, Japan). To quantify the amount of pRB, recombinant pRB (QED Bioscience, San Diego, CA, USA) was used for the standard assay.

3. Results

3.1. G1 accumulation with DFO treatment

To determine the optimal concentrations of DFO, etoposide, and AraC for growth inhibition, we added 10^{-6} to 10^{-3} M of DFO, etoposide, or AraC to ML-1 cells in the exponential growth phase, then monitored their growth with a flow cytometer after 1 to 9 h of incubation. With 10^{-4} M DFO, 10^{-5} M etoposide and 10^{-5} M AraC, cell growth was inhibited 3 h after the start of treatment and G1 accumulation became apparent 6 h treatment.

Analysis of DNA histograms after 6 h of treatment showed that 54% of cells treated with 10^{-4} M DFO accumulated in the G1 phase, while in untreated cells the proportion of G1 phase cells was 30%. Treatment with 10^{-5} M etoposide caused an increase in the number of cells in the S phase (66%), and treatment with AraC caused an increase in the number of cells in the G1 phase (47%) (Fig. 1A). G1 accumulation became apparent on the DNA histogram after 48 h of treatment with 10^{-4} M DFO (Fig. 1B). To analyze the early cellular response, we used the above-stated concentrations and the incubation periods of 3 and 6 h for the following experiments.

3.2. P53 expression

Flow cytometric analysis revealed that p53 protein expression increased after 6 h of treatment with DFO, etoposide, or AraC (Fig. 1A). To confirm that the data from FACS, we examined p53 protein expression with Western blot analysis. Enhanced p53 protein bands were detected in lysates of cells treated with DFO, etoposide, or AraC (Fig. 2A). The data from FACS and Western blot analysis were well correlated. The levels of p53 mRNA as determined by Northern blot analysis demonstrated that the mRNA level remained almost unchanged after 3 to 6 h of treatment with DFO, etoposide, or AraC (Fig. 3A).

3.3. P21 expression

To determine whether the p53 growth inhibition cascade (p53 induction of p21 expression, with p21 inhibiting cyclin-CDK kinase activity, which reduces Rb phosphorylation) is involved in DFO-induced G1 accumulation, we examined the expression of p21 mRNA and protein. As shown in Fig. 3B, after incubation for 3 h, the level of p21 mRNA increased significantly with 10^{-5} M etoposide (509% of levels in untreated cells) and increased to some extent with 10^{-4} M DFO (159%) and 10^{-5} M AraC (263%). After incubation for 6 h, p21 mRNA levels increased markedly with all three treatments: 556% with 10^{-4} M DFO, 391% with 10^{-5} M etoposide, and 304% with 10^{-5} M AraC. The expression of p21 protein showed a marked increase after etoposide treatment for 6 h (Fig. 1A). Although mRNA expression was enhanced after treatment with DFO or AraC for 3 and 6 h, p21 protein expression remained at the level of

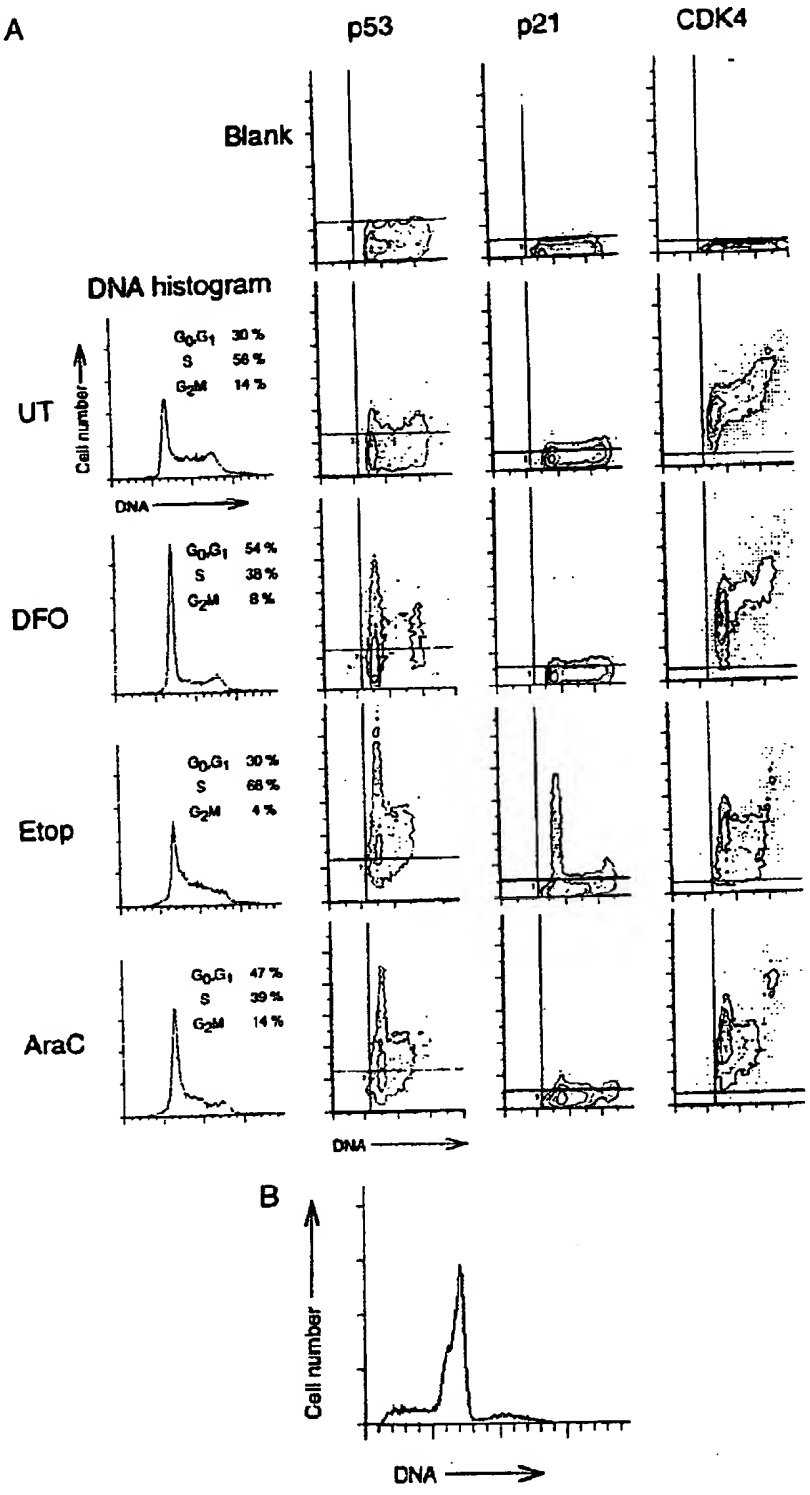
A
p53
p21
CDK4
Blank
DNA histogram
UT
DFO
Etop
AraC
G_0G_1 30 %
S 58 %
G_2M 14 %
G_0G_1 54 %
S 38 %
G_2M 8 %
G_0G_1 30 %
S 68 %
G_2M 4 %
G_0G_1 47 %
S 39 %
G_2M 14 %
Cell number
DNA
B
Cell number
DNA

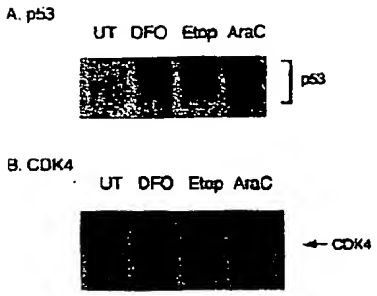

Fig. 2. Western blot analysis of p53 and CDK4. Cells were harvested 6 h after the addition of 10^{-4} M DFO, 10^{-5} M etoposide, or 10^{-5} M AraC and lysed with 1% NP40. Cell lysates were immunoprecipitated with anti-p53 monoclonal antibody or anti-CDK4 polyclonal antibody. The precipitates were electrophoresed in 10% to 20% SDS-PAGE, transferred to Hybond N+ membrane, then probed with anti-p53 monoclonal antibody (A) or anti-CDK4 polyclonal antibody (B). UT: untreated, DFO: deferoxamine, Etop: etoposide.

untreated cells (Fig. 1A). To determine whether p21 protein increased transiently with DFO or AraC, we also examined other time points. No increase in p21 protein was detected after incubation for 1 to 12 h (data not shown).

It is possible that FACS failed to detect the p21 protein in the form of cyclin-CDK complex after paraformaldehyde fixation. To confirm that p21 protein synthesis is enhanced only after treatment with etoposide, we conducted Western blot analysis of cell lysates. First, to detect the p21 protein in a cyclin-CDK4 complex, the cell lysate was immunoprecipitated with anti-CDK4 polyclonal antibody, after which the precipitate was probed with anti-p21 monoclonal antibody. Second, to detect p21 protein in any complexed form, the cell lysate was treated with 0.01% SDS and 0.1% sodium deoxycolate to dissociate the complex, immunoprecipitated with anti-p21 monoclonal antibody, then probed with anti-p21 monoclonal antibody. The protein product of p21 was observed in the lysate of only etoposide-treated cells (Fig. 4).

3.4. CDK4 expression

CDK4 is one of the most important factors controlling progression through the G1 checkpoint. Since DFO treatment causes G1 accumulation, we have examined the involvement of CDK4 in this process. To identify the level of regulation of CDK4 by DFO, we analyzed CDK4 mRNA and protein expression. CDK4 mRNA levels were not affected by treatment with DFO, etoposide, or AraC for 3 or 6 h (Fig. 3C), indicating that transcriptional regulation was not occurring. The CDK4 staining pattern showed that CDK4 protein expression after treatment with DFO was similar to that in untreated cells (Fig. 1A). After treatment with etoposide or AraC, CDK4 expression of G1-phase cells was similar to that of untreated cells and decreased in phases S through G2M (Fig. 1A). We further examined the CDK4 protein expression with Western blot analysis. The intensity of the CDK4 protein band correspond to the FACS data (Fig. 2B).

3.5. pRB phosphorylation status

To investigate CDK4 function, we examined the phosphorylation status of pRB. On Western blot analysis, phosphorylated pRB appeared as a more slower migrating band, and unphosphorylated pRB appeared as a more quickly migrating band, similar to that obtained from a confluent WI38 cell lysate (Fig. 5A) [22]. After 6 h of treatment, phosphorylated and unphosphorylated pRB bands were observed in lysates from both untreated and DFO-treated cells. With etoposide treatment, the band appeared between the phosphorylated and unphosphorylated pRB bands (Fig. 5A). To confirm that more slowly migrating band represented phosphorylated pRB, anti-pRB immunoprecipitates were subjected to Western blot analysis with anti-phosphorylated serine and threonine antibodies. Only more slowly migrating bands were detected with these antibodies (Fig. 5B).

Fig. 1. Flow cytometric analysis of deferoxamine-treated cells. (A) Cells were harvested after 6 h of treatment. DNA histograms were analyzed after ML-1 cells were stained with propidium iodide, as described in Section 2. The expression of p53, p21, and CDK4 was analyzed with monoclonal antibodies against p53 and p21 and polyclonal antibody against CDK4, as described in Section 2. Blank: preimmune mouse IgG for p53 and p21 detection or preimmune rabbit serum for CDK4 detection was used as the first antibody. (B) DNA histogram of ML-1 cells after 48 h of treatment with 10^{-4} M DFO. UT: untreated, DFO: deferoxamine, Etop: etoposide. The data are representative of three separate experiments.

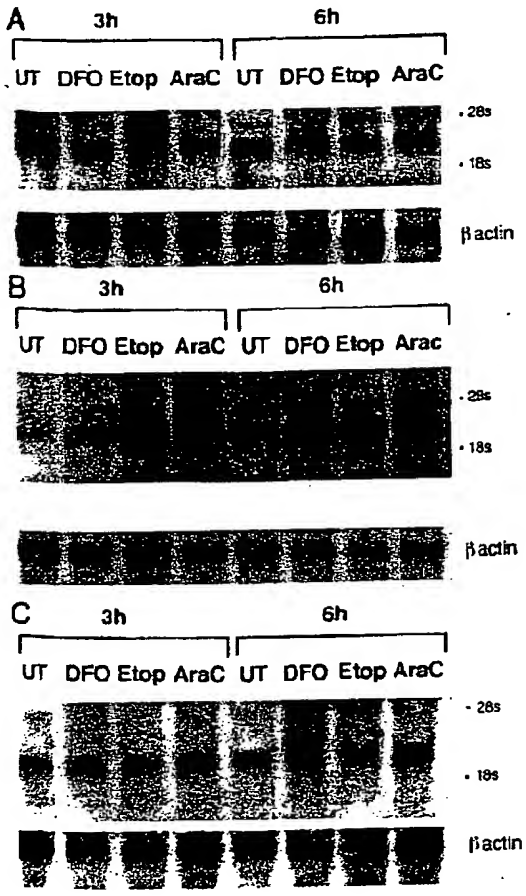

Fig. 3. Northern blot analysis. Total RNA was extracted from ML-1 cells 3 or 6 h after the addition of 10^{-4} M DFO, 10^{-5} M etoposide, or 10^{-5} M AraC. Twenty micrograms of total RNA were electrophoresed on formaldehyde agarose gel, transferred to Hybond N+ membrane, and hybridized with digoxigenin-labeled probes. (A) p53, (B) p21, (C) CDK4. The level of expression was normalized by comparison with β-actin.

To quantify the precise level of pRB and the phosphorylation status of pRB at the serine and threonine residues, we constructed an ELISA system using chemiluminescent detection. Table 1 summarizes the ELISA data obtained from four independent experiments, each of which was performed with duplicate samples. The amount of pRB was calculated from the standard assay. The amount of pRB of 9.70 ng/100 μg cell lysate of untreated cells did not change after 6 h of treatment with DFO, 10.66 ng, and decreased markedly after 6 h of treatment with etoposide, 2.61 ng, or AraC, 3.32 ng.

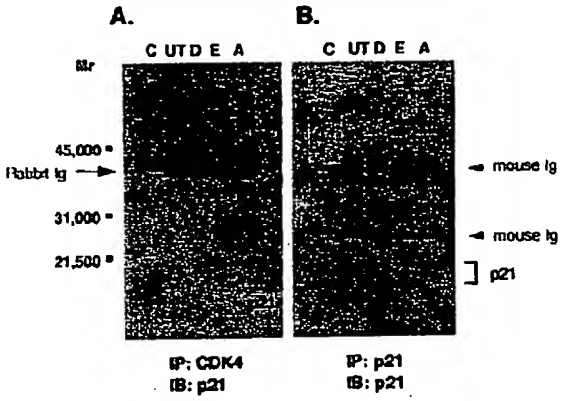

Fig. 4. Western blot analysis of p21 protein. Cells were harvested 6 h after the addition of 10^{-4} M DFO, 10^{-5} M etoposide, or 10^{-5} M AraC and lysed with 1% NP40. (A) Cell lysates were immunoprecipitated with anti-CDK4 polyclonal antibody, then electrophoresed on 10% to 20% SDS-PAGE. (B) Cell lysates were immunoprecipitated with anti-p21 monoclonal antibody after treatment with 0.01% SDS and 0.1% sodium deoxycolate, then electrophoresed on 10% to 20% SDS-PAGE. The membranes were probed with anti-p21 monoclonal antibody. (C) cell lysate(-), UT: untreated, D: deferoxamine, E: etoposide A: AraC.

The level of phosphorylation was calculated as the ratio of chemiluminescence value (KCOUNT) obtained by anti-phosphorylated serine and threonine antibodies to the chemiluminescence value obtained by anti-pRB antibody, which indicates the amount of pRB. The phosphorylation level did not change after

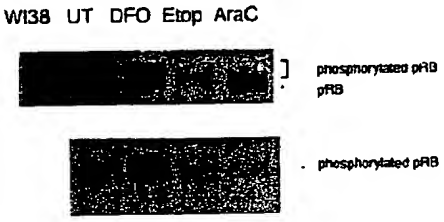

Fig. 5. Western blot analysis of pRB. Cell lysates were prepared 6 h after the addition of 10^{-4} M DFO, 10^{-5} M etoposide, or 10^{-5} M AraC. Cell lysates were immunoprecipitated with anti-pRB monoclonal antibody, and the precipitates were electrophoresed with 7.5% SDS-PAGE, transferred to Hybond N+ membrane, and probed with anti-pRB monoclonal antibody (A) or anti-phosphorylated serine and threonine (B). Confluent WI38 cells were used as a control for growth arrest. The data are representative of three separate experiments. UT: untreated, DFO: deferoxamine, Etop: etoposide.

Table 1
ELISA data obtained from four independent experiments

	Exp. 1	Exp. 2	Exp. 3	Exp. 4	Mean	S.E.
Anti-pRB (KCOUNT / 20 s)						
UT	30.40	30.60	30.50	28.30	30.50	0.10
DFO	35.80	32.98	30.30	27.85	33.03	2.75
Etoposide	11.72	14.45	9.40	7.30	11.86	2.53
AraC	10.60	19.55	11.00	11.25	13.72	5.06
Anti-phosphoreserine and threonine (KCOUNT / 20 s)						
UT	5.90	5.85	5.50	6.00	5.75	0.22
DFO	7.20	5.40	4.75	5.60	5.78	1.27
Etoposide	5.20	5.70	5.75	4.80	5.55	0.30
AraC	6.10	5.25	5.50	6.60	5.62	0.44
pRB (ng / 0.1 mg cell lysate)						
UT	9.66	9.74	9.70	8.86	9.70	0.04
DFO	11.71	10.64	9.62	8.69	10.66	1.05
Etoposide	2.56	3.60	1.68	0.88	2.61	0.96
Arac	2.14	5.54	2.29	2.39	3.32	1.92
Phosphorylation level: phosphoserine and threonine (KCOUNT) / pRB (KCOUNT)						
UT	0.19	0.19	0.18	0.21	0.19	0.01
DFO	0.20	0.16	0.16	0.20	0.17	0.02
Etoposide	0.44	0.39	0.61	0.66	0.48	0.12
AraC	0.58	0.27	0.50	0.59	0.45	0.16

Each experiment was performed with duplicate samples.

6 h of DFO treatment, and increased somewhat after etoposide treatment.

4. Discussion

We analyzed the cellular response to iron deprivation by DFO treatment in comparison with treatment with a DNA-damaging agent, etoposide, or an antimetabolite, AraC. With all three treatments, the level of p53 mRNA did not change and p53 protein levels increased in the G1 phase, findings that confirm the posttranscriptional regulation of p53 [10,23].

Expression of p21 mRNA was induced by all three treatments, suggesting that the increased p53 functioned as a transcription factor. However, FACS and Western blot analysis confirmed that p21 protein expression increased only with etoposide, but not with DFO or AraC treatment, suggesting that p21 gene expression may be posttranscriptionally regulated. Northern blot analysis showed that treatment with etoposide for 3 h resulted in the highest level of p21 mRNA. For effective expression of p21 protein, a considerable amount of p21 mRNA may be required in the early stages of the cellular response or DNA damage may be required for translation of p21 mRNA. We conclude from these results that the G1 accumulation caused by DFO is p21-independent.

Analysis of CDK4 expression showed that although mRNA levels remained constant after treatment with all three agents, protein expression was reduced by treatment with etoposide and AraC, suggesting that CDK4 may have been posttranscriptionally regulated. Ewen et al. have reported that an increase in wild-type p53 inhibits translation of CDK4 mRNA [20]. In our study, p53 accumulated with all three treatments, but CDK4 protein levels were affected only by treatments with etoposide or AraC. The elevation in p53 caused by DFO treatment was thus ineffective in blocking CDK4 translation.

ELISA and Western blot analysis revealed that treatment with DFO for 6 h did not affect expression of pRB or pRB phosphorylation. After treatment with etoposide or AraC for 6 h, expression of pRB de-

creased and the pRB phosphorylation index increased. This result may have been caused by the failure of etoposide and AraC to arrest G1 at this point, implying that although the cells pass through the G1-S checkpoint, the following cell cycle did not proceed properly, and, therefore, pRB was not dephosphorylated. Since we assayed the native form of pRB with ELISA, the bead-coated anti-pRB monoclonal antibody or the anti-pRB polyclonal antibody might not have detected pRB in the complex. In this assay, both antibodies recognize regions outside the pocket domain or phosphorylation region [22] and the results of ELISA paralleled those of Western blot analysis. Thus, results with the present ELISA system were considered reliable.

In this study, we found that although p53 accumulation occurred with all three treatments, the downstream cellular response was variable. Treatment with DFO clearly caused G1 accumulation; accordingly, a growth inhibition mechanism may exist independently from the cascade by which p53 induces p21, which inhibits CDK4 activity, and results in pRB phosphorylation. Recent studies have revealed that p21-deficient mouse embryo fibroblasts undergo G1 arrest after DNA damage [23,24]. Growth inhibition by iron deprivation would thus offer a model system to analyze the regulation of cell growth by mechanisms other than p53-inhibition of pRB phosphorylation.

Acknowledgements

This work was supported in part by a Grant-in-Aid from the Ministry of Science and Education, Japan, and the Japan Private School Promotion Foundation.

References

[1] A.V. Hoffbrand, K. Ganeshaguru, J.W.L. Hooton, M.H.N. Tattersall, Effect of iron deficiency and desferrioxamine of DNA synthesis in human cells, Br. J. Haematol. 33 (1976) 517–526.

[2] L. Dezza, M. Cazzola, M. Danova, C. Carlo-Stella, G. Bergamaschi, S. Brugnatelli, R. Invernizzi, G. Mazzini, A. Riccardi, E. Ascari, Effects of deferrioxamine on normal and leukemic human hematopoietic cell growth: in vitro and in vivo studies, Leukemia 3 (1989) 104–107.

[3] M. Cazzola, G. Bergamaschi, L. Dezza, P. Arosio, Manipulations of cellular iron metabolism for modulating normal and malignant cell proliferation: achievement and prospects, Blood 75 (1990) 1903–1919.

[4] H.M. Lederman, A. Cohen, J.W.W. Lee, M.H. Freedman, E.W. Gelfand, Deferoxamine: a reversible S-phase inhibitor of human lymphocyte proliferation, Blood 64 (1984) 748–753.

[5] J. Blatt, S.R. Taylor, S. Stitely, Mechanism of antineuroblastoma activity of deferoxamine in vitro, J. Lab. Clin. Med. 112 (1988) 433–436.

[6] C. Brodie, G. Siriwardana, J. Jucas, R. Schleicher, N. Terada, A. Szepesi, E. Gelfand, P. Seligman, Neuroblastoma sensitivity to growth inhibition by deferrioxamine: evidence for a block in G1 phase of the cell cycle, Cancer Res. 53 (1993) 3969–3975.

[7] A. Bomford, J. Isaac, S. Roberts, A. Edwards, S. Young, R. Williams, The effect of desferrioxamine of transferrin receptors, the cell cycle and growth rates of human leukaemic cells, Biochem. J. 236 (1986) 243–249.

[8] K.P. Hoyes, R.C. Hider, J.B. Porter, Cell cycle synchronization and growth inhibition by 3-hydroxypridine-4-one iron chelator in leukemia cell lines, Cancer Res. 52 (1992) 4591–4599.

[9] K. Fukuchi, S. Tomoyasu, N. Tsuruoka, K. Gomi, Iron deprivation-induced apoptosis in HL-60 cells, FEBS Lett. 350 (1994) 139–142.

[10] K. Fukuchi, S. Tomoyasu, H. Watanabe, S. Kaetsu, N. Tsuruoka, K. Gomi, Iron deprivation results in an increase in p53 expression, Biol. Chem. Hoppe-Seyler 376 (1995) 627–630.

[11] M.B. Kasten, O. Onyekwere, D. Sidransky, B. Vogelstein, R.W. Craig, Participation of p53 in the cellular response to DNA damage, Cancer Res. 51 (1991) 6304–6311.

[12] S.J. Kuerbitz, B.S. Plunkett, W.V. Walsh, M.B. Kasten, Wild-type p53 is a cell cycle checkpoint determinant following irradiation, Proc. Natl. Acad. Sci. USA 89 (1992) 7491–7495.

[13] S.W. Lowe, E.M. Schmitt, S.W. Smith, B.A. Osborne, T. Jacks, p53 is required for radiation-induced apoptosis in mouse thymocytes, Nature 362 (1993) 847–849.

[14] A.R. Clarke, C.A. Purdie, D.J. Harrison, R.G. Morris, C.C. Bird, M.L. Hooper, A.H. Wyllie, Thymocyte apoptosis induced by p53-dependent and independent pathways, Nature 362 (1993) 849–852.

[15] C. Caelles, A. Helmberg, K. Michael, p53-dependent apoptosis in the absence of transcriptional activation of p53-target genes, Nature 370 (1994) 220–223.

[16] C.J. Sherr, G1 phase progression: cycling on cue, Cell 79 (1994) 551–555.

[17] T. Hunter, J. Pines, Cyclins and cancer II: cyclin D and CDK inhibitors come of age, Cell 79 (1994) 573–582.

[18] R.A. Weinberg, The retinoblastoma protein and cell cycle control, Cell 81 (1995) 323–330.

[19] C.J. Sherr, J.M. Roberts, Inhibitors of mammalian G1 cyclin-dependent kinases, Genes Dev. 9 (1995) 1149–1163.

[20] M.E. Ewen, C.J. Oliver, H.K. Sluss, S.J. Miller, D.S. Peeper, p53-dependent repression of CDK4 translation in TGF-β-induced G1 cell-cycle arrest, Genes Dev. 9 (1995) 204–217.
[21] J. Sambrook, E.F. Fritsch, T. Maniatis, Molecular Cloning: A Laboratory Manual, 2nd ed., Cold Spring Harbor Laboratory, New York, 1982.
[22] Y. Qian, C. Luckey, L. Horton, M. Esser, D.J. Templeton, Biological function of the retinoblastoma protein requires distinct domain for hyperphosphorylation and transcription factor binding, Mol. Cell. Biol. 12 (1992) 5363–5372.
[23] C. Deng, P. Zhang, J.W. Harper, S.J. Elledge, P. Leder, Mice lacking p21CIP1/WAF1 undergo normal development, but are defective in G1 checkpoint, Cell 82 (1995) 675–684.
[24] J. Brugarolas, C. Chandrasekaran, J.I. Gordon, D. Beach, T. Jacks, G.J. Hannon, Radiation-induced cell cycle arrest compromised by p21 deficiency, Nature 377 (1995) 552–557.

EXPERIMENTAL CELL RESEARCH 229, 60–68 (1996)
ARTICLE NO. 0343

Iron Deprivation Inhibits Cyclin-Dependent Kinase Activity and Decreases Cyclin D/CDK4 Protein Levels in Asynchronous MDA-MB-453 Human Breast Cancer Cells

KRISTEN S. KULP,* SHERRIL L. GREEN,† AND P. RICHARD VULLIET*,[1]

*Department of Molecular Biosciences, School of Veterinary Medicine, University of California at Davis, Davis, California 95616-8643; and †Department of Comparative Medicine, Stanford University, Palo Alto, California 94305-5410

Iron chelation, known to block progression through the cell cycle, was examined for effects on the activity and subunit levels of the cyclin-dependent protein kinases (cdk). Treatment of asynchronous MDA-MB-453 cells with the iron chelators mimosine or desferrioxamine (DFO) for 24 h stopped cell division, but did not produce a single, synchronous block. DNA content analysis demonstrated that although a majority of the cells were blocked in G1 (87.3%), an unexpectedly large fraction of the cells were blocked in S phase (11.5%). Western blot analysis of the treated lysates demonstrated the presence of cyclin B, confirming that part of the cell population was blocked in S phase. After release from mimosine treatment, 84% of the cell population remained in G1 up to 8 h. Treating breast cancer cells with 400 μM mimosine for 24 h inhibited cyclin E- and cyclin A-associated kinase activity by 85% or more, although immunoblots using anti-cyclin A, cyclin E, cdc2, and cdk2 antibodies showed that these key subunits were still present in the cells at pretreatment levels. Interestingly, Western blot analysis also demonstrated that iron chelation decreased the protein levels of the cyclin D and cdk4 subunits as compared to control and produced a change in retinoblastoma protein phosphorylation. These results indicate that iron deprivation effects the activity and protein levels of the cyclin-dependent kinases, and ultimately, the pathways that control cell division.

INTRODUCTION

Regulation of cell cycle progression appears to be controlled by sequential activation and subsequent inactivation of a growing family of serine/threonine protein kinases, the cyclin-dependent (cdk) protein kinases (reviewed in [1–3]). The active forms of these kinases are heterodimers composed of at least two subunits: a cyclin that acts as a regulatory subunit and a catalytic subunit that acts as the kinase. The complex often contains other proteins that may act as inhibitors or activators. Many physiological substrates of the cdk kinases have been identified, including microtubules, lamins, nucleolin, and histone H1. During the G1 phase of the cell cycle an important target for the cdk kinases appears to be the retinoblastoma susceptibility gene product (pRb).

To date, eight cdk subunits have been identified in higher eukaryotes [4–8]. The kinase subunits are numbered sequentially in chronological order of discovery as cdk1 through cdk8, with p34cdc2 being cdk1. Eight cyclins or cyclin families have been identified, designated as cyclins A–H. In keeping with their periodic nature, the cyclins appear and disappear at specific regulatory points in the cell cycle. In mammalian cells, progression through G1 appears to be controlled by the C-, D-, and E-type cyclins, while progression through S, G2, and M is controlled by the A- and B-type cyclins.

Adequate intracellular iron levels are also vital for cell cycle progression, and a large body of evidence indicates that either all or part of the iron requirement is for DNA synthesis [9, 10]. The major cellular iron requirement occurs during late G1 and S phase and has been attributed to the increased activity of ribonucleotide reductase, an iron-requiring enzyme [11]. Ribonucleotide reductase catalyzes the reduction of ribonucleoside 5′-diphosphates to the corresponding 2′-deoxyribonucleoside 5′-diphosphates [12]. In proliferating cells, S phase appears to be dependent upon the rapid synthesis of the R2 subunit of ribonucleotide reductase. This subunit contains a tyrosyl-free radical that must be regenerated by a mechanism that requires ferrous (Fe^{+2}) iron and oxygen [11, 13–15]. Removal of iron, through treatment with iron chelators, has consistently been shown to inhibit cellular proliferation [16].

In 1990 Lalande reported that mimosine reversibly arrested cell cycle progression in human lymphoblastoid cells in late G1, 1–2 h before the onset of S phase

[1] To whom correspondence and reprint requests should be addressed. Fax: (916) 752-7409.

0014-4827/96 $18.00

[17]. This observation led several groups of cell cycle researchers to use mimosine as a synchronization agent in an attempt to elucidate the biochemical events leading to the initiation of S phase [18–28]. These studies demonstrated that mimosine blocked a variety of cell types including CEM leukemic human T cells [19], A549 human lung carcinoma cells [21], new-born MANCA cells [24], MG-63 osteosarcoma cells [25], and Chinese hamster ovary cells [28] in the G1 phase of the cell cycle. After release from mimosine block, these various cell types progressed uniformly into S phase within 4 to 6 h.

It is generally agreed that mimosine blocks cell cycle progression, although the exact timing and mechanism of action of the block remain controversial. Hanauske-Abel *et al.* support a G1 block by reporting that the accumulation of cells in late G1 was due to the ability of mimosine to inhibit deoxylhypusyl hydroxylase. This metallo-enzyme is necessary for the formation of hypusine, a rare amino acid found in the eukaryotic initiation factor-5A (eIF-5A) [29]. Other researchers have reported that mimosine blocks cells in S phase. Several studies by Hamlin and Mosca have demonstrated that mimosine is an effective inhibitor of DNA origins of replication in Chinese hamster ovary cells, resulting in an S phase block, rather than G1 [20, 30, 31]. Eblen *et al.* have also reported that mimosine blocks mink lung epithelial cells in S phase [32] and a report by Hughes *et al.* demonstrates that mimosine blocks HeLa cells after the cells have entered S phase [33]. As a strong iron chelator, it is possible that mimosine inhibits DNA synthesis by chelating the iron necessary for the R2 subunit of ribonucleotide reductase. Gilbert *et al.* studied the effects of mimosine on nuclear, mitochondrial, and simian virus 40 DNA replication, as well as DNA replication in *Xenopus* eggs. These investigators concluded that rather than inhibiting initiation of DNA replication, mimosine destabilizes replication forks by sequestering iron and altering deoxyribonucleotide metabolism [34]. Dai *et al.* have correlated a decrease in ribonucleotide reductase activity to an inhibition of viral DNA synthesis [35].

We have previously shown that mimosine blocks cell cycle progression in MDA-MB-453 human breast cancer cells in a time- and dose-dependent manner and that the effects of mimosine can be antagonized by treatments that increase intracellular iron [36]. Breast cancer cells treated with mimosine are iron-starved, and this can be evidenced by the movement of transferrin receptors to the cell surface. In addition, we have shown that the effects of mimosine were similar to those of another, chemically dissimilar, iron chelator, desferrioxamine (DFO). From these results, we have concluded that the effects of mimosine on cell cycle progression are caused by iron chelation.

In the current studies, we hypothesize that iron deprivation may produce cell cycle arrest by a direct or indirect effect on cdk kinases, providing a possible connection between these important regulators of cell cycle progression and intracellular iron levels. Our hypothesis was tested using DNA content analysis, kinase activity assays, and Western blot analysis. We found that treating asynchronous breast cancer cells with mimosine for 24 h reversibly arrested cell proliferation. However, we also discovered that the cells were not highly synchronized, with cells blocked in both G1 and S phases of the cell cycle. Under these conditions we found that cdk kinase activity was inhibited although the protein levels and apparent phosphorylation state of the cyclin E, cyclin A, cdk2, and cdk1 subunits were unchanged as compared to untreated controls. More interestingly, we found that the protein levels of the cyclin D and cdk4 subunits were decreased, and that there was a change in pRb phosphorylation. When taken together, these data suggest that mimosine blocks cells at multiple points in the cell cycle, and that a lack of iron, through iron chelation, causes a profound effect on the biochemical pathways that regulate G1 cdk activity.

MATERIALS AND METHODS

Materials

Mimosine (MIMO) (Sigma) was resuspended in phosphate-buffered saline (PBS) at 10 m*M* and then filtered through a 0.2 μm sterile filter. Desferrioxamine (DFO) (Ciba-Geigy) was resuspended as a 20 m*M* solution in sterile water. Aphidicolin (APH) (Sigma) was dissolved in DMSO as a 5 mg/ml solution. Cyclin A, cyclin E, cdc2, and cdk2 antibodies were kindly provided by Dr. Frederick Hall. Cdc2 antibody was also kindly provided by Dr. Joyce Yamaguchi. Cyclin E antibody was kindly provided by Dr. James Roberts. Cyclin B, cyclin E, cdk2, cyclin D, cdk4, and retinoblastoma protein antibodies were also obtained from Upstate Biologicals Inc. (Lake Placid, NY). The antibody to cyclin D recognizes p36 cyclin D1 and cross-reacts with p34 cyclin D2, which has a highly homologous epitope.

Methods

Tissue culture. MDA-MB-453 human breast cancer cells were obtained from American Type Culture Collection (Rockville, MD). The cells were maintained as monolayers in L-15 media (JRH Biosciences), supplemented with 10% fetal bovine serum (JRH), 100 units/ml penicillin, and 100 μg/ml streptomycin (JRH). For DNA content analysis, Western blot analysis, and protein kinase assays, the cells were subcultured in 75-cm^2 flasks and maintained in complete media for at least 24 h prior to drug treatment.

Flow Cytometric Analysis of DNA Content. Cells were harvested by trypsinization, washed once in cold HBSS, resuspended in cold 70% ethanol, and stored at 4°C for at least overnight. Prior to analysis, the cells were pelleted, removed from the ethanol, and washed once in PBS. RNAse (Sigma) dissolved in PBS was added to a final concentration of 100 μg/ml and the samples were incubated at 37°C for 30 min. The cell concentration was adjusted to 1 million cells/ml. Propidium iodide solution (10 mg propidium iodide, (Calbiochem), 0.37 mg EDTA, 9 ml PBS) was added to a final concentration of 50 μg/ml and the samples were subjected to flow cytometric analysis using a FACS Scan Becton–Dickinson instrument equipped with a

TABLE 1

DNA Content Analysis of the Recovery of MDA-MB-453 Cells from Cell Cycle Arrest by Mimosine or DFO

Treatment	G0/G1	S	G2/M
Control	66.8 (5.2)	23.1 (2.7)	10.1 (5)
400 μM Mimosine	87.3 (1.2)	11.5 (6.3)	1.2 (0.5)
400 μM Mimosine; Released 4 Hours	85.2 (1.2)	12.4 (3)	2.4 (2.7)
400 μM Mimosine; Released 8 Hours	84.3 (1.4)	12.2 (2.9)	3.6 (4.3)
150 μM DFO	82.8 (11.2)	15.4 (9.5)	3.2 (1.7)
150 μM DFO; Released 4 Hours	81.8 (5.7)	15 (7.9)	3.3 (2.3)
150 μM DFO; Released 8 Hours	68.0 (4.3)	29.5 (3.6)	3.0 (0.7)

Note. Exponentially growing cells were treated with 400 μM mimosine or 150 μM DFO or left untreated. After 24 h, the drug was removed and replaced with medium. Cell cycle status was determined at the times indicated by flow cytometry after staining with propidium iodide. CellFit Cell-Cycle Analysis Version 2.0 software was used to deconvolute DNA histograms. Data are averages of determinations of three different cell populations. The standard deviation is given in parenthesis.

Argon-Ion laser adjusted to emit at 488 nm. The fluorescence emission was collected at 590 nm. Mean fluorescence intensity data and contour plots were generated using CellFIT Cell-Cycle Analysis Version 2.0 software. For all samples 10,000 events were recorded and the average coefficient of variation of the mean DNA content of the G1 population was less than 3.0.

Western blotting. Cellular extracts were separated by SDS–polyacrylamide gel electrophoresis and electrophorctically transferred to nitrocellulose. Uniform protein loading and transfer were verified by Ponceau-S (Sigma) staining of the blot. Complete protein transfer was verified by staining the polyacrylamide gel. The membranes were blocked with 5% nonfat Carnation Milk in TBS-Tween (20 mM Tris–HCl, pH 7.4, 150 mM NaCl, 0.05% Tween 20). Following washing with TBS-Tween the membranes were incubated for 2 to 3 h or overnight in primary antiserum. The blots were washed again, incubated for 1–2 h in alkaline phosphatase-conjugated secondary antibody, washed again, and treated with 0.56 mM 5-bromo-4-chloro-3-indoyl phosphate and 0.48 mM nitroblue tetrazolium to develop the colored reaction product. Aphidicolin-treated samples were included as positive controls to indicate the levels of cdk subunits during an S phase block. Photographs of Western blots were scanned using a Cohu High Performance CCD Camera. Image Analysis was done using an IS-100 Digital Imaging System (Innotech Scientific Corp.)

Immunoprecipitation and protein kinase assay. After the specified treatment, the cell cultures were washed twice with cold HBSS and lysed with lysis buffer [Tris–HCl (10 mM), pH 8.5, sucrose (0.27 M), mercaptoethanol (7.5 mM), EDTA (2 mM), EGTA (2 mM), leupeptin (5 μg/ml), PMSF (0.1 mM), sodium pyrophosphate (5 mM), NaF (25 mM), and Triton-X 100 (0.2%)]. Insoluble material was pelleted by centrifugation (13,000g for 15 min). To specifically determine the cyclin E- and cyclin A-associated kinase activity, cell lysates were immunoprecipitated with polyclonal anti-cyclin E and anti-cyclin A antibodies. Protein samples were diluted (0.3 mg total cellular protein/200 μl) in ice-cold immunoprecipitating buffer. Samples were precleared with goat serum and incubated with anti-cyclin A or cyclin E antiserum for 2 h at 4°C in the presence of 45 μl of a 1:1 suspension of protein A–Sepharose beads. Immunoprecipitated material was assayed for kinase activity utilizing a synthetic peptide analog based on the consensus sequence for histone H1 (A-K-A-K-K-T-P-K-K-A-K). As a control substrate, the proline at position 7 was substituted with a glycine (A-K-A-K-K-T-G-K-K-A-K; peptides prepared by the University of California-Davis Protein Structure Laboratory). Additional controls included omission of the substrate peptides. Protein kinase assays were done according to the method of Vulliet *et al.* [37]. Briefly, the peptide (100 μM) was incubated with the protein A beads, Tris–acetate (100 mM), pH 7.5, magnesium acetate (10 mM) and [γ-^{32}P]ATP (100 μM) (sp act 1000–2000 cpm/pmol) (final volume 50 μl) for 30 min at 30°C.

RESULTS

The effects of iron chelation on cell cycle progression were examined by treating MDA-MB-453 human breast cancer cells with mimosine and DFO. As shown in Table 1, DNA content analysis demonstrated that treatment with mimosine and DFO arrested a majority (85 to 87%) of the cells in the G0/G1 phase of the cell cycle as compared to the asynchronous control. However, a relatively large fraction (11–15%) of the cells was also arrested in S phase. Four h after removal of the drug, less than 3% of the population of cells blocked in G1 had moved into S phase. After 8 h release from iron chelation the percentage of cells in S phase had not significantly changed in the cells released from mimosine block. In the cells released from DFO block the percentage of cells in S phase increased from 15 to 30%. In both cases a majority of cells remained in G1.

The presence of cyclin B, a cdk subunit that appears only in S, G2, and M phases of the cell cycle, was examined to confirm that a percentage of the chelator-treated cells were blocked in the S phase of the cell cycle. Western blotting with anti-cyclin B antibody demonstrated the presence of this cdk subunit in the lysates of cells treated for 24 h with mimosine and DFO. In Fig. 1, the level of cyclin B in the blocked cells was compared to the level of cyclin B found in the asynchronous cells as well as cells blocked by 24 h treatment with aphidicolin. Blocking the cells with aphidicolin, an S phase blocking agent, illustrates typical protein levels of cyclin B during a total S phase block. Using scanning densitometry, the amount of cyclin B in the mimosine-treated (36%) and DFO-treated (47%) cells is decreased over 50% as compared to the control cell lysates (100%). The amount of cyclin B in aphidicolin-treated (382%) cells is increased threefold.

The effect of iron chelation on cdk activity was examined using immunoprecipitation with specific antibodies. Antibodies to cyclin E and cyclin A were used to selectively precipitate these cyclins and their associ-

ated kinase activities. Treatment with 400 μM mimosine or 150 μM DFO for 24 h demonstrated that a lack of intracellular iron has an inhibitory effect on cyclin E- and cyclin A-immunoprecipitable activity (Fig. 2). Histone H1 peptide phosphorylating cyclin E activity was significantly inhibited in the mimosine-treated samples (83.5%) and in the DFO-treated samples (95%) ($P < 0.025$). Cyclin A-associated activity was undetectable.

To investigate the relative levels of the cdk kinase subunits following iron deprivation, we immunoblotted the treated cell lysates. Western blot analysis with anti- p34 cdc2, anti-p33 cdk2, anti-cyclin E, and anti-cyclin A antibodies confirmed the presence of these various subunits in the cell extracts (Fig. 3). Although the blocked cells had much less cdk kinase activity (5–10% of control) the protein levels of the subunits were not noticeably altered. Scanning denistometry confirmed that the amounts of the subunits in the treated cell lysates did not differ from the control cell lysates by more than 30%.

Although the protein levels of cyclin A, cyclin E, cdk2, and cdc2 did not change due to iron deprivation, levels of cyclin D and cdk4 were noticeably less in both the mimosine- and DFO-treated lysates, as compared to the control or aphidicolin-treated lysates (Fig. 4A and 4B). Aphidicolin-treated samples were included in these blots to illustrate that the decrease in cyclin D and cdk4 was not a general effect of cell cycle blockade. In Fig. 4A, the amount of cyclin D quantifiable by scanning densitometry dropped 70% in the mimosine-treated cells and 80% in the DFO-treated cells as compared to the control (100%) and aphidicolin-treatment (92%). The antibody to cyclin D recognizes p36 cyclin D1 and crossreacts with p34 cyclin D2, which has a highly homologous epitope. Densitometric analysis confirmed that the amount of cdk4 dropped to 42% in the mimosine-treated cells and 29% in the DFO-treated cells.

As a potential consequence of the decreased protein levels of the cyclin D/cdk4 complex, we examined the state of phosphorylation of Rb (as evidenced by altered

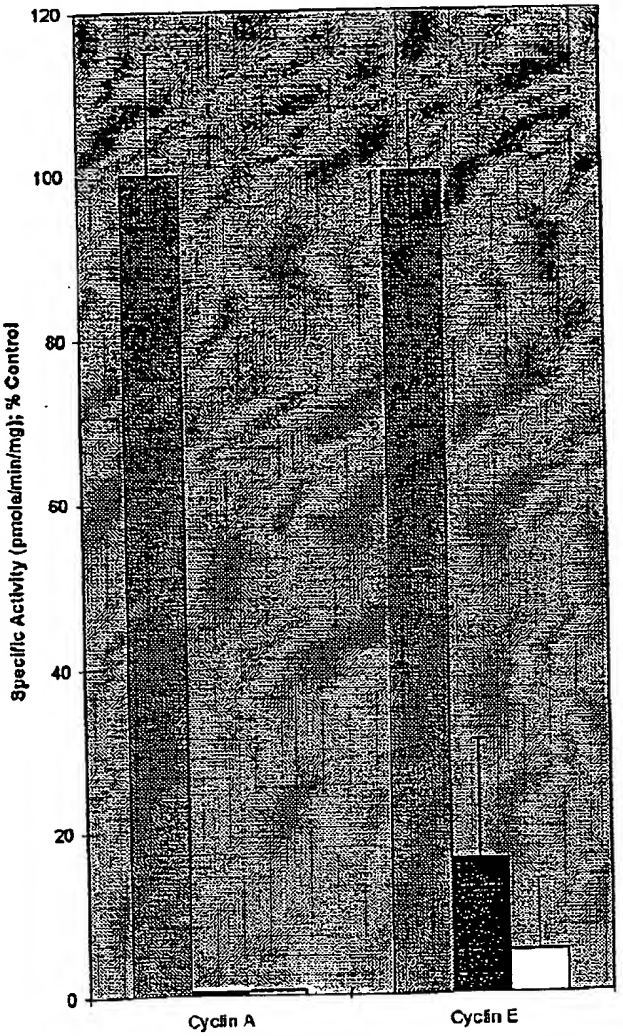

FIG. 2. Cyclin A- and cyclin E-immunoprecipitable activities in mimosine and DFO-treated cell lysates. MDA-MB-453 cells were treated for 24 h with either 400 μM mimosine or 150 μM DFO. Control ▩; Mimosine ■; DFO □. Results are the average of at least three determinations. Mimosine and DFO treatment produced results significantly different from control, $P < 0.025$.

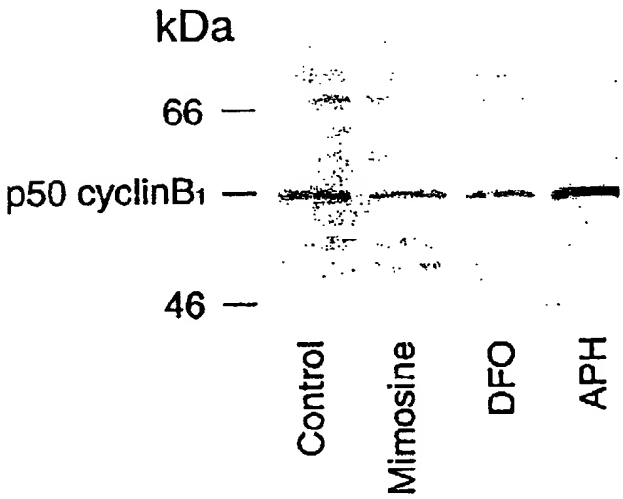

FIG. 1. Immunoblot analysis of cyclin B in MDA-MB-453 breast cancer cells. Cells were treated with 400 μM mimosine, 150 μM DFO, 10 μM aphidicolin, or left untreated (Control) for 24 h. 10% SDS–PAGE gels were loaded with 200 μg protein per lane and transferred to nitrocellulose. Cyclin B appears as a single 50-kDa molecular weight band. Scanning densitometry values: Control, 100%; Mimosine, 36%; DFO, 47%; APH, 382%.

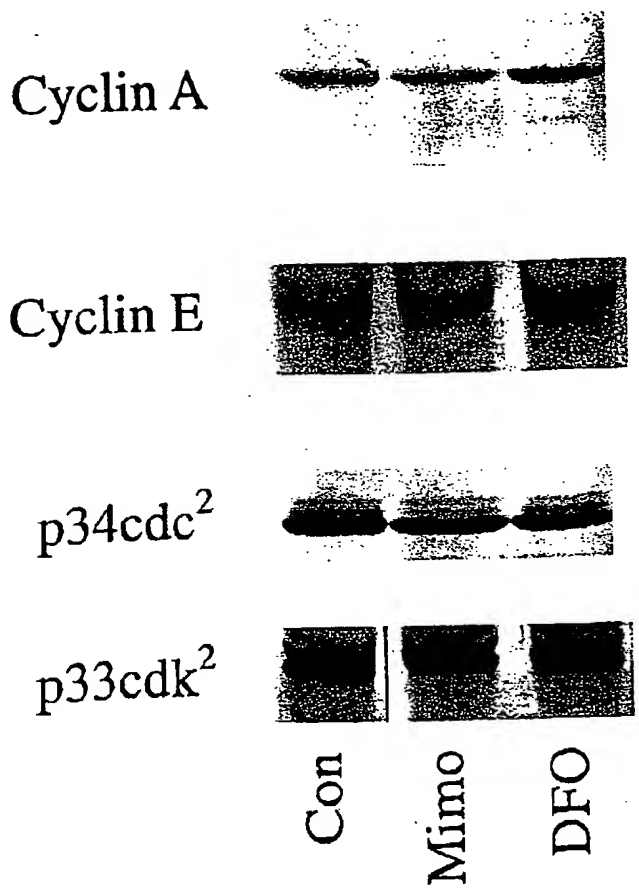

FIG. 3. Immunoblot analysis of cyclin A, cyclin E, cdc2, and cdk2 in MDA-MB-453 breast cancer cells. Cells were treated with 400 μM mimosine (Mimo), 150 μM DFO, or left untreated (Con) for 24 h. 10% SDS–PAGE gels were loaded with 200 μg protein per lane and transferred to nitrocellulose. Cyclin A appears as a single 60-kDa molecular weight band. Cyclin E appears as a single 45-kDa molecular weight band. Cdc2 appears as a triple band, indicating multiple phospho-forms. Cdk2 appears as a doublet, also indicating multiple phospho-forms. (Scanning densitometry values) Cyclin A: Control, 100%; Mimosine, 92%; DFO, 122%. Cyclin E: Control, 100%; Mimosine, 106%; DFO, 118%. p34cdc^2: Control, 100%; Mimosine, 70%; DFO, 75%. p33cdk^2: Control, 100%; Mimosine, 106%; DFO, 130%.

migration on SDS gels) by Western blotting. Retinoblastoma protein is a physiological substrate of cyclin D and cdk4, and phosphorylation of this protein is critical for progression into S phase. Immunoblotting mimosine- and DFO-treated lysates with anti-retinoblastoma protein (pRb) antibody illustrated that there was a distinct change in phosphorylation state of the Rb protein. In the mimosine- and DFO-treated cells there was less pRb in the hyperphosphorylated state (slower migrating band) (50 and 44%, respectively, by scanning densitometry) as compared to the control (100%) (Fig. 4C). In the aphidicolin-treated samples, the amount of pRb in the hypophosphorylated state (lower molecular weight), dropped 40% by scanning densitometry. In these samples most of the protein appears to be in the hyperphosphorylated, higher molecular weight form.

DISCUSSION

Iron Chelation Does Not Produce a Synchronous Block in MDA-MB-453 Cells

Although we originally became interested in iron chelation as a way to synchronize cells near the S phase border, we found that adding mimosine or DFO to an asynchronous population of MDA-MB-453 cells blocked cells in both the G1 and S phases of the cell cycle. DNA content analysis demonstrated that treating the cells with 400 μM mimosine for 24 h reduced the fraction of S phase cells by only 50%, from 23 to 11.5%. The same concentration of mimosine (400 μM) decreased the incorporation of tritiated thymidine by greater than 95% [36]. This decrease in tritiated thymidine incorporation suggests that the cells are arrested in S phase, since they are not synthesizing DNA. The presence of the cyclin B subunit in the treated lysates confirms that a portion of the cells are blocked in S phase. During the cell cycle, cyclin B is degraded in metaphase and is not produced again until the following S phase [38, 39]. A two-step synchronization treatment of these breast cancer cells that utilizes serum deprivation and 400 μM mimosine treatment blocks the cells exclusively in G1 and demonstrates that cyclin B is not present during this phase of the cell cycle (data not shown). The occurrence of cyclin B in the mimosine and DFO-treated samples (Fig. 1) is additional evidence of an S phase cell population in the blocked cells. Aphidicolin is an S phase blocker that blocks cycle progression by inhibiting DNA polymerases [40]. The amount of cyclin B in the aphidicolin-treated samples should be greater than the control or iron-deprived cells, as the entire cell population is blocked in S phase. This anticipated result is presented in Fig. 1.

Although our data do not exclude the possibility that those cells blocked in G1 are at the G1/S phase border, neither does the data support a block of this nature. The slow rate of increase in S phase cells (as well as a slow rate of increase in tritiated thymidine incorporation [36]) upon removal of the chelator suggests that the cells blocked in G1 were not highly synchronized and were not blocked near the S phase border. Up to 8 h after removal of the mimosine block, there was no appreciable increase in the S phase cell population. This, along with the apparent effect on cyclin D and cdk4, suggests that there may be another block point, earlier in G1.

In this respect, the MDA-MB-453 human breast cancer cell line appears to be unique. This breast cancer cell line is an androgen-responsive cell line that ex-

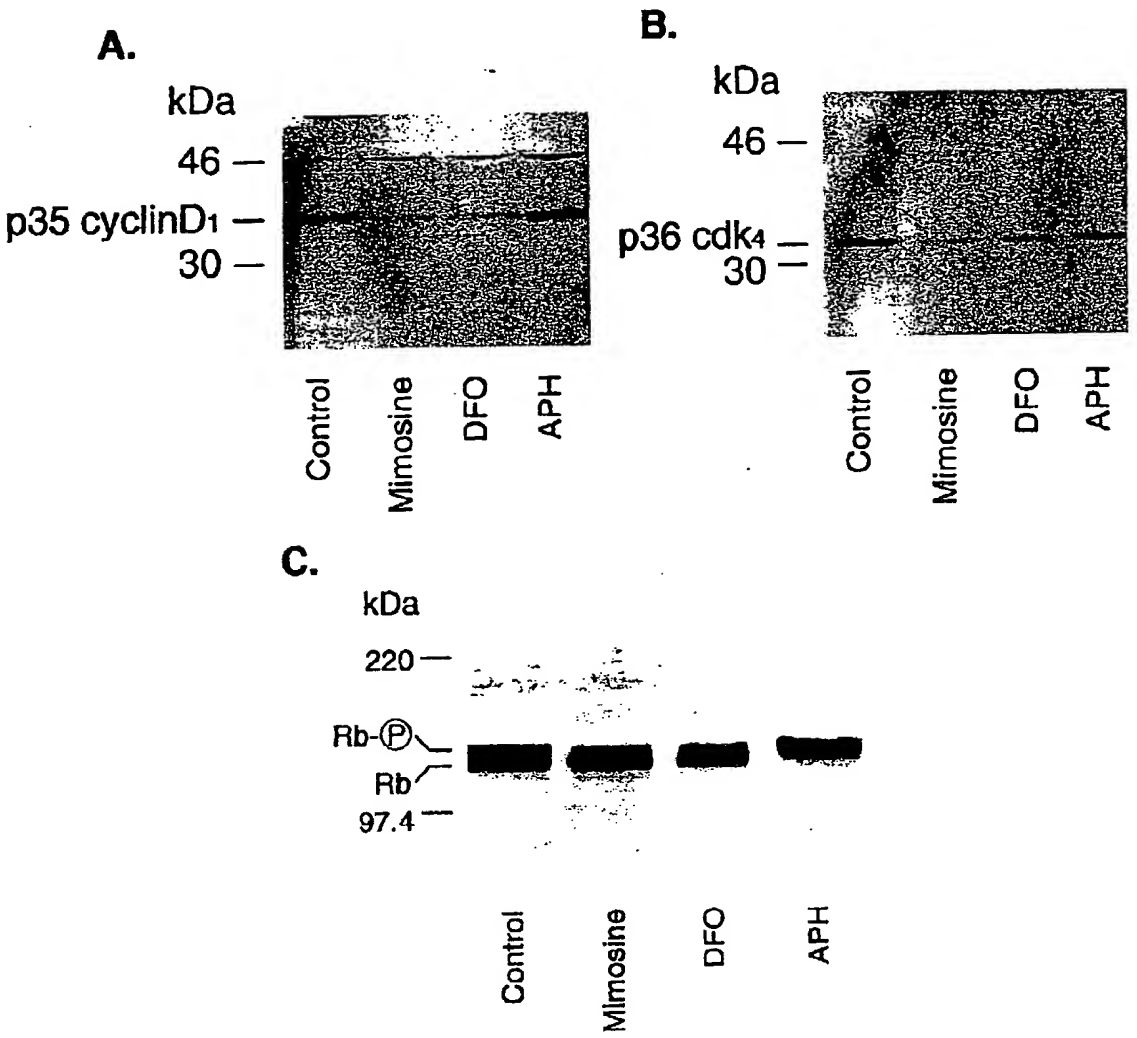

FIG. 4. (A) Immunoblot analysis of cyclin D in MDA-MB-453 breast cancer cells. Cells were treated with 400 μM mimosine, 150 μM DFO, 10 μM aphidicolin or left untreated (Control) for 24 h. 10% SDS–PAGE gels were loaded with 200 μg protein per lane and transferred to nitrocellulose. Cyclin D appears as a single 35-kDa molecular weight band. The band at 46 kDa is unidentified but consistently appears in these samples. Scanning densitometry values: Control, 100%; Mimosine, 29%; DFO, 20%; APH, 92%. (B) Immunoblot analysis of cdk4 in MDA-MB-453 breast cancer cells. Cells were treated as in A. Cdk4 appears as a single 36-kDa molecular weight band. Scanning Densitometry values: Control, 100%; Mimosine, 35%; DFO, 53%; APH, 98%. (C) Immunoblot analysis of retinoblastoma protein in MDA-MB-453 cells. Cells were treated as in A. 8% SDS–PAGE gels were loaded with 250 μg protein per lane and transferred to nitrocellulose. Retinoblastoma appears as multiple phospho-forms. (Scanning Densitometry values) Control: Rb-P, 100%; Rb, 100%; Mimosine: Rb-P, 50%; Rb, 102%; DFO: Rb-P, 44%; Rb, 80%; APH: Rb-P, 119%; Rb, 64%.

presses androgen receptors and p185erbB2 (HER2, neu) receptors, but lacks oestrogen receptors, progesterone receptors, and EGF receptors [41, 42]. These cells have also been shown to express a shortened, more stable cyclin D1 mRNA [43]. In other cell lines that have been treated with mimosine, most of the cells appear to be blocked in late G1, and progress uniformly into S phase within 4 h of release from mimosine block [17, 19, 21, 25, 28, 44]. Cell lines not blocked in G1 are reported to be stopped in S phase [32, 33, 45]. Other researchers have reported that mimosine has an effect on CDK activity in various cell types [18, 19, 32, 24, 25, 46]; however, the presence of cyclin B in a mimosine-treated lysate and the change in cyclin D and cdk4 that occur in this cell line are novel findings.

Iron Chelation Has an Effect on Cyclin-Dependent Kinases

Cyclin-dependent kinases regulate cell cycle progression, and the activities of cyclin E-, and cyclin A-depen-

dent kinases are necessary for progress through the G1 and S phases of the cell cycle [4, 6, 47]. Treating breast cancer cells with mimosine and DFO profoundly inhibited both cyclin E- and cyclin A-associated kinase activity, demonstrating that the cellular activity of these kinases requires iron. Other cyclin-associated kinase activities were not examined because previous experimentation has shown that 24-h mimosine and DFO treatment inhibits total, extractable proline-directed protein kinase (PDPK) activity by 90% or more [36]. The PDPK family of kinases includes the cdk kinases as well as mitogen-activated protein (MAP) kinases. Therefore iron chelation generally inhibits PDPK activity as well as specifically inhibiting cyclin E- and cyclin A-associated kinase activity. Inhibition of the kinase activity was not a direct effect; addition of mimosine or DFO to the assay system did not significantly affect kinase activity and the addition of iron to inhibited extracts did not reverse the effects of mimosine or DFO (data not shown).

Although there was little, if any, cyclin A-, or cyclin E-associated kinase activity detectable after 24 h treatment with mimosine and DFO, Western blot analysis using antibodies to cdc2, cdk2, cyclin A, and cyclin E demonstrated that these key subunits were still present in the cell lysates. Immunoblotting with an anti-cdc2 antibody typically results in three bands, which is generally attributed to multiple phospho-forms [48–50]. After 24 h treatment with mimosine and DFO the ratio of these bands did not change, suggesting that there is no change in the apparent phosphorylation state of the cdc2 subunit. This may indicate that the decrease in kinase activity is not due to a change in the activity of the kinases or phosphatases that regulate the cdc2 subunit. Immunoblotting treated cell lysates with antibodies to phospho-tyrosine also did not show any change from control (data not shown).

The phosphotransferase activity of the cdk kinases is regulated primarily by association and dissociation of the cyclin partner, timely phosphorylation–dephosphorylation events, and the presence or absence of inhibitor proteins (reviewed in [51, 52]). Because there is no apparent change in protein levels or phosphorylation state, the results from the Western blots suggest that the chelators may decrease cyclin A- and cyclin E-associated kinase activity by upsetting the regulation of an inhibitor protein. It is possible that the decrease in cyclin D and cdk4 protein levels produced by iron chelation causes an increase or redistribution of an inhibitor protein, and that this subsequently inhibits cyclin A- and cyclin E-associated kinase activity. Poon *et al.* have reported that in cells arrested in G1 with lovastatin, cyclin D1 was degraded and the inhibitor protein p27 was redistributed to cyclin A/cdk2 [53]. A similar phenomenon may be occurring in the iron-deprived cells, leading to an inhibition of kinase activity.

The cyclin D/cdk4 complex is growth factor-sensitive, and appears to function to translate extracellular signals into orderly progression through G1 (reviewed in [54]). The activity of cyclin D/cdk4 is strongly correlated to retinoblastoma protein phosphorylation; cyclin D-dependent kinase activity first appears in G1 at the same time as the appearance of *in vivo* phosphorylation of pRb [55]. Timely phosphorylation of pRb is critical for cell cycle progression. Hypophosphorylated pRb sequesters essential transcription factors while hyperphosphorylation of pRb reverses the inhibitory functions, allowing progression into DNA synthesis (reviewed in [56]). Immunoblotting mimosine- and DFO-treated cell lysates with antibodies specific to cyclin D and cdk4 showed a diminution of these subunits not seen in the aphidicolin-treated cell lysates. In addition to decreasing cyclin D and cdk4 protein levels, mimosine and DFO treatment caused a change in the phosphorylation state of pRb as compared to the control and aphidicolin-treated samples (Fig. 4c). In the aphidicolin-treated samples, most of the pRb appears in the upper, phosphorylated form, which is consistent with a S phase cell population. However, in the iron-deprived samples less of the pRb appeared in the upper form. A change in protein levels of the cyclin D/cdk4 subunits and a change in phosphorylation state of pRb together suggests that the decrease in these subunits may somehow prevent pRb from being phosphorylated. Terada *et al.* reported that DFO arrested cell cycle progression in stimulated human T cells earlier than aphidicolin and that this cell cycle block resulted in hypophosphorylated pRb. Adding iron restored both cell proliferation and pRb phosphorylation, leading these researchers to conclude that these effects were due to iron deprivation and that there may be iron-dependent events that lead to pRb phosphorylation [57]. Similarly, these researchers found that the synthesis of p34cdc2 in a serum-free cell culture system of human T lymphocytes required a small amount of iron [58]. The decrease in the cyclin D and cdk4 protein levels suggests that iron may be important in the biochemical pathways that control the regulation of these key cell cycle subunits, which, in turn, leads to pRb phosphorylation.

The transport and utilization of iron is vital to cell cycle control. The crucial need for iron during S phase is generally attributed to the requirements of ribonucleotide reductase [13]. While there is no doubt that the requirement for iron is due in part to the needs of this enzyme, it does not explain why iron chelators such as mimosine and DFO block cells in G1, before ribonucleotide reductase is required. In 1992, Chan *et al.* [59] observed that cdc2 and cdk2 are able to phosphorylate a physiological site on the R2 subunit of ribonucleotide reductase, leading these authors to postulate that R2 phosphorylation by a cdk kinase may play a role in regulating ribonucleotide reductase activity.

We have shown that adequate intracellular iron concentrations are essential for cdk activity. These results suggest that at least part of the cellular need for iron occurs before ribonucleotide reductase activation.

In our studies with MDA-MB-453 human breast cancer cells, we have found that iron chelation inhibits the activity of cyclin E- and cyclin A-associated kinase and decreases the protein levels of cyclin D and cdk4, key regulatory subunits in cell cycle control. These results suggest a link between an iron-sensitive G1 pathway and a G1 cdk regulatory point in this cell line. We have also found that mimosine treatment of asynchronous cells does not produce a synchronous G1 block. However, mimosine treatment following partial synchronization by serum deprivation does block cells exclusively in G1, although probably not near the G1/S phase border. Partially synchronizing the cell population prior to mimosine treatment produces a dramatic effect on cyclin subunits in G1 that is not seen in mimosine treatment of asynchronous cells (manuscript in preparation). Ongoing experimentation is in progress to define the nature of a possible iron-dependent regulatory step in G1. Further experimentation is also planned to determine if these observations are unique to this breast cancer cell line, all breast cancer cells, or is generally true for all cell types.

The authors gratefully acknowledge the assistance of Renan Acevedo for performing the FACS analysis and Robert Rigor for technical assistance.

REFERENCES

1. Norbury, C., and Nurse, P. (1992) *Annu. Rev. Biochem.* **61**, 441–470.
2. Murray, A. (1992) *Nature* **359**(6396), 599–604.
3. Pines, J. (1992) *Curr. Opin. Cell Biol.* **4**(2), 144–148.
4. Meyerson, M., Enders, G. H., *et al.* (1992) *EMBO J.* **11**(8), 2909–2917.
5. Tsai, L.-H., Harlow, E., and Meyerson, M. (1991) *Nature (London)* **353**, 174–177.
6. Bates, S., Bonetta, L., *et al.* (1994) *Oncogene* **9**, 71–79.
7. Lew, J., Beaudette, K., *et al.* (1992) *J. Biol. Chem.* **267**, 13383–13390.
8. Tassan, J., Jaquenoud, M., *et al.* (1995) *Proc. Natl Acad. Sci. USA* **92**, 8871–8875.
9. Hayashi, I., and Sato, G. H. (1976) *Nature (London)* **259**, 132–134.
10. Cherington, P. V., Smith, B. L., and Pardee, A. B. (1979) *Proc. Natl Acad. Sci. USA* **76**, 3937–3941.
11. Eriksson, S., Graslund, A., *et al.* (1984) *J. Biol. Chem.* **259**(19), 11695–11700.
12. Thelander, L., and Reichard, P. (1979) *Annu. Rev. Biochem.* **48**, 133–158.
13. Thelander, L., Graslund, A., and Thelander, M. (1983) *Biochem. Biophys. Res. Commun.* **110**, 859–865.
14. Bjorklund, S., Skog, S., *et al.* (1990) *Biochemistry* **29**, 5452–5458.
15. Wright, J. A., Chan, A. K., *et al.* (1990) *Biochem. Cell Biol.* **68**, 1364–1371.
16. Laskey, J., Webb, I., *et al.* (1988) *Exp. Cell. Res.* **176**, 87–95.
17. Lalande, M. (1990) *Exp. Cell Res.* **186**, 332–339.
18. Feldman, S. T., and Schonthal, A. (1994) *Cancer Res.* **54**, 494–498.
19. Yoshida, M., Yamamoto, M., and Nikaido, T. (1992) *Cancer Res.* **52**, 6676–6681.
20. Levenson, V., and Hamlin, J. (1993) *Nucleic Acids Res.* **21**(17), 3997–4004.
21. Bui, K. C., Wu, F., *et al.* (1993) *Am. J. Respir. Cell Mol. Biol.* **9**, 115–125.
22. Watson, P. A., Hanauske-Abel, H. H., *et al.* (1991) *Cytometry* **12**, 242–246.
23. Williams, R. T., Wu, L., *et al.* (1993) *J. Biol. Chem.* **268**(12), 8871–8880.
24. Marraccino, R. L., Firpo, E. J., and Roberts, J. M. (1992) *Mol. Biol. Cell* **3**, 389–401.
25. Carbonaro-Hall, D., Williams, R., *et al.* (1993) *Oncogene* **8**, 1649–1659.
26. Urbani, L., Sherwood, S. W., and Schimke, R. T. (1995) *Exp. Cell Res.* **219**, 159–168.
27. Alexandrow, M. G., and Moses, H. L. (1995) *Cancer Res.* **55**, 3928–3932.
28. Orren, D. K., Petersen, L. N., and Bohr, V. A. (1995) *Mol. Cell. Biol.* **15**(7), 3722–3730.
29. Hanauske-Abel, H. M., Park, M.-H., *et al.* (1994) *Biochim. Biophys. Acta* **1221**, 115–124.
30. Mosca, P. J., Dijkwel, P. A., and Hamlin, J. L. (1992) *Mol. Cell. Biol.* **12**(10), 4375–4386.
31. Hamlin, J. L., Mosca, P. J., *et al.* (1993) *Cold Spring Harbor Symp. Quant. Biol.* **58**, 467–474.
32. Eblen, S. T., Fautsch, M. P., *et al.* (1995) *Cancer Res.* **55**, 1994–2000.
33. Hughes, T., and Cook, P. (1996) *Exp. Cell Res.* **222**, 275–280.
34. Gilbert, D. M., Neilson, A., *et al.* (1995) *J. Biol. Chem.* **270**(16), 9597–9606.
35. Dai, Y., Gold, B., *et al.* (1994) *Virology* **205**, 210–216.
36. Kulp, K. S., and Vulliet, P. R. (1996) *Toxicol. Appl. Pharmacol.* **139**, 356–364.
37. Vulliet, P. R., Hall, F. L., *et al.* (1989) *J. Biol. Chem.* **264**(27), 16292–16298.
38. Murray, A. W., and Kirschner, M. (1989) *Nature* **339**, 275–279.
39. Pines, J., and Hunter, T. (1991) *J. Cell. Biol.* **115**, 1–17.
40. Wang, T.-F. (1991) *Annu. Rev. Biochem.* **60**, 513–552.
41. Hall, R. E., Birrell, S. N., *et al.* (1994) *Eur. J. Cancer* **30A**(4), 484–90.
42. Lupu, R., Colomer, R., *et al.* (1990) *Science* **249**(4976), 1552–5.
43. Lebwohl, D. E., Muise-Helmericks, R., *et al.* (1994) *Oncogene* **9**(7), 1925–9.
44. Hoffman, B. D., Hanauske-Abel, H. M., *et al.* (1991) *Cytometry* **12**, 26–32.
45. Mosca, P. J., Lin, H.-B., and Hamlin, J. L. (1995) *Nucleic Acids Res.* **23**(2), 261–268.
46. Perennes, C., Qin, L., *et al.* (1993) *FEBS Lett.* **333**, 141–145.
47. Hunt, T. (1991) *Cell Biol.* **2**, 213–222.
48. Draetta, G., and Beach, D. (1988) *Cell* **54**, 17–26.
49. Simanis, V., and Nurse, P. (1986) *Cell* **45** 261–268.
50. Solomon, M. J., Glotzer, M., *et al.* (1990) *Cell* **63**, 1013–1024.

51. Coleman, T. R., and Dunphy, W. G. (1994) *Curr. Opin. Cell Biol.* 6 877–882.
52. Hunter, T., and Pines, J. (1994) *Cell* 79, 573–582.
53. Poon, R. Y. C., Toyoshima, H., and Hunter, T. (1995) *Mol. Biol. Cell* 6, 1197–1213.
54. Druetta, G. F. (1994) *Curr. Opin. Cell Biol.* 6, 842–846.
55. Matsushime, H., Quelle, D. E., *et al.* (1994) *Mol. Cell. Biol.* 14, 2066–2076.
56. Ewen, M. E. (1994) *Cancer Metasis Rev.* 13, 45–66.
57. Terada, N., Lucas, J. J., and Gelfand, E. (1991) *J. Immunol.* 147(2), 698–704.
58. Terada, N., Or, R., *et al.* (1993) *Exp. Cell Res.* 204, 260–267.
59. Chan, A. K., Litchfield, D. W., and Wright, J. A. (1992) *Biochemistry* 32, 12835–12840.

Received May 1, 1996
Revised version received August 21, 1996

[14] Assay for Activity of Mammalian Cyclin D-Dependent Kinases CDK4 and CDK6

By DAWN E. PHELPS and YUE XIONG

Introduction

During the G1 phase of the eukaryotic cell division cycle, signals transduced from the extracellular environment converge on the cell cycle machinery and result in the decision to enter the cell cycle and proliferate, or to exit from the cell cycle either temporarily or permanently. Once cells have passed the "restriction" checkpoint, the cell cycle advances largely on its own, no longer influenced by external signals. In mammalian cells, progression through the G1 phase is primarily controlled by two cyclin-dependent kinases, CDK4–cyclin D or CDK6–cyclin D and CDK2–cyclin E. The temporal activation and inactivation of CDK kinase activity during the cell cycle are multistep processes that are tightly regulated by several complex mechanisms including cyclin binding and activation, subunit phosphorylations (either activating or inhibitory), ubiquitin-mediated cyclin destruction, and inhibition by the binding of a CDK inhibitor (reviewed in Refs. 1–3).

Both CDK4 and CDK6 preferentially, if not exclusively, associate with the D-type cyclins,[4–8] which in turn bind directly to pRb and to the pRb-related proteins, p107 and p130.[5,9–13] The Rb family of proteins is phosphorylated in a cell cycle-dependent manner beginning in mid G1, a time at

[1] C. J. Sherr, *Cell* **79**, 551 (1994).
[2] C. J. Sherr and J. M. Roberts, *Genes Dev.* **9**, 1149 (1995).
[3] D. O. Morgan, *Nature* (*London*) **374**, 131 (1995).
[4] Y. Xiong, H. Zhang, and D. Beach, *Cell* **71**, 505 (1992).
[5] Y. Xiong, H. Zhang, and D. Beach, *Genes Dev.* **7**, 1572 (1993).
[6] H. Matsushime, M. E. Ewen, D. K. Strom, J. Y. Kato, S. K. Hanks, M. F. Roussel, and C. J. Sherr, *Cell* **71**, 323 (1992).
[7] M. Meyerson and E. Harlow, *Mol. Cell Biol.* **14**, 2077 (1994).
[8] S. Bates, L. Bonetta, D. MacAllan, D. Parry, A. Holder, C. Dickson, and G. Peters, *Oncogene* **9**, 71 (1994).
[9] S. F. Dowdy, P. W. Hinds, K. Louie, S. I. Reed, A. Arnold, and R. A. Weinberg, *Cell* **73**, 499 (1993).
[10] J. Kato, H. Matsushime, S. W. Hiebert, M. Ewen, and C. J. Sherr, *Genes Dev.* **7**, 331 (1993).
[11] G. Hannon, D. Demetrick, and D. Beach, *Genes Dev.* **7**, 2378 (1993).
[12] Y. Li, C. Graham, S. Lacy, A. M. V. Duncan, and P. Whyte, *Genes Dev.* **7**, 2366 (1993).
[13] M. E. Ewen, H. K. Sluss, C. J. Sherr, H. Matsushime, J. Kato, and D. M. Livingston, *Cell* **73**, 487 (1993).

METHODS IN ENZYMOLOGY, VOL. 283 0076-6879/97 $25.00

which CDK4–cyclin D and CDK6–cyclin D kinase activity can be first detected in quiescent cells that have been stimulated to reenter the cell cycle.[7,14–17] These results have strongly implicated both D-type cyclin-dependent CDK4 and CDK6 as physiological kinases of pRb, p107, and p130. Indeed, the Rb family of proteins is thus far the only known *in vitro* substrates of cyclin D-associated CDK4 and CDK6 kinase activity. CDK4 and CDK6 are unique in that they associate with and are inhibited by both classes of CDK inhibitors (reviewed in Ref. 2). The family composed of p21, $p27^{Kip1}$, and $p57^{Kip2}$ forms ternary complexes with and inhibits the activity of most, if not all, cyclin–CDK enzymes. In contrast, members of the p16 family ($p15^{INK4b}$, $p16^{INK4a}$, $p18^{INK4c}$, and $p19^{INK4d}$) bind to the catalytic subunits CDK4 and CDK6 to form a binary complex in a competing or potentially mutually exclusive manner with activating D-type cyclins (cyclin D1, D2, and D3), thereby inhibiting the kinase. The expression of cyclin D and CDK inhibitor genes is regulated by diverse extra- and intracellular cell growth regulatory signals (reviewed in Refs. 2 and 18), linking the regulation of CDK4 and CDK6 kinase activity with the control of cell growth. The assay of CDK4 and CDK6 kinase activity, therefore, is critical for studying the mechanisms that regulate CDK4 and CDK6 and early G1 progression.

Active forms of several CDKs, such as CDC2 and CDK2, can be prepared relatively easily from several sources including recombinant protein expressed in bacteria after activation by a CDK-activating kinase (CAK),[19] in insect cells using recombinant baculoviruses[20,21] or *in vivo* by immunoprecipitation,[22–24] and readily assayed *in vitro* using commercially available histone H1 as a substrate. The analysis of cyclin D-dependent CDK4 and CDK6 kinase activity, however, has technically been more difficult. This chapter describes detailed protocols for the preparation and measurement

[14] H. Matsushime, D. E. Quelle, S. A. Shurtleff, M. Shibuya, C. J. Sherr, and J. Kato, *Mol. Cell Biol.* **14**, 2066 (1994).
[15] R. L. Beijersbergen, L. Carlee, R. M. Kerkhoven, and R. Bernards, *Genes Dev.* **9**, 1340 (1995).
[16] X. Mayol, J. Garriga, and X. Grana, *Oncogene* **11**, 801 (1995).
[17] Z. Xiao, D. Ginsberg, M. Ewen, and D. M. Livingston, *Proc. Natl. Acad. Sci. U.S.A.* **93**, 4633 (1996).
[18] T. Hunter and J. Pines, *Cell* **79**, 573 (1994).
[19] L. Connell-Crowley, M. J. Solomon, N. Wei, and J. W. Harper, *Mol. Biol. Cell* **4**, 79 (1993).
[20] D. Desai, Y. Gu, and D. O. Morgan, *Mol. Biol. Cell* **3**, 571 (1992).
[21] A. Koff, A. Giordano, D. Desai, K. Yamashita, J. W. Harper, S. Elledge, T. Nishimoto, D. O. Morgan, B. R. Franza, and J. M. Roberts, *Science* **257**, 1689 (1992).
[22] S. J. Elledge, R. Richman, F. L. Hall, R. T. Williams, N. Lodgson, and J. W. Harper, *Proc. Natl. Acad. Sci. U.S.A.* **89**, 2907 (1992).
[23] J. Rosenblatt, Y. Gu, and D. O. Morgan, *Proc. Natl. Acad. Sci. U.S.A.* **89**, 2824 (1992).
[24] L.-H. Tsai, E. Harlow, and M. Meyerson, *Nature* (*London*) **353**, 174 (1991).

of active CDK4 and CDK6 complexes from three different sources: bacterial, insect, and mammalian cells. Other techniques to study the regulation of CDK4 and CDK6 such as the yeast two-hybrid system to detect interacting proteins,[24a] CDK complex assembly,[24b] and phosphorylation of the CDK subunit by CAK[24c] are described elsewhere in this volume. Protocols for metabolic labeling of cultured cells followed by immunoprecipitation (IP) of the cell lysate to globally visualize the subunit composition of the CDK complexes and IP-Western blot analysis to quantitate the association between two proteins have been previously described in detail.[25]

Immunoprecipitation of Active CDK4 and CDK6 Kinases from Mammalian Cells

The assay of kinase activity by immunoprecipitation (IP-kinase assay) provides not only a specific and sensitive, but sometimes the only, measurement for studying the regulation of a particular growth condition (e.g., differentiation, senescence, negative and positive cytokines) on the activity of a CDK *in vivo*. The technical difficulties of detecting cyclin D-associated CDK4 and CDK6 kinase activity from mammalian cells by the IP-kinase assay have been largely overcome in the last few years.[7,14] A critical factor in quantitatively detecting the cyclin D–CDK4/6 kinase activity by IP appears to be related to the quality of the antibodies. Not all anticyclin D, anti-CDK4, or anti-CDK6 antibodies are capable of immunoprecipitating cyclin D, CDK4, or CDK6 kinase activity. In particular, crude sera of nearly all rabbit polyclonal antibodies for D cyclins, CDK4 or CDK6, were found to be incapable of immunoprecipitating kinase activity, even though they are able to coimmunoprecipitate cyclin or catalytic partners. A number of affinity-purified polyclonal antibodies raised against synthetic C-terminal peptides of rodent or human D cyclins, CDK4 and CDK6 and two cyclin D monoclonal antibodies, have been generated that are capable of immunoprecipitating kinase activity from a variety of human and mouse cell lines.[7,14] All these antibodies are commercially available [Pharmingen (San Diego, CA) #15156E (α-CDK4) and #13446E (α-CDK6); Santa Cruz Biotechnology (Santa Cruz, CA) #sc-260 (α-CDK4) and #sc-177 (α-CDK6), #sc-450 (α-Cyclin D1), #sc-181 (α-Cyclin D2), #sc-452 (α-Cyclin D2), #sc-182 (α-Cyclin D3), #sc-453 (α-Cyclin D3); Upstate Biotechnology Incorporated (Lake Placid, NY) #06-139 (α-CDK4)]. While there was concern about the

[24a] C. Bai and S. J. Elledge, *Methods Enzymol.* **283**, [11], (1997) (this volume).
[24b] L. Stepanova, X. Leng, and J. W. Harper, *Methods Enzymol.* **283**, [16], (1997) (this volume).
[24c] R. P. Fisher, *Methods Enzymol.* **283**, [19], (1997) (this volume).
[25] C. W. Jenkins and Y. Xiong, *In* "Cell Cycle: Material and Methods" (M. Pagano, ed.), pp. 250–263. Springer-Verlag, New York, 1995.

nature and concentration of detergent used in the IP/lysis buffer,[14] several reports described detection of CDK6 kinase activity by IP using a buffer that contains Nonidet P-40 (NP-40) as opposed to Tween 20.[7,26] We have included the recipes for both the NP-40 and Tween 20 containing IP/lysis buffer. The following protocol is based on our IP/kinase experience using multiple cell lines and IP/lysis buffer that contains NP-40.

Note: Keep the samples on icc and in the cold as much as possible during this protocol to help preserve the enzymatic activity.

Lysis of Mammalian Cells

1a. *For monolayer cells:* wash twice with cold 1× phosphate-buffered saline (PBS). Add 1 ml of cold IP/lysis buffer per 90 mm or 2 ml per 150-mm plate. Incubate on ice for 20 min with occasional shaking. Collect cell lysate in a 1.5-ml Eppendorf tube (distribute cell lysate into several Eppendorf tubes if the volume is greater than 1.3 ml). Continue cell lysis at 4° for 30 min with rotation.

NP-40 IP/lysis buffer (store at 4°):

452.5 ml Distilled H_2O	to final	500 ml
25 ml 1 *M* Tris, pH 7.5	to final	50 m*M*
15 ml 5 *M* NaCl	to final	150 m*M*
2.5 ml NP-40	to final	0.5%
1.05 g NaF	to final	50 m*M*

Add to each 1 ml NP-40 IP/lysis buffer immediately before use:

10 μl 100 m*M* Na_3VO_4	to final	1 m*M*
10 μl 100 m*M* Dithiothreitol (DTT)	to final	1 m*M*
10 μl 100 m*M* Phenylmethylsulfonyl fluoride (PMSF)	to final	1 m*M*
10 μl 100× Protease inhibitors	to final	1×

Tween 20 IP/lysis buffer (store at 4°):

403.5 ml Distilled H_2O	to final	500 ml
25 ml 1 *M* HEPES, pH 7.5	to final	50 m*M*
15 ml 5 *M* NaCl	to final	150 m*M*
1 ml 0.5 *M* EDTA	to final	1 m*M*
5 ml 0.25 *M* EGTA	to final	2.5 m*M*
50 ml Glycerol	to final	10%
0.5 ml Tween 20	to final	0.1%
21 mg NaF	to final	1 m*M*

Add to each 1 ml Tween 20 IP/lysis buffer immediately before use:

1 μl 100 m*M* Na_3VO_4	to final	0.1 m*M*
10 μl 100 m*M* DTT	to final	1 m*M*

[26] J. Jakus and W. A. Yeudall, *Oncogene* **12**, 2369 (1996).

1 μl 100 m*M* PMSF	to final	0.1 m*M*
10 μl 100 × Protease inhibitors	to final	1×

1b. *For suspension cells:* Count the cells on a hemacytometer. Pellet cells at 2000 rpm for 3 min. Aspirate the media and wash once with cold 1× PBS (optional). Add 1 (to 3) ml cold IP/lysis buffer per 10^7 cells, pipette to resuspend, and transfer cell lysate to a 1.5-ml Eppendorf tube (distribute cell lysate into several Eppendorf tubes if the volume is greater than 1.3 ml). Continue cell lysis at 4° for 30 min with rotation.

Save some of the IP/lysis buffer for use later as a blank for optical density measurements.

2. Clarify lysate in an Eppendorf centrifuge at maximum speed for 5–10 min at 4° to remove insoluble debris. Transfer the supernatant to a new tube (pool together lysates that were separated in step 1). Determine the optical density at 595 nm by use of the Bradford assay (Bio-Rad, Richmond, CA, Protein Assay #500-0006), in duplicate, of the lysates for future reference and use in equalizing total protein concentrations between different cell lysates. Dilute Bio-Rad protein dye (1:5, v/v) in distilled H_2O. Mix 1 ml of diluted Bio-Rad protein dye with 5 μl of clarified cell lysate. Determine optical density at 595 nm using 5 μl IP/lysis buffer as a blank. The lysate is now ready for immunoprecipitation.

Immunoprecipitation

3. Aliquot the lysate to Eppendorf tubes containing antibody (affinity purified) and rotate 2 hr at 4°. As a control, set up a reaction in which (a) the antibody has been preincubated with its corresponding antigen peptide (20 min at room temperature); (b) immunoprecipitate with preimmune serum or no antibody; and (c) immunoprecipitate with antibody but do not add substrate to the kinase reaction.

The amount of lysate needed to detect CDK4 and CDK6 kinase activity is cell line and cell cycle dependent and therefore must be empirically determined. The amount of antibody needed to immunoprecipitate CDK4 and CDK6 kinase activity is antibody dependent and therefore the reader should consult the manufacturer's recommended protocol.

4. Add 10 μl prewashed protein A beads (Gibco-BRL, Gaithersburg, MD; Pierce, Rockford, IL; or equivalent) to the IP tubes. Rotate at 4° for 1 hr.

5. Centrifuge the samples in a microcentrifuge at 3000 rpm for 5 min at 4°. Wash twice with cold IP/lysis buffer (minus leupeptin, aprotinin, benzamidine, and trypsin inhibitor). For each wash: aspirate the supernatant with a flat tip gel-loading tip, being careful not to aspirate the beads, add 1 ml wash solution for each sample down the side of the tube, gently mix by inversion, and repellet protein A beads.

6. Wash twice with cold kinase assay buffer: 1 ml for each wash and spin at low speed in the cold. (*Note:* The pellet will become clear and even harder to see. Also, the kinase assay buffer does not separate as easily from the pellet as the IP/lysis buffer does so extra care must be taken to not aspirate the beads.)

Kinase assay buffer (store at 4°):

94 ml Distilled H_2O	to final	100 ml
5 ml 1 *M* HEPES, pH 7.0	to final	50 m*M*
1 ml 1 *M* $MgCl_2$	to final	10 m*M*
0.5 ml 1 *M* $MnCl_2$	to final	5 m*M*

Add to each 1 ml kinase assay buffer immediately before use:

1 μl 1 *M* DTT	to final	1 m*M*
0.5 μl 10 m*M* ATP	to final	5 μ*M*

7. Aspirate off the final wash, resuspend the beads in 25 μl kinase assay buffer, and proceed to the kinase assay (described in CDK4 and CDK6 Kinase Assay).

Preparation of Active CDK4 and CDK6 Kinases via Recombinant Baculovirus Expression in Insect Cells

The expression of recombinant cyclin and CDK proteins in baculovirus-infected insect cells, a eukaryotic expression system, offers several advantages over bacterial expression systems. First, the folding, disulfide bond formation, and posttranslational modifications of the recombinant protein occur properly in the baculovirus system. Second, this system, which has the capability to express two or more genes simultaneously within single infected insect cells, allows active cyclin/CDK complexes to be assembled. It has been demonstrated that lysates of Sf9 (*Spodoptera frugiperda* fall armyworm ovary) cells containing recombinant CDK4/6 or cyclin D subunits alone do not exhibit detectable protein kinase activities and that mixing of Sf9 lysates in which the regulatory and catalytic subunits were expressed individually leads to only 1–5% of the expected kinase activity, as compared to when the CDK and cyclin are coexpressed.[27] Third, the insect cell lysate can be used directly for kinase assays or the cyclin–CDK complexes can be purified by immunoprecipitation using specific anti-cyclin D or anti-CDK4 or CDK6 antibodies (see Immunoprecipitation). For the culturing of insect cell lines and the production, titer, and maintenance of recombinant baculoviruses, the reader is referred to the manufacturer's protocol.

[27] J. Kato, M. Matsuoka, D. K. Strom, and C. J. Sherr, *Mol. Cell Biol.* **14**, 2713 (1994).

1. Plate 2×10^6 Sf9 cells in one well of a six-well tissue culture dish. Incubate at 27° for 30 min to allow cells to attach to dish. Infect cells at a multiplicity of infection between 5 and 10 for optimum protein production. Set up a mock-, single- (CDK or cyclin alone), and coinfection (both CDK and cyclin) expression experiments. Incubate the cells for 40 hr at 27°.

If the titer of the virus is unknown, a small scale infection can be performed to determine the amount of protein expressed and the optimal ratio of CDK virus to cyclin virus to obtain the highest amount of fully active kinase. For example, mix 100 μl of cyclin virus with 50, 100, and 200 μl CDK virus and 200 μl cyclin virus with 100, 200, and 400 μl CDK virus. Infect 2.0×10^6 Sf9 cells seeded in one well of a six-well dish with the viruses and incubate at 27° for 40 hr. Proceed to step 2 and 3 of this section. Separate 10 μl of the clarified insect cell lysate by SDS–PAGE minigel. Stain the gel with Coomassie Brilliant Blue to estimate the concentration by comparison to defined quantities of marker protein (Pharmacia, Piscataway, NJ). Perform an *in vitro* kinase assay reaction to determine the optimal ratio of CDK virus to cyclin virus needed to obtain the highest amount of active kinase.

2. Remove cells from culture dish by gentle pipetting or by scraping in the medium in which the cells have been cultured (do not aspirate the culture medium). Pellet cells at 2000 rpm for 3 min in a table-top centrifuge. Aspirate the medium and resuspend the cells in 200 μl cold hypotonic lysate buffer. Incubate on ice for 20 min. Add NaCl to 150 m*M* (6 μl of a 5 *M* NaCl stock) and transfer lysate to an Eppendorf tube. Clarify cell lysate by microcentrifugation at maximum speed for 10 min at 4°. The clarified lysate may be stored at −80° in small aliquots for future use.

Hypotonic lysis buffer (store at 4°):

445 ml Distilled H_2O	to final	500 ml
50 ml 0.5 *M* HEPES, pH 7.5	to final	50 m*M*
5 ml 1 *M* $MgCl_2$	to final	10 m*M*
0.21 g NaF	to final	10 m*M*

Add to each 1 ml immediately before use:

1 μl 100 m*M* Na_3VO_4	to final	0.1 m*M*
10 μl 100 m*M* DTT	to final	1 m*M*
1 μl 100 m*M* PMSF	to final	0.1 m*M*
10 μl 100 × Protease inhibitors	to final	1×

3. For kinase assays, mix 5 μl of clarified lysate with 20 μl kinase assay buffer containing DTT to 1 m*M* and ATP to 5 μ*M*. Proceed to the kinase assay.

Preparation of Active CDK4 and CDK6 Kinases from Bacterially Expressed Fusion Proteins

The procedure for the expression and purification of glutathione *S*-transferase (GST) fusion proteins is based on published procedures[28] and have been modified based on our experience in expressing GST–CDK4/6 and GST–cyclin D proteins. The assembly of active CDK4/CDK6–cyclin D kinases using bacterially expressed and purified proteins has been found to be inefficient and requires additional incubation with mammalian cell lysate, presumably because of the requirement of an activating phosphorylation by CAK that has been found to be necessary for the full activation of CDK2 and CDK4.[19,27] Cell lysates derived from many cells are capable of activating CDK4/6–cyclin D enzymes, including proliferating NIH 3T3[29] and Jurkat cells.[27]

Expression and Purification of GST Fusion Protein

1. Transform *Escherichia coli* BL21 with GST-fusion protein expression plasmid. Although other *E. coli* strains (e.g., HB101, TG1) allow expression from pGEX vectors, BL21 and its derivative strains are preferred because of a deficiency in two protease genes (*lon* and *ompT*). As a control, transform the BL21 cells with the parental pGEX vector.

2. Inoculate a 10-ml overnight culture in 2× YT or LB containing ampicillin (100 μg/ml final concentration). Dilute the overnight culture 1:100 into 1 liter of 2× YT or LB. Grow at 37° until the OD_{600} is 0.6–1.0 (approximately 2 hr). Add 0.5 ml of 400 m*M* IPTG to a final concentration of 0.2 m*M* and continue to grow for another 3 hr. Growing the bacterial culture at a lower temperature (30, 25, or even 18°) may help to stabilize some proteins or to increase the solubility of some proteins. GST–CDK4, GST–CDK6, GST–D1, D2, and D3 fusion proteins are partially soluble.

3. Harvest bacterial culture by centrifugation for 5 min at 3000 rpm in a table-top centrifuge at 4°.

4. Resuspend bacterial pellet in 10 ml (1/5 original volume) cold PBS-T buffer. Incubate on ice for 20 min with slow shaking.

PBS-T buffer (store at 4°):

380 ml Distilled H_2O	to final	500 ml
100 ml 0.1 *M* sodium phosphate buffer, pH 6.8	to final	20 m*M*
15 ml 5 *M* NaCl	to final	150 m*M*
5 ml Triton X-100	to final	1%

[28] K. L. Guan and J. E. Dixon, *Anal. Biochem.* **192**, 262 (1991).
[29] K. L. Guan, C. W. Jenkins, Y. Li, C. L. O'Keefe, S. Noh, X. Wu, M. Zariwala, A. G. Matera, and Y. Xiong, *Mol. Cell Biol.* **7**, 57 (1996).

Add to 10 ml PBS-T buffer immediately before use:

100 μl 100 m*M* PMSF	to final	1 m*M*
100 μl 100 m*M* DTT	to final	1 m*M*
100 μl 50 mg/ml lysozyme	to final	500 μg/ml

5. Lyse cells by passing through a French press, twice, at 1200 lb/in^2. Alternatively, sonicate the cells three times at full microtip power for 20 sec with 1 min intervals between each sonication. The lysis of bacterial cells by sonication is less efficient than using the French press. To check the level of expression, transfer 100 μl of the sonicated lysate to a 1.5-ml microfuge tube and add 100 μl 2× SDS–DTT dye. Boil for 4 minutes. Store at 4° until loading of SDS–PAGE minigel.

2× SDS–DTT gel loading buffer (store at room temperature):

30 ml 0.5 *M* Tris-Cl, pH 6.8	to final	100 m*M*
60 ml 10% SDS	to final	4%
30 ml Glycerol	to final	20%
0.3 g bromphenol blue	to final	0.2%

Before use add 200 μl 1M DTT to 800 μl stock solution, store at −20°.

6. Clarify the crude lysate by centrifugation at 4° for 10 min at 10,000 *g*. Transfer the supernatant to a new tube. Resuspend the pellet in 10 ml bacterial cell lysate buffer by vortexing. Transfer 100 μl of the supernatant and pellet suspension to 1.5-ml microfuge tubes and add 100 μl 2× SDS–DTT dye. Boil for 4 minutes and store at 4° until loading of SDS–PAGE minigel.

7. Mix the clarified cell lysate with 4 ml glutathione-Sepharose 4B resin (Pharmacia; or equivalent) in PBS-T. Incubate at 4° for 30 min with rotation. Pack the glutathione-Sepharose 4B resin into a column. Wash the column with 100 ml PBS-T. Elute the GST-fusion protein with 10 m*M* glutathione (prepared fresh in 50 m*M* Tris, pH 8.0). Collect 10 1-ml fractions. Add 100 μl of 10× PBS to fractions. Separate 10 μl of the purified protein fractions by SDS–PAGE minigel. Stain the gel with Coomassie Brilliant Blue to estimate the purity and concentration by comparison to defined quantities of marker protein (Pharmacia).

Activation of CDK4–Cyclin D Kinases

8. Lyse exponentially growing mammalian cells in 50 μl cold mammalian cell lysis buffer per 10^6 cells.

Mammalian cell lysis buffer (store at 4°):

452.5 ml Distilled H_2O	to final	500 ml
40 ml 1 *M* HEPES, pH 7.4	to final	80 m*M*
7.5 ml 1 *M* $MgCl_2$	to final	15 m*M*

Add to each 1 ml immediately before use:

10 μl 100 m*M* Na_3VO_4	to final	1 m*M*
10 μl 100 m*M* DTT	to final	1 m*M*
10 μl 100 m*M* PMSF	to final	1 m*M*
10 μl 100× Protease inhibitors	to final	1×

9. Sonicate the cells three times at full microtip power for 20 sec with 1 min intervals between each sonication.

10. Centrifuge the lysate at maximum speed for 10 min at 4° in a microcentrifuge to remove insoluble debris. Transfer the supernatant to a new tube.

11. Mix 50 μl mammalian cell lysate, 2 μg purified GST–cyclin D protein, and 2 μg purified GST–CDK4 or CDK6 protein. Add ATP to 1 m*M*. Incubate for 1 hr at room temperature.

12. Centrifuge at maximum speed for 5 min at 4° and transfer the supernatant to a new tube.

13. Recover the activated GST–cyclin D/GST–CDK4 or CDK6 complex by adding 20 μl glutathione-Sepharose 4B resin. Incubate for 30 min at 4°.

14. Pellet the resin in a microcentrifuge at 3000 rpm for 3 min at 4°.

15. Wash the resin six times with mammalian cell lysis buffer—for each wash: aspirate the supernatant with a flat gel-loading tip being careful not to aspirate the beads, add 1 ml wash solution down the side of the tube, gently mix by inversion, and repellet beads in a microcentrifuge at 3000 rpm for 3 min at 4°.

16. Aspirate off the final wash and elute the activated cyclin–CDK complex by resuspending the resin in 50 μl kinase assay buffer containing 10 m*M* glutathione.

Kinase assay buffer (+ glutathione):

94 ml Distilled H_2O	to final	100 ml
5 ml 1 *M* HEPES, pH 7.0	to final	50 m*M*
1 ml 1 *M* $MgCl_2$	to final	10 m*M*
0.5 ml 1 *M* $MnCl_2$	to final	5 m*M*
0.3 g glutathione	to final	10 m*M*

Add to each 1 ml immediately before use:

1 μl 1 *M* DTT	to final	1 m*M*
0.5 μl 10 m*M* ATP	to final	5 μ*M*

17. Use 5 μl of the activated cyclin–CDK complex for kinase assays. Bring volume up to 25 μl with kinase assay buffer (which contains DTT to 1 m*M* and ATP to 5 μ*M* but which does not contain glutathione) and proceed to the kinase assay (described in the next section).

CDK4 and CDK6 Kinase Assay

1. Start the reaction by adding to each tube 5 μl of mixture:
   2 μl (approximately 0.5–2 μg) GST-pRb/p107/p130 fusion protein substrate
   0.5 μl [γ-^{32}P]ATP (10 μCi/μl; 3000 Ci/mmol)
   2.5 μl kinase assay buffer

Incubate for 30 min at 30° in a water bath designed for radioactive samples.

There are three substrates available to measure the *in vitro* kinase activity of the cyclin D-associated kinases CDK4 and CDK6: pRb, p107, and p130. The most commonly used substrate is a fusion protein between GST and the C-terminal 137 amino acids (792–928) of human pRb.[7] GST fusion proteins containing the pocket region and C terminus (amino acids 252–936) of human p107 or the spacer region of p130 can also serve as CDK4 and CDK6 substrates *in vitro*[6,13,16] (D. Phelps and Y. Xiong, unpublished data, 1997). As a negative control, the GST protein can be used as a substrate. The preparation and purification of GST-pRB/p107/p130 substrates was outlined previously in this chapter.

2. Stop the reactions by adding 20 μl 2× SDS–DTT sample buffer to each tube. Boil the samples for 3 min.

3. Load 20 μl of each sample onto a denaturing polyacrylamide gel (10–12.5%) being careful to avoid lane-to-lane leakage. The remaining sample may be stored at −20° should they be needed.

4. Run the gel until the dye front has reached the bottom. Cut the upper left corner of the gel (for ease of orientation) and stain it in Coomassie dye (50% (v/v) methanol, 7% (v/v) acetic acid, 0.2% (w/v) Coomassie Brilliant Blue) for approximately 10–15 min. Destain for 30 min to 1 hr in destain solution (37.5% (v/v) methanol, 7% (v/v) acetic acid, 0.75% (v/v) glycerol). Observe the relative levels of both the IgG heavy chain for each sample and the substrate. If the loading was unequal, the remaining stored samples can be used to repeat the experiment.

5. Dry the gel for 1 hr at 80°. After drying, cover the gel with Saran Wrap and expose the gel either on a phosphorimage plate (about 2 to 4 hr) or on X-ray film (overnight to several days) with an intensifying screen.

Stock Solutions

400 m*M* IPTG (isopropyl-β-thiogalactopyranoside, Promega, Madison, WI): 0.95 g in 10 ml distilled H_2O, dispense into 1-ml aliquots and store at −20°.

100 m*M* PMSF (phenylmethylsulfonyl fluoride, Sigma, St. Louis, MO): 174 mg in 10 ml 100% ethanol, store at 4°.

1 *M* DTT (1,4-dithiothreitol, Sigma): 1.54 g in 10 ml distilled H_2O, dispense into aliquots and store at −20°. To prepare 100 m*M* DTT dilute 1 ml 1 *M* DTT in 9 ml distilled H_2O.

50 mg/ml lysozyme (Sigma): 50 mg in 1 ml distilled H_2O, dispense into 100-μl aliquots and store at −20°.

100 m*M* Na_3VO_4 (sodium orthovanadate, Sigma): 1.83 g Na_3VO_4 in 100 ml distilled H_2O, store at 4°.

100× Protease inhibitors: Prepare 400× stocks of leupeptin (Sigma, 10 mg/ml), aprotinin (Sigma, 10 mg/ml), benzamidine (Sigma, 60 mg/ml), and trypsin inhibitor (Boehringer Mannheim, Indianapolis, IN, 4 mg/ml) in distilled H_2O. To prepare 100× stocks, mix equal volumes of 400× stocks and dispense into small aliquots. Store 400× and 100× stocks at −80 or −20° for 6 months.

10 m*M* ATP (adenosine 5′-triphosphate, Boehringer Mannheim): 60.5 mg in 10 ml distilled H_2O, dispense into small aliquots and store at −20°.

10 m*M* glutathione (Sigma): 30.7 mg in 10 ml 50 m*M* Tris-HCl, pH 8.0.

Acknowledgments

We thank Drs. Kunliang Guan and Wade Harper for providing protocols for the preparation of active kinases from bacterially expressed fusion proteins and via recombinant baculovirus expression in insect cells, respectively. We thank Mike Nichols for help with the expression of recombinant proteins in insect cells using baculoviruses and the subsequent kinase assays. D. E. P. is a recipient of the National Research Service Award from the NIH (NIGMS). Y. X. is a Pew Scholar in Biomedical Science and recipient of the American Cancer Society Junior Faculty award. This study was supported by a National Institute of Health grant CA 65572 to Y. X.

[15] Functional Analysis of E2F Transcription Factor

By JOSEPH R. NEVINS, JAMES DEGREGORI, LASZLO JAKOI, and GUSTAVO LEONE

Introduction

Originally identified as a transcriptional activity important for the regulation of the adenovirus E2 gene,[1] the E2F (E2 factor) transcription factor has now been shown to play a critical role in the control of transcription

[1] I. Kovesdi, R. Reichel, and J. R. Nevins, *Cell* 45, 219 (1986).

METHODS IN ENZYMOLOGY, VOL. 283
0076-6879/97 $25.00

Experimental Cell Research 253, 372–384 (1999)
Article ID excr.1999.4664, available online at http://www.idealibrary.com on IDEAL®

The Expression and Activity of D-Type Cyclins in F9 Embryonal Carcinoma Cells: Modulation of Growth by RXR-Selective Retinoids

Yong Li,*,[1] Michele A. Glozak,*,[1] Susan M. Smith,* and Melissa B. Rogers*,†,‡,[2]

Department of Biology, †Department of Pharmacology, and ‡Institute for Biomolecular Science, University of South Florida, 4202 E. Fowler Avenue, Tampa, Florida 33620

The growth rate of malignant F9 embryonal carcinoma cells slows considerably following all-*trans*-retinoic acid-induced differentiation into benign parietal endoderm. To determine the mechanism of this process, we examined the expression of cyclins D1, D2, and D3 and the activity of their associated kinases. Cyclin D1 and D3 mRNA levels decreased during complete differentiation induced by all-*trans*-retinoic acid and dibutyryl cAMP, while the levels of cyclin D2 and the cyclin-dependent kinase (Cdk) inhibitor p27 mRNAs increased. Ultimately, terminally differentiated cells possessed 50% of the Cdk4-associated kinase activity observed in undifferentiated cells. Since numerous genes are differentially regulated during parietal endoderm differentiation, it is difficult to determine whether retinoic acid affects cell cycle gene expression directly or if these changes are caused by differentiation. We found that the retinoid X receptor (RXR)-selective agonists LG100153 and LG100268 significantly inhibited F9 cell growth without causing overt terminal differentiation as assessed by anchorage-independent growth and differentiation-associated gene expression. As seen in cells induced to differentiate by the RAR agonist all-*trans*-retinoic acid, RXR activation led to an increase in the number of cells in G1 phase. RXR agonists also sharply induced the levels of the Cdk regulatory subunits, cyclin D2 and D3. However, Cdk4-dependent kinase activity was reduced by RXR-selective retinoid treatment. These observations suggest that some retinoids can directly inhibit proliferation and regulate Cdk4-dependent kinase activity without inducing terminal differentiation. © 1999 Academic Press

Key Words: retinoids; RXR; F9 embryonal carcinoma; differentiation; cyclins.

INTRODUCTION

Vitamin A and its chemical relatives, the retinoids, are important regulators of cell proliferation and differentiation in a diverse array of tissues. Cell types whose *in vitro* differentiation is influenced by retinoids include keratinocytes, chondrocytes, adipocytes, hematopoietic cells, and numerous neoplastic cell lines [1, 2]. Retinoids slow or arrest the growth of many transformed cell lines by inducing differentiation. This observation contributed to the development of a novel chemotherapeutic approach known as differentiation therapy. Rather than selectively killing tumor cells, tumor cells are induced to differentiate. These nonproliferating cells often lose the markers characteristic of the malignant state and gain markers of terminal differentiation.

One promising differentiation agent is the vitamin A derivative retinoic acid (RA). RA reverses the malignancy of several tumor lines *in vitro* and represses acute promyelocytic leukemia and aerodigestive tract tumors [3]. *In vitro,* and presumably *in vivo,* RA exerts its effect by activating a cascade of differential gene expression ending in terminal differentiation and the loss of malignancy.

RA-regulated gene expression is mediated by nuclear retinoid receptors which act as ligand-dependent transcription factors [4]. These receptors are encoded by six different genes, the *RARs* α, β, and γ and the *RXRs* α, β, and γ. Numerous isoforms arising from differential promoter usage and alternate splicing have been identified and the expression of these isoforms is developmentally regulated [5]. Furthermore, the receptors can act as homodimers and heterodimers, each with unique characteristics [see 6, 7]. While the RARs bind to and are activated by all-*trans*-RA and 9-*cis*-RA, the RXRs are activated only by 9-*cis*-RA. The RXRs form heterodimers with the RARs and several other receptors, including the thyroid hormone, vitamin D, oxysterol, peroxisome proliferator-activated receptors, and Nurr77/NGFI-B [8–10]. This plethora of receptors and gene pathways may begin to explain the multiple effects retinoids have on differentiation.

[1] These two authors contributed equally to this work.

[2] To whom correspondence and reprint requests should be addressed at Department of Biology, BSF119, University of South Florida, 4202 E. Fowler Avenue, Tampa, FL 33620. Fax: (813) 974-1614. E-mail: rogers@chuma.cas.usf.edu.

0014-4827/99 $30.00

Unfortunately, toxic side effects limit the clinical use of retinoids. For example, retinoids are extremely teratogenic. Accutane (13-*cis*-RA), used for treatment of chronic cystic acne, is one of the most potent human teratogens. Babies who survive to birth exhibit malformations of the cardiovascular system, face, and central nervous system and absence of the thymus [11]. The pleiotropic effects of natural retinoids indicate that multiple mechanisms contribute to these detrimental outcomes. To ameliorate the toxicity and teratogenicity of retinoids, receptor-selective agonists have been synthesized which possess a narrower spectrum of activity [12]. These retinoids have clinical and research value, as they affect the expression of a subset of the target genes (e.g., *Bmp-2* and *Bmp-4*) regulated during RA-induced differentiation [13]. Understanding the effects of these retinoids will aid in designing more effective and safe therapeutic agents.

F9 embryonal carcinoma cells are a classic model system for studying the mechanisms underlying RA-induced terminal differentiation. F9 cells can be induced by RA and drugs that increase cellular cAMP levels to differentiate into a pure population of parietal endoderm-like cells [14]. This differentiation is characterized by a change in morphology to that typical of parietal endoderm and the induction of numerous parietal endoderm genes. This synchronous and reproducible differentiation is ideal for biochemical analyses of retinoid-induced responses. As occurs during the terminal differentiation of many cell types, F9 cells cease growing rapidly and lose their malignant phenotype, including their ability to grow in the absence of substrate. The decreased growth rate could be purely the result of terminal differentiation or retinoids could directly inhibit the cell cycle system controlling growth rate. Most likely, a combination of these mechanisms plays a role.

To understand the mechanism that lengthens the F9 G1 phase during terminal differentiation, we have analyzed the expression and activity of several G1 phase regulatory proteins. Cyclins D1, D2, and D3 are generally considered to be positive regulatory subunits of the cyclin-dependent kinase 4 (Cdk4) and Cdk6 kinases. As such, increased cyclin D levels promote G1 progression in several cell types [15]. The G1 Cdks are also regulated by the Cdk inhibitors $p21^{waf1/cip1/Sdi1/CDKN1}$, $p27^{kip}$, $p16^{ink4a/MTS1/CDKN2}$, and $p15^{ink4B/MTS2}$. For a general review, see Ref. [16]. We show here that cyclins D1 and D3 levels are reduced and cyclin D2 and $p27^{kip}$ levels are increased in terminally differentiated parietal endoderm cells relative to undifferentiated F9 stem cells. It was not clear, however, whether these changes required terminal differentiation or whether all-*trans*-RA directly influenced the expression of these genes.

It has been reported that untreated F9 cells lacking a functional RXR gene grow more rapidly than wild-type cells [17]. We now report the complementary observation. Specifically, RXR-activating retinoids decrease the rate of F9 cell growth. We also show that RXR activation alters the expression of distinct cell cycle proteins in the absence of RAR-activating retinoids. This occurs without complete terminal parietal endoderm differentiation, suggesting that retinoids can directly influence the cell cycle apparatus.

MATERIALS AND METHODS

Cell proliferation and differentiation. All-*trans*-RA (RAR agonist), dibutyryl cAMP, theophylline, calf serum, L-glutamine, and β-mercaptoethanol were obtained from Sigma Chemical Co. (St. Louis, MO). 9-*cis*-RA (RAR and RXR panagonist) and TTNPB (RAR agonist) were obtained from Hoffman–LaRoche (Nutley, NJ). LG100153 (LG153, RXR agonist) [18] and LG100268 (LG268, RXR agonist) [19] were obtained from Ligand Pharmaceuticals (San Diego, CA). Stocks (1 mM) of retinoid solutions were prepared in ethanol and diluted to the appropriate concentration into media before use. Monolayer F9 or RA-5-1 embryonal carcinoma cells [20] were maintained in DMEM (Gibco BRL, Gaithersburg, MD) supplemented with 10% heat-inactivated calf serum, 2 mM L-glutamine, and 0.1 mM β-mercaptoethanol on gelatinized tissue culture plates in 10% CO_2 at 37°C. For differentiation, monolayers were dispersed into single cells with trypsin–EDTA (Gibco-BRL) and replated at the desired density. After cell attachment, the medium was replaced with medium containing the desired concentration of retinoid plus 250 μM dbcAMP and 500 μM theophylline (CT). On the third day of long experiments, the medium was replaced with fresh medium containing drugs.

Cell proliferation assays. F9 cells (4.5×10^3) were plated in 0.15 ml DMEM in 96-well flat-bottomed culture plates. After cells attached, the medium was replaced with drug-containing medium. For the MTS assay, separate stock solutions of MTS (3-(4,5-dimethylthiazol-2-yl)-5-(3-carboxymethoxyphenyl)-2-(4-sulfophenyl) 2*H*-tetrazolium, inert salt) and phenazine methosulfate (PMS) were prepared and added to the cultures to a final concentration of 100 mM MTS and 5 mM PMS. The amount of formazan product was assayed by measuring the absorbance at 570 nm [21]. For toluidine blue staining, cells grown similarly in 96-well plates were fixed with 0.1 ml of 4% paraformaldehyde for 30 min and then 0.05 ml 0.5% toluidine blue was added and incubated 1 h. The cells were solubilized with 0.1 ml 2% SDS per well and the absorbance was read at 650 nm [22]. For cell counting assays, 3×10^4 cells were plated in 1.0 ml medium in 24-well plates. Drugs were added as described above. After 3 or 4 days, cells were trypsinized and counted on a hemacytometer.

Flow cytometry. Cells were dispersed with trypsin–EDTA and then fixed with 70% ethanol at −20°C for at least 30 min. The fixed cells were washed with PBS and then resuspended in PBS containing 100 μg/ml RNaseA and 40 μg/ml propidium iodide. Cells were incubated at 37°C for 30 min. Samples were analyzed for DNA content on a Becton Dickinson FACSCAN using MODFIT software.

Anchorage-independent growth. The anchorage independent growth assay was adapted from Chen *et al.* [23]. The bottom agar layer was prepared by mixing equal volumes of sterilized 1.4% agar (Difco, Sparks, MD) and 2× DMEM supplemented with 20% heat-inactivated calf serum, 4 mM L-glutamine, and 0.2 mM β-mercaptoethanol. A quantity of 3.0 ml was pipetted into 60-mm non-tissue culture petri dishes and incubated at 37°C in 10% CO_2 overnight. A cell slurry was prepared by mixing one part 1.4% agar at 45°C, two parts cell suspension (1.3×10^3 cells/ml suspended in 1× DMEM), and one part 2× DMEM. The cell slurry also contained 250 μM dbcAMP, 500 μM theophylline, and 0.1 μM retinoid or ethanol vehi-

TABLE 1

Percentage of F9 Cells in G1, S, and G2/M Phases Following All-*trans*-RACT and LG153 CT Treatment

	G1			S			G2/M		
Time	CT	RACT	LG153 CT	CT	RACT	LG153 CT	CT	RACT	LG153 CT
Day 1	21.2 ± 0.6	24.1 ± 0.2	20.9 ± 0.2	54.7 ± 0.8	49.9 ± 0.3	55.0 ± 2.0	24.1 ± 1.4	26.0 ± 0.1	24.1 ± 1.8
Day 2	21.4 ± 1.2	45.1 ± 0.6	24.9 ± 0.1	54.0 ± 1.2	42.3 ± 0.7	56.4 ± 0.4	24.6 ± 0.01	12.6 ± 0.2	18.8 ± 0.6
Day 3	26.6 ± 1.0	47.5 ± 0.5	38.9 ± 1.0	61.2 ± 6.4	39.3 ± 1.5	48.0 ± 0.2	12.2 ± 5.4	13.2 ± 0.9	13.1 ± 1.1
Day 4	27.8 ± 1.1	44.8 ± 0.1	43.4 ± 0.04	59.8 ± 1.9	38.8 ± 1.2	44.1 ± 0.6	12.4 ± 0.8	16.4 ± 1.3	12.5 ± 0.5

cle. A quantity of 4.5 ml prewarmed cell slurry mixture containing 3.0×10^3 cells was poured on the preincubated bottom agar layer. Following a 6-h incubation (37°C, 10% CO_2), 3.0 ml 1× DMEM supplemented as above was pipetted onto the second layer. Colonies were visible within 11 days.

RNA isolation and blotting. RNA isolation and northern blotting procedures are described in Li *et al.* [24].

Preparation of protein extracts and Western blotting. F9 cell monolayers were lysed on ice for 30 min in 50 mM Tris–HCl (pH 8), 120 mM NaCl, and 0.5% Triton X-100, containing a cocktail of protease and phosphatase inhibitors. Lysates were passaged though a 26-gauge needle several times and then spun in a microcentrifuge for 15 min at 4°C to pellet cellular debris. The supernatants were frozen in liquid N_2 and stored at −80°C until used. Protein concentration was determined by Bradford assay (Bio-Rad, Hercules, CA).

For Western blotting, 20–25 μg protein was loaded on SDS–PAGE minigels [25]. Following electroblotting, filters were blocked in 5% nonfat dry milk and then exposed to antibodies overnight. Protcins were visualized by enhanced chemiluminescence (Amersham) and quantified by densitometry. Antibodies were obtained from Santa Cruz Biotechnology (Santa Cruz, CA) (cyclin D1, SC-450; cyclin D2, SC-593; cdk4, SC-260) and Neomarkers (Union City, CA) (p27, MS-256; cyclin D3, MS-215; and p21, MS-5387).

Cyclin-dependent kinase assays. Kinase assays were done essentially as described by DeGregori *et al.* [26]. Equivalent amounts of protein extract, as determined by Bradford assay (Bio-Rad), were then added to protein A/protein G agarose beads (Santa Cruz) that had been precoated with 2 μg polyclonal anti-Cdk4 (Santa Cruz SC-260) or polyclonal anti-Cdk6 (Santa Cruz SC-177) antibodies. Complexes were immunoprecipitated for 3 h at 4°C with constant rotation. Immunoprecipitates were washed and then resuspended in 30 μl kinase reaction mix (50 mM Hepes, pH 8.0, 10 mM $MgCl_2$, 1 mM DTT, 2.5 mM EGTA, 10 mM β-glycerophosphate, 0.1 mM sodium orthovanadate, 1 mM NaF, 20 μM ATP, and 10 μCi [γ-^{32}P]ATP (3000 Ci/mmol, DuPont NEN, Boston, MA), containing 2 μg bacterially expressed GST-Rb (amino acids 379–928, kindly provided by Doug Cress, Moffitt Cancer Center) as substrate. After incubation at 30°C for 30 min, the reactions were stopped by the addition of SDS sample buffer and then boiled for 5 min, electrophoresed though 7.5% SDS–PAGE, and exposed to X-ray film. The amount of kinase activity was quantified by use of a phosphorimager (Molecular Dynamics).

RESULTS

All-trans-RACT Treatment Increases the Length of the F9 Cell Cycle

Cells induced to differentiate into parietal endoderm by exposure to all-*trans*-RA, 250 μM dbcAMP, and 500 μM theophylline (RACT) for 4 days grow much slower than undifferentiated cells. The decreased growth rate and induction of complete differentiation depends on all-*trans*-RA, because cells treated only with 250 μM dbcAMP and 500 μM theophylline (CT) fail to differentiate and continue to divide rapidly. We compared the percentage of cells in each phase of the cell cycle during 4 days of treatment with CT or 0.1 μM all-*trans*-RACT by staining with propidium iodide and measuring DNA content by flow cytometry. Results are shown in Table 1. By the second day of treatment, 45% of the RACT-treated cells, compared to 21% of the CT-treated cells, were in G1 phase. All-*trans*-RACT treatment eventually caused the number of cells in S phase to decline from 60 to 39%. Thus, the decreased growth of all-*trans*-RACT-treated cells was largely due to an increase in the length of G1 phase relative to that of undifferentiated CT-treated cells.

Regulation of Cyclin D1, D2, and D3 Transcripts in F9 Embryonal Carcinoma Cells

The cyclin D proteins are major regulatory subunits of the G1 Cdks. Since their concentrations directly regulate G1 progression, we measured the abundance of the cyclin D transcripts in F9 embryonal carcinoma cells induced to terminally differentiate into parietal endoderm *in vitro*. A time course of cyclin D expression was obtained by isolating RNA from cells treated with 0.1 μM all-*trans*-RA (Figs. 1A and 1B) or 1.0 μM all-*trans*-RA (Figs. 1C and 1D) and CT for 1, 2, 3, or 4 days. As controls, RNA was isolated from cells treated only with CT at the same time points. Figures 1A and 1C show the autoradiographs of Northern blots of this RNA and Figs. 1B and 1D show the data normalized to the constitutive message 36B4 [27].

Cyclin D1 mRNA abundance in cells induced to differentiate by exposure to 0.1 μM all-*trans*-RA and CT for 4 days was 26% of that observed in undifferentiated cells treated only with CT ($P < 0.05$, $n = 4$, Figs. 1A and 1B, compare lanes 4 and 8; Fig. 4; and data not shown). A similar repression was observed in cells treated with 1.0 μM all-*trans*-RA and CT (Figs. 1C and 1D and data not shown). We also observed a decline in cyclin D1 mRNA levels during culture in CT-containing medium (Figs. 1A and B). Since all-*trans*-RACT-

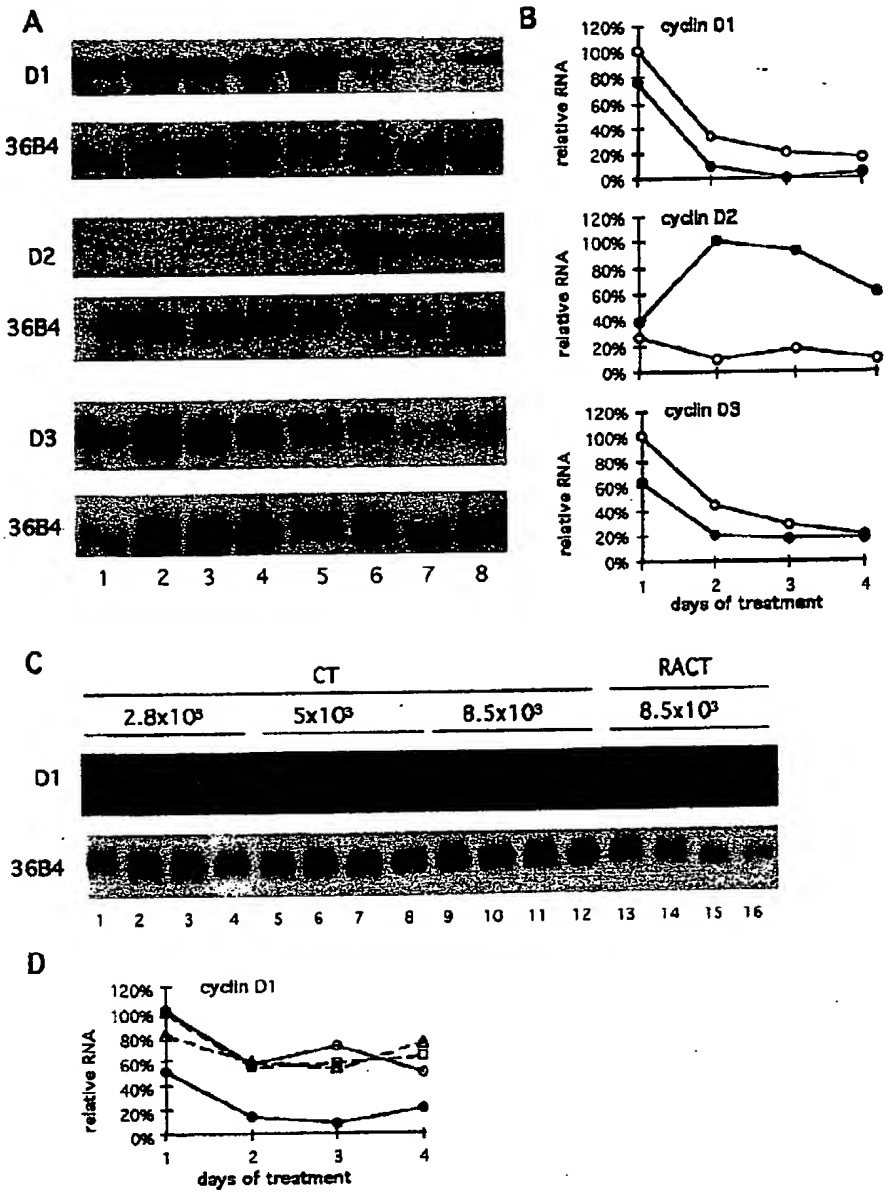

FIG. 1. Time course of cyclin D1-3 RNA levels during F9 cell differentiation. (A) Representative autoradiographs of Northern blots of RNA isolated from F9 cells seeded at 8.5×10^3 cells/cm^2 and treated with 250 μM dbcAMP and 500 μM theophylline (CT, lanes 1–4) or CT with 0.1 μM all-*trans*-RA (RACT, lanes 5–8) for 1 day (lanes 1, 5), 2 days (lanes 2, 6), 3 days (lanes 3, 7), or 4 days (lanes 4, 8). 25 μg of RNA was loaded per lane. Blots were probed for the cyclin D1, D2, D3, and 36B4 RNAs as indicated. Similar results were obtained with three to four independent Northern analyses. (B) Graphs indicate the transcript levels shown in A normalized to the level of the constitutive RNA, 36B4. In each graph, RNA levels are expressed as a percentage of those observed in the cells having the highest abundance of that RNA. (C) RNA was isolated and analyzed for cyclin D1 RNA abundance exactly as in A and B except that cells were seeded in CT only (lanes 1–12) at 2.8×10^3 cells/cm^2 (lanes 1-4), 5×10^3 cells/cm^2 (lanes 5–8), or 8.5×10^3 cells/cm^2 (lanes 9–12) or in 1 μM all-*trans*-RACT seeded at 8.5×10^3 cells/cm^2 (lanes 13–16). Cells were grown for 1 day (lanes 1, 5, 9, 13); 2 days (lanes 2, 6, 10, 14); 3 days (lanes 3, 7, 11, 15); or 4 days (lanes 4, 8, 12, 16). (D) Transcript levels shown in C normalized to the level of the constitutive RNA, 36B4. ●, RACT-treated, seeded at 8.5×10^3 cells/cm^2; ○, CT-treated, seeded at 8.5×10^3 cells/cm^2; □, CT-treated, seeded at 5×10^3 cells/cm^2; △, CT-treated, seeded at 2.8×10^3 cells/cm^2.

treated cells have a decreased growth rate, CT-treated cultures seeded at the same density contain approximately three times as many cells after 4 days of culture. Therefore, we measured cyclin D1 levels in CT-treated cells seeded at the usual density of 8.5×10^3 cells/cm^2 or at 5×10^3 or 2.8×10^3 cells/cm^2. The data

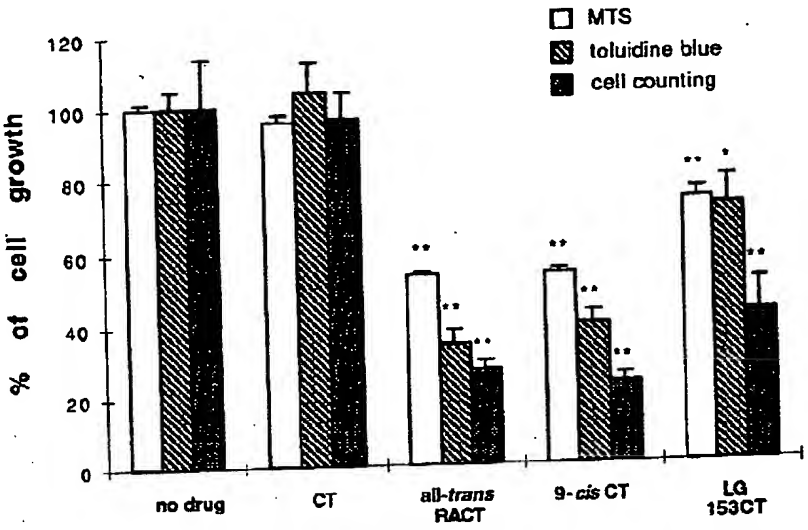

FIG. 2. The effects of various retinoids on F9 cell growth. Cells were grown 3 days in DMEM containing CT and 0.1 μM retinoids as indicated under each bar. For the MTS assay, cells in 96-well plates were assayed by increased conversion to formazan and absorption at 570 nm was determined on microplate reader ($n = 8$). For toluidine blue staining, absorption at 630 nm was measured in 96-well plates ($n = 8$). The growth of cells in 24-well plates was measured by cell counting ($n = 4$). The values were normalized relative to the number of untreated cells. Bars, SEM. $^*P < 0.05$, $^{**}P < 0.01$ relative to undifferentiated (untreated or CT-treated) cells.

shown in Figs. 1C and 1D indicate that, although cyclin D1 levels may decline in cells grown at high density, all-*trans*-RACT further decreases the abundance of the cyclin D1 mRNA.

In contrast to the observed decrease in cyclin D1 mRNA level, 0.1 μM all-*trans*-RA and CT induced the cyclin D2 RNA eightfold over that observed in CT-treated cells within 48 h of treatment ($P = 0.005$, $n = 4$, Figs. 1A and 1B, lane 6; and data not shown). Likewise, 1.0 μM all-*trans*-RA and CT induced the cyclin D2 RNA strongly by 48 h (data not shown). As observed for the cyclin D1 transcript, the abundance of the cyclin D3 RNA declined with culture in both all-*trans*-RACT and CT-containing medium (Fig. 1). Cell density failed to affect this decline (data not shown). Together, these data indicate that the cyclin D1 and D2 transcript levels are differentially regulated by all-*trans*-RACT during F9 cell growth and differentiation.

RXR Agonists Inhibit F9 Cell Proliferation

The decreased F9 cell growth rate caused by all-*trans* RA could involve genes regulated by factors associated with terminal differentiation. This could be an indirect retinoid effect, because many transcription factors are regulated by RA. Alternatively, all-*trans*-RA-bound receptors could directly regulate the cell cycle genes controlling growth rate. Most likely, a combination of these mechanisms plays a role. All-*trans*-RA, which directly activates RARα, β, and γ, may be metabolized to 9-*cis*-RA and thus indirectly activate the RXRs as well. One approach to distinguish direct from indirect regulation of the cyclin D genes would require a laborious analysis of the genetic regulatory elements controlling each gene. An alternative pharmacological approach using receptor-selective retinoids is more suitable for analyzing many genes. These retinoids can activate a subset of receptors and thus a subset of the genes activated in all-*trans*-RA-treated F9 cells.

We compared the growth of F9 cells treated with 0.1 μM all-*trans*-RA, an RAR agonist; 9-*cis*-RA, an RAR and RXR panagonist; and LG100153 (LG153), an RXR agonist [18]. Three independent cell proliferation assays were used to measure cell growth (Fig. 2). Each assay showed that CT treatment alone did not change the growth rate relative to untreated F9 cells. In contrast, exposure to 0.1 μM all-*trans*-RA or 9-*cis* RA and CT resulted in significantly fewer cells (Figs. 2 and 3A). The RXR agonist LG153 and CT also repressed the number of cells by 50%, although the morphology typical of differentiated cells was not induced. The difference in growth was statistically significant as determined by the Student's *t* test assuming equal variances (MTS assay, $P < 0.01$; cell counting, $P < 0.01$; toluidine blue assay, $P < 0.05$). Since LG153 specifically activates RXRs, these observations suggest that ligand activation of RXRs by LG153 inhibits the growth of F9 cells. LG153 has also been observed to block the cell cycle of the myelomonocytic cell line U937 [28].

To examine the effect of LG153 activation on cell cycle traverse, we determined the percentage of cells in each phase of the cell cycle by flow cytometry. As shown

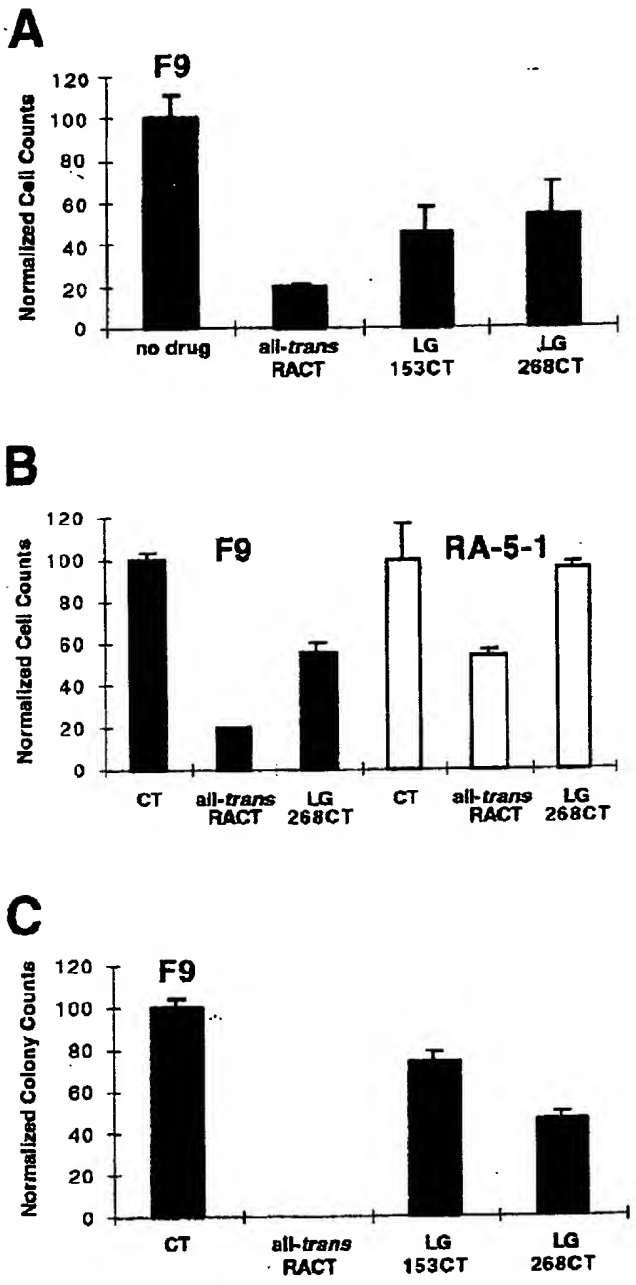

FIG. 3. RXR activation selectively inhibit F9 but not RA-5-1 cell growth. F9 (A, B) or RA-5-1 (B) cells were seeded at 2×10^4 cells per well in 24-well plates and grown for 4 days in medium containing 0.1 μM retinoid and CT as indicated. Cells were then trypsinized and counted on a hemacytometer (n = 3–4). (C) F9 cells were grown in semisolid agarose in medium containing 0.1 μM retinoid and CT as indicated. After 11 days, visible colonies were counted (n = 9–13). All values are normalized to the number of cells or colonies in the CT-treated cultures. There was no difference in the size of colonies formed in CT or RXR-selective retinoids. Solid bars, F9 cells; open bars, RA-5-1 cells. Bars, SEM.

in Table 1, treatment with LG153 and CT for 4 days caused an increase in the number of cells in G1 phase from 21 to 43%. This did not differ significantly from the 45% G1 phase cells found in the RACT-treated cultures. The kinetics of this change in G1 length were different. RACT nearly doubled the number of G1 cells within 48 h of treatment. In contrast, the number of LG153-treated cells in G1 phase were not significantly different until 72 h of treatment. Thus, while RXR activation can inhibit the growth of F9 cells, the kinetics of this inhibition are distinct from that induced by RAR activation.

To determine whether or not the significant inhibition of F9 cell growth rate by LG153 was caused by the selective activation of RXRs, we tested another RXR-selective agonist, LG100268 (LG268) [19]. Figure 3A demonstrates that 4 days of exposure to 0.1 μM LG153 or LG268 and CT repressed F9 cell growth by 49 and 47% respectively. The average doubling times of the cells over 4 days were 16.6 h in the absence of retinoids, 27.8 h in all-*trans*-RACT, 19.8 h in LG153CT, and 20.7 h in LG268CT-containing medium. The receptor selectivity of these retinoids has been confirmed by binding studies and mammalian reporter assays [18, 19]. Therefore, our observations are consistent with the growth inhibition resulting from the ability of each drug to activate RXRs.

The RXR-Selective Agonist LG268 Fails to Inhibit the Proliferation of an F9 Cell Line That Cannot Differentiate

Wang and Gudas isolated a mutant clone of F9 cells, RA-5-1, that cannot differentiate into either parietal [20] or visceral endoderm [29]. These cells, which have a defective prolyl-4-hydroxylase enzyme, were selected by virtue of their ability to grow without anchorage in medium containing all-*trans*-RA [30]. All-*trans*-RA fails to induce differentiation or complete growth arrest in RA-5-1 cells, although *Hoxa-1*, a directly RA-responsive gene, is induced [29]. Thus RA-5-1 cells begin, but fail to complete, the series of events leading to terminal differentiation. To test whether or not the RXR-selective agonists were nonselectively cytotoxic, we examined the effect of LG268 on RA-5-1 growth. As shown in Fig. 3B, all-*trans*-RACT causes a 47% decrease in RA-5-1 growth rate. This is significantly less than the 80% decrease observed in wild-type F9 cells (Fig. 3B, compare bars 2 and 5) and is consistent with published data [30]. In contrast, LG268CT did not alter the growth of RA-5-1 cells (Fig. 3B, compare bars 4 and 6), although this drug inhibited F9 cell growth by 45%. This proves that LG268 is not generally cytotoxic. This result also suggests that RXR-selective retinoids inhibit cell growth by a mechanism that is impaired in RA-5-1 cells.

RXR-Selective Retinoids Inhibit, but Do Not Abolish, Anchorage-Independent Growth

The previous results indicate that LG153 and LG268 decrease F9 cell growth rate in monolayer cultures. F9 cells induced to differentiate by all-*trans*-RACT are, like most benign cells, incapable of anchorage-independent growth. In contrast, untreated F9 embryonal carcinoma cells are highly malignant and readily form colonies in semisolid agar. To further assess the effects of the RXR-selective retinoids on growth control in F9 cells, we compared the number of colonies formed in soft agar containing 0.1 μM LG153, LG268, or all-*trans*-RA and CT. Cells (3×10^3) were plated in 0.35% agar and colonies were counted after 11 days. Cells treated with CT alone formed an average of 520 ± 78 colonies per plate. As expected for terminally differentiated cells, all-*trans*-RACT-treated cells failed to form colonies in soft agar. LG153CT- and LG268CT-treated cells formed 385 ± 82 and 242 ± 51 colonies per plate, respectively. Figure 3C shows the number of colonies normalized to the average number of colonies in CT-treated plates. Thus, both RXR-selective retinoids impair colony formation, although not to the same extent as all-*trans*-RA. These data are consistent with two hypotheses: (1) a subset of RXR agonist-treated cells terminally differentiates and these fail to form colonies, or (2) the RXR agonists fail to induce complete terminal differentiation, but cause some cells to become anchorage-dependent though partial differentiation or another mechanism. We do not favor the first hypothesis, because the RXR agonist-treated cells did not assume the characteristic parietal endoderm morphology. Also, as described below, the pattern of gene expression in RXR agonist-treated cells resembles that of undifferentiated cells.

LG153-Treated Cells Express Undifferentiated Stem Cell Markers

All-*trans*-RA regulates cell differentiation and proliferation by modulating gene expression [31]. To learn which genes are involved in RXR-mediated growth inhibition, we used Northern analyses to quantify the expression of several genes known to be regulated during all-*trans*-RA-induced F9 cell differentiation (Fig. 4). These genes included those expressed in undifferentiated stem cells and down-regulated by all-*trans*-RA, as well as those induced by all-*trans*-RA. Previous work showed that LG153 does not affect the expression of *H218*, which functions as a receptor for sphingosine 1-phosphate and related compounds and is down-regulated during RA-induced differentiation [24]. We also tested five other genes normally expressed in undifferentiated cells: the transcription factors *Rex1* (*Zfp-42*) [32], *Oct3/4* [33], and *Sox2* [34] and the growth factors *Bmp4* [13] and *Fgf4* [35]. As expected, each gene was down-regulated by RAR agonists (all-*trans*-RA, TTNPB, or 9-*cis* RA) but not by the RXR-selective agonist LG153. TTNPB activates RARs highly selectively and cannot be metabolized to 9-*cis*-RA.

LG153 also failed to fully up-regulate the expression of the genes encoding the extracellular matrix protein *laminin B1*, the growth factor *Bmp2*, or the transcription factors *Hoxa-1* and *RARβ*, as occurs in differentiated cells [32 and Refs. therein]. If the 25 to 50% decreases in colony formation shown in Fig. 3C were caused by terminal differentiation of 25 to 50% of the cells, then a corresponding decrease in the expression of all stem cell markers and an increase in all parietal endoderm markers should have been observed. Since this was not observed, LG153 does not appear to induce parietal endoderm in a subset of the F9 cell population.

LG153 Induces Cyclin D2 and D3 mRNA

All-*trans*-RA slows the F9 cell cycle by increasing the length of the G1 phase (Table 1) [17, 36]. We also observed that cyclins D1, D2, and D3 were regulated during F9 cell differentiation (Fig. 1). Therefore, we measured the expression of RNAs encoding G1 phase regulatory proteins which are directly involved in the cell cycle and growth control in cells treated with a panel of retinoids (Fig. 5). Retinoids that induced differentiation (all-*trans*-RA, TTNPB, and 9-*cis*-RA) down-regulated *cyclin D1* and *cyclin E*. Conversely, as observed for the stem cell markers *H218*, *Rex1*, *Oct3/4*, *Sox2*, *Bmp4*, and *Fgf4*, the levels of *cyclin D1* and *E* RNAs were unaltered in LG153-treated cells. Thus regulation of these genes is linked to RAR- activation and parietal endoderm differentiation.

Cyclin D2 and D3 message abundance, however, was changed in RXR agonist-treated cells. Both LG153 (Fig. 5) and LG268 (data not shown) induced cyclin D2 RNA levels as efficiently as RAR agonists or panagonist (8-fold). Further, cyclin D3 mRNA levels were induced by the RXR agonist LG153, but not by all-*trans*-RACT. The RNA-encoding $p27^{Kip}$, a major Cdk inhibitor, was modestly, but reproducibly, up-regulated by both all-*trans*-RACT (2-fold, $P < 0.01$, $n = 6$) and LG153CT (1.4-fold, $P < 0.05$, $n = 6$). These observations suggest that cyclin D2, cyclin D3, and $p27^{Kip}$ may be involved in the partial growth suppression caused by RXR agonists. More importantly, the striking elevation of cyclin D2 levels during all-*trans*-RACT-induced differentiation may not be involved in differentiation, but rather in cell cycle exit.

RAR- and RXR-Selective Retinoids Differentially Regulate Cell Cycle Protein Levels

Having shown distinct modulations of mRNAs encoding cell cycle proteins upon treatment with RAR or RXR-selective retinoids, we next examined the relative

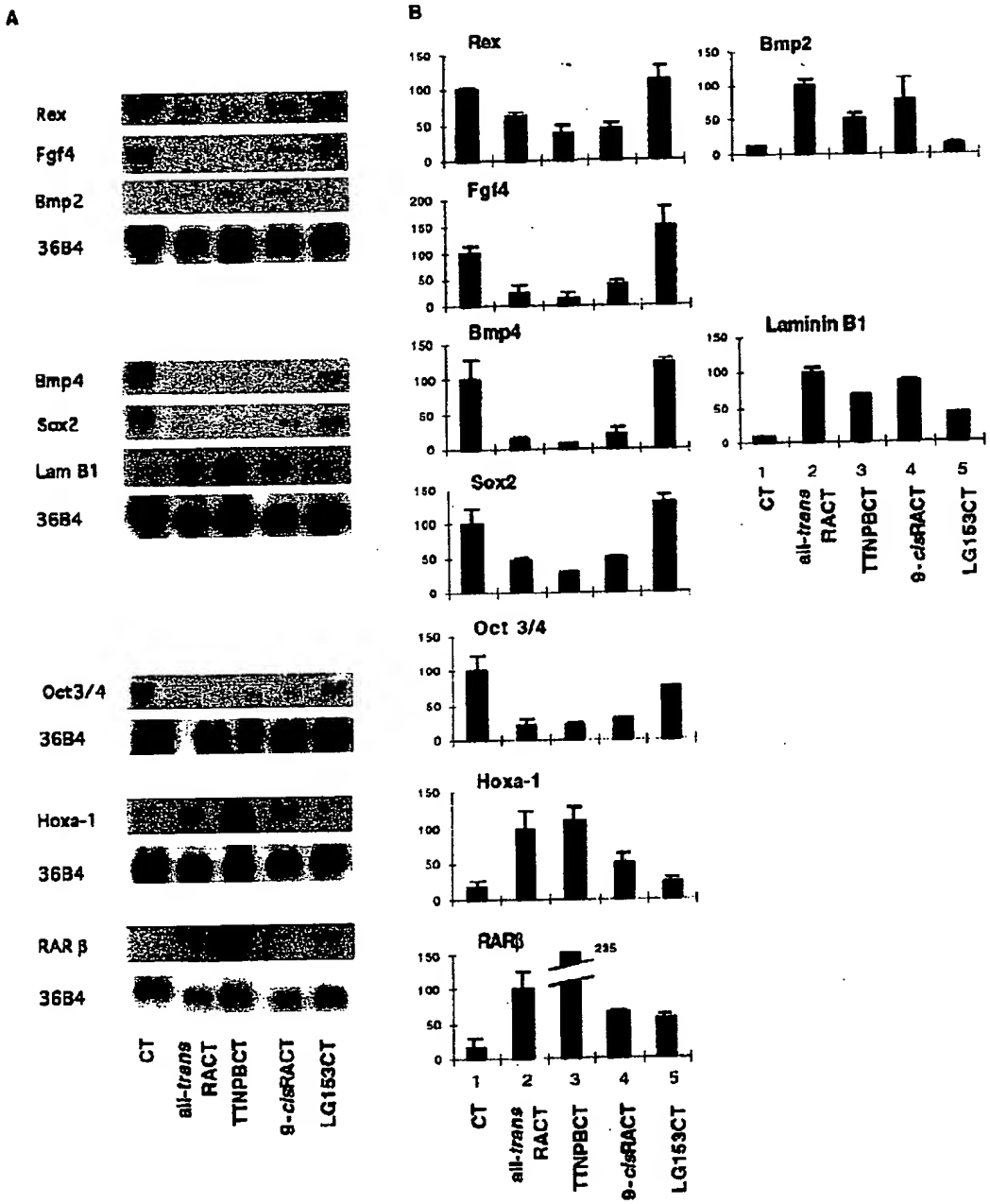

FIG. 4. Northern analyses of genes expressed in F9 cells treated with different retinoids. (A) Representative autoradiographs of Northern blots of RNA isolated from F9 cells treated for 102 h with CT and 0.1 μM retinoids as indicated at the bottom of each lane. 22 μg total cellular RNA per lane was loaded on formaldehyde-containing agarose gels. Following electrophoresis, RNA was transferred to nylon filters and hybridized to the indicated radiolabeled cDNA probes (Lam B1, *Laminin B1*). The autoradiographs of the representative blots hybridized to the constitutive RNA, 36B4, is shown at the bottom of each set of blots. (B) The amount of signal was quantified on a phosphorimager. Bar graphs indicate a compilation of the data from several Northern blots, normalized to 36B4. Loading variation between lanes was less than threefold. $n = 2$ for all blots, except $n = 4$ for *Hoxa-1*. The mRNA levels are expressed as a percentage of the average value observed in cells treated with CT alone (down-regulated genes: *Rex1, Oct 3/4, Fgf4, Bmp4,* and *Sox2*) or all-*trans*-RACT (up-regulated genes: *Bmp2, Hoxa-1, laminin B1,* and *RARβ*). Bars, range or SEM.

protein levels directly (Fig. 6A). The amount of cyclin D1 protein in all-*trans*-RACT-treated cells was approximately one-half the amount in undifferentiated cells (Fig. 6A). In contrast, treatment with the RXR-selective retinoid (LG268CT) did not cause any appreciable change in the amount of cyclin D1 protein. While the

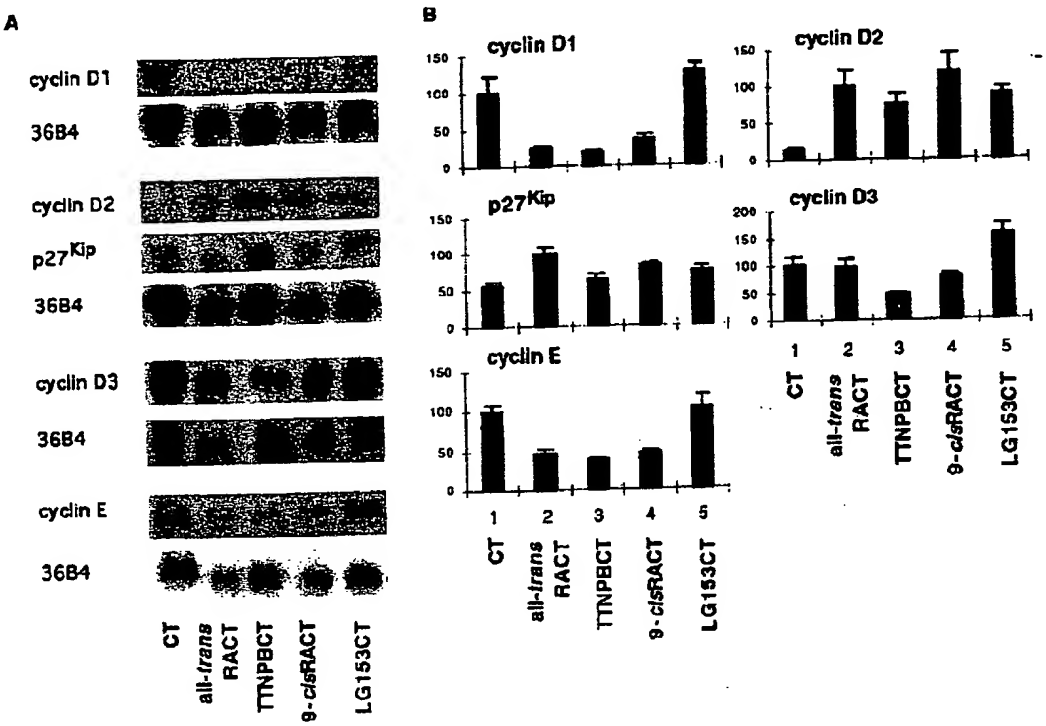

FIG. 5. Cell cycle mRNA levels in F9 cells treated with different retinoids. (A) Representative autoradiographs of Northern blots of RNA isolated from F9 cells treated with CT and retinoids as indicated for Fig. 4. (B) Bar graphs indicate a compilation of the data from several Northern blots, normalized to 36B4. $n = 6$ for $p27^{Kip}$, *cyclin D1*, and *D2*. $n = 2$ for *cyclin D3* and *cyclin E*.

cyclin D2 protein was barely detectable in undifferentiated cells, cyclin D2 protein levels were strongly induced by all-*trans*-RACT. Treatment with LG268CT induced cyclin D2 expression to a level almost one-half that of all-*trans* RACT. Cyclin D3 levels declined by approximately 40% upon treatment with all-*trans*-RACT, but were induced threefold by the RXR-selective retinoid and CT. Thus, overall cyclin D levels increased in RXR-treated cells, despite their decreased rate of proliferation.

Cdk4 protein levels did not change appreciably following any treatment (Fig. 6A). In contrast to treatment with all-*trans*-RACT which induced $p27^{Kip}$, RXR-selective agonist and CT did not change the abundance of the Cdk inhibitors p21 or p27 (Fig. 6B). Thus, in RXR agonist-treated cells, the levels of cyclin D1, p21, and $p27^{Kip}$ proteins resemble those of undifferentiated cells, while cyclin D2 and D3 protein levels are specifically induced.

Like All-trans-RA, Treatment with RXR-Selective Retinoid Decreases Cdk4-Dependent Kinase Activity

Having shown that RXR-selective retinoids modulate the expression of D-type cyclins in a manner distinct from that of all-*trans*-RA, we next examined the functional consequences of this regulation. In extracts prepared from all-*trans*-RACT-treated cells, the amount of Cdk4-dependent kinase activity was 50% that observed in cells treated with CT alone (Fig. 6C). In these fully differentiated cells, decreased Cdk4 kinase activity correlates with decreased proliferation rate. RXR-selective retinoids, which cannot cause full differentiation (Fig. 4), also impair proliferation (Figs. 2 and 3). *In vitro* kinase assays showed that treatment with the RXR-selective retinoid LG153 and CT decreased Cdk4-dependent kinase activity by 36% (Fig. 6C). Cdk6-dependent kinase activity was not appreciably affected by any treatment. The magnitude of the LG153-associated decline in Cdk4 activity correlates with the antiproliferative effect of this retinoid.

DISCUSSION

The retinoid-induced complete differentiation of F9 embryonal carcinoma stem cells into parietal endoderm is accompanied by a sharply decreased proliferation rate as the cells become benign (Table 1) [17, 36]. Changes occur in numerous cellular systems during this process. Cells activate and inactivate various transcription factor genes, change shape and adhesive properties, and begin to secrete specialized extracellular matrix proteins. Some of these changes result from the direct regulation of specific genes by retinoids and

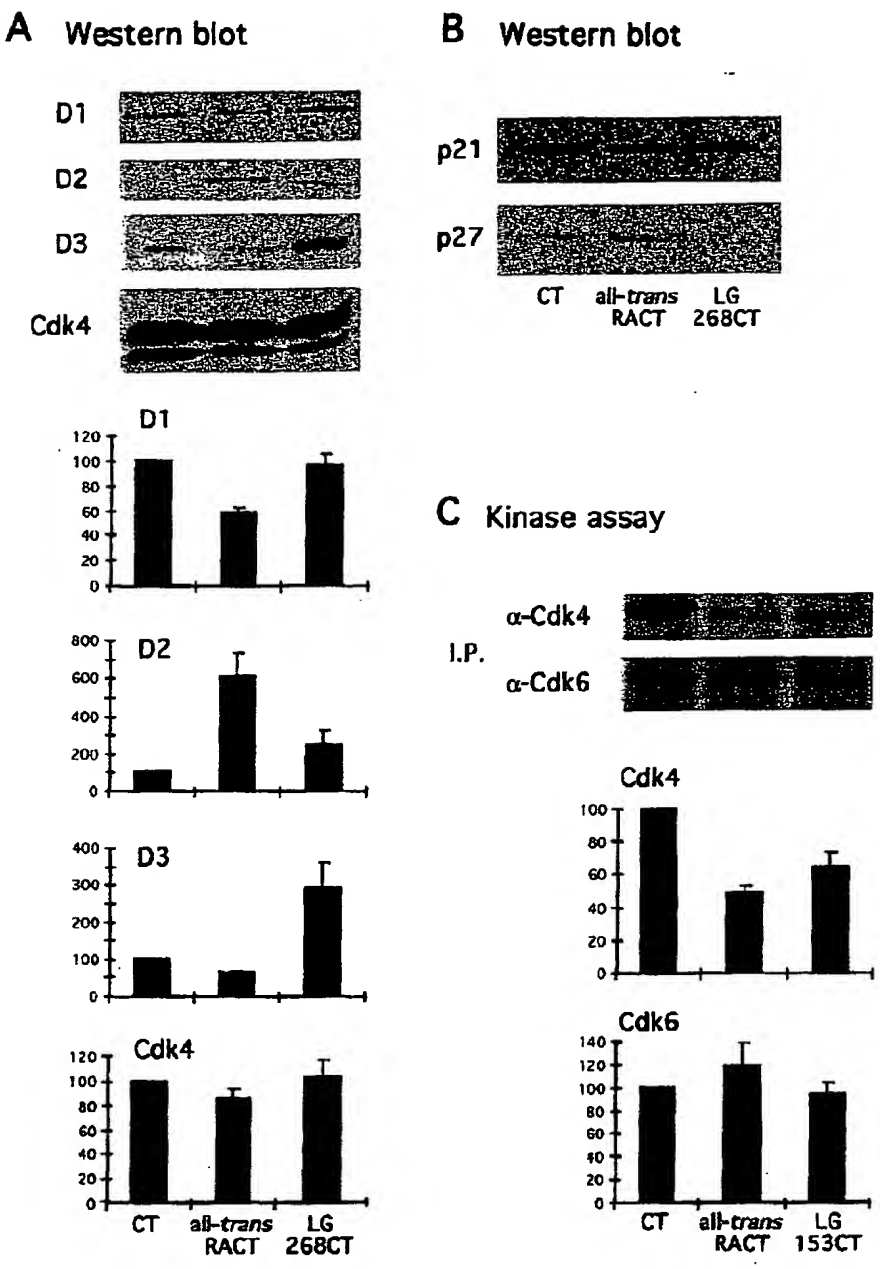

FIG. 6. Cell cycle protein levels and Cdk activity in retinoid-treated cells. F9 cells were treated with CT alone or 1 μM of the indicated retinoid and CT for 3 or 4 days. Representative autoradiographs of ECL-visualized Western blots (A, B) or phosphorylated GST-Rb (C) are shown. (A and B) 25 μg of whole cell extract was electrophoresed though 12% (A) or 15% (B) SDS–PAGE gels and then the proteins were electroblotted to nitrocellulose. Blots were incubated with antibodies to the indicated proteins and were visualized by enhanced chemiluminescence. Protein levels were quantitated by densitometry and expressed as a percentage of the value observed in cells treated with CT alone. Data represent two to four experiments; bars, range or SEM. (C) Whole cell extracts were immunoprecipitated with antibodies to Cdk4 or Cdk6. Immunoprecipitates were then tested for their ability to phosphorylate bacterially produced GST-Rb. Reactions were electrophoresed on 7.5% SDS–PAGE gels. Kinase activity was quantitated with a phosphorimager and expressed relative to the kinase activity measured in CT-treated cells. Extracts immunoprecipitated with normal rabbit serum were not capable of phosphorylating Rb, indicating the specificity of the assay (data not shown). Data represent four experiments. Bars, SEM. RACT- and LGCT-treated cells differed significantly from the CT-treated cells in the cdk4 kinase assay ($P < 0.01$). For the Cdk6 kinase assay, none of the samples differed significantly.

their receptors, e.g., *Hoxa-1* [37, 38], while others are secondarily regulated by the products of directly regulated genes encoding transcription factors. The decreased growth rate of RA-treated F9 cells could result from direct regulation of cell cycle genes or by other genes regulated during parietal endoderm differentiation. We have presented an analysis of the changing expression levels of key cell cycle regulatory genes, cyclins D1, D2, D3, and E, and $p27^{kip}$, during F9 cell differentiation. We also present evidence that a retinoid-stimulated decrease in proliferation can be unlinked from terminal differentiation.

We observed that two different RXR agonists increased the doubling time of F9 cells from 16.6 to 20 h (Figs. 2 and 3). RXR activation can also slow proliferation, without inducing differentiation of a melanoma cell line [39]. The inhibition of Cdk4 activity we observed in F9 cells (Fig. 6C) might explain this decreased growth rate. Unexpectedly, however, cyclin D2 and D3 protein levels were induced in F9 cells treated with RXR agonist (Fig. 6A). The best characterized function of the cyclin Ds is to activate Cdk4 and Cdk6. However, recent observations support a distinct role for the G1 cyclins in differentiated cells [40]. Cyclin D2 or D3 have been shown to enter into unique protein complexes in cells exiting the cell cycle. For example, cyclin D3 bound both cyclin E and p130 in differentiated myotubes [41] and cyclin D2 bound catalytically inactive Cdk2 in fibroblasts entering quiescence [42]. In fact, overexpression of cyclin D2 alone inhibited G1 progression. An increase in cyclin D3 protein abundance has also been recently reported as a relatively early event in HL-60 cell differentiation [43]. Whether or not the induction of cyclin D2 and D3 is required for the RXR-mediated growth suppression remains to be tested. However, the fact that RXR-selective retinoids can inhibit proliferation and induce cyclin D2 without inducing the complex differentiation program suggests that the induction of cyclin D2 during all-*trans*-RACT-induced differentiation may be involved in cell cycle exit rather than differentiation *per se*.

Retinoids inhibit the proliferation of most cells; however, some normal and malignant cells are stimulated to proliferate by retinoids or require retinoids for survival [see 44 and Refs. therein]. Indeed, supplements of β-carotene, a major dietary precursor to vitamin A, were found to increase the cancer rate in smokers [45], suggesting that some retinoids promote tumor cell survival *in vivo*. Undifferentiated F9 cells may possess a repressive function that prevents growth despite retinoid-induced upregulation of cyclin D2 and D3. This function may be absent in cells that require retinoids for survival.

The complete differentiation of parietal or visceral endoderm from F9 embryonal carcinoma stem cells is a multistep process initiated by various retinoids that activate RARs [13]. Retinoids that activate the RXRs do not induce differentiation alone, but can synergize with suboptimal RAR agonist concentrations to cause complete differentiation [46, 47]. During F9 cell differentiation, the expression of numerous genes is up-regulated or down-regulated [31]. We tested the anti-proliferative effects of an RXR agonist on an F9 cell line that is RA responsive, but cannot differentiate. RA-5-1 cells transcribe *Hoxa-1* in response to all-*trans*-RA, but fail to terminally differentiate or completely growth arrest [20, 29]. All-*trans*-RA-treated RA-5-1 cells grew slower than untreated cells, but the response was limited relative to that of wild-type F9 cells (Fig. 3B). In contrast, the RXR agonist did not alter RA-5-1 cell growth. Since RA-5-1 cells were selected by their mutant phenotype of growth in soft agar containing all-*trans*-RA [20] and since they initiate, but fail to complete, the differentiation program [20, 29], RXR-mediated decreased growth rate may require a process that is impaired in these cells.

Normal F9 cell differentiation clearly requires the activity of both RARs and RXRs, because F9 cells lacking functional RARs or RXRs were impaired in their ability to differentiate in response to all-*trans*-RA [17, 48, 49]. Interestingly, the phenotypes of these cell lines suggested that regulation of proliferation by retinoids was partially separable from differentiation. Although all-*trans*-RA and other retinoids failed to induce the normal gene markers of differentiation in RARγ-null cells, these cells were as sensitive as wild-type cells to the antiproliferative effects of the retinoids [17, 48]. In contrast, the RXRα-null cells also failed to differentiate, but resisted the antiproliferative effects of the retinoids [17]. Likewise, dominant-negative RXR mutant proteins inhibited RA-induced growth arrest in F9 cells [50] and RXRα-null cells proliferated more rapidly in the absence of retinoid [17]. Our observation that two chemically distinct RXR-selective ligands decrease the rate of F9 cell proliferation is consistent with the hypothesis that an RXR-mediated event directly influences cell cycle control in F9 cells. Additionally, the antiproliferative effect of retinoids does not require activation of the entire differentiation program.

The majority of retinoid-regulated genes are efficiently activated by ligand-bound RAR in a heterodimer with an unbound RXR [4, 7]. At least one dozen, however, bind and are activated by RXR homodimers *in vivo* and *in vitro* [7, 51, 52]. The RXRs also bind other hydrophobic ligand receptors such as the thyroid hormone, vitamin D, oxysterol, and peroxisome proliferator-activated receptors and Nurr77/NGFI-B [8–10]. One of the RXR-agonists with antiproliferative effects on our F9 cells (LG268) has been shown to directly stimulate the expression of 25-hydroxy-vitamin D3-24-hydroxylase, a key enzyme catalyzing 1,25-dihydroxyvitamin D metabolism, in reporter assays and in mice [52]. RARβ has been previously shown to

be induced by RXR homodimers *in vitro* [6] and in yeast [53] and by RXR agonist in chick limb buds [54] and all-*trans*-RA-resistant breast cancer cells [55]. We also observed that the RXR agonist induced RARβ modestly in F9 cells (Fig. 4). Finally, we have shown here that RXR agonists induced the abundance of the cyclin D2 and D3 RNAs and proteins without RAR agonist (Figs. 5 and 6), suggesting that RXRs may activate these important cell cycle genes by a mechanism independent of ligand-bound RARs.

The evidence indicates that all-*trans*-RA exerts its effects mainly via RAR/RXR heterodimers [4]. However, the ability of RXR ligands to alter the level of key proteins in the metabolic and signaling pathways of diverse signals, such as growth hormone, retinoids, and vitamin D [51–53], suggests that they can unexpectedly alter the response of cells to other ligands and thus influence proliferation. Our work also indicates that RXR ligands can directly influence the cell cycle apparatus.

We thank CIRD Galderma, Hoffmann LaRoche, and Ligand Pharmaceuticals for the gift of the various selective retinoids. For plasmids encoding various genes, we thank Drs. C. Sherr (*cyclins D1, D2,* and *D3* and *Cdk4*), T. Hunter ($p27^{Kip}$), J. DeGregori (*cyclin E*), C. Basilico (*Fgf4* and *Sox2*), and H. Schöler (*Oct3/4*). We are also indebted to Dr. W. D. Cress for GST-Rb and helpful discussion. Technical assistance was provided by student researchers Joseph Johnson, Rocio Martinez-Angel, and Juan P. Richiusa. We acknowledge the use of the Molecular Imaging and Flow Cytometry Core Facilities at the H. Lee Moffitt Cancer Center and Research Institute. This work was supported by a National Institute of Child Health and Human Development grant to M.B.R. (R29 HD31117) and a postdoctoral fellowship from the American Heart Association, Florida Affiliate, to M.A.G.

REFERENCES

1. Amos, B., and Lotan, R. (1990). Retinoid-sensitive cells and cell lines. *Methods Enzymol.* **190,** 217–225.
2. Sporn, M., Roberts, A., and Goodman, D. (Eds.) (1994). "The Retinoids: Biology, Chemistry, and Medicine," Raven Press, New York.
3. Lotan, R. (1996). Retinoids in cancer prevention. *FASEB J.* **10,** 1031–1039.
4. Chambon, P. (1996). A decade of molecular biology of retinoic acid receptors. *FASEB J.* **10,** 940–954.
5. Smith, S., and Eichele, G. (1991). Temporal and regional differences in the expression pattern of distinct retinoic acid receptor-β transcripts in the chick embryo. *Development* **111,** 245–252.
6. Zhang, X., Lehmann, J., Hoffmann, B., Dawson, M., Cameron, J., Graupner, G., Hermann, T., Tran, P., and Pfahl, M. (1992). Homodimer formation of retinoid X receptor induced by 9-*cis* retinoic acid. *Nature* **358,** 587–591.
7. Mangelsdorf, D. J., Umesano, K., and Evans, R. M. (1994). The retinoid receptors. *In* "The Retinoids: Biology, Chemistry, and Medicine" (M. Sporn, A. Roberts, and D. Goodman, D., Eds.), Raven Press, New York.
8. Leblanc, B., and Stunnenberg, H. (1995). 9-*cis*-Retinoic acid signaling: Changing partners causes some excitement. *Genes Dev.* **9,** 1811–1816.
9. Lehmann, M., Kliewer, S., Moore, L., Smith-Oliver, T., Oliver, B., Su, J., Sundseth, S., Winegar, D., Blanchard, D., Spencer, T., and Willson, T. (1997). Activation of the nuclear receptor LXR by oxysterols defines a new hormone response pathway. *J. Biol. Chem.* **272,** 3137–3140.
10. Mangelsdorf, D. J., Thummel, C., Beato, M., Herrlich, P., Schutz, G., Umesono, K., Blumberg, B., Kastner, P., Mark, M., Chambon, P., and Evans, R. M. (1995). The nuclear receptor superfamily: The second decade. *Cell* **83**(6), 835–839.
11. Lammer, E. J., Chen, D. T., Hoar, R. M., Agnish, N. D., Benke, P. J., Braun, J. T., Curry, C. J., Fernoff, P. M., Grix, A. W., Lott, I. T., Richard, J. M., and Sun, S. C. (1985). Retinoic acid embryopathy. *N. Engl. J. Med.* **313,** 837–841.
12. Dawson, M., and Hobbs, P. (1994). The synthetic chemistry of retinoids. *In* "The Retinoids: Biology, Chemistry, and Medicine" (M. Sporn, A. Roberts, and D. Goodman, Eds.), Raven Press, New York.
13. Rogers, M. (1996). Receptor-selective retinoids implicate RAR alpha and gamma in the regulation of *bmp-2* and *bmp-4* in F9 embryonal carcinoma cells. *Cell Growth Differ.* **7,** 115–122.
14. Strickland, S., Smith, K. K., and Marotti, K. R. (1980). Hormonal induction of differentiation in teratocarcinoma stem cells: Generation of parietal endoderm by retinoic acid and dibutyryl cAMP. *Cell* **21,** 347–355.
15. Hunter, T., and Pines, J. (1994). Cyclins and cancer II: Cyclin D and CDK inhibitors come of age. *Cell* **79,** 573–582.
16. Thomas, N. (Ed.) (1996). "Apoptosis and Cell Cycle Control," BIOS, Oxford.
17. Clifford, J., Chiba, H., Sobieszczuk, D., Metzger, D., and Chambon, P. (1996). RXRα-null F9 embryonal carcinoma cells are resistant to the differentiation, anti-proliferative and apoptotic effects of retinoids. *EMBO J.* **15,** 4142–4155.
18. Boehm, M. F., Zhang, L., Badea, B. A., White, S. K., Mais, D. E., Berger, E., Suto, C. M., Goldman, M. E., and Heyman, R. A. (1994). Synthesis and structure–activity relationships of novel retinoid X receptor-selective retinoids. *J. Med. Chem.* **37**(18), 2930–2941.
19. Boehm, M. F., Zhang, L., Zhi, L., McClurg, M. R., Berger, E., Wagoner, M., Mais, D. E., Suto, C. M., Davies, P. J. A., Heyman, R. A., and Nadzan, A. M. (1995). Design and synthesis of potent retinoid X receptor selective ligands that induce apoptosis in leukemia cells. *J. Med. Chem.* **38**(16), 3146–3155.
20. Wang, S.-Y., and Gudas, L. J. (1984). Selection and characterization of F9 teratocarcinoma stem cell mutants with altered responses to retinoic acid. *J. Biol. Chem.* **259**(9), 5899–5906.
21. Buttke, T. M., McCubrey, J. A., and Owen, T. C. (1993). Use of an aqueous soluble tetrazolium/formazan assay to measure viability and proliferation of lymphokine-dependent cell lines. *J. Immunol. Methods* **157**(1–2), 233–240.
22. Coll, J. L., Ben-Ze'ev, A., Ezzell, R. M., Rodriguez Fernandez, J. L., Baribault, H., Oshima, R. G., and Adamson, E. D. (1995). Targeted disruption of vinculin genes in F9 and embryonic stem cells changes cell morphology, adhesion, and locomotion. *Proc. Natl. Acad. Sci. USA* **92**(20), 9161–9165.
23. Chen, J. Y., Penco, S., Ostrowski, J., Balaguer, P., Pons, M., Starrett, J. E., Reczek, P., Chambon, P., and Gronemeyer, H. (1995). RAR-specific agonist/antagonists which dissociate transactivation and AP1 transrepression inhibit anchorage-independent cell proliferation. *EMBO J.* **14**(6), 1187–1197.
24. Li, Y., MacLennan, A. J., and Rogers, M. B. (1998). A putative G-protein coupled receptor, H218, is down-regulated during the retinoic acid-induced differentiation of F9 embryonal carcinoma cells. *Exp. Cell Res.* **230,** 320–325.
25. Ausubel, F. M., Brent, R., Kingston, R. E., Moore, D. D., Seidman, J. G., Smith, J. A., and Struhl, K. (Eds.) (1997). "Current Protocols in Molecular Biology", Wiley, New York.

26. DeGregori, J., Kowalik, T., and Nevins, J. R. (1995). Cellular targets for activation by the E2F1 transcription factor include DNA synthesis- and G1/S-regulatory genes. *Mol. Cell. Biol.* **15**(8), 4215–4224.
27. Rio, M. C., Bellocq, J. P., Gairard, B., Rasmussen, U. B., Krust, A., Koehl, C., Calderoli, H., Schiff, V., Renaud, R., and Chambon, P. (1987). Specific expression of the pS2 gene in subclasses of breast cancers in comparison with expression of the estrogen and progesterone receptors and the oncogene ERBB2. *Proc. Natl. Acad. Sci. USA* **84**, 9243–9247.
28. Liu, M., Iavarone, A., and Freedman, L. (1996). Transcriptional activation of the human p21$^{WAF1/CIP1}$ gene by retinoic acid receptor. *J. Biol. Chem.* **271**, 31723–31728.
29. Rogers, M. B., Watkins, S. C., and Gudas, L. J. (1990). Gene expression in visceral endoderm: A comparison of mutant and wildtype embryonal carcinoma cell differentiation. *J. Cell. Biol.* **110**, 1767–1777.
30. Wang, S.-Y., Roguska, M. A., and Gudas, L. J. (1989). Defective post-translational modification of collagen IV in a mutant F9 teratocarcinoma cell line is associated with delayed differentiation and growth arrest in response to retinoic acid. *J. Biol. Chem.* **264**(26), 15556–15564.
31. Gudas, L., Sporn, M., and Roberts, A. (1994). Cellular biology and biochemistry of the retinoids. *In* "The Retinoids: Biology, Chemistry, and Medicine" (M. Sporn, A. Roberts, and D. Goodman, Eds.), Raven Press, New York.
32. Rogers, M. B., Hosler, B. A., and Gudas, L. J. (1991). Specific expression of a retinoic acid-regulated, zinc-finger gene, Rex-1, in preimplantation embryos, trophoblast, and spermatocytes. *Development* **113**, 815–824.
33. Schöler, H. (1991). Octamania: The POU factors in murine development. *Trends Genet.* **7**, 323–329.
34. Yuan, H., Corbi, N., Basilico, C., and Dailey, L. (1995). Developmental-specific activity of the FGF-4 enhancer requires the synergistic action of Sox2 and Oct-3. *Genes Dev* **9**(21), 2635–2645.
35. Velcich, A., Delli-Bovi, P., Mansukhani, A., Ziff, E. B., and Basilico, C. (1989). Expression of the K-fgf protooncogene is repressed during differentiation of F9 cells. *Oncogene Res.* **5**(1), 31–37.
36. Rosenstraus, M., Sundell, C., and Liskay, R. (1982). Cell-cycle characteristics of undifferentiated and differentiating embryonal carcinoma cells. *Dev. Biol.* **89**, 516–520.
37. LaRosa, G. J., and Gudas, L. J. (1988). Early retinoic acid-induced F9 teratocarcinoma stem cell Gene ERA-1: Alternate splicing creates transcripts for a homeobox-containing protein and one lacking the homeobox. *Mol. Cell. Biol.* **8**, 3906–3917.
38. Langston, A., and Gudas, L. (1992). Identification of a retinoic acid responsive enhancer 3′ of the murine homeobox gene Hox 1.6. *Mech. Dev.* **38**, 217–228.
39. Spanjaard, R. A., Ikeda, M., Lee, P. J., Charpentier, B., Chin, W. W., and Eberlein, T. J. (1997). Specific activation of retinoic acid receptors (RARs) and retinoid X receptors reveals a unique role for RARγ in induction of differentiation and apoptosis of S91 melanoma cells. *J. Biol. Chem.* **272**, 18990–18999.
40. Gao, C., and Zelenka, P. (1997). Cyclins, cyclin-dependent kinases and differentiation. *BioEssays* **19**, 307–315.
41. Kiess, M., Gill, R., and Hamel, P. (1995). Expression and activity of the retinoblastoma protein (pRB)-family proteins, p107 and p130, during L6 myoblast differentiation. *Cell Growth Differ.* **6**, 1287–1298.
42. Meyyappan, M., Wong, H., Hull, C., and Riabowol, K. (1998). Increased expression of cyclin D2 during multiple states of growth arrest in primary and established cells. *Mol. Cell. Biol.* **18**, 3163–3172.
43. Bartkova, J., Lukas, J., Strauss, M., and Bartek, J. (1998). Cyclin D3: Requirement for G1/S transition and high abundance in quiescent tissues suggest a dual role in proliferation and differentiation. *Oncogene* **17**, 1027–1037.
44. Rogers, M. (1997). Life and death decisions influenced by retinoids. *Curr. Top. Dev. Biol.* **35**, 1–46.
45. Omenn, G. S., Goodman, G. E., Thornquist, M. D., Balmes, J., Cullen, M. R., Glass, A., Keogh, J. P., Meyskens, F. L., Valanis, B., Williams, J. H., Barnhart, S., and Hammar, S. (1996). Effects of a combination of beta carotene and vitamin A on lung cancer and cardiovascular disease. *N. Engl. J. Med.* **334**(18), 1150–1155.
46. Roy, B., Taneja, R., and Chambon, P. (1995). Synergistic activation of retinoic acid (RA)-responsive genes and induction of embryonal carcinoma cell differentiation by an RA receptor alpha (RAR alpha)-, RAR beta-, or RAR gamma-selective ligand in combination with a retinoid X receptor-specific ligand. *Mol. Cell. Biol.* **15**(12), 6481–6487.
47. Taneja, R., Roy, B., Plassat, J., Zusi, C., Ostrowski, J., Reczek, P., and Chambon, P. (1996). Cell-type and promoter-context dependent retinoic acid receptor (RAR) redundancies for *RARβ2* and *Hoxa-1* activation in F9 and P19 cells can be artefactually generated by gene knockouts. *Proc. Natl. Acad. Sci. USA* **93**, 6197–6202.
48. Boylan, J. F., Lohnes, D., Taneja, R., Chambon, P., and Gudas, L. J. (1993). Loss of retinoic acid receptor gamma function in F9 cells by gene disruption results in aberrant Hoxa-1 expression and differentiation upon retinoic acid treatment. *Proc. Natl. Acad. Sci. USA* **90**(20), 9601–9605.
49. Chiba, H., Clifford, J., Metzger, D., and Chambon, P. (1997). Distinct retinoid X receptor-retinoic acid receptor heterodimers are differentially involved in the control of expression of retinoid target genes in F9 embryonal carcinoma cells. *Mol. Cell. Biol.* **17**(6), 3013–3020.
50. Minucci, S., Zand, D., Dey, A., Marks, M., Nagata, T., Grippo, J., and Ozato, K. (1994). Dominant negative retinoid X receptor beta inhibits retinoic acid-responsive gene regulation in embryonal carcinoma cells. *Mol. Cell. Biol.* **14**, 360–372.
51. Davis, K. D., Berrodin, T. J., Stelmach, J. E., Winkler, J. D., and Lazar, M. A. (1994). Endogenous retinoid X receptors can function as hormone receptors in pituitary cells. *Mol. Cell. Biol.* **14**(11), 7105–7110.
52. Allegretto, E. A., Shevde, N., Zou, A., Howell, S. R., Boehm, M. F., Hollis, B. W., and Pike, J. W. (1995). Retinoid X receptor acts as a hormone receptor in vivo to induce a key metabolic enzyme for 1,25-dihydroxyvitamin D3. *J. Biol. Chem.* **270**(41), 23906–23909.
53. Allegretto, E., McClurg, M., Lazarchik, S., Clemm, D., Kerner, S., Elgort, M., Boehm, M., White, S., Pike, J., and Heyman, R. (1993). Transactivation properties of retinoic acid and retinoid X receptors in mammalian cells and yeast: Correlation with hormone binding and effects of metabolism. *J. Biol. Chem.* **268**, 26625–26633.
54. Lu, H. C., Eichele, G., and Thaller, C. (1997). Ligand-bound RXR can mediate retinoid signal transduction during embryogenesis. *Development* **124**(1), 195–203.
55. Wu, Q., Dawson, M. I., Zheng, Y., Hobbs, P. D., Agadir, A., Jong, L., Li, Y., Liu, R., Lin, B., and Zhang, X. K. (1997). Inhibition of trans-retinoic acid-resistant human breast cancer cell growth by retinoid X receptor-selective retinoids. *Mol. Cell. Biol.* **17**(11), 6598–6608.

Received March 3, 1999
Revised version received June 14, 1999

Breast Cancer Research and Treatment 59: 27–39, 2000.

Report

Cyclin D1 overexpression in a model of human breast premalignancy: preferential stimulation of anchorage-independent but not anchorage-dependent growth is associated with increased cdk2 activity

Qun Zhou[1], Julia Wulfkuhle[1], Taoufik Ouatas[1], Paula Fukushima[2], Maryalice Stetler-Stevenson[2], Fred R. Miller[3], and Patricia S. Steeg[1]

[1]*Women's Cancers Section and* [2]*Flow Cytometry Unit, Laboratory of Pathology, Division of Clinical Sciences, National Cancer Institute, Bethesda, MD;* [3]*Breast Cancer Program, Barbara Ann Karmanos Cancer Institute, Wayne State University, Detroit, MI, USA*

Key words: cyclin D1, premalignant disease progression, anchorage-independent growth, MCF-10A cells

Summary

Cyclin Dl is frequently overexpressed in human breast ductal carcinoma *in situ* (DCIS) specimens, which confer a high risk for the development of infiltrating ductal carcinoma. If causally involved in the genesis of human breast malignancy, cyclin D1 may represent an interesting target for chemopreventive approaches, as it sits at the junction of many growth factor and hormonal pathways. We have used the MCF-10A human breast cell line, derived from a mastectomy containing a low risk premalignant lesion, as a model system. Three cyclin D1 transfectants exhibited physiologically relevant levels of transgene overexpression, but no coordinate overexpression of other cell cycle related genes. Proliferation assays, flow cytometry, and cdk enzymatic assays of anchorage-dependent proliferation indicated only a minimal and transient effect of cyclin D1. In contrast, cyclin D1 overexpression significantly stimulated anchorage-independent colonization in soft agar or methylcellulose, accompanied by greater Gl-S progression. The cdk4 activity of the control- and cyclin D1 transfectants in colonization assays was comparable, but the cdk2 activity was higher in the latter. Injection of control- and cyclin D1 transfected MCF-10A cells in matrigel into nude mice failed to produce tumors within 1.5 years. The data suggest that cyclin D1 overexpression is an early feature of breast neoplastic progression, and can contribute to cancer development through the promotion of colonization.

Introduction

While prevention approaches to the development of hormone receptor-positive breast cancer have been developed [1], continued investigation of the molecular pathways contributing to breast malignancy will undoubtedly fuel the rational development of improved or more widely applicable preventive agents. One approach to this molecular characterization examines altered gene or protein expression levels among human breast biopsy specimens containing premalignant or ductal carcinoma *in situ* (DCIS) lesions, which have been associated with stratified risk estimates for patient development of invasive breast cancer [2–11].

We reported that 80% of DCIS specimens overexpressed cyclin D mRNA, as compared to normal ductal/lobular units in the margin of the biopsy specimen. A diagnosis of DCIS confers on the patient an 8–10 fold increased risk for the development of invasive breast cancer. Overexpression of cyclin D mRNA was infrequent in atypical ductal hyperplasia (ADH) or proliferative lesions, which confer lower risks [12]. This finding associated cyclin D overexpression with a relatively high risk for breast cancer development. Gillett et al. [13] confirmed and extended these data to the protein level, where 64% of DCIS overexpressed cyclin D1, in comparison to few lower risk ADH cases. Using a different cutpoint, where a case was

considered positive if 5% of the tumors stained, Alle et al. [14] reported that cyclin D1 expression increased from normal epithelial cells, to proliferative lesions and ultimately to DCIS. Two additional reports found cyclin D1 overexpression in DCIS, and that overexpression resulted from multiple mechanisms: gene amplification in many comedo or high grade forms, and protein overexpression in noncomedo or low grade forms [15, 16]. These observations indicate that cyclin D1 overexpression is a frequent event in DCIS, associated with a high risk estimate, and suggests the hypothesis that it functionally contributes to breast cancer development.

Cyclin D1 is one of the three members of a set of short-lived proteins which are essential activators of the cyclin-dependent kinases cdk4 and cdk2 involved in G1 cell cycle progression; the cyclin-cdk complexes can be inhibited by binding of several inhibitors ($p16^{ink4a}$, $p15^{ink4b}$, $p18^{ink4c}$, and $p19^{ink4d}$ specific for cyclin D-cdk complexes, and, $p21^{cip1}$, $p27^{kip1}$, and $p57^{kip}$ which are inhibitory to other cyclin-cdk complexes as well) (reviewed in [17, 18]). Recent reports indicate that cyclin D1 can serve additional functions, including the promotion of gene amplification in fibroblasts, participation in neuronal differentiation and apoptosis, modulation of DNA repair, direct activation of the estrogen receptor response element in breast cells, and binding of the DMP1 transcription factor [17, 19–25].

Despite years of investigation, the phenotypic role of cyclin D1 overexpression in breast cancer development remains incompletely understood. Transgenic mice overexpressing cyclin D1 tethered to a MMTV-LTR produced hyperplasias, and 8/12 mice developed mammary carcinomas with a mean latency of 551 days [26]. This hyperplastic phenotype differs from the human situation, where cyclin D overexpression was infrequent in typical or atypical hyperplasias [12, 13], and the long latency of carcinoma induction has suggested that other molecular events are required. This study underscores the need for careful analysis in human model systems. Two transfection studies using 'normal' human breast epithelial cells have been reported to date, with somewhat conflicting results – Han et al. [27] reported that cyclin D1 overexpressing HBL-100 clones were inhibited in anchorage-dependent and -independent growth and tumorigenicity. In contrast, Kamalati et al. [28] reported a growth advantage with cyclin D1 overexpression, similar to that reported in immortal fibroblasts and several other cell types. Interpretation of the data, however, was complicated by the SV40 large T antigen expression by both cell lines (which may alter the RB pathway that cyclin D1 affects), and potentially also by the variable presence of other cell cycle related proteins.

We report herein the effects of cyclin D1 transfection on the MCF-10A human mammary epithelial cell line. The MCF-10A line was derived from a mastectomy specimen containing premalignant, low risk fibrocystic changes and a focus of typical hyperplasia [29, 30]. It exhibits wild type p53, and is nontumorigenic. We report that cyclin D1 overexpression augmented anchorage-independent colonization, suggesting a contributory role to the genesis of human breast cancer.

Materials and methods

Cell culture and transfection

MCF-10A cells were grown in DMEM/F-12 (1:1) medium supplemented with 20 mM HEPES, 5% heat inactivated horse serum, 0.1 μg/ml cholera toxin, 10 μg/ml insulin, 100 U/ml penicillin, 100 μg/ml streptomycin, 10 ng/ml EGF, and 0.5 μg/ml hydrocortisone. The cells were maintained in a humidified atmosphere of 95% air, 5% CO_2 at 37°C. MCF-10A cells were infected with culture supernatants from the amphotropic packaging cell line PA317 (ATCC) transfected with pBabe retrovirus vector [31] with or without a cyclin D1 cDNA insert [32] under the control of a Mo MuLV LTR. Three cyclin D1 overexpressing clones were selected from 18 puromycin resistant colonies, based on cyclin D1 overexpression and lack of other cell cycle protein overexpression; three control transfectants (pBabe vector) were randomly selected. Where indicated, pools of control- or cyclin D1 transfectants were used, and were made by combining equal numbers of cells from the three clonal transfectants.

The KE and GH mutant forms of cyclin D1 [33] were subcloned into the pBabe vector. Virus supernatants from PA317 cells, which had been transfected with pBabe, pBabe-cyclin D1, pBabe-cyclin D1KE, and pBabecyclin D1GH were used to infect MCF-10A cells, as described above.

Cell proliferation assay

To assay anchorage-dependent growth, 200 MCF-10A cells in 100 μl medium were plated into each well of

96-well plates, which were coated in some experiments with fibronectin or matrigel. Cell proliferation was determined using the Cell Titer 96 TM kit according to the manufacturer's instructions (Promega) [34].

Anchorage-independent proliferation assay

Cell anchorage-independent growth was determined by soft agar [35] and methylcellulose culture [36]. For the soft agar assay, $0.5 - 1 \times 10^4$ cells/ml of MCF-10A control and cyclin D1 transfectants were grown in 0.5 ml of 0.3% Difco agar (Difco) in MCF-10A growth medium. The cell suspensions were layered over 0.5 ml of 0.7% bottom agar in 24-well plate. After two weeks of culture the colonies (>50 cells) in soft agar were counted using a grid on the bottom of the dish and a microscope. Each point represents the mean of three cultures and each experiment shown is representative of at least three conducted.

Cell cycle analysis

For monolayer culture, 2×10^5 cells per 60 mm culture dish of MCF-10A control and cyclin D1 transfectants were trypsinized and flow cytometric analysis was conducted on day 3 using propidium iodide staining on a Becton Dickinson FACScan flow cytometer [37]. For methylcellulose experiments, 1×10^6 cells from exponential cultures of MCF-10A control or cyclin D1 transfectants were grown in 8 ml of 1% methylcellulose (Sigma) in 15-ml conical tubes and harvested after 24 h of culture for flow cytometry.

Immunoprecipitation and western blot analysis

5×10^5 cells per 100 mm culture dish of MCF-10A control- or cyclin D1 transfectants were cultured for 2.5 days before they were lysed in buffer 1 (PBS with 1% NP-40, 1 mM PMSF, 5 μg/ml aprotinin, 5 μg/ml pepstatin, 10 μg/ml leupeptin, 1 mM NaF, 10 mM β-glycerophosphate, 0.1 mM sodium vanadate, and 5 mM EDTA). Cellular lysates equivalent to 60 or 100 μg protein were resolved on an 8–16% SDS–PAGE and were transferred to a nitrocellulose membrane. Western blots were performed using 1 μg/ml antibodies incubated overnight at 4°C and detected by chemiluminescence (DuPont NEN or Pierce). The antibodies to cyclin D1, cyclin D3, p21, p27, p16 (Lab. Vision), and cyclin E, Cdk2, Cdk4, Cdk6, p53 (Santa Cruz) were used. For immunoprecipitations, 500 μg lysates were precleared with protein A-sepharose (Pharmacia LKB) for 1 h, and the supernatants were incubated overnight at 4°C with 5 μg cyclin D1 polyclonal antibody (Upstate). The immune complexes were precipitated by protein A-sepharose and resolved on an 8–16% SDS–PAGE which was transferred to nitrocellulose. The cell cycle related proteins in cyclin D1 complex were detected by western blot.

Cyclin D1 kinase (cdk 4) assay

Exponential cultures of MCF-10A control or cyclin D1 transfectants were lysed in lysis buffer 2 (50 mM HEPES, pH7.5, containing 150 mM NaCl, 2.5 mM EGTA, 1 mM EDTA, 0.1% Tween-20, 10% glycerol, 1 mM DTT, 0.1 mM PMSF, 5 μg/ml pepstatin, 1 mM NaF, 10 μg/ml aprotinin, 10 mM β-glycerophosphate, and 0.1 mM sodium vanadate). Five hundred microgram lysates were precleared with protein A-sepharose before the supernatants were incubated with 5 μg cyclin D1 antibody (Upstate) for 3 h at 4°C. The immune complexes were precipitated by protein A-sepharose and cyclin D1 kinase activity was determined using 0.45 μg GST-Rb (Santa Cruz) and 10 μCi [γ-^{32}P]ATP (ICN) as described previously [37].

Cdk 2 kinase assay

Exponential cultures of MCF-10A control- or cyclin D1 transfectants were lysed in lysis buffer 3 (50 mM Tris–HCl, pH 7.5, containing 250 mM NaCl, 0.1% TritonX-100) with 0.1 mM PMSF, 5 μg/ml pepstatin, 1 mM NaF, 10 μg/ml aprotinin, 10 mM B-glycerophosphate, 0.1 mM sodium vanadate, and 1 mM EDTA. Five hundred micrograms of lysate was incubated with 2 μg anti-cdk2 (Santa Cruz) which had been precoated to protein A-sepharose for 3 h at 4°C. Cdk2 activity was determined using 5 μg histone H1 and 10 μCi [γ-^{32}P] ATP (ICN) as described previously [38].

Tumorigenicity assay using nude mice

Each of MCF-10A control and cyclin D1 transfectants was injected subcutaneously into ten 4–6 week old female NIH nu/nu mice. 1×10^7 cells suspended in 0.1 ml of matrigel were injected into the right and left dorsal flanks of the mouse [39]. After subcutaneous injection, animals were checked for palpable lesions at weekly intervals. All *in vivo* procedures were per-

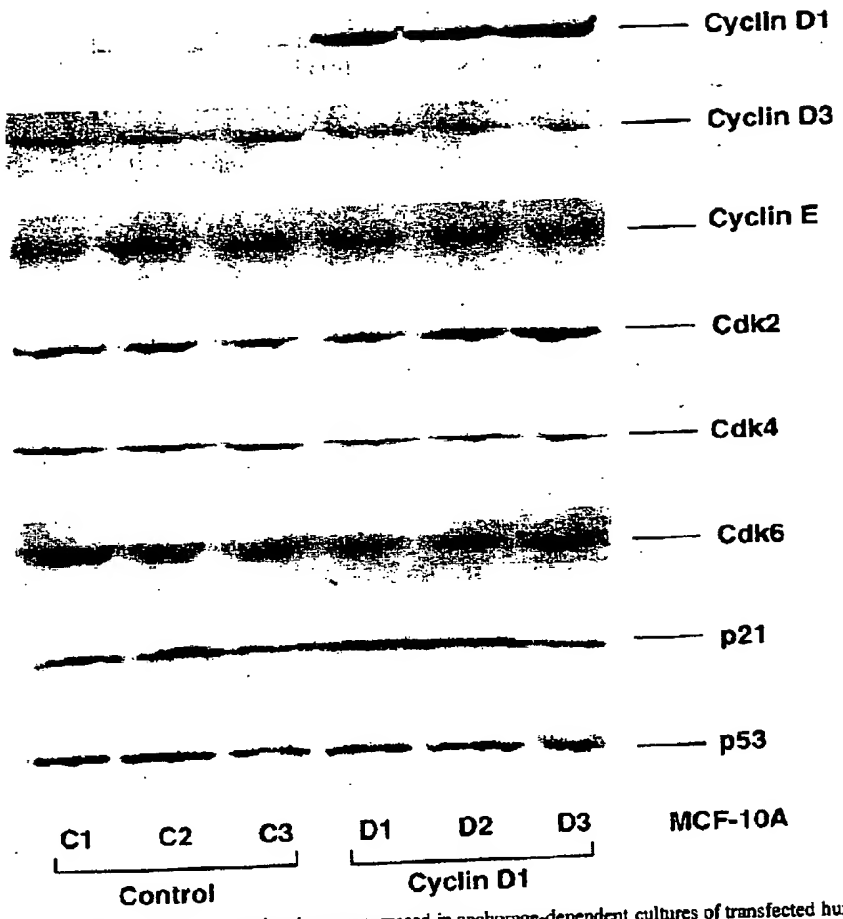

Figure 1. Cyclin D1, but not other cell cycle proteins, is overexpressed in anchorage-dependent cultures of transfected human MCF-10A breast clones. Western blots of total cell lysates from three independent cyclin D1 transfectants (D1, D2, and D3) and three independent control transfectants (C1, C2, C3) are shown for multiple proteins.

formed in compliance with approved NIH animal use proposal LP-008.

Results

Characterization of cyclin D1-transfected MCF-10A breast cells

MCF-10A cells were transfected with a pBabe retroviral vector containing a cyclin D1 cDNA or empty insert. Figure 1 shows the cyclin D1 protein levels among three independent control clones (C1, C2, C3) and three cyclin D1 transfectants (D1, D2, D3). Five–ten fold overexpression was noted in the cyclin D1 transfectants. Because studies have reported the overexpression of other cell cycle related genes coincident with cyclin D1 transfection (27, 40), clones were analyzed for cyclin, cdk, and cdk-inhibitor protein levels by western blot analysis. We did not find frequent overexpression of other cell-cycle proteins in the majority of the MCF-10A clonal transfectants. As shown in Figure 1, cyclins D3 and E, cdks 2, 4 and 6, p21, and p53 were expressed at comparable levels in the two sets of transfected clones. p27 was difficult to visualize in 100 μg of cell lysate but appeared equally expressed (data not shown); other proteins which were undetectable in 100 μg of cell lysate included cyclin D2 and p16.

Effect of cyclin D1 transfection on anchorage-dependent growth

In the experiments shown in Figure 2, MCF-10A clones were cultured under various conditions in microtiter wells, and anchorage-dependent growth quantitated using a MTT assay. At normal serum concen-

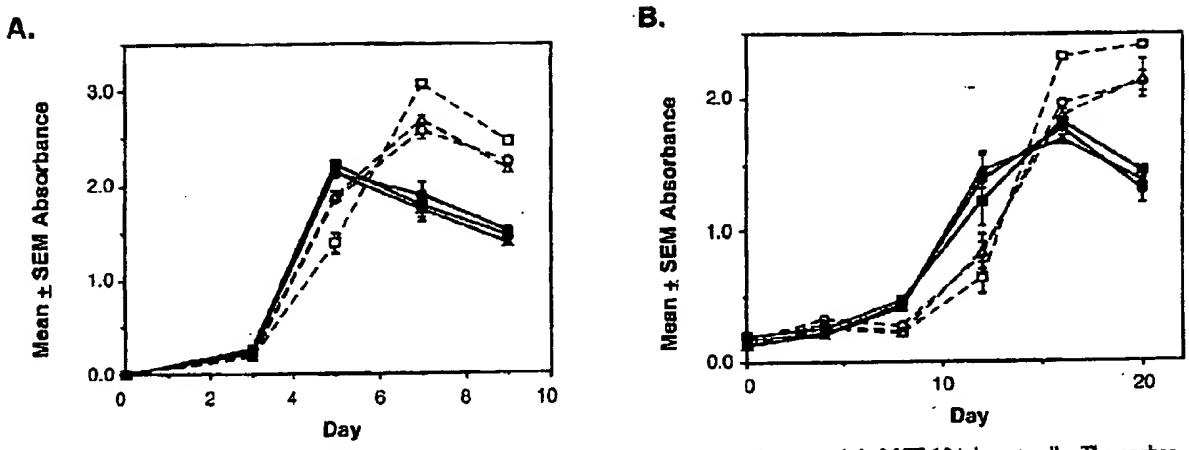

Figure 2. Cyclin D1 overexpression induces only a transient increase in anchorage-dependent growth in MCF-10A breast cells. The anchorage-dependent growth of three independent control transfectants (C1, C2, and C3, dashed lines) and three independent cyclin D1 transfectants (D1, D2, and D3, solid lines) was determined on multiple days of culture using a spectrophotometric assay. The mean ± sem absorbance of triplicate cultures at each timepoint is graphed under two culture conditions: (A) Normal (10%) serum; (B) Low (0.1%) serum. Cyclin D1 transfectants significantly varied from the control transfectants ($p < 0.01$, student's *t*-test): Panel A, days 5,7,9; Panel B: days 12, 20.

trations (Figure 2A), each of the three independent cyclin D1 transfectants (solid lines) exhibited a slight (30%) increase in cell density through the exponential phase of growth (days 3–5 of culture), as compared to control transfectants (dashed lines). This increase was not maintained, as the cyclin D1 transfectants subsequently exhibited a 30% decrease in cell number as compared to the control transfectants on days 7–9 of culture. Similar trends were observed if the cells were cultured on fibronectin or matrigel (data not shown). Growth in low serum media is often considered an assay of growth factor independence. The cyclin D1 transfectants exhibited similar anchorage-dependent growth trends in 0.5% serum, but with a longer time course (20 days) and a maximum of 2-fold growth stimulation over controls (Figure 2B).

The relatively minor growth advantage of the cyclin D1 transfectants was mirrored in their cell cycle distribution (Table 1). Flow cytometry of each clone on day 1 of culture indicated that 33–35% of the cyclin D1 transfectants were in S-phase, as compared to 24–30% of control transfectants. The increased S-phase expression of the cyclin D1 transfectants was at the expense of G0/G1 participation. G2/M levels remained comparable in all of the transfectants.

Increased cyclin D1 was observed in the D1–D3 clones upon immunoprecipitation (Figure 3), confirming the western blot data. The increased amount of cyclin D1 in these clones was associated with a 2-fold increase in cdk4 binding, and a 4-fold increase in the amount of p21 bound. Low but comparable amounts of p27 were found in the cyclin D1 and control transfectant complexes (data not shown). The enzymatic activities of the cyclin D1-cdk complexes from each transfectant were assayed by immunoprecipitation and kinase assays (Figure 3B). When anti-cyclin D1 immunoprecipitated complexes were incubated with ^{32}P-γATP and RB in an assay of cdk4 function, a minor (25% by densitometry) but repeatable increase in RB kinase activity was observed in the cyclin D1 transfectants. The RB phosphorylation status of the control- and cyclin D1 transfectants was comparable on western blots (data not shown). Cyclin D1 has been reported to indirectly affect Cdk2 activity, via its binding of common cdk inhibitors [41]. When lysates were immunoprecipitated with anti-Cdk2 and tested in a histone kinase assay, comparable activity was demonstrated in all lysates (Figure 3B) suggesting that this

Table 1. Cell cycle distribution of control- and cyclin D1 transfected MCF-10A breast cells under anchorage-dependent culture conditions

Clone	G0+G1 (%)	S (%)	G2+M (%)
C1	50.5	30.4	19.1
C2	52.0	24.5	23.5
C3	52.1	28.4	19.5
D1	43.9	33.6	22.5
D2	44.9	34.9	20.2
D3	47.1	34.2	18.8

Cells were harvested from semiconfluent cultures and the cell cycle distribution analyzed by flow cytometry. Data are from a single culture of each transfectant, and representative of three independent experiments conducted.

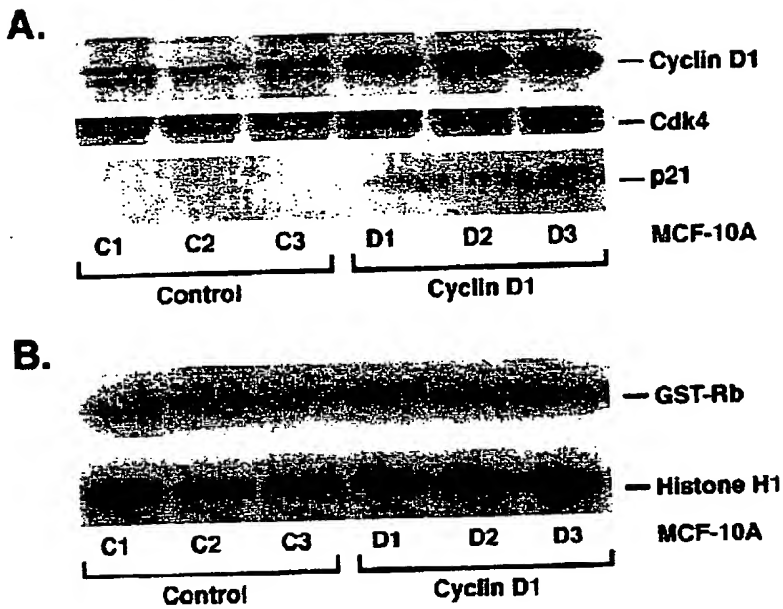

Figure 3. Cyclin D1 complex formation and cdk enzymatic activities under anchorage-dependent conditions. A. Cell lysates from three control transfectants (C1, C2, and C3) and three cyclin D1 transfectants (D1, D2, and D3) were immunoprecipitated with anticyclin D1, and proteins in the complex resolved by western blot analysis. B. Anti-cyclin D1 or anti-cdk2 immunoprecipitated cell lysates were assayed for kinase activity using GST-RB and Histone as substrates, respectively.

titration of cdk inhibitors had not occurred. Taken together, the data indicate that overexpression of cyclin D1 in the MCF-10A breast cell line resulted in a minor and ephemeral increase in anchorage-dependent growth, which was correlated with a minor increase in cdk4 activity.

Effect of cyclin D1 transfection on anchorage-independent growth

In contrast to anchorage-dependent assays, a significant increase in anchorage-independent colonization was observed in each of the cyclin D1 transfectants. This increase was observed using either 0.3% agar (Figure 4A) or 1.0% methylcellulose (Figure 4B) in the cultures, the latter of which permitted harvest of the cells for subsequent assays. A photograph showing representative colonies formed by the cyclin D1 transfectants is included as Figure 4C; the three-dimensional nature of the soft-agar culture necessarily makes some colonies poorly focused. The increased colonization potential of the cyclin D1 transfectants was maintained through the limit of our culture conditions, approximately five weeks.

Flow cytometry of control- and cyclin D1 transfectants harvested from methylcellulose cultures is summarized in Table 2. Overall levels of S-phase participation were lower than under anchorage-dependent conditions (Table 1), with a greater percentage of cells in G0/G1. However, the cyclin D1 transfectants contained 18–21% of cells in S-phase, as compared to 9–10% of control transfectants. This represents a larger difference than under anchorage-dependent conditions.

In order to investigate the mechanism of anchorage-independent colonization further, we determined the relative expression levels of cell-cycle proteins in total cell lysates from methylcellulose cultures. While cyclin D1 was overexpressed in the D1–3 transfectants, comparable levels of cyclins D3 and E, cdks 2, 4 and 6, p16, p21, p53, and p27 were observed in the cyclin D1 and control-transfectants (data not shown). Immunoprecipitation of cyclin D1 from anchorage-independent cultures and western blot analysis of complexes is shown in Figure 5A. The immunoprecipitations resemble those conducted under anchorage-dependent conditions, exhibiting a relatively minor increase in cdk4 binding, and a substantial increase in p21 binding. Enzymatic activities of the lysates under anchorage-independent conditions are shown in Figure 5B. The cdk4 activity of the transfectants was comparable. In data not shown, the Rb protein level and phosphorylation status were also comparable. In a significant diversion from data under

anchorage-dependent conditions, the cdk2 activity of the cyclin D1 transfectants was present, and virtually undetectable in the control transfectants. Thus,

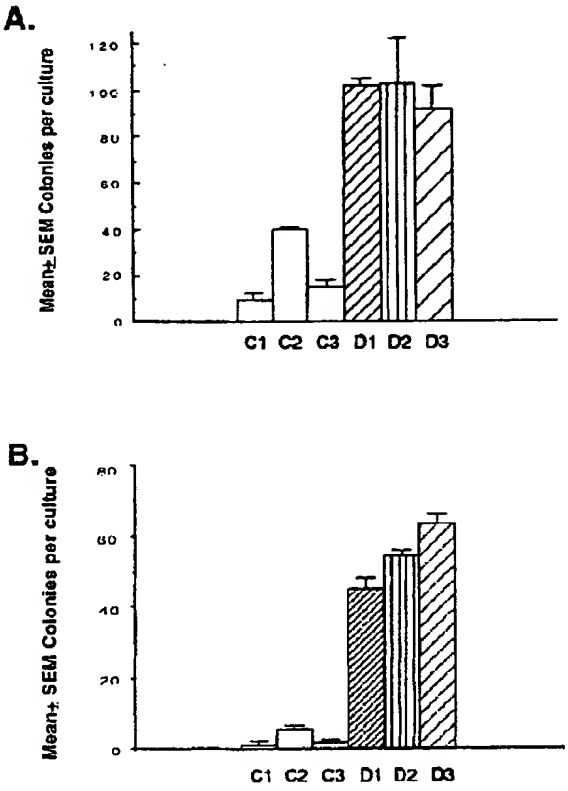

Figure 4. Cyclin D1 overexpression by MCF-10A breast cells increases anchorage-independent colonization. The colonization of control transfectants (open bars) and cyclin D1 transfectants (filled bars) in anchorage-independent assays using 0.3% soft agar (Panel A) or 1% methylcellulose (Panel B) was determined after 2 weeks of culture. Each point represents the mean ± sem of triplicate cultures. The colonization of the control- and cyclin D1 transfectants was significantly different, $P < 0.01$, student's *t*-test. Panel C shows a representative photomicrograph of soft agar colonies produced by the cyclin D1 transfectant.

Table 2. Cell cycle distribution of control- and cyclin D1 transfected MCF-10A breast cells under anchorage-independent culture conditions

Clone	G0+G1 (%)	S (%)	G2+M (%)
C1	76.4	8.9	14.7
C2	74.6	9.6	15.8
C3	76.0	9.8	14.2
D1	65.3	17.9	16.8
D2	63.3	21.3	15.4
D3	62.8	20.4	16.8

Cells were harvested after 24 h culture in methylcellulose, and the cell cycle distribution analyzed by flow cytometry. Data were obtained from a single culture of each transfectant, and are representative of three independent experiments conducted.

the increased anchorage-independent colonization of cyclin D1 overexpressing human MCF-10A clones was associated with a relative increase in cdk2 activity. While western blot data established that the control- and cyclin D1 transfectants expressed comparable amounts of p21, we asked if overall levels of p21 varied between culture conditions. The western blot shown in Figure 5C indicates that, while p21 levels were comparable between the control- and cyclin D1 pooled transfectants, p21 was decreased by anchorage-independent culture conditions.

Site directed mutagenesis of cyclin D1

MCF-10A cells were transfected side-by-side with a control vector, wild type cyclin D1, and two cyclin D1 mutant constructs. The KE mutation alters the 'cyclin box' of cyclin D1 such that interaction with cdk4 is inhibited [33]; the GH mutation abrogates cyclin D1 binding to the RB protein [32]. Three clones expressing each mutant transfectant were compared to control and wild type transfectants (Figure 6A). Expression of the KE mutant was high among 14 clones analyzed, and three representative independent clones were selected; expression levels of the GH mutant were lower overall. Three wild type cyclin D1 clones (D4–D6) were selected which reflected the range of overall protein expression, and three control clones were randomly selected (C4–C6).

The colonization potential of each clone is graphed in Figure 6B. Three wild type cyclin D1 transfectants produced significantly more colonies than control transfectants. Colonization by KE overexpressing clones was comparable to that of the control transfectants, implicating the cdk binding and/or activity

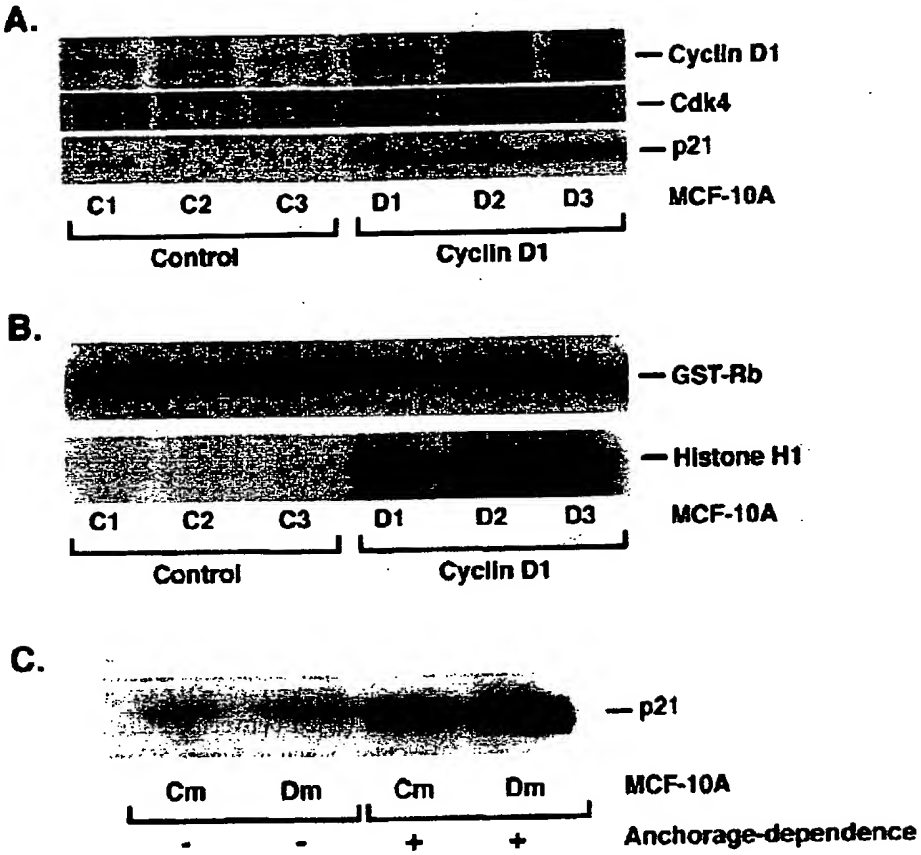

Figure 5. Cyclin D1 complex formation and cdk enzymatic activities under anchorage-independent conditions. A. Cell lysates from three control transfectants (C1, C2, and C3) and three cyclin D1 transfectants (D1, D2, and D3) were immunoprecipitated with anticyclin D1, and proteins in the complex resolved by western blot analysis. B. Anti-cyclin D1 or anti-cdk2 immunoprecipitated cell lysates were assayed for kinase activity using GST-RB and histone as substrates, respectively. C. Pools of the three control transfectants (Cm) and three cyclin D1 transfectants (Dm) were grown under anchorage-dependent and -independent conditions, harvested, and western blot analysis of p21 conducted.

of cyclin D1 in its colonization potential in this model system. However, destruction of the RB binding motif in cyclin D1 did not inhibit colonization. Thus, the cyclin D1-cdk interactive and not the RB associative properties of cyclin D1 were required for its potentiation of colonization.

In vivo *growth of the cyclin D1 transfectants*

Injection of a bolus ($\geq 10^7$ cells) of the parent MCF-10A line into mice, either in the presence or absence of matrigel, resulted in the presence of small palpable nodules which disappeared after several weeks. Derivatives of this line containing mutated *ras* have occasionally produced premalignant lesions and tumors when injected sc in matrigel [29], so this procedure was adopted to test the tumorigenicity of the cyclin D1 and control transfectants. Figure 7 shows the results of one of two experiments conducted, in which 10^7 cells were injected sc within matrigel in each flank of the mice. The initial lesion size at injection was comparable between the control- and cyclin D1 transfected clones. The lesions from all of the transfectants disappeared by week 8. At one year postinjection no lesions appeared palpable, and histological examination of H&E stained sections from the injection site contained only normal mammary fat-pad structures (personal communication, Drs. Maria Merino and Gil Smith, NCI). Thus, despite increased colonization potential, the cyclin D1 transfectants remained nontumorigenic.

Discussion

In order to determine the contribution of cyclin D1 overexpression to the genesis of human breast can-

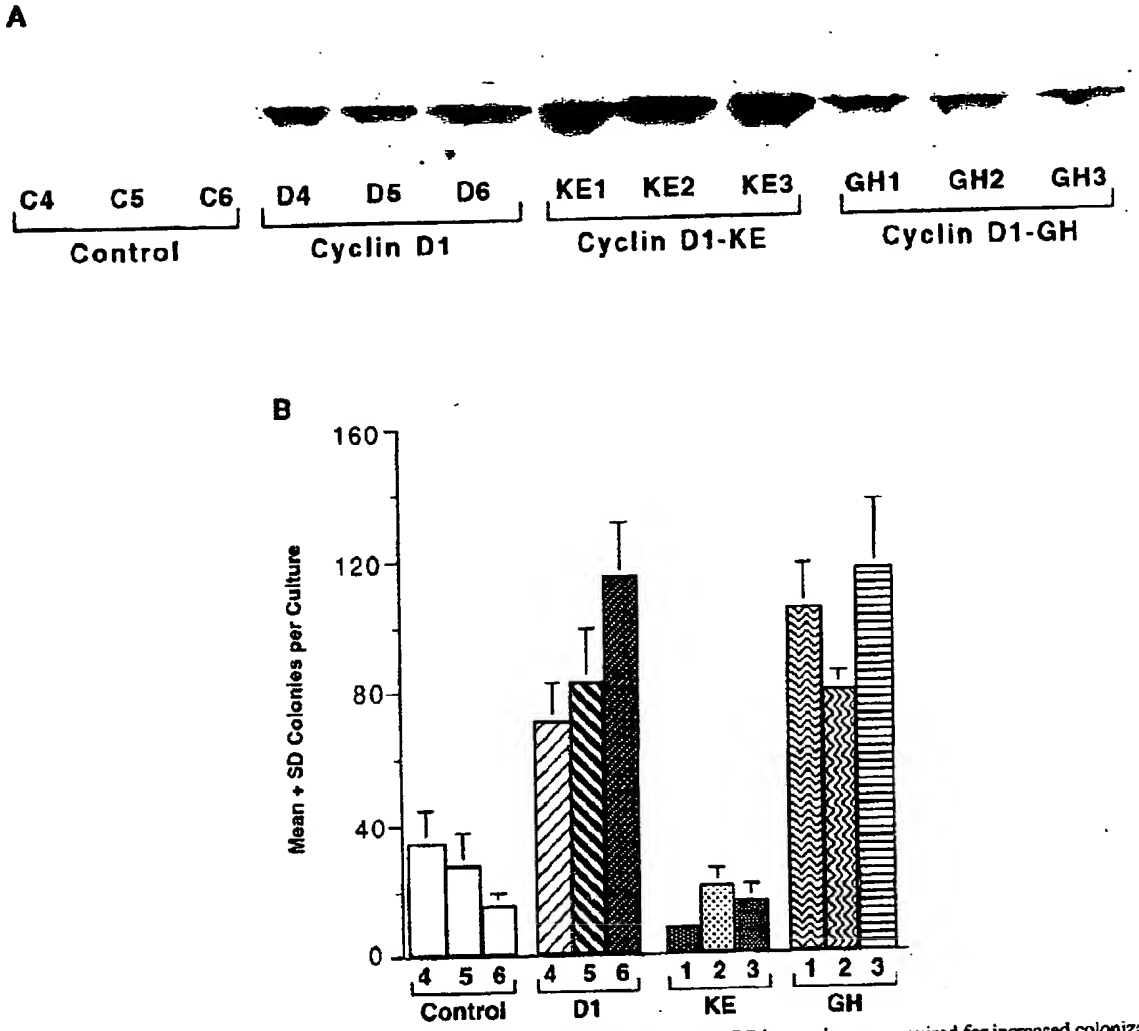

Figure 6. Site directed mutagenesis of cyclin D1 reveals that its cdk association, but not RB interaction, are required for increased colonization. MCF-10A cells were transfected, and overexpressing independent clones identified for a control vector (C4, C5, and C6), wild type cyclin D1 (D4, D5, and D6), the KE mutant of cyclin D1 involved in the cyclin box (KE1, KE2, and KE3) (significantly different from cyclin D1 transfectants, $p < 0.05$, student's t-test), and the GH mutant of cyclin D1 involved in RB binding (GH1, GH2, and GH3). Panel A: Total cyclin D1 protein levels determined by western blot. Panel B: Anchorage-independent colonization in soft agar, with each bar representing the mean ± sem of triplicate cultures.

cer, model systems which faithfully reflect the disease process must be developed. Several features of the model system described herein have been optimized. First, cyclin D1 overexpression was obtained in the range of 5–10 fold. When grains of *in situ* hybridization were counted in our cohort study, the minimal difference denoting overexpression was 2–3 fold, and many lesions were double this, in the 4–9 fold range [12]. Thus, the degree of overexpression in this transfection study was consistent with values observed in nature. Second, the transfected MCF-10A clones did not vary in overall levels of a number of other cell cycle related genes, including other cyclins, cdks, cdk inhibitors, and p53. Secondary or random changes in gene expression have hampered the interpretation of other cyclin D1 transfection studies [27, 40]. Third, the recipient cell line, MCF-10A, was derived from a mastectomy specimen containing low risk premalignant breast disease, and approximates the premalignant phenotype. MCF-10A cells exhibit advanced features such as immortalization, but normal phenotypes in p53, tumorigenicity, etc. To our knowledge,

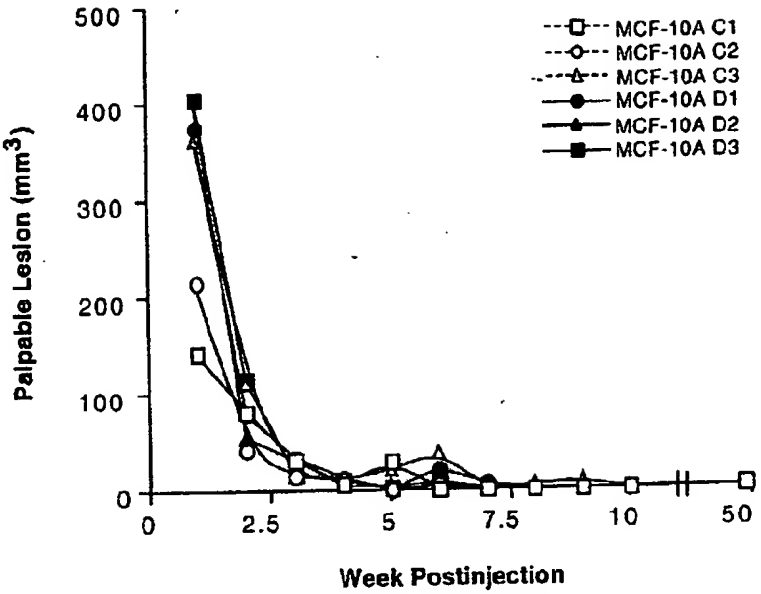

Figure 7. Cyclin D1 overexpression by human MCF-10A breast cells is insufficient to produce tumorigenicity *in vivo*. Three control transfectants (C1, C2, and C3, open symbols) and three cyclin D1 transfectants (D1, D2, and D3, closed symbols) were injected sc in matrigel into each flank of nu/nu mice, and lesion size estimated as $l \times w \times h$, determined weekly by calipers, for one year.

no cell lines exist from a DCIS lesion. Fourth, the use of methylcellulose cultures for anchorage-independent assays has enabled some of the first molecular characterization of this complex phenomenon. The model can be extended in future studies in several directions. For instance, the additive or synergistic role of genes whose altered expression is prevalent in comedo DCIS would be of interest. Candidates include erb-B-2/Her-2/neu, mutated p53, angiogenesis stimulators and inhibitors, etc. Also, studies for other functions of cyclin D1 not directly related to G1 progression, are of interest to determine if they also affect the breast cancer phenotype.

We present a characterization of the growth effects of cyclin D1 transfection *in vitro* and *in vivo*. The most salient finding is that overexpression of cyclin D1 significantly increased anchorage-independent colonization of the MCF-10A cells. This can be postulated to promote colonization of 'normal' epithelial cells in the breast architecture, which may contribute to their neoplastic progression. In this model system overexpression of cyclin D1 failed to promote full tumorigenicity within a period of 1.5 years. This would be consistent with transgenic mouse data if the long latency and focal nature of the mammary carcinomas were due to a requirement for additional molecular events [26, 42]. Thus, if our model system is relevant to human breast cancer, it is likely that cyclin D1 overexpression is contributory but not sufficient.

The complexity of cyclin D1 action is suggested by its stimulation of anchorage-independent, but not dependent, growth in our model system. Similar trends have been reported for cyclin D1 overexpression in other cell types, including rodent fibroblasts and human gliomas [43], suggesting the generality of this phenotype. Other cell cycle genes have also exerted varying effects on anchorage-independent and -dependent growth in transfection studies, but the mechanism of differential regulation was unknown [44, 45]. Overall levels of many cell-cycle proteins as well as those proteins binding cyclin D1 were examined from both anchorage-dependent and methylcellulose cultures, and appeared comparable between the control- and cyclin D1 transfectants. Our data from anchorage-dependent conditions indicated that cdk4 activity was not significantly increased by cyclin D1 overexpression, perhaps because of the additional p21 binding to the complex. Based on the site-directed mutation data, the binding of cyclin D1 to cdks was necessary for colonization, however. The formation of a cyclin D1-cdk complex is now known to require additional proteins, including p21 and/or p27 [46–48]. Given the observation that the enzymatic activity of this complex was not dramatically changed, the

data suggest that the binding activity of the complex may be important. Another potential contributor to the anchorage-dependent data is a block in S-phase, which could involve additional unstudied mechanisms.

The most profound difference between the anchorage-dependent and -independent cultures lies in the dramatic difference in cdk2 activity between the cyclin D1 and control transfectants under the latter culture conditions. The loss of normal, but not transformed, cell growth when changed to anchorage-independence has been previously correlated with reduced cdk2, kinase activity [49]. One explanation for the observed data is that two events, (1) increased cyclin D1 which bound p21 and cdk4, and (2) an overall decrease in p21 levels in anchorage-independent conditions, served to titrate-out free p21, resulting in enhanced cdk2 activity. Other proteins unstudied herein may also contribute to the observed colonization. A similar sequestration of p21, with concomitant activation of cdk2, was recently proposed to mediate estrogen induced growth of breast cells [50, 51]. p21 has also been reported to participate in other pathways not directly involved in G1 progression, including DNA repair, centrosome duplication, and mRNA splicing [52–54], and these pathways may be participatory. Immunohistochemical studies have detected heterogeneous expression and potential mutations of p21 in human breast DCIS specimens [55, 56], suggesting the potential relevance of this pathway to the human disease. Several reports have found opposite trends, whereby overexpression of cyclin D1 induced p21 expression [43], or where anchorage-independence resulted in increased p21 expression [57, 58]. Many of these findings were mediated by p53, and it may be that p53-dependent and -independent pathways exist.

If confirmed in additional human model systems, cyclin D1 may represent an interesting target for pilot breast cancer chemoprevention studies. Our data suggesting a facilitation of G1-S progression in colonization represents a point at which many growth factor and hormonal signaling pathways converge, and thus may be more widely applicable, including the estrogen-receptor negative subpopulation for which we have no effective chemoprevention regimens yet. Indeed, our laboratory and others have reported that retinoids, which are being considered in a chemopreventative setting, decrease breast tumor cell line cyclin D1 expression *in vitro* [37, 59, 60].

Acknowledgements

The authors are grateful to Dr. Hynda Klienman, NIDR, for provision of matrigel; to Dr. Steven Dowdy, HHMI, Washington University, Dr. Philip Hinds, Harvard Medical School, and Dr. Robert Weinberg, Whitehead Institute for Biomedical Research, for provision of pBabe, cyclin D1, cyclin D1-KE, and cyclin D1-GH; to Dr. Maria Merino and Dr. Gil Smith, NCI, for pathologic analysis of H&E stained sections; and to Mr. Andrew McMarlin for animal technical assistance.

References

1. Fisher B, Constantino J, Wickerham D, Redmond C, Kavanah M, Cronin W, Vogel V, Robidoux A, Dimitrov N, Atkins J, Daly M, Wieland S, Tan-Chiu E, Ford L, Wolmark N, et al.: Tamoxifen for prevention of breast cancer: report of the National surgical adjuvant breast and bowel project P-1 study. J National Cancer Inst 90: 1371–1388, 1998
2. DuPont W, Page D: Risk factors for breast cancer in women with proliferative breast disease. New Engl J Med 312: 146–151, 1985
3. DuPont W, Parl F, Hartmann W, Brinton L, Winfeld A, Worrell J, Schuyler P, Plummer W: Breast cancer risk associated with proliferative breast disease and atypical hyperplasia. Cancer 71: 1258–1265, 1993
4. London S, Connolly J, Schnitt S, Colditz G: A prospective study of benign breast disease and the risk of breast cancer. JAMA 267: 941–944, 1992
5. Marshall L, Hunter D, Connolly J, Schnitt S, Byrne C, London S, Colditz G: Risk of breast cancer associated with atypical hyperplasia of lobular and ductal types. Cancer Epidemiology, Biomarkers and Prev 6: 297–301, 1997
6. Ottesen GL, Graversen HP, Blichert TM, Zedeler K, Andersen JA: Ductal carcinoma *in situ* of the female breast: short term results of a prospective nationwide study. Amer J Surg Pathol 16: 1183–1196, 1992
7. Page D: Cancer risk assessment in benign breast biopsies. Human Pathol 17: 871–874, 1986
8. Page D, DuPont W: Anatomic indicators (histologic and cytologic) of increased breast cancer risk. Breast Cancer Res Treat 28: 157–166, 1993
9. Tavassoli F, Norris H: A comparison of the results of long-term follow-up for atypical intraductal hyperplasia and intraductal hyperplasia of the breast. Cancer 65: 518–529, 1990
10. Ward BA, McKhann CF, Ravikkumar TS: Ten year follow-up of breast carcinoma *in situ* in Connecticut. Archives of Surgery 127: 1392–1395, 1992
11. Jacobs T, Byrne C, Colditz G, Connolly J, Schnitt S: Radial scars in benign breast-biopsy specimens and the risk of breast cancer. New Engl J Med 340: 430–436, 1999
12. Weinstat-Saslow D, Merino MJ, Manrow RE, Lawrence JA, Bluth RF, Wittenbel KD, Simpson JF, Page DL, Steeg PS: Overexpression of cyclin D mRNA distinguishes invasive and *in situ* breast carcinomas from non-malignant lesions. Nature Med 1: 1257–1260, 1995

13. Gillett C, Lee A, Millis R, Barnes D: Cyclin D1 and associated proteins in mammary ductal carcinoma *in situ* and atypical ductal hyperplasia. J Pathol 184: 396–400, 1998
14. Alle K, Henshall S, Field A, Sutherland R: Cyclin D1 protein is overexpressed in hyperplasia and intraductal carcinoma of the breast. Clin Cancer Res 4: 847–854, 1998
15. Simpson J, Quan D, O'Malley F, Odom-Maryon T, Clarke P: Amplification of CCND1 and expression of its protein product, cyclin D1, in ductal carcinoma *in situ* of the breast. Am J Pathol 151: 161–168, 1997
16. Vos C, Haar NT, Peterese J, Cornelisse G, Vijer MVd: Cyclin D-1 gene amplification and overexpression are present in ductal carcinoma *in situ* of the breast. J Pathol 187: 279–284, 1999
17. Hunter T, Pines J: Cyclins and Cancer II: Cyclin D and CDK inhibitors come of age. Cell 79: 573–582, 1994
18. Sherr C: Cancer cell cycles. Science 274: 1672–1677, 1996
19. Asano K, Sakamoto H, Sasaki H, Ochiya T: Tumorigenicity and gene amplification potentials of cyclin D1-overexpressing NIH3T3 cells. Biochem Biophys Res Commun 217: 1169–1176, 1995
20. Freeman R, Estus S, EM Johnson J: Analysis of cell cycle-related gene expression in postmitotic neurons: selective induction of cyclin D1 during programmed cell death. Neuron 12: 343–355, 1994
21. Inoue K, Sherr C: Gene expression and cell-cycle arrest mediated by transcription factor DMP1 is antagonized by D-type cyclins though a cyclin-dependent-kinase-independent mechanism. Mol Cell Biol 18: 1590–1600, 1998
22. Kranenburg O, Eb Av, Zantema A: Cyclin D1 is an essential mediator of apoptotic neuronal cell death. EMBO J 15: 46–54, 1996
23. Neuman E, Ladha M, Lin N, Upton T, Miller S, Renzo JD, Pestell R, Hinds P, Dowdy S, Brown M, Ewen M: Cyclin D1 stimulation of estrogen receptor transcriptional activity independent of cdk4. Mol Cell Biol 17: 5338–5347, 1997
24. Zhou P, Jiang W, Weghorst CM, Weinstein IB: Overexpression of cyclin D1 enhances gene amplification. Cancer Res 56: 36–39, 1996
25. Zwijsen R, Wientjens E, Klompmaker R, Sman JVd, Bernards R, Michalides R: CDK-independent activation of estrogen receptor by cyclin D1. Cell 88: 405–415, 1997
26. Wang T, Cardiff R, Zukerberg L, Lees E, Arnold A, Schmidt E: Mammary hyperplasia and carcinoma in MMTV-cyclin D1 transgenic mice. Nature 369: 669–671, 1994
27. Han EK-H, Sgambato A, Jiang W, Zhang Y-J, Santella R, Doki Y, Cacace A, Schieren I, Weinstein I: Stable overexpression of cyclin D1 in a human mammary epithelial cell line prolongs the S-phase and inhibits growth. Oncogene 953–961, 1995
28. Kamalati T, Davies D, Titley J, Crompton M: Functional consequences of cyclin D1 overexpression in human mammary luminal epithelial cells. Clin Exp Metast 16: 415–426, 1998
29. Miller F, Soule H, Tait L, Pauley R, Wolman S, Dawson P, Heppner G: Xenograft model of progressive human proliferative breast disease. J Nat'l Cancer Inst 85: 1725–1732, 1993
30. Soule H, Maloney T, Wolman S, WD Peterson J, Brenz R, McGrath C, Russo J, Pauley R, Jones R, Brooks S: Isolation and characterization of a spontaneously immortalized human breast epithelial cell line, MCF-10. Cancer Res 50: 6075–6086, 1990
31. Morgenstern J, Land H: Advanced mammalian gene transfer: High titer retroviral vectors with multiple drug selection markers and complimentary helper free packaging cell line. Nucl Acids Res 18: 3587–3596, 1990
32. Dowdy SF, Hinds PW, Louie K, Reed SI, Arnold A, Weinberg RA: Physical interaction of the retinoblastoma protein with human D cyclins. Cell 73: 499–511, 1993
33. Hinds PW, Dowdy SF, Eaton EN, Arnold A, Weinberg RA: Function of a human cyclin gene as an oncogene. Proc Natl Acad Sci USA 91: 709–713, 1994
34. Preije JMP, Lawrence JA, Hollingshead MG, Rosa ADL, Narayanan V, Grever M, Sausville EA, Paull K, Steeg PS: Identification of compounds with preferential *in vitro* inhibitory activity against low Nm23 expressing human breast carcinoma and melanoma cell lines. Nature Med 3: 395–401, 1997
35. Freshney R: Culture of Animal Cells, 2nd edition. Alan R. Liss, Inc. New York, 1987, pp. 137–153
36. Kang J, Krauss R: Ras induces anchorage-independent growth by subverting multiple adhesion regulated cell cycle events. Mol Cell Biol 16: 3370–3380, 1996
37. Zhou Q, Stetler-Stevenson M, Steeg P: Inhibition of cyclin D expression in human breast carcinoma cells by retinoids *in vitro*. Oncogene 15: 107–115, 1997
38. Gorospe M, Liu Y, Xu Q, Chrest FJ, Holbrook NJ: Inhibition of G1 cyclin-dependent kinase activity during growth arrest of human breast carcinoma cells by prostaglandin A2. Mol Cell Biol 14: 762–770, 1996
39. Dawson P, Wolman S, Tait L, Heppner G, Miller F: MCF10AT: a model for the evolution of cancer from proliferative breast disease. Am J Pathol 148: 313–319, 1996
40. Han E-H, Begemann M, Sgambato A, Soh J-W, Doki Y, Xing W-Q, Liu W, Weinstein I: Increased expression of cyclin D1 in a murine mammary epithelial cell line induces p27kipl, inhibits growth and enhances apoptosis. Cell Growth Diff 7: 699–710, 1996
41. Sherr C, Roberts J: Inhibitors of mammalian G1 cyclin dependent kinases. Genes Dev 9: 1149–1163, 1995
42. Barnes D: Cyclin D1 in mammary carcinoma. J Pathol 181: 267–269, 1997
43. Hiyama H, Iavarone A, LaBaer J, Reeves S: Regulated ectopic expression of cyclin D1 induces transcriptional activation of the cdk inhibitor p21 gene without altering cell cycle progression. Oncogene 14: 2533–2542, 1997
44. Michieli P, Li W, Lorenzi M, Miki T, Zakut R, Givol D, Pierce J: Inhibition of oncogene-mediated transformation by ectopic expression of p21 (Waf) in NIH3T3 cells. Oncogene 12: 775–784, 1996
45. Castellano M, Gabrielli B, Hussussian C, Dracopoli N, Hayward N: Restoration of CDKN2A into melanoma cells induces morphologic changes and reduction in growth rate but not anchorage-independent growth reversal. J Invest Dermatol 109: 61–68, 1997
46. Cheng M, Olivier P, Diehl J, Fero M, Roussel M, Roberts J, Sherr C: The p2lcipl and p27kipl CDK 'inhibitors' are essential activators of cyclin D-dependent kinases in murine fibroblasts. EMBO J 18: 1571–1583, 1999
47. Parry D, Mahony D, Wills K, Lees E: Cyclin D-CDK subunit arrangement is dependent on availability of competing INK4 and p21 class inhibitors. Moll Cell Biol 19: 1775–1783, 1999
48. Welcker M, Lukas J, Strauss M, Bartek J: p21 WAF/CIP1 mutants deficient in inhibiting cyclin-dependent kinases (CDKs) can promote assembly of active cyclin D/CDK4 (6)

complexes in human tumor cells. Cancer Res 58: 5053–5056, 1998
49. Fang F, Orend G, Watanabe N, Hunter T, Ruoslahti E: Dependence of cyclin E-CDK2 kinase activity on cell anchorage. Science 271: 499–502, 1996
50. Plana-Silva M, Weinberg R: Estrogen-dependent cyclin E-cdk2 activation through p21 redistribution. Mol Cell Biol 17: 4059–4069, 1997
51. Prall O, Rogan E, Musgrove E, Watts C, Sutherland R: c-myc or cyclin D1 mimics estrogen effects on cyclin E-cdk2 activation and cell cycle reentry. Mol Cell Biol 18: 4499–4508, 1998
52. Lacey K, Jackson P, Stearns T: Cyclin-dependent kinase control of centrosome duplication. Proc Natl Acad Sci USA 96: 2817–2822, 1999
53. Shivji M, Ferrari E, Ball K, Hubacher U, Wood R: Resistance of human nucleotide excision repair synthesis *in vitro* to p21 cdnl. Oncogene 17: 2827–2838, 1999
54. Seghezzi W, Chua K, Shanahan F, Reed G, Lees E: Cyclin E associates with components of pre-mRNA splicing machinery in mammalian cells. Mol Cell Biol 18: 4526–4536, 1998
55. Lukas J, Groshen S, Saffari B, Niu N, Reles A, Wen W, Felix J, Jones L, Hall F, Press M: WAF1/Cip1 gene polymorphism and expression in carcinomas of the breast, ovary, and endometrium. Am J Pathol 150: 167–175, 1997
56. Barbareschi M, Caffo O, Doglioni C, Finn P, Marchetti A, Buttitta F, Leek R, Morelli L, Leonardi E, Bevilacqua G, Dallapalma P, Harris A: p21 (WAF1) immunohistochemical expression in breast carcinoma: correlations with clinicopathological data, oestrogen receptor status, MIB1 expression, p53 gene and protein alterations and relapse-free survival. Br J Cancer 74: 208–215, 1996
57. Kuzumaki T, Ishikawa K: Loss of cell adhesion to substratum up-regulates p21 (Cip1/WAF1) expression in BALB/c3T3 fibroblasts. Biochem Biophys Res Comm 238: 169–172, 1997
58. Wu R, Schonthal A: Activation of p53-p21waf1 pathway in response to disruption of cell-matrix interactions. J Biol Chem 272: 29091–29098, 1997
59. Bardon S, Razanamahefa L: Retinoic acid suppresses insulin-induced growth and cyclin D1 gene expression in human breast cancer cells. Int J Oncol 12: 355–359, 1998
60. Seewaldt V, Kim J-H, Caldwell L, Johnson B, Swisshelm K, Collins S: All-trans-retinoic acid mediates G1 arrest but not apoptosis of normal human mammary epithelial cells. Cell Growth Diff 8: 631–641, 1997

Address for offprints and correspondence: Patricia S. Steeg, Women's Cancers Section, Laboratory of Pathology, National Cancer Institute, Building 10, Room 2A33, Bethesda MD 20892; *Tel.:* (301) 496-9753; *Fax:* (301) 402-8910

Journal of Cellular Biochemistry 67:223–230 (1997)

Role of Cell Cycle Regulators in Tumor Formation in Transgenic Mice Expressing the Human Neurotropic Virus, JCV, Early Protein

Barbara Krynska,[1] Jennifer Gordon,[1] Jessica Otte,[1] Roberta Franks,[2] Robert Knobler,[3], Antonio DeLuca[4] Antonio Giordano,[4] and Kamel Khalili[1]*

[1]Center for NeuroVirology and NeuroOncology, Allegheny University of the Health Sciences, Philadelphia, Pennsylvania 19102
[2]Department of Genetics, College of Medicine, University of Illinois, Chicago, Illinois 60612
[3]Department of Neurology, Jefferson Medical College, Thomas Jefferson University, Philadelphia, Pennsylvania 19107
[4]Department of Pathology, Anatomy, and Cell Biology, Thomas Jefferson University, Philadelphia, Pennsylvania 19107

Abstract Transgenic mice harboring the early genome from the human neurotropic JC virus, JCV, develop massive abdominal tumors of neural crest origin during 6–8 months after birth and succumb to death a few weeks later. The viral early protein, T-antigen, which possesses the ability to transform cells of neural origin, is highly expressed in the tumor cells. Immunoblot analysis of protein extract from tumor tissue shows high level expression of the tumor suppressor protein, p53, in complex with T-antigen. Expression of p21, a downstream target for p53, which controls cell cycle progression by regulating the activity of cyclins and their associated kinases during the G1 phase, is extremely low in the tumor cells. Whereas the level of expression and activity of cyclin D1 and its associated kinase, cdk6, was modest in tumor cells, both cyclin A and E, and their kinase partners, cdk2 and cdk4, were highly expressed and exhibited significant kinase activity. The retinoblastoma gene product, pRb, which upon phosphorylation by cyclins:cdk induces rapid cell proliferation, was found in the phosphorylated state in tumor cell extracts, and was detected in association with JCV T-antigen. The transcription factor, E2F-1, which dissociates from the pRb–E2F-1 complex and stimulates S phase-specific genes upon phosphorylation of pRb and/or complexation of pRb with the viral transforming protein, was highly expressed in tumor cells. Accordingly, high level expression of the E2F-1-responsive gene, proliferating cell nuclear antigen (PCNA), was detected in the tumor cells. These observations suggest a potential regulating pathway that, upon expression of JCV T-antigen, induces formation and progression of tumors of neural origin in a whole animal system. J Cell. Biochem. 67:223–230, 1997.

Key words: human JC virus; p53; T-antigen; transgenic mice; tumor cells

Tumors of neural origin are among the most common malignancies seen in both children and adults. Analysis of the genetic abnormalities that underlie such tumors has implicated a functional role for several oncogenes and tumor suppressor genes, including p53 and pRb [for review, see Wong et al., 1994]. De-regulation of both p53 and pRb has been extensively examined, with indications of a high incidence of mutations in these genes in astrocytoma [Wong et al., 1994]. The paradigm of virus-induced tumors represents an excellent model system for in vivo analysis of tumor progression. The association of viral oncogenic proteins, including SV40 T antigen and adenovirus E1A, with p53 and pRb, which may functionally inactivate these cell proliferation controllers is reminiscent of de-regulatory events observed in human tumors [Lang et al., 1994; Manfredi et al., 1991; Schlegel et al., 1993]. While the association between viruses and human tumors of neural origin has been weakly established, there have been several documented cases of patients with central nervous system (CNS) neoplasms

Contract grant sponsor: National Institutes of Health.

*Correspondence to: Kamel Khalili, Center for NeuroVirology and NeuroOncology, Allegheny University of the Health Sciences, Broad and Vine, Philadelphia, PA 19102.

Received 6 June 1997; accepted 26 June 1997

and reactivation of papovaviruses including simian virus 40 (SV40) and JC virus (JCV) [Bergsagel et al., 1992; GiaRusso et al., 1978; Lednicky et al., 1995; Rencic et al., 1996; Sima et al., 1983].

JCV is a human papovavirus known to cause the fatal demyelinating disease, progressive multifocal leukoencephalopathy (PML) [Padgett et al., 1971; ZuRhein and Chou, 1965]. Similar to other papovaviruses, the early region of the viral genome encoding the early protein, T-antigen is expressed prior to viral DNA replication. The early genome is separated by the viral regulatory sequences from the late region, which is responsible for production of the capsid proteins during the late phase of the viral lytic cycle [for review, see Frisque and White, 1992]. The neuro-oncogenic potential of JCV has been well established in several experimental animals, including Syrian hamsters, owl, and squirrel monkeys [London et al., 1978; Miller et al., 1984; Nagashima et al., 1984; Varakis et al., 1976; Walker et al., 1973; ZuRhein and Varakis, 1975, 1979]. The ability of JCV to induce neural origin tumors is likely attributed to the viral early protein, T-antigen, whose expression is restricted to neural cells [Raj and Khalili, 1995] and exhibits greater that 75% sequence homology to its well-characterized SV40 counterpart [Frisque et al., 1984]. In support of this concept, earlier reports along with our recent findings [Franks et al., 1996; Small et al., 1986] indicate that expression of JCV T-antigen in mice leads to the development of neural crest origin tumors in which the JCV early protein is highly expressed in the tumor tissue. This paper presents the results of our biochemical analysis of tumor tissue from transgenic mice in which levels of expression and activity of several cell cycle regulatory proteins including the tumor suppressors p53 and pRb have been evaluated.

METHODS

Transgenic Mice

Transgenic mice were generated by conventional methods as described previously [Gordon and Ruddle, 1983]. Briefly, a 3.2-kb *BalI/Nci*I DNA restriction fragment of the JCV early-control region and the coding sequence for the viral early gene was injected into fertilized mouse oocytes generated by FVB/N mouse mating. The transgenic animals were identified by Southern blot analysis of DNA isolated from the tails upon treatment with *Eco*RI. The positive mice were observed daily for phenotypic manifestations, i.e., sluggish appearance with disheveled fur and distended lower abdomen, and formation of tumors as described previously [Franks et al., 1996].

Reagents

Monoclonal antibodies to SV40 T-antigen (Ab-2) and to p53 (Ab-1) were obtained from Oncogene Science. Purified mouse anti-human Rb (G3-245) detecting mouse Rb protein was obtained from Pharminigen (San Diego, CA). Antibodies to cyclins, cyclin-dependent kinases (cdks), E2F (KH95), PCNA (PC10), and p21 (M-164) were obtained from Santa Cruz Biotechnology (Santa Cruz, CA).

Protein Extract Preparation and Analysis

Total protein extracts were prepared from tumor, brain, spleen, and kidney of adult transgenic mice and age-matched control animals by the method described previously [Franks et al., 1996]. Briefly, 0.5 mg of tissue was homogenized in TNN buffer containing 50 mM Tris–HCl (pH 8.0), 150 mM NaCl, 0.05% NP40, and a mixture of protease inhibitor containing aprotinin 2 μg/ml, leupeptin 10 μg/ml, pepstatin 10 μg/ml, PMSF 100 μg/ml, and TPCK 100 μg/ml. The homogenate was centrifuged for 15 min at 14,000 rpm, and the supernatant was collected and stored at −70°C for further analysis. All procedures for protein preparation were performed at 4°C. To measure the level of protein by direct Western blot analysis, approximately 50 μg of protein was fractionated by 12% sodium dodecyl sulfate–polyacrylamide gel electrophoresis (SDS–PAGE) and, after transfer to nitrocellulose, reacted with the specific antibodies as described previously [Franks et al., 1996]. To examine the association of T-antigen with p53 or pRb, 200 μg of nuclear extract were incubated with anti-T-antigen, anti-p53, or anti-pRb antibodies overnight and the immune complexes pulled down with Pansorbin and washed and analyzed by immunoblotting with the secondary monospecific antibodies. Proteins were detected by enhanced chemi luminescence (ECL, Amersham, Arlington Heights, IL).

Assay of Kinase Activity

Kinase activity was measured as a result of histone H1 phosphorylation in the presence of a given kinase or cdk as described previously [Kim et al., 1994]. Briefly, 150 μg of total pro-

tein extract from normal and transgenic tissues was immunoprecipitated overnight at 4°C with specific antibodies. Twenty µl of a 50% suspension of packed protein A–Sepharose beads in TNN lysis buffer was added and incubated at 4°C for 1 h. The immunoprecipitates were assayed for kinase activity for 20 min in reaction buffer containing 50 mM Tris–HCl (pH 7.5), 10 mM $MgCl_2$, 1 mM DTT, 50 µM ATP, 5 µCi [γ^{32}P]-ATP, and 200 µg/ml calf thymus histone H1 (Sigma, St. Louis, MO) in a final volume of 50 µl. The reaction was carried out at 30°C for 20 min and stopped by the addition of 50 µl of sample loading buffer. Phosphorylated histone H1 was identified following SDS–PAGE and autoradiography.

RESULTS AND DISCUSSION

The large T-antigen of JCV is composed of 695 amino acids with 70% sequence homology to the well-characterized SV40 large T-antigen [Frisque et al., 1984]. One of the most highly homologous regions between JCV and SV40 T-antigen (amino acid residues 259–517) partially overlaps with the region important for complex formation with the cellular tumor suppressor protein, p53. Despite sequence conservation in the regions encompassing p53 binding sites, the interaction between p53 and JCV T-antigen has not been completely established. In earlier studies, analysis of protein from owl monkey brain tumors induced by intracerebral inoculation of JCV revealed nuclear expression of JCV T-antigen, which was not associated with the host p53 protein [Major and Traub, 1986; Major et al., 1984]. However, in later studies, the association of JCV T-antigen with p53 was detected in cell extracts from a glioblastoma developed upon intracerebral inoculation of a juvenile owl monkey with a cell suspension of an explanted JCV-induced glioma [Major et al., 1987]. In order to determine the level of p53 in tumors developed in the JCV T-antigen transgenic mice and to assess its association with JCV T-antigen, protein extract from tumor and several nontumor tissues were prepared and reacted with anti-p53 and anti-T-antigen antibodies and immunocomplexes were analyzed by Western blot utilizing antibodies against T-antigen and p53, respectively. Figure 1A illustrates results from immunoprecipitation, using anti-p53 antibody (lanes 1–4) and anti-T-antigen antibody (lane 5), followed by Western blot using anti-p53 antibody. As evident from this study, in contrast to its undetectable level in brain, spleen, and kidney, substantial levels of p53 are expressed in tumor tissue (compare lanes 1–3 with lane 4) and significant amounts of this protein were found associated with T-antigen (compare lanes 4 and 5). It is likely that the association of T-antigen with p53 prolongs the half-life of p53 and results in the high-level accumulation of this protein in tumor tissue. In the reciprocal experiment, the level of T-antigen and its association with p53 was determined by immunoprecipitation and Western blot. As shown in Figure 1B, an extremely low level of T-antigen was detected in brain and kidney, but not in the spleen of transgenic mice (lanes 1–3). JCV T-antigen was highly expressed in tumor tissue and was found in complex with p53 (Fig. 1B, lanes 4 and 5).

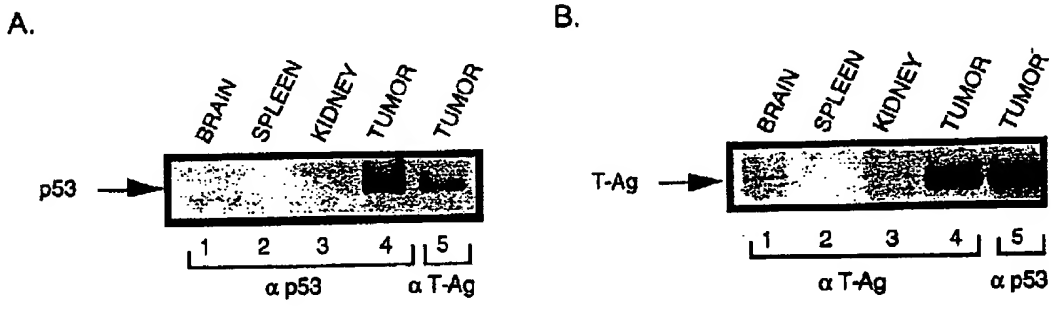

Fig. 1. Expression of p53 and JCV T-antigen in tumor and nontumor tissue of a transgenic animal. A: Protein extracts from brain, spleen, kidney and tumor of JCV T-antigen transgenic mice were immunoprecipitated with monoclonal antibody against p53 (lanes 1–4) or with monoclonal antibody against SV40 T-antigen that cross reacts with JCV T-antigen (lane 5). Immunocomplexes were resolved by SDS–PAGE and, after transfer to nitrocellulose, were subjected to Western blot analysis with antibody detecting p53. B: Protein extracts from brain, spleen, kidney, and tumor of transgenic mice were incubated with monoclonal antibody against SV40 T-antigen (lanes 1–4) or with monoclonal antibody against p53 (lane 5), and immunoprecipitates were subjected to Western blot analysis using anti-T-antigen antibody.

Previous studies have indicated that expression of p21, an inhibitor of cell proliferation, is upregulated by p53 [for review, see Cox and Lane, 1995; Hartwell and Kastan, 1994]. To examine the level of p21 in tumor tissue where a high amount of p53 has been detected in association with T-antigen, we performed Western blot analysis of protein extracts from tumor and nontumor tissues obtained from transgenic and age-matched control animals. As shown in Figure 2, despite a high level of p53 in the tumor tissue, extremely low levels of p21 were detected in these cells, suggesting that upon its association with JCV T-antigen, p53 may lose its ability to stimulate transcription of the p21 gene. Also, we observed that the level of p21 is significantly higher in the brains of transgenic mice compared to its level in age-matched control mouse brain. This is an intriguing observation, suggesting that overexpression of p21, through a p53 independent pathway, may participate in a pathway that prevents formation of tumors in the brains of transgenic mice.

p21 prevents cell cycle progression by binding to regulatory complexes composed of one of the cyclins and their partner kinases, cyclin dependent kinases (cdks) [Scherr, 1996]. Therefore, in the next series of studies, we assessed the level and activity of cyclins and their associated kinases in tissue from transgenic and age-matched control animals. As shown in Figure 3A, a high level of cyclin E was detected in tumor tissues. No dramatic variations in the level of cyclin E were observed in various tissues from transgenic mice versus those from control animals. The examination of H1 kinase activity of complexes obtained by immunoprecipitation with anti-cyclin E antibody revealed substantial kinase activity in extracts from tumor tissue as well as in brains and spleens of transgenic mice. Of interest, in control mouse brain where the level of cyclin E was comparable to that from transgenic animals, cyclin E exhibited no kinase activity. The evaluation of cyclin A expression by Western blot and its kinase activity by H1 kinase assay revealed a pattern very similar to that described for cyclin E. As shown in Figure 3B, a high level of cyclin A which correlated with its kinase activity was observed in the tumor tissue (lane 7). Similar to cyclin E, significant kinase activity was associated with the cyclin A complex obtained from the brains of transgenic mice. Next, we evaluated the kinase activity of cdk2, a cyclin-dependent kinase which is found in complex with cyclins E and A during G1 and S phases, respectively. As illustrated in Figure 3C, different levels of cdk2 were detected in various tissues from transgenic mice, and all were comparable to those seen in tissues from control animals. Of interest, the cdk2 complex from tumor tissue exhibited high levels of kinase activity as determined by H1 kinase assay (lane 7). These observations suggest that in nontumor tissue cdk2 may be associated with inhibitors which prevent its kinase ability.

We next extended our studies and focused our attention on the early G1 regulators, including cyclin D and its associated kinases, cdk4 and cdk6. As demonstrated in Figure 4A, cyclin D1 was expressed in a variety of tissues, including tumor and exhibited a modest kinase activity. Similarly, as shown in Figure 4B, cdk4 was produced in a variety of tissues from control and transgenic mice with the highest levels observed in tumor cells. Interestingly, in contrast to its high level, no significant kinase activity was associated with the cdk4 complexes in tumor and non-tumor tissue. Analysis of cdk6 expression indicates lower levels of cdk6 in tumor and in brains of normal and transgenic mice (Fig. 4C). Regardless of its high levels in spleen and kidney, cdk6 showed no significant kinase activity in these cells. The cdk6 complex from brain, spleen, and tumor of transgenic mouse exhibits a modest kinase activity (Fig. 4C).

In the next series of experiments, we raised the question of whether the observed increased kinase activity of cyclin E, cyclin A, and cdk2 in tumor tissue correlates with the levels of phosphorylated pRb, a tumor suppressor which upon

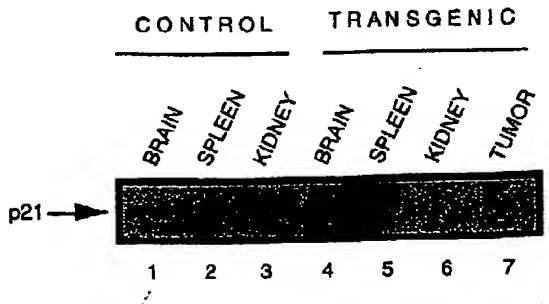

Fig. 2. Expression of p21 in various tissues from transgenic and control age-matched mice. Equal amounts of crude protein extracts (50 μg) from various tissues of normal (lanes 1–3) and transgenic animals (lanes 4–7) were analyzed by Western blotting using anti-p21 antibody.

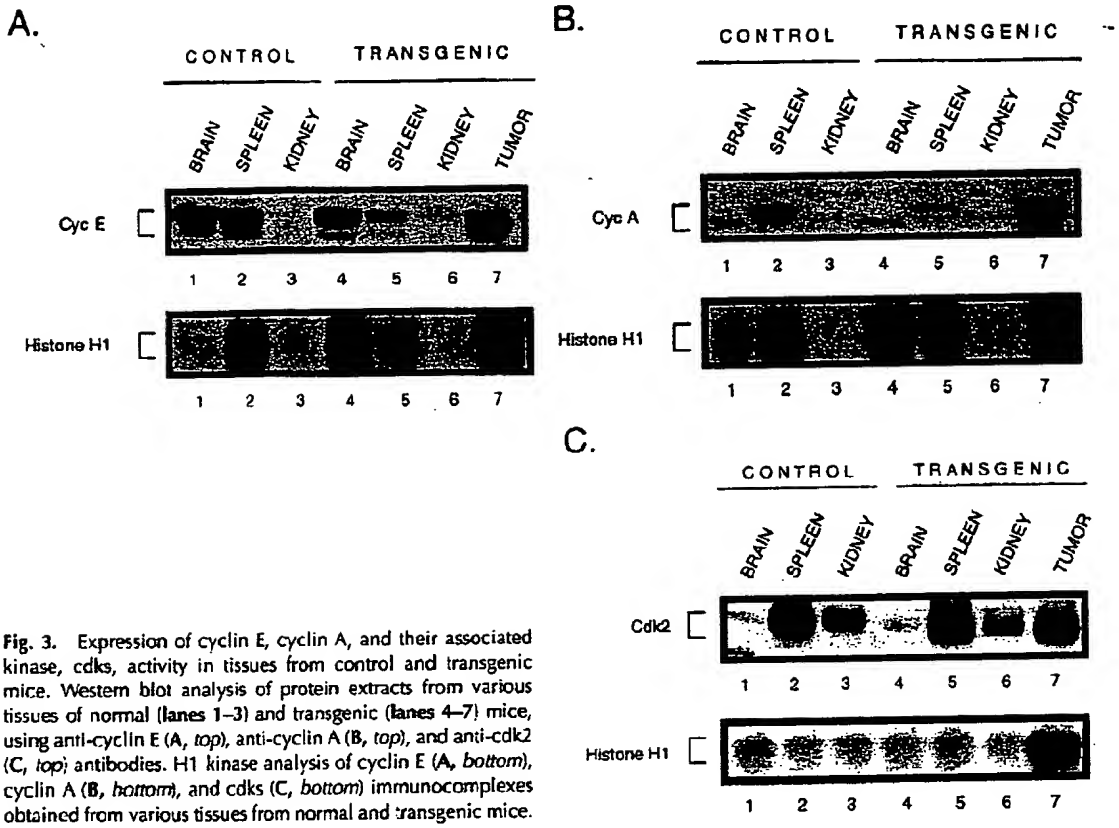

Fig. 3. Expression of cyclin E, cyclin A, and their associated kinase, cdks, activity in tissues from control and transgenic mice. Western blot analysis of protein extracts from various tissues of normal (**lanes 1–3**) and transgenic (**lanes 4–7**) mice, using anti-cyclin E (**A**, *top*), anti-cyclin A (**B**, *top*), and anti-cdk2 (**C**, *top*) antibodies. H1 kinase analysis of cyclin E (**A**, *bottom*), cyclin A (**B**, *bottom*), and cdks (**C**, *bottom*) immunocomplexes obtained from various tissues from normal and transgenic mice.

phosphorylation loses its ability to restrain cells in the G1 phase [Scherr, 1996]. Also, as complexation of several viral oncoproteins, including JCV T-antigen with pRb, may lead to functional inactivation of pRb, as well as induction of uncontrolled cell proliferation [Scherr, 1996], we sought to examine the state of pRb phosphorylation and the level of its association with JCV T-antigen. As shown in Figure 5, whereas a hypophosphorylated form of pRb was detected in a variety of tissues from transgenic mice, extracts from tumor tissue showed an additional band corresponding to the phosphorylated form of pRb. Moreover, results from Western blot analysis of the protein complexes pulled down by anti-T-antigen antibody suggest that JCV T-antigen may remain in complex with pRb in tumor tissue (Fig. 5A, lane 5). Results from the reciprocal experiment in which anti-T-antigen-specific immunocomplexes were analyzed for the presence of pRb verified the association of pRb and T-antigen in extract from tumor tissue.

One consequence of pRb phosphorylation and/or its association with JCV T-antigen would be liberation of E2F-1 from the pRb–E2F-1 complex. E2F-1 is a DNA binding transcription factor which upon binding to its consensus sequence stimulates expression of a group of S phase specific genes including its own. Hence, in the next study, we determined the level of E2F-1 in tissues from transgenic animals. As shown in Figure 6A, whereas the lowest level of E2F-1 was detected in the brain of the transgenic animal (lane 1), a high level of E2F-1 was observed in tumor tissue (lane 4). Thus it is likely that the liberated E2F-1 in tumor cells positively autoregulates transcription of its own promoter and results in high level production of this protein in tumor tissue.

In the last series of studies, we examined the level of proliferating cell nuclear antigen (PCNA), a protein whose expression is enhanced by E2F-1 during the S phase [Scherr, 1996]. As shown in Figure 6B, significant amounts of PCNA were detected in tumor tissue (lane 7). The level of PCNA in other tissues from transgenic mice was comparable to those from control animals.

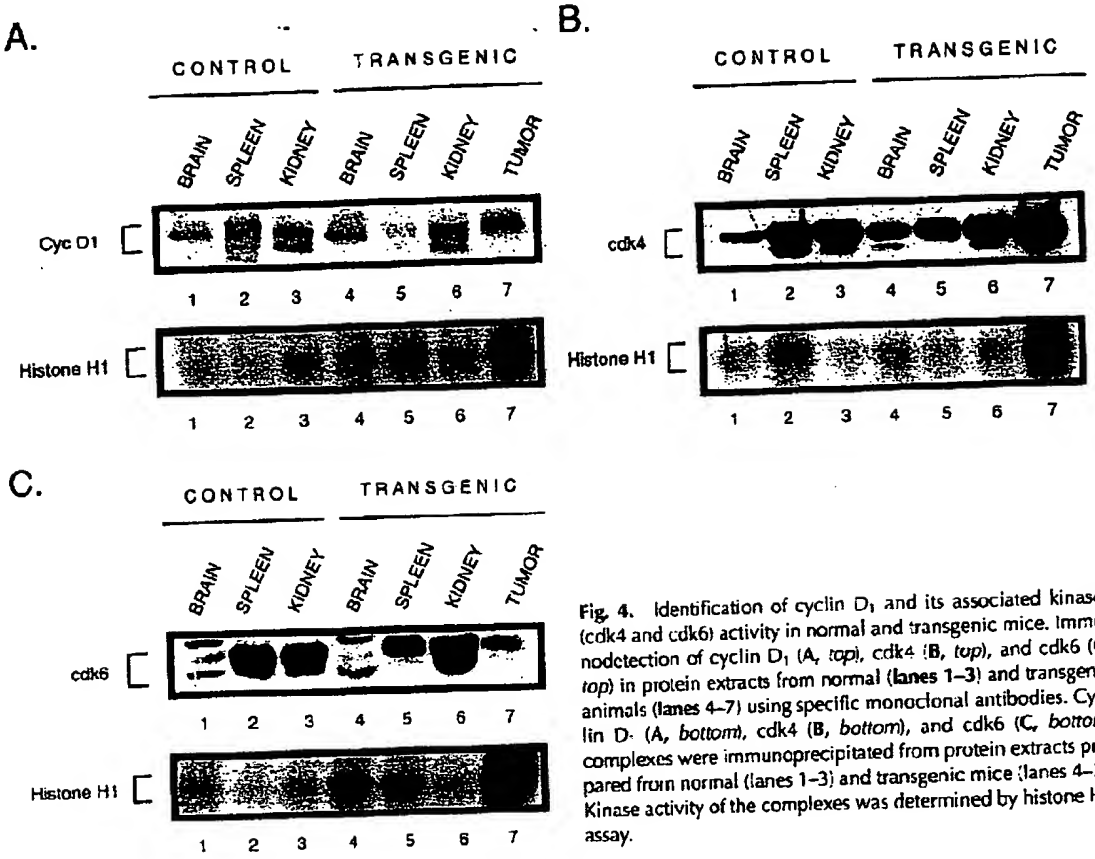

Fig. 4. Identification of cyclin D_1 and its associated kinases (cdk4 and cdk6) activity in normal and transgenic mice. Immunodetection of cyclin D_1 (A, *top*), cdk4 (B, *top*), and cdk6 (C, *top*) in protein extracts from normal (lanes 1–3) and transgenic animals (lanes 4–7) using specific monoclonal antibodies. Cyclin D- (A, *bottom*), cdk4 (B, *bottom*), and cdk6 (C, *bottom*) complexes were immunoprecipitated from protein extracts prepared from normal (lanes 1–3) and transgenic mice (lanes 4–7). Kinase activity of the complexes was determined by histone H1 assay.

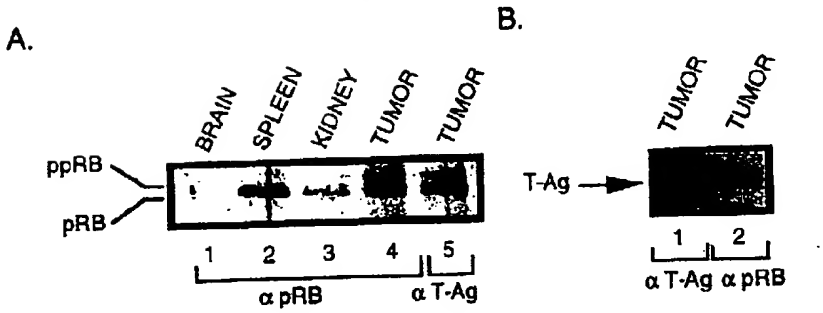

Fig. 5. Expression and association of JCV T-antigen with the tumor suppressor protein, pRb. A: Proteins extracted from brain, spleen, kidney, and tumor of transgenic mouse were immunoprecipitated with monoclonal antibody against retinoblastoma protein (pRb) (lanes 1–4) and with monoclonal antibody against T-antigen (lane 5). Immunoprecipitates were fractionated by SDS–PAGE, transferred to nitrocellulose, and subjected to Western blot analysis with a monoclonal antibody against retinoblastoma protein that detects both phosphorylated (ppRb) and its hypophosphorylated (pRb) forms. B: Proteins from tumor tissue of transgenic mice were prepared and immunoprecipitated with monoclonal antibody against T-antigen (lane 1) or with monoclonal antibody against pRb (lane 2). Immunoprecipitates were fractionated by SDS–PAGE, and after transfer to nitrocellulose, incubated with antibody to T-antigen.

In summary, we performed an interrelated series of experiments to evaluate the level of expression and activity of various cell cycle controllers in order to obtain some insight into the molecular pathogenesis of JCV T-antigen-induced CNS tumors in transgenic animals. Based on our observations, we provide a working model as schematized in Figure 7. According to this model, the association of JCV T-antigen with p53 may block the ability of p53 to induce p21WAF1, a protein which inhibits cyclin:cdk activity. De-regulation of the participant cyclins, in particular cyclins E and A, and their associated kinases, may in turn lead to

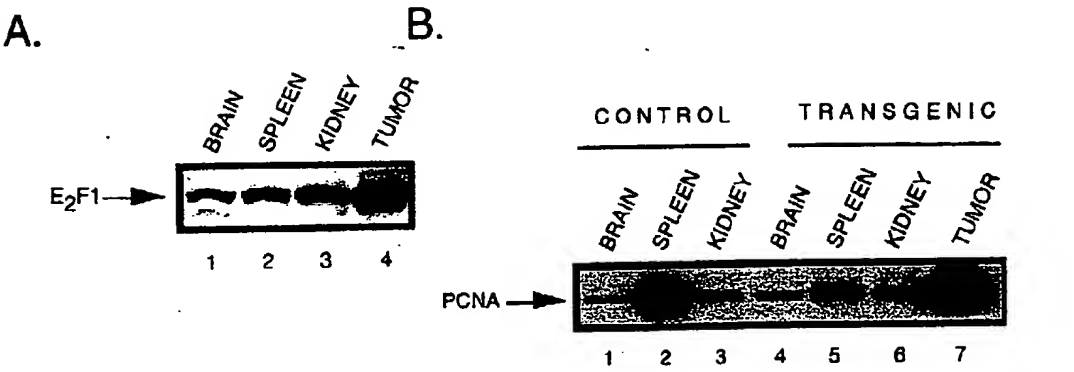

Fig. 6. Expression of transcription factor E2F-1 and its responsive gene, PCNA, in experimental animals. A: Equal amounts of protein extract (50 μg) isolated from brain, spleen, kidney and tumor of transgenic mice were subjected to Western blot analysis with monoclonal antibody against the transcription factor, E2F-1. B: Fifty μg of total protein extracted from various tissues of normal (lanes 1–3) and transgenic animals (lanes 4–7) were analyzed by Western blotting with antibody that recognizes PCNA.

the phosphorylation of pRb and the liberation of E2F-1. The release of E2F-1 from the pRb–E2F-1 complex may also be accomplished by the association of JCV T-antigen with pRb. As levels of E2F-1 increase in cells, E2F-1 may induce its own gene expression, as well as those from other S-phase-specific promoters such as PCNA, and promote rapid entry of cells into S phase. Perhaps it should be mentioned that none of the transgenic mice created in our laboratory [Franks et al., 1996] and others [Small et al., 1986] developed tumors in brain. The results of this study may also provide important clues as to why JCV T-antigen fails to induce tumors in the brains of experimental animals. For example, elevated levels of p21 in the brains of transgenic mice by a p53-dependent pathway may be an underlying mechanism for the control of cell proliferation and the lack of tumors in brains of these mice. Results from studies on cyclins A and E suggest that despite their comparable levels, complexes associated with these two cyclins in transgenic mouse brain possess more kinase activity than those from control mice. The issue may become even more complicated as their cdk partner, cdk2, which is produced at modest but detectable levels, exhibits no kinase activity. Thus, one may speculate on the involvement of other kinases in association with cyclins A and E in these cells. In light of our data showing high level kinase activity of cyclins A and E, one may anticipate the detection of the phosphorylated form of pRb in tumor cells. It was noted, however, that the increased kinase activity of cyclins A and E in the brain may not correlate with the level and status of pRb in brain cells, as low but detectable levels of pRb in the phosphorylated state were present in brain tissue.

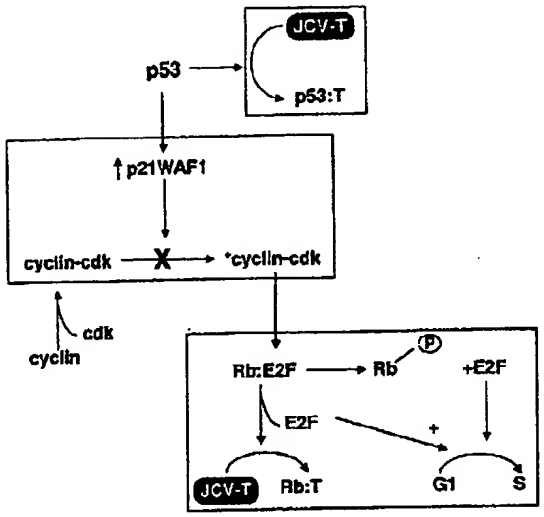

Fig. 7. Proposed pathway by which JCV T-antigen induces tumors in experimental animals. Wild type p53 has the capacity to augment transcription of p21WAF-1, an inhibitor of cyclin kinases, including cyclins E and A and their associated kinases. A decrease in kinase activity of cyclin:kinase maintains pRb in a hypophosphorylated state, which in turn sequesters the transcription factor, E2F1. The association of JCV T-antigen with p53 abrogates the ability of p53 to exert its regulatory action via p21WAF-1. In addition, the association of JCV T-antigen with pRb may liberate E2F-1 from pRb:E2F-1 complex and permit E2F-1 to induce transcription of S-phase-specific genes.

Currently we are in the process of evaluating the role of other tumor suppressor proteins which may regulate cyclin activity in tumor and brains of transgenic mice, and are investigating the role of other Rb family members in JCV-induced tumors in transgenic animals.

ACKNOWLEDGMENTS

We thank members of the Center for NeuroVirology and NeuroOncology for their helpful insight and suggestions and sharing of reagents. We also thank Cynthia Schriver for editorial assistance and Bassel Sawaya for assistance in preparation of figures. This work was made possible by grants awarded by the National Institutes of Health (to K.K.).

REFERENCES

Bergsagel DJ, Finegold MJ, Butel JS, Kupky WJ, Garcea RL (1992): DNA sequences similar to those of simian virus 40 in ependymomas and choroid plexus tumors of childhood. N Engl J Med 326:988–993.

Cox LS, Lane DP (1995): Tumour suppressors, kinases and clamps: How p53 regulates the cell cycle in response to DNA damage. BioEssays 17:501–508.

Franks R, Rencic A, Gordon J, Zoltick PW, Curtis M, Knobler RL, Khalili K (1996): Formation of undifferentiated mesenteric tumors in transgenic mice expressing human neurotropic polyomavirus early protein. Oncogene 12: 2573–2578.

Frisque RJ, White FA (1992): The molecular biology of JC virus, causative agent of progressive multifocal leukoencephalopthy. In Roos RP (ed): "Molecular Neurovirology." Towana, NJ: Humana Press, pp 25–258.

Frisque RJ, Bream GL, Cannella MT (1984): Human polyomavirus JC virus genome. J Virol 51:458–469.

GiaRusso MH, Koeppen AH (1978): Atypical progressive multifocal leukoencephalopathy and primary cerebral malignant lymphoma. J Neurol Sci 35:391–398.

Gordon JW, Ruddle FH (1983): Gene transfer into mouse embryos: Production of transgenic mice by pronuclear injection. Methods Enzymol 101:411–433.

Hartwell LH, Kastan MB (1994): Cell cycles control and cancer. Science 266:1821–1828.

Kim TA, Ravitz M, Wenner C (1994): Transforming growth factor-beta regulation of retinoblastoma gene product and E2F transcription factor during cell cycle progression in mouse fibroblasts. J Cell Physiol 160:1–9.

Lang FF, Miller DC, Koslow M, Newcomb EW (1994): Pathways leading to glioblastoma multiforme: A molecular analysis of genetic alterations in 65 astrocytic tumors. J Neurosurg 81:427–436.

Lednicky JA, Garcea RL, Bergsagel DJ, Butel JS (1995): Natural simian virus 40 strains are present in human choroid plexus and ependymoma tumors. Virology 212: 710–717.

London W, Houff SA, Madden DL, Fuccillo DA, Gravell M, Wallen WC, Palmer AE, Sever JL, Padgett BL, Walker DL, ZuRhein GM, Ohashi T (1978): Brain tumors in owl monkeys inoculated with a human polyomavirus (JC virus). Science 201:1246–1249.

Major EO, Traub R (1986): JC virus T protein during productive infection in human fetal brain and kidney cells. Virology 148:221–225.

Major EO, Mourrain P, Cummins C (1984): JC virus-induced owl monkey glioblastoma cells in culture: Biological properties associated with the viral early gene product. Virology 136:359–367.

Major EO, Vacante DA, Traub RG, London WT, Sever JL (1987): Owl monkey astrocytoma cells in culture spontaneously produce infectious JC virus which demonstrates altered biological properties. J Virol 61:1435–1441.

Manfredi JJ, Prives C (1994): The transforming activity of simian virus 40 large tumor antigen. The transforming activity of simian virus 40 large tumor antigen. Biochim Biophys Acta 1198:65–83.

Miller N, McKeever P, London W, Padgett BL, Walker DL, Wallen W (1984): Brain tumors of owl monkeys inoculated with JC virus contain the JC virus genome. J Virol 49:848–856.

Nagashima K, Yasui K, Kimura J, Washizu K, Yamaguchi K, Mori W (1984): Induction of brain tumors by a newly isolated JC virus (Tokyo-1 strain). Am J Pathol 116:455–463.

Padgett BL, ZuRhein GM, Walker D, Echoroade R, Dessel B (1971): Cultivation of papova-like virus from human brain with progressive multifocal leukoencephalopathy. Lancet 1:1257–1260.

Raj GV, Khalili K (1995): Transcriptional regulation: Lessons from the human neurotropic polyomavirus, JCV. Virology 213:283–291.

Rencic A, Gordon J, Otte J, Curtis M, Kovatich A, Zoltick PW, Khalili K, Andrews D (1996): Detection of JC virus DNA sequence and expression of the viral oncoprotein, tumor antigen, in brain of immunocompetent patient with oligoastrocytoma. Proc Natl Acad Sci USA 93:7352–7357.

Scherr C (1996): Cancer cell cycles. Science 274:672–1677.

Schlegel U (1993): Mechanisms of molecular development of human glioma. (Review.) Nervenarzt 64:485–493.

Sima AF, Finkelstein SD, McLachlan DR (1983): Multiple malignant astrocytomas in a patient with spontaneous progressive multifocal leukoencephalopathy. Ann Neurol 14:183–188.

Small J, Khoury G, Jay G, Howley P, Scangos G (1986): Early regions of JC virus and BK virus induce distinct and tissue-specific tumors in transgenic mice. Proc Natl Acad Sci USA 83:8288–8292.

Varakis J, ZuRhein GM, Padgett BL, Walker DL (1976): Induction of peripheral neuroblastomas in Syrian hamsters after injection as neonates with JC virus, a human polyoma virus. Cancer Res 38:1718–1722.

Walker DL, Padgett BL, ZuRhein GM, Albert A, Marsh RF (1973): Human papovavirus (JC): Induction of brain tumors in hamsters. Science 181:674–676.

Wong A, Zoltick P, Moscatello D (1994): The molecular biology and molecular genetics of astrocytic neoplasms. Semin Oncol 21:139–148.

ZuRhein GM, Chou SM (1965): Particles resembling papovaviruses in human cerebral demyelinating disease. Science 148:1477–1479.

ZuRhein GM, Varakis J (1975): Morphology of brain tumors induced in Syrian hamsters after inoculation with JC virus, a new human papovavirus. In Kornyey S, Tariska S, Gosztonyi G (eds): "Proceedings of the Seventh International Congress of Neuropathology." Vol. 1. Budapest: Akademia Kiado, pp 479–481.

ZuRhein GM, Varakis J (1979): Perinatal induction of medulloblastomas in Syrian Golden hamsters by a human polyomavirus (JC). In Rice JM (ed): "Perinatal Carcinogenesis." National Cancer Institute Monograph 51. Bethesda: National Cancer Institute, pp 205–208.

Activation of Cdk4 and Cdk2 During Rat Liver Regeneration Is Associated With Intranuclear Rearrangements of Cyclin-Cdk Complexes

MONTSERRAT JAUMOT,[1] JOSEP-MARIA ESTANYOL,[1] JOAN SERRATOSA,[2] NEUS AGELL,[1] AND ORIOL BACHS[1]

Partial hepatectomy (PH) triggers the entry of rat liver cells into the cell cycle. The signals leading to cell-cycle activation converge into a family of kinases named cyclin-dependent kinases (cdks). Specific cyclin-cdk complexes are sequentially activated during the cell cycle. Cyclin D-cdk4 and cyclin E-cdk2 are activated during the G_1 phase, cyclin A-cdk2 is activated during the S phase, and cyclin B-cdk1 during mitosis. In the present study, we have examined the timing of the activation of cdk4 and cdk2, the intracellular location of G_1/S cyclins and cdks, and the relationship between location and cdk4 and cdk2 activities during rat liver regeneration after a PH. Results showed that the activity of both kinases started at 13 hours and showed maximal levels at 24 hours after hepatectomy. In quiescent cells, cyclin D3 and cdk4 were cytoplasmatic, whereas cyclin D1 was nuclear. At 5 hours after hepatectomy, cyclin D3 and cdk4 began to move into the nucleus, and at 13 hours, they were mostly nuclear. During the first 13 hours after hepatectomy, significant amounts of cyclin D1-cdk4 and cyclin D3-cdk4 complexes were formed, but they were mostly inactive. At 24 hours, these complexes were maximally activated. This activation was associated with the accumulation of cyclin D1, cyclin D3, and cdk4 in a nuclear subfraction extractable with nucleases. At 28 hours, the activity of cdk4 in this nuclear subfraction decreased when cyclin D1 moved from this fraction to the nuclear matrix (NM) and the levels of cyclin D3 diminished. The maximal activation of cdk2 at 24 hours was also associated with the accumulation of cyclin E, cyclin A, and cdk2 in this nuclease-sensitive fraction. The inactivation of cdk2 at 28 hours was associated with a strong decrease in cdk2 in this nuclear subfraction. Thus, results reported here indicate that the activation of cdk4 and cdk2 observed in rat liver cells after a PH is associated with a specific intranuclear location of these cdks and their associated cyclins. (HEPATOLOGY 1999;29:385-395.)

In pluricellular organisms, the cell cycle is regulated by growth factors, anchorage to the extracellular matrix, and contact inhibition. These extracellular factors generate intracellular signals that finally converge into a family of serine-threonine kinases, named cyclin-dependent kinases (cdks), which act as molecular integrators of the signals that regulate cell-cycle progression.

The liver contains hepatocytes (85%-95% of the hepatic mass) and nonhepatocytes (5%-15% of hepatic mass). In normal livers from adult animals, all these cells are quiescent. They can proliferate in response to the loss of liver mass produced, for example, by partial hepatectomy (PH).[1] Liver regeneration triggered by PH is a useful model for the study of the cell cycle, because it permits the analysis of cell proliferation *in vivo*. Hepatocytes from hepatectomized rats enter the G_1 phase immediately after PH. DNA synthesis begins 14 hours after surgery and is maximal at 22 to 24 hours. A peak of mitosis is produced at 28 to 30 hours. The nonhepatocytes start DNA synthesis 24 hours later than hepatocytes. Seven days after PH, all liver cells have divided once or twice and the liver has recovered its original mass (for review, see Steer[2] and Michalopoulos and DeFrances[3]).

The proliferation of hepatocytes after PH occurs in response to the action of transforming growth factor α,[4] epidermal growth factor,[5] and hepatocyte growth factor[6] (for review, see Fausto et al.[7]). Before responding to these growth factors, hepatocytes must be sensitized by a process called "priming," which seems to be induced by agents such as tumor necrosis factor α.[8] Sensitized hepatocytes' respond to the growth factors activating the cell-cycle regulatory machinery and thus entering into the cell cycle. How the cell-cycle regulatory machinery is activated after PH is mostly unknown.

To become active, cdks must be associated with regulatory subunits called cyclins. Specific cyclin-cdk complexes are activated at different intervals during the cell cycle. Thus, cyclin D-cdk4 complexes are activated at mid-G_1, cyclin E-cdk2 complexes are necessary for G_1/S transition, cyclin A-cdk2 for progression of DNA replication, and cyclin B-cdk1 for mitosis entry (for review, see Sherr,[9] Pines,[10] and Grafia and Reddy[11]). In addition to cyclin binding, the activity of

Abbreviations: PH, partial hepatectomy; cdk, cyclin-dependent kinase; CAK, cdk-activating kinase; CKI, cdk-inhibitor; PCNA, proliferating cell nuclear antigen; PMSF, phenylmethylsulfonyl fluoride; NM, nuclear matrix; TBS, Tris-buffered saline; IP, immunoprecipitation; DTT, dithiothreitol; EGTA, ethylene glycol-bis(β-aminoethyl ether)-*N*,*N*,*N*',*N*'-tetraacetic acid; ATP, adenosine triphosphate; PBS, phosphate-buffered saline.

From the [1]Department of Cell Biology, Faculty of Medicine, Institut d'Investigacions Biomèdiques August Pi Sunyer (IDIBAPS), University of Barcelona, and [2]Department of Pharmacology and Toxicology, Institut d'Investigacions Biomèdiques de Barcelona (IIBB-CSIC), Barcelona, Spain.

Received April 8, 1998; accepted September 21, 1998.

Supported by grants SAF96-0187-C02-01, SAF97-0069, and SAF98-0067 from the Comisión Interministerial de Ciencia y Tecnología (CICYT), and by grants 94/1017 and 94/0792 from the Fondo de Investigaciones Sanitarias de la Seguridad Social (FISss).

Address reprint requests to: Prof. Oriol Bachs, Departament de Biologia Cellular, Facultat de Medicina, Universitat de Barcelona Casanova 143, 08036-Barcelona, Spain. E-mail: bachs@medicina.ub.es; fax: 34-93-402-19-07.

0270-9139/99/2902-0011$3.00/0

cdks is regulated by a variety of mechanisms (reviewed in Morgan[12]): 1) phosphorylation of a conserved threonine residue by the cdk-activating kinase (CAK), which is formed by cdk7 associated with cyclin H[13,14]; 2) dephosphorylation of specific threonine and tyrosine residues by the phosphatase, cdc25[15]; and 3) binding of a number of proteins called cdk inhibitors (CKIs). Two families of CKIs have been described: the Ink4 family and the Cip/Kip family.[16] The Ink4 members include $p16^{ink4a}$, $p15^{ink4b}$, $p18^{ink4c}$, and $p19^{ink4d}$. They bind specifically to cdk4 and to its homologue, cdk6. The Cip/Kip proteins ($p21^{Cip1}$, $p27^{Kip1}$, and $p57^{Kip2}$) bind to and inhibit the activity of a wide range of cyclin-cdk complexes, including cyclin D-cdk4/6, cyclin E-cdk2, and cyclin A-cdk2.

In spite of the increasing amount of information concerning the regulation of the activity of cdks, the mechanisms of how cdk4 and cdk2 are activated and inactivated *in vivo* remain obscure. In some cell types such as T lymphocytes, macrophages, fibroblasts, and epithelial cells, it is assumed that quiescent cells contain low levels of D-type cyclins. Upon stimulation by growth factors, the expression of D-type cyclins increases, and then cyclin D-cdk4 complexes can be formed.[17,18] The assembly of cyclin D-cdk4 complexes requires an assembly factor whose activity is also induced by the mitogenic factors.[18,19] The full activation of cyclin D-cdk4 complexes also needs the action of CAK and cdc25A.[20]

During progression of the G_1 phase, the activation of cyclin D-cdk4 complexes is responsible for the phosphorylation of the retinoblastoma protein (pRb)[21] and the other members of the pocket family (p107 and p130).[22] When hypophosphorylated, the pocket proteins bind to the members of the E2F family of transcription factors and inactivate their function.[22] Free E2Fs are able to transactivate the expression of certain genes, *e.g.*, dihydrofolate reductase, Orc1, proliferating cell nuclear antigen (PCNA), and DNA polymerase α, which are necessary for G_1/S transition (reviewed in Lam and La Thangue,[23] and Mayol and Graña[22]). When pocket proteins are phosphorylated during G_1, E2Fs are released and the transcription of S-phase genes is activated. Cyclin E-cdk2 complexes also phosphorylate the pocket proteins, although the major role of these complexes is accomplished in the transition G_1/S, possibly by phosphorylating key proteins involved in the "firing" of DNA replication.[24]

The mechanisms leading to the inactivation of cyclin D-cdk4 and cyclin E/A-cdk2 complexes are also unclear. A possible way for cdk inactivation is by degradation of the cyclin subunits; however, because at least the levels of the D-type cyclins exhibit only moderate variations during the cell cycle, other processes to explain cdk inactivation must be considered.

Recently, it has been reported that most of the proteins of the cell-cycle regulatory machinery are already present in normal rat liver cells.[25-32] These reports also revealed that the levels of some of these proteins increase during liver regeneration. However, studies on the mechanisms involved in the activation and inactivation of the cdks are lacking in this *in vivo* model. Here, we analyze the formation, activation, and inactivation of cyclin D-cdk4 and cyclin E/A-cdk2 complexes during rat liver regeneration.

MATERIALS AND METHODS

Animals and PHs. Two-month-old male Sprague-Dawley rats (200-250 g) were used for all the experiments. The animals were treated according to the European Community laws for animal care. Rats were maintained on a 12-hour-light/12-hour-darkness schedule. Food and water were provided *ad libitum*, and before PH, rats were fasted overnight. PHs were performed according to Higgings and Anderson,[1] in which 66% of liver mass was removed under light ether anesthesia. Rats were refed immediately after surgery. Sham-operated rats were used as controls.

Antibodies. The antibodies used in this study are summarized in Table 1.

Preparation of Cellular and Nuclear Fractions. Three to six livers from nonoperated, from animals at different times after PH, or at different times after a sham operation were homogenized with a Potter-Elvehjem Teflon-glass homogenizer (Wheaton, Millville, NJ) in 10 vol of STM buffer (250 mmol/L sucrose, 50 mmol/L Tris-HCl [pH 7.4], and 5 mmol/L $MgSO_4$) containing 1 mmol/L phenylmethylsulfonyl fluoride (PMSF) and 0.5 μg/mL aprotinin. Homogenates were filtered through four layers of cheesecloth. Nuclei were prepared from homogenates as described by Kaufman and Shaper.[33] Nuclear subfractions were obtained according to Bachs and Carafoli.[34] Briefly, nuclei were resuspended in STM buffer containing 250 μg/mL DNase I and 250 μg/mL RNase A. After a 1-hour incubation at 4°C, the nuclei were sedimented at 800g for 10 minutes. The supernatant was collected and named S1. The pellet was resuspended in LS buffer (10 mmol/L Tris-HCl [pH 7.4] and 0.2 mmol/L $MgSO_4$) containing 1 mmol/L PMSF and 0.5 μg/mL aprotinin. Buffer HS (10 mmol/L Tris-HCl [pH 7.4], 0.2 mmol/L $MgSO_4$, and 2 mol/L NaCl) containing 1 mmol/L PMSF and 0.5 μg/mL aprotinin was added slowly to a final NaCl concentration of 1.6 mol/L. After a 15-minute incubation, the sample was sedimented at 5,000g for 20 minutes. The pellet was extracted again with 1.6 mol/L NaCl, and the new pellet, corresponding to the nuclear matrix (NM), was resuspended in STM buffer and stored at −80°C.

Gel Electrophoresis and Immunoblotting. Proteins were separated electrophoretically in sodium dodecyl sulfate–polyacrylamide gels as described by Laemmli.[35] The gels were transferred onto Immobilon-P membranes (Millipore) for 2 hours at 60 V. The membranes were preincubated in Tris-buffered saline (TBS) containing 5% defatted milk powder for 1 hour at room temperature. The antigens were identified by using the antibodies summarized in Table 1 diluted in TBS containing 0.5% defatted milk powder and 1% bovine serum albumin. After washing in TBS-0.05% Tween 20, the strips were incubated with an alkaline phosphatase– (Promega, Madison, WI; 1:10,000 dilution) or a horseradish peroxidase– (BioRad, SA, Madrid, Spain; 1:2,000 dilution) coupled secondary antibody for 45

TABLE 1. Antibodies to Cell-Cycle–Related Proteins

Target	Host	Specificity	Source	Code
CDK4 (IH)	r	p	Santa Cruz Biotechnology	sc-260
CDK4	r	p	Clontech	3516-1
CYC D1 (IH)	m	m	Santa Cruz Biotechnology	sc-6281
CYC D	r	p	UBI	06-137
CYC D3 (IH)	r	p	Santa Cruz Biotechnology	sc-182
$p21^{CIP}$ (IH)	r	p	Santa Cruz Biotechnology	sc-756
$p21^{CIP}$	g	p	Santa Cruz Biotechnology	sc-397G
$p27^{KIP1}$	r	p	J. Massagué (New York)	
$p16^{ink4a}$	m	m	Santa Cruz Biotechnology	sc-1661
CDK2	r	p	UBI	06-505
CYC E	r	p	Santa Cruz Biotechnology	sc-481
CYC A	r	p	Santa Cruz Biotechnology	sc-596
CDC25A	r	p	Santa Cruz Biotechnology	sc-97
CDK7	r	p	Santa Cruz Biotechnology	sc-857
CYC H	r	p	Santa Cruz Biotechnology	sc-855
PCNA	m	m	Boehringer	1170406
p107	r	p	Santa Cruz Biotechnology	sc-318
p130	r	p	Santa Cruz Biotechnology	sc-317

Abbreviations: IH, immunochemistry; r, rabbit; g, goat; m, mouse; p, polyclonal; m, monoclonal; UBI, Upstate Biotechnology.

minutes. After washing in TBS-0.05% Tween 20 and TBS, the reaction was visualized with nitro blue tetrazolium/5-bromo-4-chloro-3-indoyl-1-phosphate or with the enhanced chemiluminescence system (Amersham Iberica, Madrid, Spain).

Protein Determination. The protein content was measured by the procedure of Bradford,[36] using bovine serum albumin as standard.

Immunoprecipitations. Samples were lysed in buffer A (50 mmol/L Tris-HCl [pH 7.4], 0.1% Triton X-100, 5 mmol/L ethylenediaminetetraacetic acid, and 250 mmol/L NaCl) containing 50 mmol/L NaF, 0.1 mmol/L Na_3VO_4, 1 mmol/L PMSF, and 10 μg/mL leupeptin. Immunoprecipitations (IPs) were performed as described by Harlow and Lane.[37] Briefly, lysates were clarified by centrifugation at 10,000g for 10 minutes at 4°C. The supernatants were incubated with the indicated antibodies for 8 hours at 4°C, followed by an incubation with protein A beads for 1 hour at 4°C. After washing in buffer A, the immunocomplexes were subjected to immunoblotting as described above.

Determination of Cdk4 and Cdk2 Activities. To determine cdk4 activity, samples were lysed in buffer G (50 mmol/L HEPES [pH 7.5], 150 mmol/L NaCl, 1 mmol/L ethylenediaminetetraacetic acid, 2.5 mmol/L ethylene glycol-bis(β-aminoethyl ether)-*N,N,N',N'*-tetraacetic acid [EGTA], 1 mmol/L dithiothreitol [DTT], and 0.1% Tween 20) containing 10% glycerol, 1 mmol/L NaF, 0.1 mmol/L Na_3VO_4, 0.1 mmol/L PMSF, 10 μg/mL leupeptin, 0.5 μg/mL aprotinin, and 10 mmol/L β-glycerophosphate. IPs were performed as described above. The kinase assays were performed as described by Matsushime et al.[18] Briefly, after IP, the beads were washed four times in G buffer and twice in 50 mmol/L HEPES (pH 7.5), containing 1 mmol/L DTT. Cdk4 immunoprecipitates were incubated at 30°C for 30 minutes in kinase buffer (50 mmol/L HEPES [pH 7.5], 10 mmol/L $MgCl_2$, and 1 mmol/L DTT) containing 5 μg of soluble GST-pRb fusion protein, 2.5 mmol/L EGTA, 10 mmol/L β-glycerophosphate, 0.1 mmol/L Na_3VO_4, 1 mmol/L NaF, 20 μmol/L adenosine triphosphate (ATP), and 10 μCi of γ-^{32}P–ATP (Amersham; 3,000 Ci/mmol) in a total volume of 25 μL. Reaction was stopped by adding Laemmli sample buffer, and then the samples were electrophoresed in 10% sodium dodecyl sulfate–polyacrylamide gels. The gels were dried and the phosphorylated proteins were visualized by autoradiography.

To determine cdk2 activity, the samples were lysed in buffer A and then subjected to IP using anti-cdk2 antibodies. The immunoprecipitates were incubated at 30°C for 20 minutes in 20 mmol/L HEPES (pH 7.5), 10 mmol/L Mg acetate, and 1 mmol/L DTT containing 3 μg of histone H1 (Boehringer Mannheim, Germany), 20 μmol/L ATP, and 10 μCi of γ-^{32}P–ATP (Amersham; 3,000 Ci/mmol) in a total volume of 25 μL. After incubation, the samples were processed as for cdk4 determination.

Obtention of GST-pRb Protein. pGEX-SG-pRb was a gift from Dr. Wang (San Diego, CA). The recombinant protein was expressed in BL21 pLysE strain of *Escherichia coli* transformed with pGEX-SG-pRb. Induction, solubilization, and purification of the recombinant protein was made as described by Neet and Hunter.[38]

Immunohistochemistry. Fresh samples of liver tissue were cut into pieces and immediately fixed in 10% neutral buffered formalin for 24 hours. Fixed livers were dehydrated in ethanol, cleared in xylene, and embedded in paraffin blocks. Five-micrometer sections of each liver sample were cut and mounted on gelatin-coated slides. They were deparaffinized with xylene and then hydrated in decreasing concentrations of ethanol and rinsed in phosphate-buffered saline (PBS). For each antibody, slices were processed simultaneously, and after endogenous peroxidase blocking procedures, they were placed in Coplin jars, immersed in 10 mmol/L citrate buffer (pH 6.0), and autoclaved for 10 minutes at 15 psi (121°C). The slices were allowed to cool for a further 25 minutes and were then rinsed in distilled water and PBS. Treated slices were immunostained as described below.

The ABC detection system was used for immunostaining. Horse or goat serum, a blocking kit to avoid nonspecific binding of biotin-avidin system reagents, biotinylated secondary antisera, and avidin-biotin-horseradish peroxidase (ABC kits for mouse monoclonal or rabbit polyclonal antibodies) were obtained from Vector (Burlingame, CA). Immunohistochemical staining was performed as follows: after pretreatment of the slices, a normal serum incubation (horse or goat) of 20 minutes was used to reduce nonspecific background staining. Then, primary antibodies were incubated overnight at 4°C. Incubations with the linking antibody (biotinylated anti-mouse or biotinylated anti-rabbit sera) and then the labeled ABC, each for 45 minutes, followed. A 10-minute rinse of the slices with PBS was performed between each of the three incubations. Then, diaminobenzidine, as a chromogen, was applied and incubated for 10 minutes. Finally, the slices were rinsed with PBS and mounted for examination. The negative control slices were treated in an identical manner, except that the primary antibodies were omitted. For histological examination of liver samples, slices of each treatment (control and regenerating livers) were stained with hematoxylin-eosin according to conventional procedures.

Measurement of DNA Synthesis In Vivo. ^{3}H-thymidine was injected intraperitoneally at a dose of 0.5 μCi/g body weight (5 Ci/mmol/L; Radiochemical Center, Amersham) 1 hour before killing the animals. Autoradiography was performed as described by Baserga and Malamud.[39] Briefly, fresh liver tissue was cut into pieces and immediately fixed in 10% neutral buffered calcic-formalin for 24 to 72 hours. Fixed livers were dehydrated in ethanol, cleared in xylene, and embedded in paraffin blocks. Five-micrometer sections of each liver sample were cut and mounted on gelatin-coated slides. They were deparaffinized in xylene, then hydrated in decreasing concentrations of ethanol and rinsed in distilled water. The slices were submerged into the nuclear emulsion Ilford L-4 (Ilford Limited) at 40° to 45°C and subsequently dried and exposed in darkness for 3 weeks at 4°C. After photographic processing (developing and fixing), the slices were stained with hematoxylin-eosin according to conventional procedures. Under light-microscopic examination, the DNA-synthetic activity was estimated and expressed as the index of labeled hepatocytes (%).

RESULTS

Activities of Cdk4 and Cdk2 During Rat Liver Regeneration. To determine the activities of cdk4 and cdk2 during rat liver regeneration, 66% PHs or sham operations were performed, and livers were excised at 5 hours, 13 hours, 24 hours, and 28 hours after surgery. Three to six livers from each time after surgery were homogenized together, and the activities of both cdks were measured in these homogenates. The activity of cdk4 was undetectable in quiescent cells and at 5 hours after PH (Fig. 1A); at 13 hours, some activity was detected, and at 24 hours, the activity was maximal. Then, at 28 hours, it decreased. The kinetics of cdk2 activity was similar to that of cdk4 (Fig. 1B). Neither cdk4 nor cdk2 activities were detected after sham operations (data not shown). The peaks of cdk4 and cdk2 activities correlated well with both the expression of PCNA (a cofactor of DNA polymerase α whose expression correlates with DNA synthesis) (Fig. 1C) and the wave of DNA replication (Fig. 1D).

Levels of Proteins of the Cell-Cycle Regulatory Machinery During Rat Liver Regeneration. Our first approach to examining the mechanisms involved in the activation of cdk4 and cdk2 was to determine the levels of the proteins involved in their regulation at different times after PH. Samples from liver homogenates were subjected to Western blotting using specific antibodies against cdks: cdk4 and cdk2; cyclins: cyclins D1, D3, E, and A; CKIs: $p16^{Ink4a}$, $p21^{Cip1}$, and $p27^{Kip1}$; and cdk activators: cdc25A and CAK (cdk7 and cyclin H).

All these proteins, with the exception of $p21^{Cip1}$, whose levels were very low, were clearly detected in quiescent cells (Fig. 2A-2D). After PH, the amount of some of these proteins

($p16^{Ink4a}$, cyclin H, cdk7, and cdc25A) remained unmodified, whereas the levels of the other proteins (with the exception of $p27^{Kip1}$, which decreased at 24 hours) increased to variable degrees at different times after PH (Fig. 2A-2D).

Because the main known substrates for G_1/S cyclin-cdk complexes are the proteins of the pocket family (pRb, p107, and p130), we also analyzed the levels and the phosphorylation status of these proteins after PH. Unfortunately, in spite of using a panel of different anti-pRb antibodies, we were not able to detect pRb either in quiescent cells or at any time after PH. Quiescent cells contained significant levels of p130 (Fig. 2E). The levels of this protein increased progressively from 5 hours to 28 hours. Changes in the mobility of p130, as a result of phosphorylation, were clearly seen at 24 hours and 28 hours after PH, in coincidence with the induction of cdk4 and cdk2 activities. p107 was not detectable either in quiescent cells or at 5 or 13 hours, but it was observed at 24 hours and 28 hours. At these later times, p107 was found phosphorylated (as detected by a gel mobility shift). The phosphorylation of p107 coincides with the peaks of cdk4 and cdk2 activities.

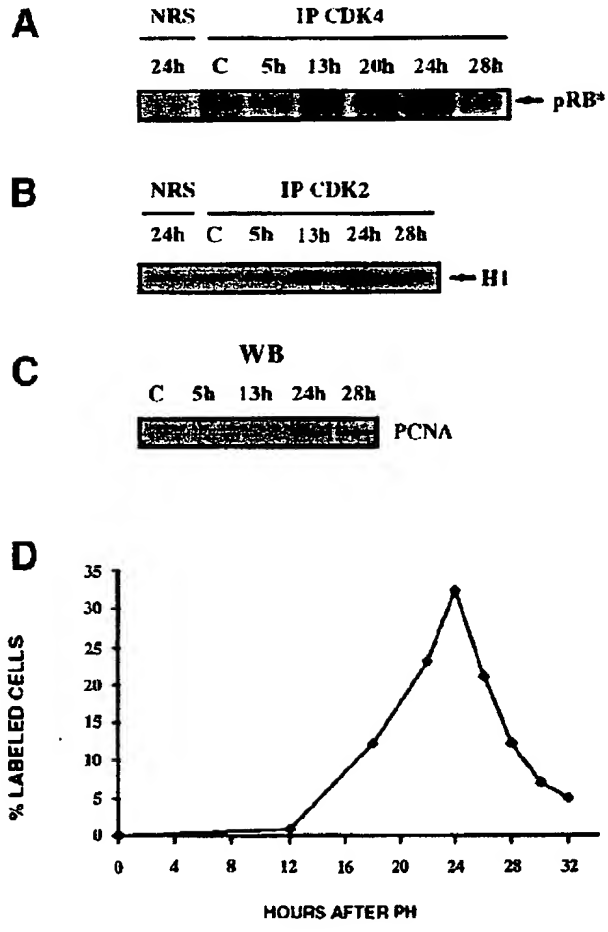

FIG. 1. Time course of (A) cdk4 activity, (B) cdk2 activity, (C) expression of PCNA, and (D) DNA synthesis after PH. Cdk4 and cdk2 activities were measured by IP, followed by kinase assays using liver homogenates as described in Materials and Methods. IPs were performed using specific antibodies against cdk4, cdk2, or normal rabbit serum (NRS), which was used as a control. GST-pRb or histone H1 were used as exogenous substrates for cdk4 and cdk2, respectively. PCNA expression was studied by Western blotting (WB) using 50 μg of homogenate. DNA synthesis was measured as the incorporation of ^{3}H-thymidine into the DNA by autoradiography as described in Materials and Methods. The DNA-synthetic activity was estimated and expressed as the index of labeled hepatocytes. Values are the mean of five slices from three rats for each point.

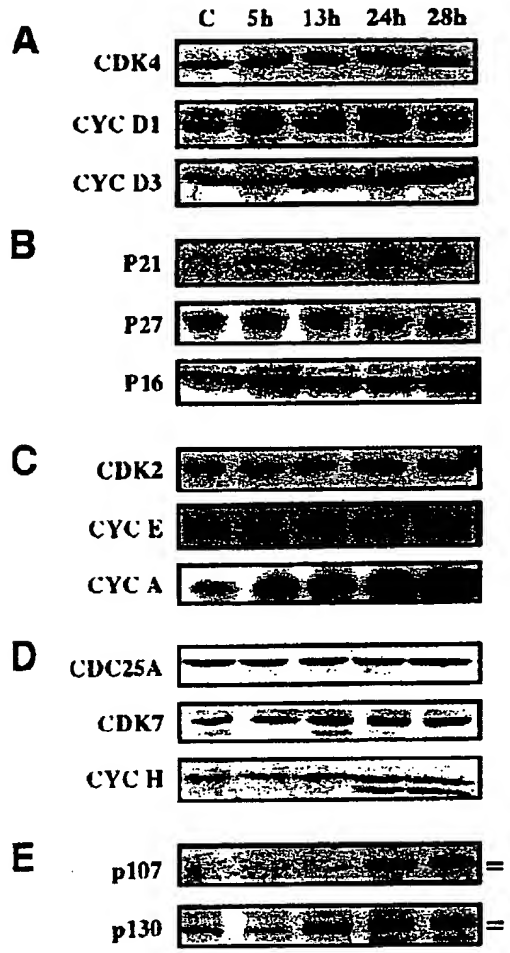

FIG. 2. Levels of cell-cycle regulatory proteins during rat liver regeneration. Fifty micrograms of liver homogenates from nonoperated rats (c) and from rats at different times after PH was subjected to Western blotting using antibodies against (A) cdk4, cyclins D1 and D3; (B) $p21^{Cip1}$, $p27^{Kip1}$, and $p16^{Ink4a}$; (C) cdk2, cyclins E and A; (D) cdc25A, cdk7, and cyclin H; and (E) p107 and p130. In (E), the *bars* indicate the hyperphosphorylated (*upper bar*) and the hypophosphorylated (*lower bar*) forms of p107 and p130.

These results indicate that in quiescent cells and at 5 hours after PH, the key proteins involved in the regulation of cdk4 and cdk2 were present in liver cells; however, both cdk4 and cdk2 were inactive. Although no significant changes in the levels of these proteins were observed at 13 hours, the activity of both enzymes started to increase, and at 24 hours, both kinases were maximally activated. Only slight increases in cyclin D1 and cdk2 and a decrease in $p27^{Kip1}$ were observed between 13 hours and 24 hours; however, the extent of these changes does not seem to be high enough to explain the sharp activation of both kinases. Thus, to better understand how cdk4 activity was induced after PH, analysis of the cyclin D-cdk4 complexes at different times after PH was subsequently performed.

Analysis of Cyclin D-Cdk4 Complexes During Rat Liver Regeneration. The status of the cyclin D-cdk4 complexes at different times after PH was analyzed by IP, followed by Western blotting. IP experiments using antibodies against cdk4 did not permit the detection of cyclin D1-cdk4 complexes in quiescent cells (Fig. 3A). However, when using anti-cyclin D1 antibodies, low amounts of these complexes could be detected (Fig. 3B). The amount of these complexes was still low at 5 hours but increased at 13 to 28 hours (Fig. 3A and 3B). In contrast, cyclin D3-cdk4 complexes were clearly detected in quiescent cells when using both anti-cdk4 or anti-cyclin D3 antibodies (Fig. 3A and 3C). The levels of cyclin D3-cdk4 complexes increased slightly until 24 hours and then decreased at 28 hours (Fig. 3A and 3C). Both cyclin D1-cdk4 and cyclin D3-cdk4 complexes contained $p27^{Kip1}$ in quiescent cells and after PH. However, the levels of $p27^{Kip1}$ associated with these complexes decreased at 24 hours and 28 hours (Fig. 3A-3C), coinciding with the decrease in the total levels of $p27^{Kip1}$ observed in the homogenates (Fig. 2B). The amount of $p21^{Cip1}$ associated with cyclin D-cdk4 complexes in quiescent cells was very low. The $p21^{Cip1}$ protein associated with these complexes was undetectable when the IPs were performed using anti-cdk4 antibodies (Fig. 3A). However, when anti-cyclin D1 or anti-cyclin D3 antibodies were used, it was observed that in quiescent cells, low amounts of $p21^{Cip1}$ were associated with cyclin D3-cdk4 but not with cyclin D1-cdk4 (Fig. 3B and 3C). The amount of $p21^{Cip1}$ bound to both complexes increased progressively after PH (Fig. 3A-3C). IPs using anti-$p21^{Cip1}$ antibodies confirmed these results and revealed that at 28 hours, the binding of $p21^{Cip1}$ to cyclin D1-cdk4, but not to cyclin D3-cdk4, was increased (Fig. 3D).

IP experiments also detected the presence of cdk4-$p16^{ink4a}$ complexes in quiescent cells and also during regeneration (Fig. 3A).

These results suggest that the binding of $p27^{Kip1}$ and $p21^{Cip1}$ could be involved in the regulation of cdk4 activity during regeneration. Because the increase in cdk4 activity at 24 hours coincides with a strong decrease in the amount of $p27^{Kip1}$ bound to both cyclin D1-cdk4 and cyclin D3-cdk4 complexes (Fig. 3A-3C), it can be suggested that the dissociation of $p27^{Kip1}$ from the complexes could facilitate this increase in cdk4 activity. Likewise, the increased association of $p21^{Cip1}$ to cdk4 and cyclin D1 at 28 hours (Fig. 3D) could be involved in the inactivation of cdk4 activity observed at this time after PH.

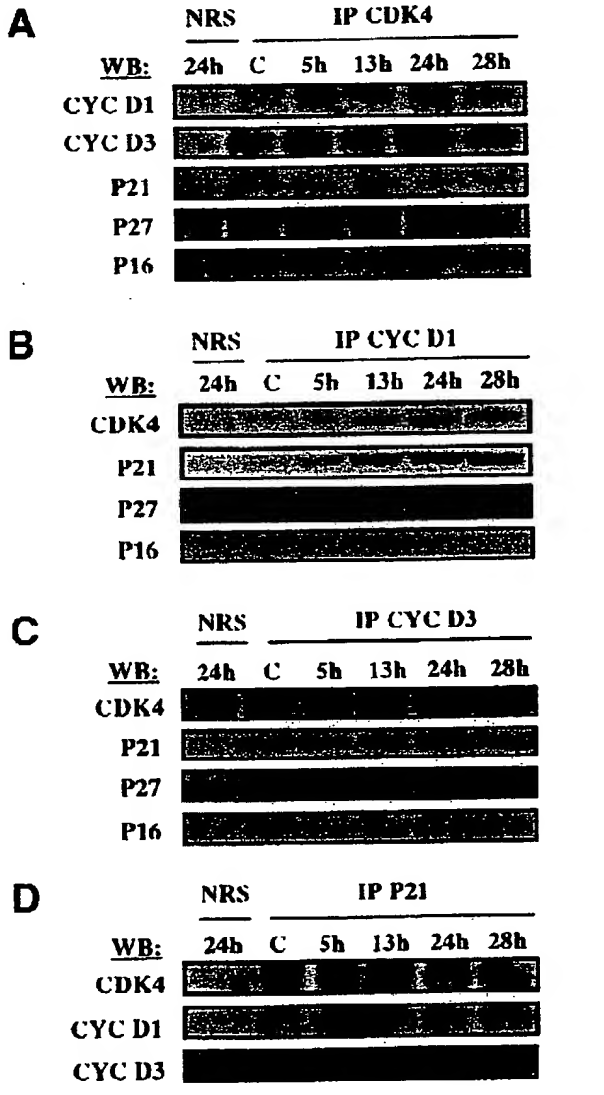

FIG. 3. Analysis of cdk4, cyclin D1, cyclin D3, and $p21^{Cip1}$ complexes during rat liver regeneration. Liver homogenates were immunoprecipitated using antibodies against cdk4 (A), cyclin D1 (B), cyclin D3 (C), or $p21^{Cip1}$ (D). The immunoprecipitates (IP) were subjected to Western blot analysis (WB) with antibodies against cyclin D1, cyclin D3, $p21^{Cip1}$, $p27^{Kip1}$, and $p16^{ink4a}$ (A); against cdk4, $p21^{Cip1}$, $p27^{Kip1}$, and $p16^{ink4a}$ (B and C); and against cdk4, cyclin D1, and cyclin D3 (D). In all the cases, a control was performed using a normal rabbit serum (NRS) to immunoprecipitate samples of 24-hour regenerating livers.

Immunocytochemical Analysis of D-Type Cyclins, Cdk4, and $p21^{Cip1}$ During Rat Liver Regeneration. As mentioned above, quiescent cells contained significant levels of cyclin D3-cdk4 complexes, but only low levels of cyclin D1-cdk4. However, the total amounts of both cyclins were similar in quiescent cells (Fig. 2A). Thus, a possibility for the explanation of this distinct ability of both D-type cyclins to form complexes with cdk4 could be a differential intracellular location of both cyclins in these cells. It could also be possible that their intracellular location was modified during liver regeneration, leading to the increase of the formation of cyclin D1-cdk4 complexes. To test these possibilities, the intracellular distribution of cyclin D1, cyclin D3, and cdk4 was studied by immunocytochemistry using slices obtained from livers at different times after PH. In quiescent cells, cdk4 and cyclin D3 were mainly located in the cytoplasm, whereas cyclin D1 was mostly nuclear (Fig. 4). At 5 hours after PH, cdk4 and cyclin D3 were detected in both cytoplasm and nuclei. Interestingly, at this time, both proteins were significantly associated with the nuclear envelope, although staining in intranuclear domains was also observed. These results suggest that both proteins translocate from cytoplasm into the nucleus at this time after PH. Cyclin D1, which was already nuclear in quiescent cells, also showed a clear association with the nuclear envelope at 5 hours after PH (Fig. 4). At 13 hours after PH and thereafter, all these proteins (cyclin D1, cyclin D3, and cdk4) were mostly intranuclear and displayed similar patterns (Fig. 4).

The intracellular location of $p21^{Cip1}$ was also analyzed, because a recent report suggested that this protein could be involved in the translocation of cyclin D-cdk4 from cyto-

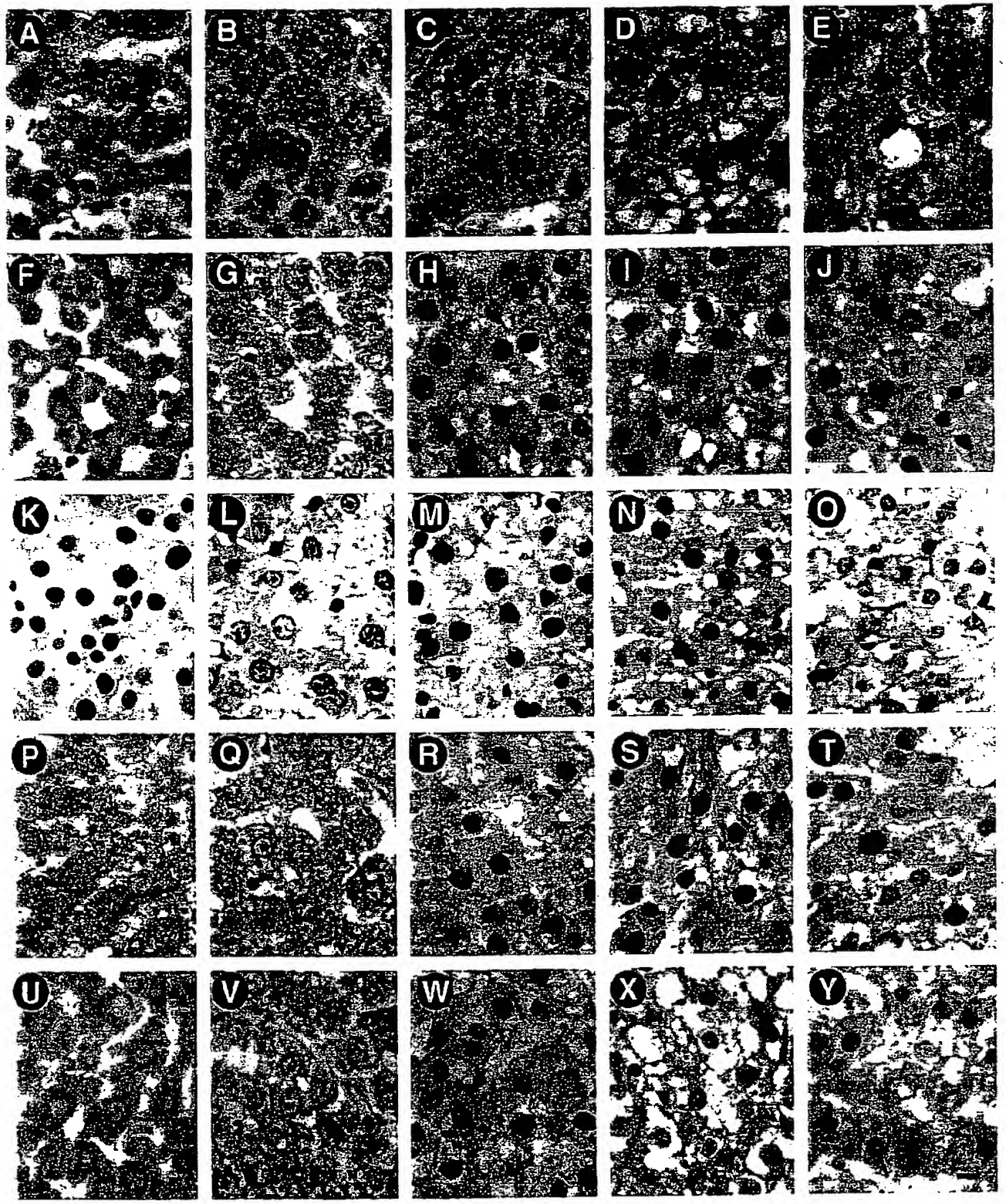

FIG. 4. Immunocytochemical detection of cdk4, cyclin D1, cyclin D3, and $p21^{Cip1}$ during rat liver regeneration. Rat liver sections from control (A, F, K, P, and U) and hepatectomized rats at different times after surgery: 5 hours (B, G, L, Q, and V), 13 hours (C, H, M, R, and W), 24 hours (D, I, N, S, and X), and 28 hours (E, J, O, T, and Y) were stained with hematoxylin-eosin (A-E), or immunostained with anti-cdk4 (F-J), anti-cyclin D1 (K-O), anti-cyclin D3 (P-T), or anti-$p21^{Cip1}$ (U-Y). *Bar* = 10 μm.

plasm into the nucleus in epithelial cells.[40] In quiescent cells, $p21^{Cip1}$ was mostly cytoplasmatic (Fig. 4). After PH, $p21^{Cip1}$ translocated into the nucleus in a way and timing similar to that of cyclin D3 and cdk4. At 5 hours, $p21^{Cip1}$ also associated with the nuclear envelope. The concomitant translocation of $p21^{Cip1}$, cdk4, and cyclin D3 from the cytoplasm to the nucleus, at 5 hours, is compatible with the possible role of $p21^{Cip1}$ as a translocation factor for cyclin D-cdk4 complexes.[40] Figure 5 shows magnifications of typical nuclei from quiescent cells and from 5-hour hepatectomized rats immunostained with antibodies against each of these proteins.

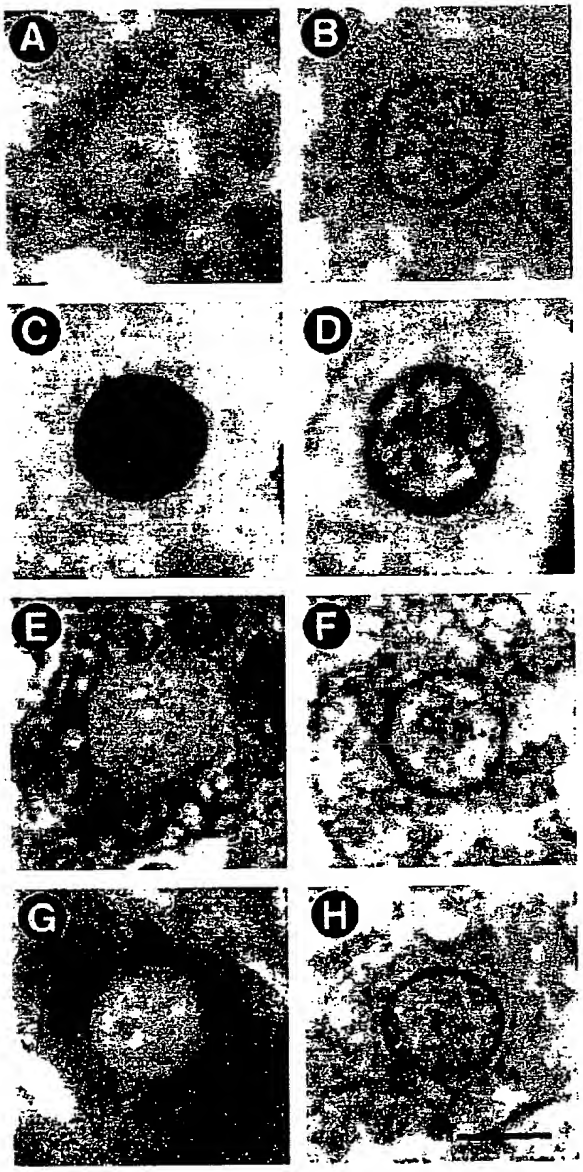

FIG. 5. Immunocytochemical detection of cell-cycle regulatory proteins in rat liver nuclei from nonoperated (A, C, E, and G) and 5-hour hepatectomized rats (B, D, F, and H). Liver sections were immunostained with antibodies against cdk4 (A and B), cyclin D1 (C and D), cyclin D3 (E and F), and $p21^{Cip1}$ (G and H). At 5 hours after surgery, the intranuclear immune reaction is diffuse, with only a few aggregates visible, and in all cases, the immunoreactivity is clearly associated with the nuclear envelope. *Bar* = 10 μm.

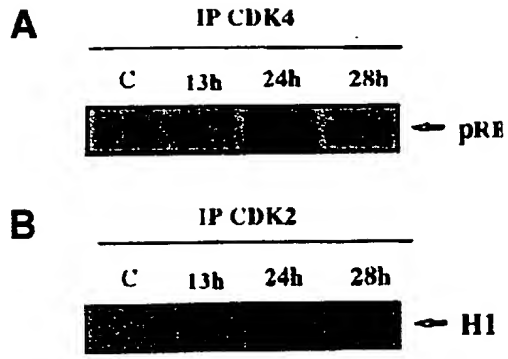

FIG. 6. Time course of cdk4 (A) and cdk2 (B) activities in the S1 nuclear fraction after PH. Cdk4 and cdk2 activities were measured by immunoprecipitation (IP) followed by kinase assays in samples from nonoperated rats (c) and from rats at different times after PH. IPs were performed using specific antibodies against cdk4 or cdk2. GST-pRb or histone H1 were used as exogenous substrates for cdk4 and cdk2 activity, respectively.

These results indicate that the existence of cyclin D3-cdk4 complexes in quiescent cells can be the result of the simultaneous presence of both proteins in the same cellular compartment, i.e., the cytoplasm. In contrast, the different intracellular location of cyclin D1 (nuclear) and cdk4 (cytoplasmatic) explains the low levels of cyclin D1-cdk4 complexes in quiescent cells. The translocation of cdk4 from cytoplasm into the nucleus at 5 hours after PH may account for the progressive increase in the formation of cyclin D1-cdk4 complexes. However, as reported in other cell types, mitogenic stimuli induce the expression of an assembly factor that increases the rate of formation of cyclin D-cdk4 complexes. Thus, the induction of such an assembly factor after PH may also participate in the increase in the number of both types of D-type cyclins-cdk4 complexes.

Activities of Cdk4 and Cdk2 and Levels of the Proteins of the Cell-Cycle Regulatory Machinery in Rat Liver Nuclear Subfractions After PH. Although the specific association of the CKIs, $p27^{Kip1}$ and $p21^{Cip1}$, with cyclin D-cdk4 complexes could be related to the activation and inactivation of cdk4, we wanted to analyze whether intranuclear redistribution of D-type cyclins, cdk4, and both CKIs, could be associated with the activation or inactivation of cdk4. To test this possibility, the activity of cdk4 and the levels of the proteins involved in its regulation were analyzed at different times after PH in two nuclear subfractions named S1 and NM. S1 fraction is a soluble fraction obtained after the treatment of purified nuclei with nucleases. NM is the insoluble residual fraction obtained after the extraction of purified nuclei with nucleases and high-salt–containing buffers.

The activity of cdk4 in the S1 fraction was undetectable in quiescent cells until 13 hours after PH (Fig. 6A). It increased sharply at 24 hours and subsequently decreased at 28 hours. These results are essentially consistent with the activity of cdk4 observed in homogenates (Fig. 1A). The only difference between these results is that in homogenates, a low activity was observed at 13 hours, whereas no activity was found in the S1 fraction at this time.

We did not detect cdk4 activity in the NM fraction. Because this fraction is highly insoluble, IP experiments cannot be performed directly. Thus, in spite of treating NM with detergents and then performing IPs using anti-cdk4 antibod-

ies, no cdk4 activity was detected. We also attempted to determine cdk4 activity directly in the NM by adding the exogenous substrate (pRb) and radioactive ATP to entire NM fractions and then analyzing the phosphorylation of the exogenous pRb after incubation. With this approach, we were also unable to determine any cdk4 activity in this fraction.

Cyclin D1 was clearly detected in the S1 fraction from quiescent cells. In contrast, only low amounts of cdk4 and cyclin D3 were detected (Fig. 7A). This is consistent with results obtained by immunocytochemistry, indicating that cdk4 and cyclin D3 were mostly cytoplasmatic and cyclin D1 mostly nuclear in quiescent cells. In S1 fraction, the amount of cyclin D1 remained high until 24 hours. In contrast, the levels of cdk4 and cyclin D3 increased slightly until 13 hours and then more sharply at 24 hours. Finally, a decrease in the amount of all these three proteins in the S1 fraction was observed at 28 hours. The most dramatic reduction was that of cyclin D1, whose levels were almost undetectable at 28 hours after PH. Coincident with this dramatic decrease of cyclin D1 in the S1 fraction, a sharp increase of this protein was observed in the NM fraction at this time after PH (Fig. 7A). These results suggest that at 28 hours after PH, cyclin D1 moved from S1 fraction to NM. A slight increase of cdk4 was also observed in the NM at this time after PH, suggesting that cdk4 also moved from S1 to NM at 28 hours after PH.

These results indicate that the activity of cdk4 in the S1 fraction correlates well with the levels of D-type cyclins and cdk4 in this fraction. Thus, the low levels of cdk4 during the first 13 hours after PH can explain why cdk4 activity was very low in this fraction during this period. The sharp increase of cdk4 and cyclin D3 at 24 hours could explain the elevation of cdk4 activity at this time after PH. Finally, the decrease of cdk4 activity at 28 hours could be explained by the translocation of cyclin D1 to the NM and the diminution of cyclin D3 and cdk4 in this fraction. The remaining cdk4 activity at 28 hours could be the result of the reduced levels of cyclin D3 and cdk4 observed in this fraction.

We also analyzed whether the levels of CKIs were modified in the nuclear subfractions after PH. Both $p27^{Kip1}$ and $p21^{Cip1}$ proteins were detected in the S1 fraction from quiescent cells (Fig. 7B). The levels of both proteins displayed a similar pattern during regeneration: their amount remained low until 13 hours, increased at 24 hours and decreased at 28 hours. In contrast, the amount of $p16^{ink4a}$ remained constant during regeneration.

The pattern of cdk2 activity in the S1 fraction was similar to that of cdk4 (Fig. 6B). It was undetectable in quiescent cells and until 13 hours after PH. It was maximal at 24 hours, and then decreased at 28 hours. Cdk2 activity correlated well with the levels of cyclin E, cyclin A, and cdk2 in this fraction. The cdk2 protein was undetectable during the first 13 hours after PH, whereas those of cyclin E and A were very low during this period (Fig. 7C). The levels of the three proteins increased sharply at 24 hours, and then decreased at 28 hours. The decrease of cdk2 was very strong, whereas that of cyclins E and A were quite modest. Thus, the concomitant presence of cyclin E, cyclin A, and cdk2 in the S1 fraction at 24 hours after PH could be responsible for the high activity of cdk2, whereas the decrease of cdk2 in this fraction at 28 hours could explain the reduction of cdk2 activity.

The accumulation of D-type cyclins and cdk4 in the S1 fraction could lead to the increase of cdk4 activity, because the activators (CAK or cdc25A) could phosphorylate/dephosphorylate the cyclin D-cdk4 complexes when they appear in this fraction at 24 hours after PH. To analyze this possibility, the levels of cdk7, cyclin H, and cdc25A were also measured in both nuclear subfractions. Cdc25A and cdk7 were present in both S1 fraction and NM from quiescent cells (Fig. 7D). The amount of both proteins remained constant during the entire cell cycle in both subfractions. In contrast, cyclin H was only present in S1 fraction, and its amount increased progressively from control to 28 hours. Thus, it is possible that cyclin D-cdk4 complexes could be activated by CAK and cdc25A only in the S1 fraction. A similar explanation could be possible in the case of cdk2.

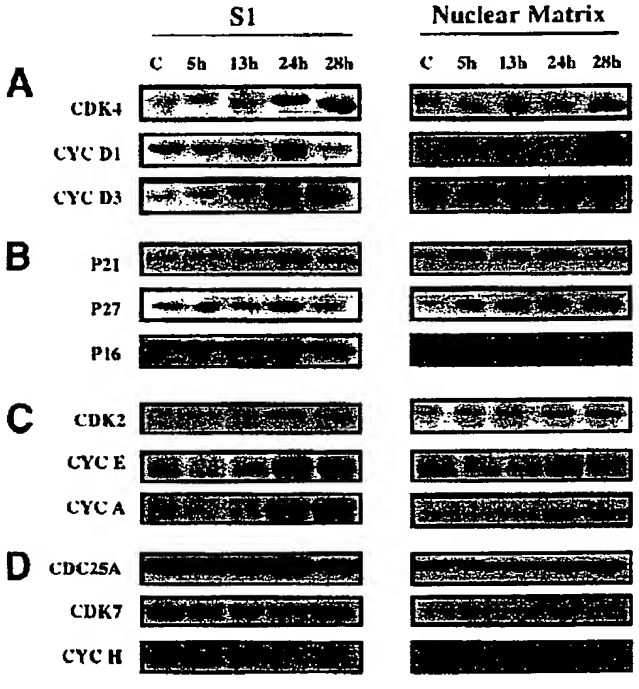

FIG. 7. Levels of cell-cycle regulatory proteins in nuclear subfractions during rat liver regeneration. S1 and nuclear matrix fractions from nonoperated rats (c) and from rats at different times after PH were obtained as described in Materials and Methods. Fifty micrograms of each sample was analyzed by Western blotting using antibodies against (A) cdk4, cyclin D1, and cyclin D3; (B) $p21^{Cip1}$, $p27^{Kip1}$, and $p16^{ink4a}$; (C) cdk2, cyclin E, and cyclin A; (D) cdc25A, cdk7, and cyclin H.

DISCUSSION

Although significant insight has been gained into the factors that promote hepatocyte proliferation, very little is known about mechanisms that regulate cell-cycle progression in the hepatocytes proliferating *in vivo* after PH. During the last few years, a number of articles reported new information about the mechanisms involved in the regulation of cdk4 and cdk2 during liver regeneration. However, many points still remain obscure, and some aspects are controversial.

The first aspect for discussion concerns the levels of proteins of the G_1/S cell-cycle regulatory machinery in quiescent liver cells and their variations after PH. All the reports, including our results, coincide that all these proteins, with the exception of $p21^{Cip1}$, are detectable in quiescent cells from young rats or mice. There is also agreement with the fact that cyclins D1, D3, E, and A, cdk4, cdk2, and $p21^{Cip1}$ are

induced after PH.[25-32] Interestingly, results reported here indicate that the levels of $p27^{Kip1}$ decreased at 24 to 28 hours after PH in rats, in agreement with results reported by others.[25-32] However, PH in mice did not induce any alteration in the levels of this protein[31] (Jaime and Bachs, unpublished data, March 1998). This behavior of $p27^{Kip1}$ in hepatectomized mice is surprising, because in most of the cell types proliferating in culture,[16] the levels of $p27^{Kip1}$ decrease at the mid-late G_1. Thus, rat hepatocytes respond to PH similarly to most of the cell types proliferating in culture, whereas those from mice respond differently.

We report here for the first time the analysis of the levels of the cdk activators, cdc25A and CAK (cyclin H-cdk7) during rat liver regeneration. The levels of these activators remained unmodified after PH.

In summary, it can be concluded that the induction of the proteins of the G_1/S cell-cycle regulatory machinery in rat liver cells proliferating *in vivo* behaves similarly to that observed in the different cell types proliferating in culture.

A second important point of discussion is related to the formation of cyclin D-cdk4 complexes after PH and their relationship with the activation of cdk4. Very little information has been previously reported about the status of cyclin D-cdk4 complexes after PH. As far as we know, only two reports describe the formation of these complexes, and both analyzed only the status of cyclin D1-cdk4, but not the complexes of cdk4 with the other D-type cyclins. Our results are in agreement with both articles in the sense that quiescent cells contain very low amounts of cyclin D1-cdk4 complexes and that these complexes are formed during G_1.[31,32] Results reported here indicate that in quiescent cells, cyclin D1 is mostly nuclear, whereas cdk4 and cyclin D3 are cytoplasmic; thus, one can argue that cyclin D1 could not form complexes with cdk4 in quiescent cells, because they are located in different intracellular compartments. Likewise, the presence of cyclin D3 and cdk4 in the cytoplasm of quiescent cells could explain the existence of cyclin D3-cdk4 complexes in these cells. The progressive formation of cyclin D1-cdk4 complexes after PH could be possible, because cdk4 translocates from cytoplasm into the nucleus during G_1. Thus, these complexes are formed in the nucleus. In contrast, cyclin D3-cdk4 are originally formed in the cytoplasm and subsequently translocated into the nucleus during G_1.

It is assumed that cyclin D-cdk4 complexes are active when located in the nucleus. However, our data show that these complexes were not always active in the nucleus, because at 13 hours after PH, both cyclin D3-cdk4 and cyclin D1-cdk4 complexes were nuclear, but cdk4 activity was very low. At 24 hours after PH, cdk4 activity was maximal, although no differences in the levels of cyclin D-cdk4 complexes were observed. Thus, the activation of cdk4 at 24 hours is not directly related to the levels of cyclin D-cdk4 complexes. A mechanism to explain cdk4 activation could be related to the differential association of the inhibitors, $p21^{Cip1}$ and $p27^{Kip1}$, with cyclin D-cdk4 complexes during regeneration. Results reported here suggest a role of $p27^{Kip1}$ in the inhibition of cdk4 during the first 13 hours after PH. The $p27^{Kip1}$ protein is associated with both types of cyclin D-cdk4 complexes during this period. Then, $p27^{Kip1}$ is suddenly released from both complexes at 24 hours, in coincidence with cdk4 activation. Thus, it can be suggested that the binding of $p27^{Kip1}$ to cyclin D-cdk4 complexes during the first 13 hours after PH prevents the activation of cdk4. The subsequent separation of this inhibitor would permit cdk4 activation.

A second mechanism involved in the activation of cdk4 could be the change in the intranuclear location of cyclin D-cdk4 complexes, which could permit the interaction with the activators, CAK and cdc25A. The analysis of cdk4 activity in the S1 nuclear subfraction showed a peak of activity at 24 hours after PH, similar to the activity in homogenates. Thus, it can be assumed that most of the activity detected in the homogenates corresponds to that detected in the S1 fraction, although it cannot be excluded that a part of cdk4 activity could also be found in other nuclear fractions. The simultaneous accumulation of cyclin D1, cyclin D3, and cdk4 in the S1 fraction at 24 hours correlates with the increase of cdk4 activity. These results suggest that some factors present in S1—CAK and cdc25A being the best candidates—activate cdk4 at this time after PH. Cdk7 and cyclin H are always present in this fraction. Because it has been reported that CAK is always active during the cell cycle, it is possible that as soon as cyclin D-cdk4 complexes accumulate in this fraction, they can be activated by CAK. In addition, cdc25A can play a role in cdk4 activation. Because the activity of cdc25A is regulated during the cell cycle, it can also be possible that the accumulation of cyclin D-cdk4 complexes at 24 hours in the S1 fraction could coincide with the activation of cdc25A. However, this is something that has yet to be proven. Thus, the release of $p27^{Kip1}$ from cyclin D-cdk4 complexes and the movement of the complexes to the S1 fraction where they can be activated by CAK and cdc25A could be the mechanisms involved in the activation of cdk4 between 13 and 24 hours after PH.

Two possible mechanisms could contribute to the inactivation of cdk4 at 28 hours after PH. One is the increase in the binding of $p21^{Cip1}$ to cyclin D1-cdk4 complexes. The second mechanism could be the translocation of cyclin D1, and a portion of cdk4 from S1 fraction to the NM. The remaining cdk4 activity observed in the S1 fraction at 28 hours could be a result of the cyclin D3-cdk4 complexes that still were retained in this fraction.

A similar hypothesis could explain the activation of cdk2 during liver regeneration. Cyclin E, cyclin A, and cdk2 accumulate in the S1 fraction at 24 hours, in parallel with the induction of maximal cdk2 activity. There, the complexes could be activated by CAK and cdc25A as in the case of cdk4. The strong decrease in the amount of cdk2 in this fraction at 28 hours after PH can be responsible for the decrease of its activity observed at this time after PH. The role of $p21^{Cip1}$ and $p27^{Kip1}$ in the regulation of cdk2 activity during liver regeneration is currently being investigated in our laboratory.

A third aspect for discussion is the mechanisms involved in the intracellular movements of D-type cyclins, cdk4, and $p21^{Cip1}$ during liver regeneration. The induction of cdk4 activity was preceded by the translocation of cyclin D3-cdk4 from the cytoplasm into the nucleus and by the increase in the formation of cyclin D1-cdk4 complexes. Because at 5 hours after PH cyclin D3, cdk4, and cyclin D1 were mostly located in the nuclear envelope, it can be suggested that cyclin D1 could associate with cdk4 in the nuclear envelope, just during the time of cdk4 translocation. The evidence that $p21^{Cip1}$ was also associated with the nuclear envelope at 5 hours after PH suggests that $p21^{Cip1}$ could translocate in association with cyclin D3-cdk4 complexes. This possibility is consistent with previous results showing that $p21^{Cip1}$ is

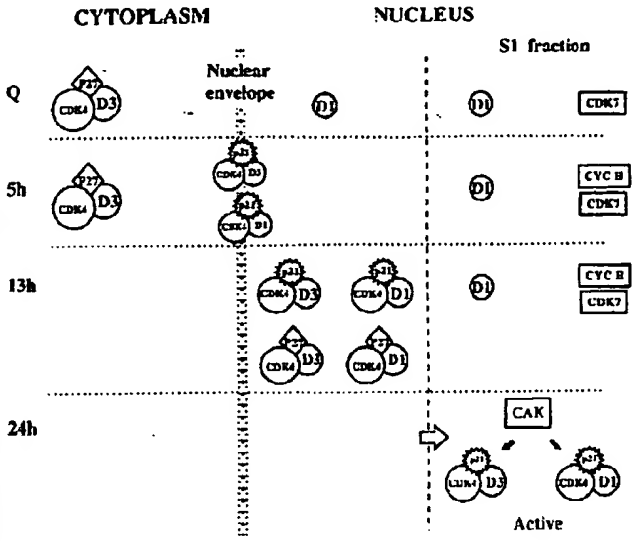

FIG. 8. Model of the intracellular rearrangements of D-type cyclins, cdk4, $p27^{Kip1}$, and $p21^{Cip1}$ during rat liver regeneration. Quiescent rat liver cells contain significant levels of cyclin D3-cdk4-$p27^{Kip1}$ and low levels of cyclin D3-cdk4-$p21^{Cip1}$ complexes in the cytoplasm. After PH, these complexes translocate into the nucleus. The first step (at 5 hours) is their association with the nuclear envelope. At this time, cyclin D1, which was already nuclear in quiescent cells, moved and associated with the nuclear envelope. It is possible that there, cyclin D1 could bind to cdk4, $p21^{Cip1}$, and $p27^{Kip1}$. At 13 hours, cyclin D3-cdk4-$p27^{Kip1}$, cyclin D3-cdk4-$p21^{Cip1}$, cyclin D1-cdk4-$p27^{Kip1}$, and cyclin D1-cdk4-$p21^{Cip1}$ complexes were located in a still-unknown intranuclear domain. At 24 hours, $p27^{Kip1}$ is eliminated from the complexes, and cyclin D3-cdk4-$p21^{Cip1}$ and cyclin D1-cdk4-$p21^{Cip1}$ moved to the S1 fraction, where they become active, possibly as a result of the phosphorylation of the complexes by CAK.

involved in the translocation of cyclin D-cdk4 from cytoplasm into the nucleus.[40] The association of these complexes with the nuclear envelope could be mediated by a 70-kd protein (p70) that is able to bind $p21^{Cip1}$ in this compartment (Estanyol J-M, Bachs O, unpublished data, March 1998). It is possible that p70 may associate not only with $p21^{Cip1}$, but also with $p21^{Cip1}$-cyclin D3-cdk4 and $p21^{Cip1}$-cyclin D1-cdk4 complexes at 5 hours after PH.

Interestingly, $p21^{Cip1}$ moved to S1 fraction in parallel with cyclin D3 and cdk4, suggesting that $p21^{Cip1}$ could also participate in the movement of these proteins to the S1 fraction. The strong association of $p21^{Cip1}$ with cyclin D-cdk4 complexes when they are active indicates that $p21^{Cip1}$ is not inhibiting these complexes, but performing another unknown function that can be related to the movement of the complexes from one cellular compartment to another.

A model summarizing how cyclin D-cdk4 complexes could be activated after a PH is showed in Fig. 8.

To establish the mechanisms inducing the translocation of G_1/S cyclins and cdks from cytoplasm to the nucleus during G_1, and those responsible for the intranuclear movements of these proteins are important goals for the understanding of how cdk4 and cdk2 are activated after PH. Experiments to elucidate these mechanisms are currently under way in our laboratory.

REFERENCES

1. Higgings GM, Anderson RM. Experimental pathology of the liver. I. Restoration of the liver of the white rat following partial surgical removal. Arch Pathol 1931;12:186-202.
2. Steer CJ. Liver regeneration. FASEB J 1995;9:1396-1400.
3. Michalopoulos GK, DeFrances MC. Liver regeneration. Science 1997;276: 60-66.
4. Mead JE, Fausto N. Transforming growth factor alpha may be a physiological regulator of liver regeneration by means of an autocrine mechanism. Proc Natl Acad Sci U S A 1989;86:1558-1562.
5. Skov-Olsen P, Boesby S, Kirkegaard P, Thorkelsen K, Almdal T, Poulsen SS, Nexo E. Influence of epidermal growth factor on liver regeneration after partial hepatectomy in rats. HEPATOLOGY 1988;8:992-996.
6. Lindroos PM, Zarnegar R, Michalopoulos GK. Hepatocyte growth factor (hepatopoietin A) rapidly increases in plasma before DNA synthesis and liver regeneration stimulated by partial hepatectomy and carbon tetrachloride administration. HEPATOLOGY 1991;13:743-750.
7. Fausto N, Laird AD, Webber EM. Role of growth factors and cytokines in hepatic regeneration. FASEB J 1995;9:1527-1536.
8. Yamada Y, Kirillova I, Peschon JJ, Fausto N. Initiation of liver growth by tumor necrosis factor: deficient liver regeneration in mice lacking type I tumor necrosis factor receptor. Proc Natl Acad Sci U S A 1997;94:1441-1446.
9. Sherr CJ. G1 phase progression: cycling on cue. Cell 1994;79:551-556.
10. Pines J. Cyclins and cyclin-dependent kinases: a biochemical view. Biochem J 1995;308:697-711.
11. Graña X, Reddy PE. Cell cycle control in mammalian cells: role of cyclins, cyclin-dependent kinases (CDKs), growth suppressor genes and cyclin-dependent kinase inhibitors (CKIs). Oncogene 1995;11:211-219.
12. Morgan DO. Principles of CDK regulation. Nature 1995;374:131-134.
13. Sclafani RA. Cyclin dependent kinase activating kinases. Curr Opin Cell Biol 1996;8:788-794.
14. Lew DL, Kornbluth S. Regulatory roles of cyclin dependent kinase phosphorylation in cell cycle control. Curr Opin Cell Biol 1996;8:795-804.
15. Strausfeld U, Labbe JC, Fesquet D, Cavadore JC, Picard A, Sadhu K, Russell P, et al. Dephosphorylation and activation of a p34cdc2/cyclin B complex in vitro by human CDC25 protein. Nature 1991;351:242-245.
16. Sherr C, Roberts JM. Inhibitors of mammalian G1 cyclin-dependent kinases. Genes Dev 1995;9:1149-1163.
17. Matsushime H, Roussel MF, Ashmun RA, Sherr CJ. Colony stimulating factor I regulates novel cyclins during the G1 phase of the cell cycle. Cell 1991;65:701-713.
18. Matsushime H, Quelle DE, Shurtleff SA, Shibuya M, Sherr CJ, Kato J. D-Type cyclin-dependent kinase activity in mammalian cells. Mol Cell Biol 1994;3:2066-2076.
19. Kato JY, Matsuoka M, Strom DK, Sherr CJ. Regulation of cyclin D-dependent kinase 4 (cdk4) by cdk4-activating kinase. Mol Cell Biol 1994;14:2713-2721.
20. Jinno S, Suto K, Nagata A, Igarashi M, Kanaoka Y, Nojima H, Okayama H. Cdc25A is a novel phosphatase functioning early in the cell cycle. EMBO J 1994;13:1549-1556.
21. Resnitzky D, Reed SI. Different roles for cyclins D1 and E in regulation of the G1-to-S transition. Mol Cell Biol 1995;15:3463-3469.
22. Mayol X, Graña X. pRb, p107 and p130 as transcriptional regulators: role in cell growth and differentiation. In: Meijer L, Guidet S, Philippe M, eds. Progress in Cell Cycle Research. Vol 3. New York: Plenum, 1997:157-169.
23. Lam EWF, La Thangue NB. DP and E2F proteins: coordinating transcription with cell cycle progression. Curr Opin Cell Biol 1994;6:859-866.
24. Dulic V, Lees E, Reed SI. Association of human cyclin E with a periodic G1-S phase protein kinase. Science 1992;257:1958-1961.
25. Lu XP, Koch KS, Lew DJ, Dulic V, Pines, J, Reed SI, Hunter T, Leffer HL. Induction of cyclin mRNA and cyclin-associated histone H1 kinase during liver regeneration. J Biol Chem 1992;267:2841-2844.
26. Loyer P, Glaise D, Cariou S, Baffet G, Meijer L, Guguen-Guillouzo C. Expression of activation of cdks (1 and 2) and cyclins in the cell cycle progression during liver regeneration. J Biol Chem 1994;269:2491-2500.
27. Rininger JA, Goldsworthy TL, Babish JG. Time course comparison of cell cycle protein expression following partial hepatectomy and WY14,643 induced hepatic cell proliferation in F344 rats. Carcinogenesis 1997;18: 935-941.
28. Ehrenfried JA, Ko TC, Thompson A, Evers BM. Cell cycle-mediated regulation of hepatic regeneration. Surgery 1997;122:927-935.
29. Albrecht JH, Meyer AH, Hu MY. Regulation of cyclin-dependent kinase inhibitor $p21^{CIP}$ (WAF1/Cip1/Sdi1) gene expression in hepatic regeneration. HEPATOLOGY 1997;25:557-563.
30. Timchenko NA, Harris TE, Wilde M, Bylyeu TA, Burgess-Beusse BL, Finegold MJ, Darlington GJ. CCAAT/Enhancer binding protein regulates p21 protein and hepatocyte proliferation in newborn mice. Mol Cell Biol 1997;17:7353-7361.

31. Albrecht JH, Poon RYC, Ahonen CL, Rieland BM, Deng C, Crary GS. Involvement of p21 and p27 in the regulation of CDK activity and cell cycle progression in the regenerating liver. Oncogene 1998;16:2141-2150.
32. Kato A, Ota S, Bamba H, Wong RM, Ohmura E, Imai Y, Matsuzaki F. Regulation of cyclin D-dependent kinase activity in rat liver regeneration. Biochem Biophys Res Commun 1998;245:70-74.
33. Kaufman SH, Shaper JH. A subset of non-histone nuclear proteins reversibly stabilized by the sulfhydryl cross-linking reagent tetrathionate. Exp Cell Res 1984;155:477-495.
34. Bachs O, Carafoli E. Calmodulin and calmodulin-binding proteins in rat liver cell nuclei. J Biol Chem 1987;262:10786-10790.
35. Laemmli, UK. Cleavage of structural proteins during the assembly of the head of bacteriophage T4. Nature (London) 1970;227:680-685.
36. Bradford, MM. A rapid and sensitive method for the quantitation of microgram quantities of protein utilizing the principle of protein-dye binding. Anal Biochem 1976;72:248-254.
37. Harlow E, Lane D. Antibodies: A Laboratory Manual. New York: CSHL Press Plainview, 1988.
38. Neet K, Hunter T. The nonreceptor protein-tyrosine kinase CSK complexes directly with the GTPase-activating protein-associated p62 protein in cells expressing v-Src or activated c-Src. Mol Cell Biol 1995;15:4908-4920.
39. Baserga R, and Malamaud D. Autoradiography: Techniques and Application of Modern Methods in Experimental Pathology. New York: Hoeber Medical Division, Harper and Row, 1969.
40. LaBaer J, Garrett MD, Stevenson LF, Slingerland JM, Sandhu C, Chou HS, Fattaey A, et al. New functional activities for the $p21^{CIP}$ family of cdk inhibitors. Genes Dev 1997;11:847-862.

ANNALS OF SURGERY
Vol. 223, No. 5, 620–628

Intestinal Cell Cycle Regulation

Interactions of Cyclin D1, Cdk4, and $p21^{Cip1}$

R. Daniel Beauchamp, M.D.,*† Hong Miao Sheng, M.D.,* Jin Yi Shao, M.D.,*
E. Aubrey Thompson, Ph.D.,‡ and Tien C. Ko, M.D.‡§

From the Departments of Surgery and Cell Biology,† Vanderbilt University School of Medicine, Nashville, Tennessee; and the Departments of Human Biological Chemistry and Genetics‡ and Surgery,§ The University of Texas Medical Branch, Galveston, Texas*

Objective

The $p21^{Cip1}$ protein is a potent stoichiometric inhibitor of cyclin-dependent kinase activity, and $p21^{Cip1}$ mRNA expression is localized to the nonproliferative compartment of the intestinal villus, suggesting an *in vivo* growth-inhibitory role in the gut. The authors determined whether nontransformed rat intestinal epithelial cells (IECs) underwent reversible cell cycle arrest by contact inhibition, and determined whether increases in the relative amount of p21 associated with Cyclin D/Cdk4 protein complexes were associated with cell growth arrest.

Methods

Density arrest was achieved by prolonged culture of IEC-6 in confluent conditions (5 or more days). Release from density arrest was achieved by detaching the cells from the culture plate and reseeding them at a 1:4 ratio. The DNA synthesis was estimated by [^{3}H]-thymidine incorporation and expressed as mean plus or minus standard error of the mean (n = 4). Cyclin D1, Cdk4, and p21 mRNA and protein levels were determined by standard Northern and Western blot analyses, respectively. Cyclin D1, Cdk4, and p21 protein complex formation was analyzed by immunoprecipitating the complexes from cell lysates with an antibody to one of the constituents, followed by SDS polyacrylamide gel electrophoresis (SDS-PAGE) and Western blot analysis of the precipitated complexes using antibodies to the other proteins. The kinase activity of the immunoprecipitated Cdk4 was determined using recombinant Rb as substrate.

Results

The IEC-6 [^{3}H]-thymidine incorporation was decreased 7.5-fold from day 1 of confluence to day 7 of confluence. Twenty-four hours after release from density arrest, there was a 43-fold increase in [^{3}H]-thymidine incorporation. Cyclin D1 and Cdk4 mRNA levels remained relatively constant during contact inhibition, whereas immunoblotting showed that the levels of cyclin D1 and Cdk4 proteins decreased by 70.9% and 68.7%, respectively, comparing day 3 with day 9 during density arrest. The levels of cyclin D1 increased 5.8-fold and Cdk4 increased by 4.4-fold by 24 hours after reseeding the day 9 density-arrested cultures, coincident with the increase in DNA synthesis. The amount of p21 associated with the cyclin D1 and Cdk4 complex in the density-arrested cells was 170% of that observed in the reseeded, proliferating cells. More important, the p21::Cdk4 ratio was 6.4-fold higher in the density-arrested (quiescent) cells as compared with rapidly proliferating cells by 24 hours after release from growth arrest. Recovery of Cdk4-dependent kinase activity occurred by 4 hours after release from growth arrest, coincident with decreased binding of p21 to the complex.

Conclusions

Intestinal epithelial cells in culture can undergo density-dependent growth arrest. This process involves downregulation of cyclin D1 and Cdk4 at the level of protein expression, whereas the mRNA levels remain relatively unchanged. Further, during contact inhibition, there is more p21 associated with cyclin D1/Cdk4, which further contributes to the inhibition of the kinase complex. The authors also have shown that the process of contact inhibition is reversible, which may explain partly the ability of the intestinal epithelium to increase proliferative activity in response to injury.

The intestinal epithelium is one of the most rapidly proliferating tissues in the body with complete cellular turnover occurring every 3 to 8 days.[1-3] Renewal of the intestinal epithelium is a complex process, with cell proliferation restricted to a subpopulation of enterocytes located in the crypts at the bases of the villi. Enterocytes migrate from the crypt as new enterocytes are produced by anchored intestinal stem cells. The intestinal epithelial crypt cells have the ability to continuously replicate, but as cells migrate up the villus, they lose the ability to enter the DNA synthesis (S) phase of the cell cycle. As cells migrate out of the crypts, they undergo differentiation, as reflected by the expression of gene products necessary for differentiated function. Migration of differentiating and differentiated enterocytes continues along the villus surface until the cells reach the tips of the villi, where they either undergo apoptosis or extrusion into the intestinal lumen. Reversible mucosal atrophy occurs under conditions of enteral nutrient deprivation. Mucosal injury is followed by increased epithelial migratory activity to close the epithelial defect and then increased proliferative activity until homeostasis is restored. These processes are necessarily tightly regulated to maintain homeostasis. Pathologic conditions such as hyperplasia and polyposis with progression to malignancy may be the result of either unrestrained cell proliferation or inappropriate resistance to programmed cell death.

In eukaryotic cells, the initiation of DNA replication (entry into S phase) as well as mitotic division (entry into M phase) is controlled by sequential activation and inactivation of a family of cyclin-dependent serine/threonine protein kinases (Cdks). Progression through early to mid-G_1 is dependent on Cdk4 and, perhaps, Cdk6, which are activated by association with one of the D-type cyclins, D1, D2, or D3. Progression through the G_1/S transition period appears to require activation of Cdk2 through association with cyclin E. Cyclins A and B and their major catalytic partners cdk2 and cdc2 (Cdk1) are required in S and G2/M phases of the cell cycle, respectively. The rate-limiting period in the cell cycle is the first gap interval (G_1) that precedes DNA synthesis.[4] A critical substrate for the activated cyclin D-Cdk4 and cyclin D-Cdk6 kinase complexes is Rb, the protein product of the retinoblastoma susceptibility gene Rb-1.[5-7] Hyperphosphorylation of the Rb protein occurs in mid- to late G_1 and is required for entry into S phase, whereas accumulation of underphosphorylated Rb prevents DNA synthesis.[8] Neutralization of cyclin D1 function in Rb-positive cells prevents them from entering S phase,[9,10] whereas Rb-deficient cells do not require cyclin D-Cdk4 activity.[11,12]

Recently, another layer of regulatory control for these cell cycle checkpoints has been identified in the form of cyclin-dependent kinase inhibitory proteins. One family of Cdk inhibitors includes $p21^{Cip1}$ and $p27^{Kip1}$. Both p21 and p27 inhibit the activities of cyclin D-Cdk4, cyclin D-Cdk6, cyclin E-Cdk2, and cyclin A-Cdk2 kinases *in vitro*. In addition, when bound to inactive cyclin-Cdk complexes, these cyclin kinase inhibitors can inhibit phosphorylation (activation) by cyclin-activating kinase.[13,14] Another family of cyclin kinase inhibitors is typified by the $p16^{INK4A}$ and $p15^{INK4B}$ proteins that appear to interact preferentially with Cdk4 and Cdk6, and their association with the kinase subunit leads to dissociation of cyclin from the complex.[15]

The $P21^{Cip1}$ expression is induced by the tumor suppressor protein p53 and facilitates G_1 arrest in response to DNA damage (caused by ionizing radiation, *etc.*).[16] Expression of p21 is not entirely p53 dependent as tissue expression is preserved in p53 "knockout" mice.[17] Furthermore, MyoD, a skeletal muscle-specific transcriptional regulator, induces p21 as an effector of terminal cell cycle arrest that occurs during muscle cell differentiation.[17,18] In addition to inhibiting Cdk activity, p21 can associate directly with the proliferating cell nuclear antigen, and p21 inhibits proliferating cell nuclear antigen-dependent DNA synthesis catalyzed by DNA polymerase-δ *in vitro*. Thus, it has been hypothesized that through its ability to inhibit DNA replication and cause cells to exit from the cell cycle, p21 serves at least dual

Presented at the 107th Annual Session of the Southern Surgical Association, December 3–6, 1995, Hot Springs, Virginia.

Supported by NIH grants R01 CA69457(RDB), R01 CA64701(EAT), and K08 CA4191(TCK).

Address reprint requests and corresponding to R. Daniel Beauchamp, M.D., Department of Surgery, Vanderbilt University School of Medicine, Nashville, TN 37232-5729.

Accepted for publication December 27, 1995.

functions: to facilitate differentiation and to enable repair of damaged DNA.

In situ hybridization studies have shown a highly selective pattern of p21 mRNA expression in the mouse.[17] In the intestine and stomach, p21 mRNA expression was localized to the differentiated columnar epithelium only and was not observed in the regions of active cell proliferation. These observations imply an important *in vivo* role for p21 in intestinal cell growth arrest and differentiation; however, little is currently known of cell cycle regulation in intestinal epithelial cells (IECs). The purpose of our study was to determine whether nontransformed rat IECs underwent reversible cell cycle arrest by contact inhibition and, further, to determine whether increases in the relative amount of $p21^{Cip1}$ associated with cyclin D/Cdk4 protein complexes are associated with cell growth arrest. We find that DNA synthesis is profoundly inhibited in the IEC-6 cells when grown to high density and that this inhibition is reversible upon reseeding the cells at lower density. Steady-state levels of cyclin D1, Cdk4, and p21 proteins all decrease during density arrest and increase to near-peak levels by 6 hours after reseeding, whereas the mRNA levels for the cyclin D and Cdk4 remain relatively constant regardless of proliferative state. Despite the decrease in the total cellular content of p21, the ratio of p21 that is associated with Cdk4 and cyclin D1 is greatly increased in the density-arrested cells as compared with that of rapidly proliferating cells. Further, Rb kinase activity is very low in the Cdk4 immunoprecipitates from density-arrested cells but increases by 4 hours after release from growth arrest, coincident with a decrease in cyclin D1-associated p21, and increases in cyclin D1/Cdk4 complexes.

METHODS

Cell Culture

The IEC-6 cells were obtained from the American Type Culture Collection at passage 14, and all experiments were performed on cells within 6 weeks of thawing frozen stocks. The cells were maintained as a monolayer culture in Dulbecco's modified Eagle medium (Mediatech, Cellgrow, Washington, DC) supplemented with 5% dialyzed fetal bovine serum (Gibco, BRL, Gaithersburg, MD). Density-dependent growth arrest was achieved by seeding cultured IEC-6 cells at 50% confluence in Dulbecco's modified Eagle medium with 5% fetal bovine serum, then allowing them to remain in culture for 9 days so that they were confluent for more than 6 days. Release from density arrest was achieved by detaching the cells from the culture plate and reseeding them at a 1:4 ratio. The DNA synthesis was estimated by [^{3}H]-thymidine incorporation into trichloroacetic acid insoluble material as previously described.[19] The [^{3}H]-thymidine 1 μCi/mL was added to cells in 24-well plates 3 hours before harvesting cells, and the data were expressed as disintegrations per minute per 100,000 cells. This method has been validated previously by determination of nuclear labeling indexes in these cells.[20]

RNA Extraction and Northern Blot Analysis

Total cellular RNA was extracted as we have described previously.[21] The RNA samples (20 μg/lane) were separated on formaldehyde–agarose gels and blotted onto nitrocellulose membranes as described previously.[20] The blots were hybridized[21] with cDNA probes labeled with [α-^{32}P]dCTP (400 Ci/mmol, DuPont, New England Nuclear, Boston, MA) by the random primer extension. After hybridization and washes, the blots then were exposed to x-ray film at -70 C for autoradiography. The 18S rRNA signals were used as internal controls to determine integrity of RNA and equality of loading among lanes.

Immunoblot Analysis and Immunoprecipitations

Immunoblot analysis of IEC-6 cell protein lysates was done as described previously.[20] Briefly, the cells were lysed for 30 minutes in RIPA buffer, then clarified cell lysates (50 μg/lane) were denatured and fractionated by SDS-PAGE. After electrophoresis, the proteins were transferred to nitrocellulose membrane (Micron Separations, Inc., Westbury, MA). The filters then were probed with the indicated antibodies as described previously and developed by the ECL chemiluminescence system (Amersham Life Science, Inc., Arlington Heights, IL) and exposed to XAR5 film (Kodak, Rochester, NY). Quantitation was by video densitometry.

For coimmunoprecipitation of protein complexes, cells were lysed by incubation at 4 C for 30 minutes in NP40 lysis buffer (50 mM TRIS [pH 7.4], 150 mM NaCl, 0.5% NP40, 50 mM NaF, 1 mM sodium vanadate, 1 mM DTT, 1 mM PMSF, 25 μg/mL aprotinin, 25 μg/mL leupeptin, 1 mM benzamidine, 10 μg/mL trypsin inhibitor, and 10 mM β-glycerophosphate). The lysates were clarified by centrifugation at 10,000 X g for 15 minutes, and the supernatants were precipitated for 16 hours at 4 C with protein A-sepharose beads precoated with saturating amounts of the polyclonal anti-cyclin D antibody (Upstate Biotechnology, Inc., Lake Placid, NY) or anti-cdk4 antibody (Santa Cruz Biotechnology, Inc., Santa Cruz, CA). After the beads were washed with NP40 lysis buffer four times, they were suspended in 2X Laemmli's buffer, boiled for 5 minutes, then separated by SDS-PAGE. The proteins were blotted to nitrocellulose filters and the blots then were probed with the indicated anti-

bodies as described above for immunoblot analysis. The p21 antibody is of rabbit origin and was raised against a carboxyl terminus peptide from the mouse sequence (Santa Cruz Biotechnology, Inc.).

Rb Kinase Assay

The cells were dispersed into IP buffer (50 mM HEPES [pH 7.5], 150 mM NaCl, 1 mM EDTA; 2.5 mM EGTA; 0.1% Tween 20; 10% glycerol; 1 mM DTT; 10 μg/mL leupeptin; 25 μg/mL aprotinin; 5 μg/mL pepstatin; 10 mM β-glycerophosphate; and 0.1 mM sodium vanadate). The cells were lysed by sonication, then the lysates were clarified by microcentrifugation for 5 minutes at 14,000 rpm at 4 C. The protein concentrations of each lysate then were determined, and equivalent amounts of protein were subjected to kinase assay. After preclearing the lysates with *Staphylococcus aureus* (Cowan), antiserum to cdk4 was added and the samples were incubated at 4 C for 2 hours, after which protein-A sepharose was added and mixed for 60 minutes at 4 C. After centrifugation for 1 minute at 14,000 rpm, the pellets were washed four times in IP buffer, then twice with 50 mM HEPES (pH 7.5) and 1 mM DTT. The Rb kinase assay then was performed for 30 minutes at 30 C in Rb kinase buffer (50 mM HEPES, pH 7.5, 1 mM NaF, 2.5 mM EGTA, 1 mM DTT, 10 mM β-glycerophosphate, 0.1 mM sodium vanadate, and 10 mM $MgCl_2$) with the addition of 0.1 μg GST-Rb, 20 μM cold ATP, and 10 μCi [γ-^{32}P]ATP in a final volume of 30 μL. The reactions were stopped with the addition of 30 mL 2X Laemmli buffer and then boiling for 5 minutes, then were analyzed by SDS-PAGE and autoradiography. The recombinant GST-Rb fusion protein was purchased from Santa Cruz Biotechnology, Inc., and the Rb fusion fragment consisted of amino acids 769-921 of the carboxyl terminal domain of the mouse pRb, linked to glutathione-S-transferase.

RESULTS

DNA Synthesis

The DNA synthesis in IEC-6 cells, as estimated by [^{3}H]-thymidine incorporation (Fig. 1), was determined daily after the cells appeared confluent by microscopic inspection (3 days after plating is the same as day 1 after confluence). The [^{3}H]-thymidine incorporation was 4302 (±220) dpm/10^5 cells at the initial determination after confluence was achieved, then progressively decreased to a nadir by approximately 5 days after confluence was achieved. [^{3}H]-thymidine incorporation was 575 (mean ± 58) dpm/10^5 cells by day 7 after confluence. This decrease from day 1 to day 7 after confluence represents a 7.5-fold decrease in [^{3}H]-thymidine incorporation. The cells appeared microscopically normal and attached to the culture plate throughout the experiment. The growth-arrested IEC-6 cells were then released from density arrest by replating in fresh medium at a density of 1:4. [^{3}H]-thymidine incorporation was 24,715 (mean ± 1193) dpm/10^5 cells 24 hours after release from density arrest. [^{3}H]-thymidine incorporation 24 hours after release from density-dependent arrest was 43-fold greater than at day 7 of confluence, and 5.7-fold greater than at day 1 of confluence. These results indicate that the IEC-6 cells can undergo reversible density-dependent growth arrest, but maximal growth arrest requires prolonged culture in confluent conditions.

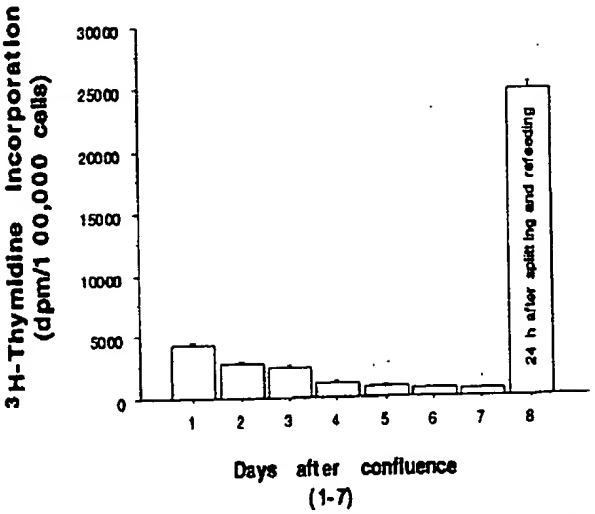

Figure 1. The intestinal epithelial cell-6 (IEC-6) cell DNA synthesis. [3H]-thymidine incorporation was determined in cultured cells maintained in Dulbecco's modified Eagle medium and 5% fetal bovine serum at intervals after achieving confluence and expressed as dpm/100,000 cells. Day 8 counts were obtained 24 hours after the cells were split at a 1:4 ratio and refed fresh medium.

Cell Cycle Protein Levels

The levels of cyclin D1 (CcnD1), Cdk4, and p21 in IEC-6 cells grown under identical conditions as described for Figure 1 were determined by immunoblot analysis (Fig. 2). Total cellular steady-state levels of all three of these proteins decreased progressively after the IEC-6 cells became confluent until day 5 after confluence (Fig. 2A). The level of CcnD1 was decreased by 70.9% by day 7 after confluence as compared with day 1, and the level of Cdk4 was decreased by 68.7% over the same interval. The levels of these proteins were greatly increased (by 5.8-fold and 4.4-fold, respectively) over day 7 confluent levels by 24 hours after release from growth arrest. Near-maximal increases in CcnD1 and Cdk4 levels were apparent by 6 hours after replating of the cells (Fig. 2B).

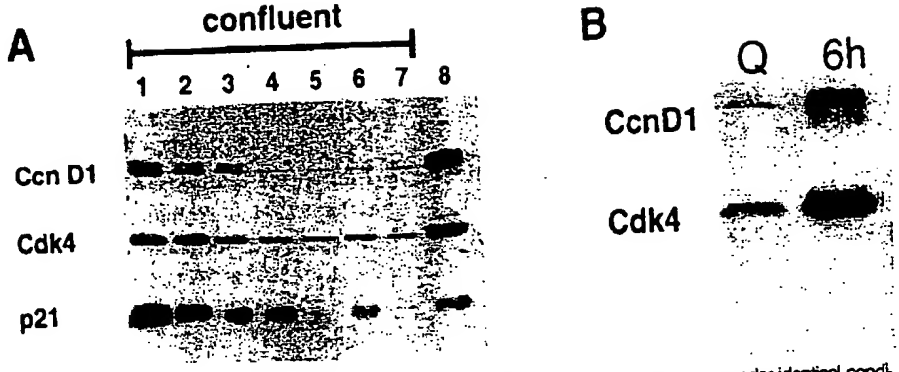

Figure 2. Immunoblot of intestinal epithelial cell-6 (IEC-6) cell lysates. (A) Cells were grown under identical conditions as described in Figure 1, and total cellular lysates were analyzed by Western blot analysis using antibodies specific for the indicated proteins. Again, the cells were confluent from days 1 to 7. Day 8 represents 24 hours after release from density arrest. (B) Identically cultured cells were examined for cyclin D1 and Cdk4 levels under growth-arrested conditions (quiescent, Q) and 6 hours after release from density arrest.

Previous experiments have shown that these cells do not begin to enter S phase until approximately 12 hours after mitogen stimulation.[22] Therefore, the maximum induction of cyclin D1 and Cdk4 occurs well before the G_1/S transition. This experiment indicates that the decreases in cyclin D1 and Cdk4 levels correlated with decreased [^{3}H]-thymidine incorporation that was observed in the experiment depicted in Figure 1. Surprisingly, the level of the p21 cyclin kinase inhibitor also decreased during density-dependent growth arrest of the IEC-6 cells.

Cell Cycle mRNA Levels

The mRNA levels for CcnD1, CcnD3, and Cdk4 were examined from IEC-6 cells cultured under confluent conditions (Fig. 3). The levels of mRNA for the D cyclins and Cdk4 remained relatively constant during density-dependent growth arrest, despite the obvious decreases in levels of cyclin D1 and Cdk4 proteins. Release from growth arrest resulted in increases in the levels of CcnD3 and Cdk4 mRNAs but little change in the level of cyclin D1 mRNA. Interestingly, levels of TGF-β1 mRNA were slightly increased by day 5 after confluence and were decreased in cells released from density arrest. We have shown previously that TGF-β1 is a potent inhibitor of [^{3}H]-thymidine incorporation in the IEC-6 cells, and this inhibition is coincident with a decrease in the expression of CcnD1 mRNA.[20] In the present experiment, we found that TGF-β1 treatment decreased the level of CcnD1 mRNA, had no effect on CcnD3 mRNA, and very little effect on the level of Cdk4 mRNA. As was expected, TGF-β1 treatment resulted in autoinduction of TGF-β1 mRNA. The results of the TGF-β1 treatment showed that these cells retained their normal responsiveness to physiologic growth inhibitory factors after release from density-dependent growth arrest.

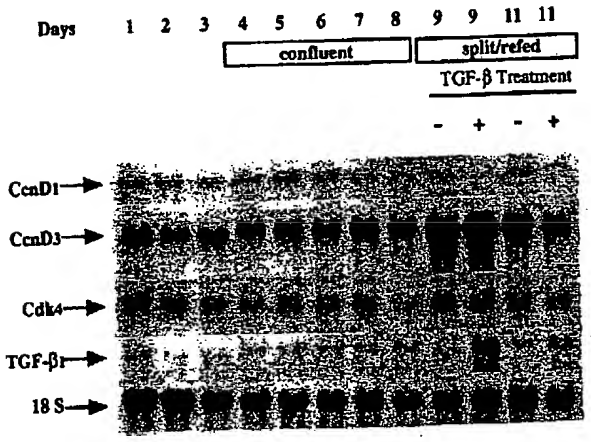

Figure 3. Northern blot analysis of intestinal epithelial cell-6 (IEC-6) mRNA. Total cellular RNA (20 μg/lane) was separated, blotted, and then hybridized with the indicated cDNA probes. Confluence was achieved after 3 days in culture, and days 9 and 11 represent cells at 24 and 72 hours after release from density arrest. The TGF-β1 (120 pM) treatment was added on release from density arrest as indicated (+).

Association of p21 With the Cyclin D/Cdk4 Complex and Rb Kinase Activity

To further explore the potential involvement of p21 in the density-dependent growth arrest of IEC-6 cells, the association of p21 with Cdk4 was examined (Fig. 4). Cell lysates were obtained under conditions designed to preserve noncovalent protein::protein associations. Coimmunoprecipitations were done with either αCcnD antibody or αCdk4 antibody, then the precipitated proteins were separated by SDS-PAGE, and the associated proteins were examined by immunoblot analysis. As expected, there was an increase in the amount of Cdk4 associated with CcnD1 in proliferating cells (lane P) that had been released from density arrest 24 hours pre-

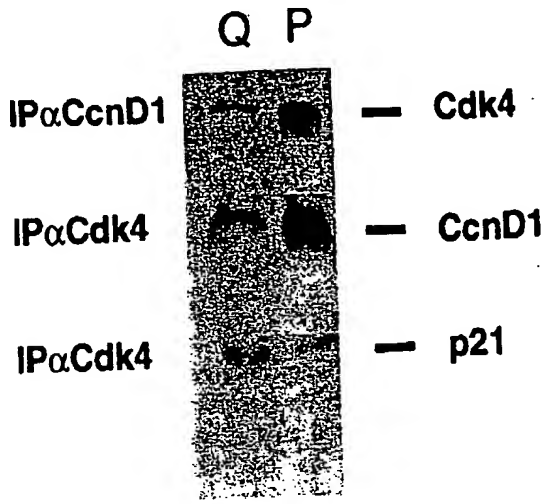

Figure 4. Association of cyclin D1, Cdk4, and p21. The intestinal epithelial cell-6 (IEC-6) cell lysates were obtained in density-arrested cells (Q) and in proliferating cells (P) 24 hours after release from density arrest. Immunoprecipitation (IP) was accomplished with the indicated antibody (e.g., IPαCcnD1), followed by SDS-PAGE separation and immunoblotting of the protein complex. The antibodies used for probing the immunoblots are indicated on the right of the figure.

viously, as compared with the density-arrested quiescent cells (lane Q). Similarly, more CcnD1 was detected in immunoprecipitated Cdk4 complexes from proliferating cells. The amount of p21 found in association with Cdk4 in the density-arrested cells was greater (170%) than that found in the Cdk4 complexes in cells after release from growth arrest. This is particularly impressive when considering the great differences in total cellular levels of Cdk4 when comparing density arrested to proliferating cells (Fig. 2A, lanes 7 and 8). The ratio of p21 to Cdk4 was 6.4-fold greater in the density-arrested (quiescent) cells as compared with the rapidly proliferating cells that had been released from density arrest.

To more closely examine the kinetics of these protein:: protein associations, a similar experiment was conducted, but lysates were obtained at 0, 4, and 8 hours after the density-arrested cells were split and replated in fresh medium (Fig. 5). In the experiment shown in Figure 5A, at intervals after release from growth arrest, the IEC-6 cell lysates were first immunoprecipitated with αcyclin D1 antibody, then the immunoprecipitated protein complexes were analyzed by immunoblotting as described above. As expected, low levels of cyclin D1 and cdk4 were found in these immunoprecipitates; however, there was abundant p21 associated with this relatively low-level cyclin D1. There was a slight increase in the amounts of cyclin D1 and cyclin D1-associated Cdk4 by 4 hours, and these proteins were abundant by 8 hours after release from growth arrest. The cyclin D1-associated p21 was decreased at 4 hours and was recovering by 8 hours after release from growth arrest.

To examine the functional significance of these changes in cyclin D1/Cdk4/p21 associations, we next determined the Rb kinase activity in the IEC-6 cell lysates obtained from identical culture conditions (Fig. 5B). Immunoprecipitation was accomplished using an αCdk4 antibody, then the precipitated complex was assayed for the ability to phosphorylate recombinant pRb substrate. The Cdk4-dependent Rb kinase activity is low in confluent, quiescent cells, but increases maximally by 4 hours after release from growth arrest, coincident with the decrease in p21 levels and rising cyclin D1/Cdk4 association.

DISCUSSION

In the present study, we have shown that cultured IEC-6 undergo density-dependent growth arrest when grown

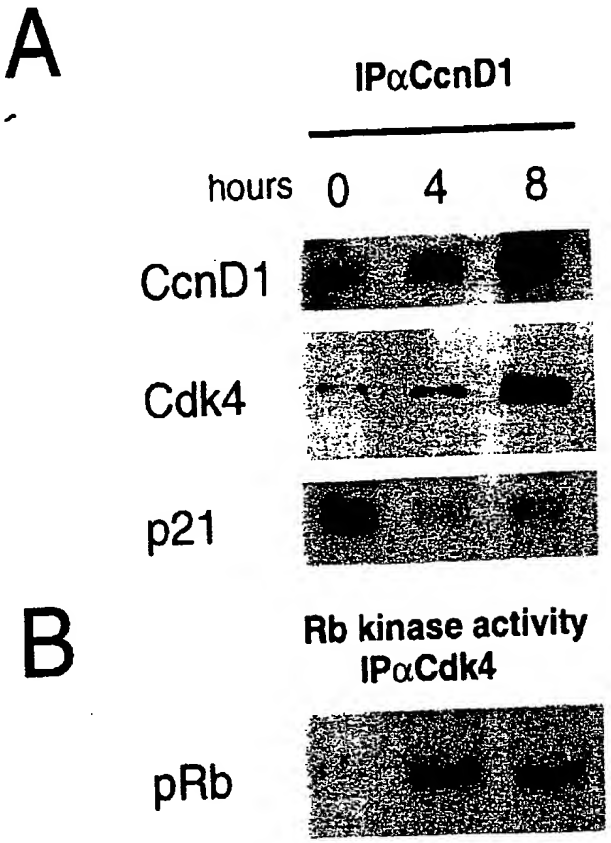

Figure 5. Kinetics of cyclin D1, Cdk4, and p21 protein interactions and Rb kinase activity. Lysates obtained at 0, 4, and 8 hours after release from density arrest (0 hour timepoint is 5 days postconfluent) were subjected to immunoprecipitation with αCcnD1 antibody, then immunoblot analysis of the precipitated complex using antibodies to the proteins as indicated to the left of the figure (A). At the same intervals, the kinase activity of the protein complex immunoprecipitated with antisera to Cdk4 was examined using recombinant GST-Rb as substrate (pRb). Lanes 2 and 3 show increased phosphorylation of the GST-Rb substrate protein that was added in equal amounts (0.1 μg/reaction).

to confluence in complete medium containing fetal bovine serum. The nadir of [^{3}H]-thymidine incorporation is achieved by approximately 5 days after the cells are estimated to be confluent by visual inspection. We have observed that the cell number continues to increase for up to 3 days after the cells appear to be confluent, but cell number plateaus between 4 and 5 days after confluence is achieved (R.D.B. and H.M.S., unpublished observations, 1995). This plateau would correspond with the cells achieving true growth arrest and with the nadir of [^{3}H]-thymidine incorporation.

At the same time that the nadir of [^{3}H]-thymidine incorporation was observed, immunoblot analysis showed that CcnD1 and Cdk4 proteins had reached their trough levels. In the present study, after release from growth arrest by replating the cells at lower density in fresh medium, the [^{3}H]-thymidine incorporation increased by 43-fold by 24 hours. This increase in [^{3}H]-thymidine incorporation was preceded by near-maximal increases in CcnD1 and Cdk4 that occurred by 6 hours after release from quiescence. In previous studies,[20,22] we have found that entry into S phase for the IEC-6 cells occurs ~ 12 hours after mitogenic stimulation. Therefore, abundant induction of these peptides at 6 hours occurs in G_1, well before the G_1 to S phase transition.

The D cyclins are induced during the G_1 phase after mitogenic stimulation of quiescent macrophages and fibroblasts,[10,23] and withdrawal of growth factor from macrophages results in disappearance of cyclin D1 and withdrawal from the cell cycle (quiescence). Abrogation of cyclin D1 by antisense or antibody microinjection prevents fibroblasts from entering S phase.[9,10] Similarly, we have found that TGF-β1 treatment of rapidly growing IEC-6 and RIE-1 intestinal cell cultures resulted in a rapid decrease in cyclin D_1 that preceded inhibition of DNA synthesis. The TGF-β1 inhibition of cyclin D1 induction after serum stimulation of quiescent intestinal cells also was associated with failure to enter S phase.[20] Taken together, the above-described findings along with our current observations suggest that cyclin D1 expression is essential for cell cycle progression in cultured IECs and that decreases in cyclin D1 are accompanied by withdrawal from the cell cycle.

The major catalytic partner for cyclin D1 is Cdk4.[24] In the present study, the decrease in Cdk4 was comparable to the decrease in cyclin D1 during density-dependent growth arrest in the cultured IECs. Although there were clear decreases in the levels of both cyclin D1 and Cdk4 proteins, the mRNAs encoding these proteins were changed very little during density-dependent growth arrest. Consistent with this observation, we have observed previously that fasting resulted in decreased levels of Cdk4 protein in the jejunal mucosa of rats that recovered within 6 hours of refeeding, whereas there was little change in the jejunal level of Cdk4 mRNA under the same conditions.[25] This would indicate that there remains a pool of mRNAs encoding the G_1 cyclin kinase, but that there is repression of the protein product. We postulate that translation of these mRNAs is prevented under conditions in which growth arrest is required, but that the available pool of mRNA allows rapid synthesis of these proteins after the cells receive the mitogenic signal.

The level of p21 decreased after cells reached confluence and the level was increased by 24 hours after release from growth arrest. Although total cellular p21 levels decreased in concert with the decreases in cyclin D1 and Cdk4, the level achieved after release from density-dependent growth arrest was less than that observed on days 1 and 2 of confluence. Also, despite the decrease in total p21 level observed during density arrest, the amount of p21 associated with Cdk4 was greater in growth-arrested as compared with proliferating cells. It is particularly interesting to note that the ratio of p21 to Cdk4 was increased more than sixfold in density-arrested IEC-6 cells as compared with rapidly proliferating cells. The increased association of p21 with cyclin D1 provides further confirmation of this observation. Harper and colleagues[26,27] have recently shown that p21 is an inhibitor of cyclin/Cdk kinase activity with high affinity for all of cyclin-dependent kinase complexes (Cdk2, Cdk4, Cdk6, and probably Cdk3) that are known to have a direct role in the G_1- to S-phase transition. Furthermore, binding of multiple p21 molecules is required for the inhibition of cyclin/Cdk kinase activity, and overexpression of p21 is sufficient to cause G_1 arrest, even in cells that lack functional p53, or pRb.[27] Thus, p21 is a stoichiometric inhibitor of G_1 cyclin/Cdk kinase activity, and a high ratio of p21 to cyclin/Cdk should prevent Rb phosphorylation and result in cell growth arrest as we have observed in the confluent IEC-6 cells.

We conclude that IECs in culture can undergo density-dependent growth arrest. This process involves downregulation of cyclin D1 and Cdk4 at the level of protein expression, whereas the mRNA levels remain relatively unchanged. Further, during contact inhibition, there is increased $p21^{cip1}$ association with the cyclin D1/Cdk4 complex, which contributes to the inhibition of the kinase complex. Release from growth arrest results in dissociation of p21 from the cyclin D1/Cdk4 complex, coincident with recovery of Rb kinase activity. We also have shown that the process of contact inhibition is reversible, which may explain partly the ability of the intestinal epithelium to increase proliferative activity in response to injury.

Acknowledgments

The authors thank Brooke Hooten for providing excellent technical assistance; Raymond N. DuBois for re-

viewing the manuscript before submission; Dr. C. Sherr, St. Jude's Children's Research Hospital, Memphis, Tennessee, for providing the mouse cyclins D1 and D3 cDNAs; Dr. S.K. Hanks, Vanderbilt University School of Medicine, Nashville, Tennessee, for providing the mouse cdk4 cDNA; Dr. R. Derynck, University of California, San Francisco, for providing the mouse TGF-β1 cDNA; and Dr. Ed Leof, Mayo Clinic, Rochester, Minnesota, for donating the cdk4 antisera used for precipitation of the active Cdk4 complex.

References

1. Cairnie AB, Lamerton LF, Steel GG. Cell proliferation studies in the intestinal epithelium of the rat. I. determination of the kinetic parameters. Exp Cell Res 1965; 39:528–538.
2. Cheng H, LeBlond CP. Origin, differentiation and renewal of the four main epithelial cell types in the mouse small intestine. I. columnar cell. American Journal of Anatomy 1974; 141:461–479.
3. Babyatsky MW, Podolsky DK. Growth and development in the gastrointestinal tract. In: Yamada T, Alpers DH, Owyang C, et al., eds. Textbook of Gastroenterology. Philadelphia: JB Lippincott, 1991.
4. King RW, Jackson PK, Kirschner MW. Mitosis in transition. Cell 1994; 79:563–571.
5. Matsushime H, Ewen ME, Strom DK, et al. Identification and properties of an atypical catalytic subunit ($p34^{PSK-J3}$/cdk4) for mammalian D type G1 cyclins. Cell 1992; 71:323–334.
6. Dowdy SF, Hinds PW, Louie K, et al. Physical interaction of the retinoblastoma protein with human D cyclins. Cell 1993; 73:499–511.
7. Kato J, Matsushime H, Hiebert SW, et al. Direct binding of cyclin D to the retinoblastoma gene product (pRb) and pRb phosphorylation by the cyclin D-dependent kinase CDK4. Genes Dev 1993; 7:331–342.
8. Goodrich DW, Wang NP, Qian YW, et al. The retinoblastoma gene product regulates progression through the G1 phase of the cell cycle. Cell 1991; 67:293–302.
9. Quelle DE, Ashmun RA, Shurtleff SA, et al. Overexpression of mouse D-type cyclins accelerates G1 phase in rodent fibroblasts. Genes Dev 1993; 7:1559–1571.
10. Baldin V, Lukas J, Marcote MJ, et al. Cyclin D1 is a nuclear protein required for cell cycle progression in G1. Genes Dev 1993; 7: 812–821.
11. Tam SW, Theodoras AM, Shay JW, et al. Differential expression and regulation of Cyclin D1 protein in normal and tumor human cells: association with Cdk4 is required for Cyclin D1 function in G1 progression. Oncogene 1994; 9:2663–2674.
12. Lukas J, Bartkova J, Rohde M, et al. Cyclin D1 is dispensable for G1 control in retinoblastoma gene-deficient cells independently of cdk4 activity. Mol Cell Biol 1995; 15:2600–2611.
13. Slingerland JM, Hengst L, Pan CH, et al. A novel inhibitor of cyclin-Cdk activity detected in transforming growth factor beta-arrested epithelial cells. Mol Cell Biol 1994; 14:3683–3694.
14. Zhang H, Hannon G, Beach D. p21-containing kinases exist in both active and inactive states. Genes Dev 1994; 8:1750–1758.
15. Sherr CJ, Roberts JM. Inhibitors of mammalian G1 cyclin-dependent kinases. Genes Dev 1995; 9:1149–1163.
16. Sherr CJ. D-type cyclins. Trends Biochem Sci 1995; 20:187–190.
17. Parker SB, Eichele G, Zhang P, et al. p53-independent expression of p21Cip1 in muscle and other differentiating cells (see comments). Science 1995; 267:1024–1027.
18. Halevy O, Novitch BG, Spicer DB, et al. Correlation of terminal cell cycle arrest of skeletal muscle with induction of p21 by MyoD (see comments). Science 1995; 267:1018–1021.
19. Ko TC, Beauchamp RD, Townsend CM Jr., Thompson JC. Glutamine is essential for epidermal growth factor-stimulated intestinal cell proliferation (see comments). Surgery 1993; 114:147–154.
20. Ko TC, Sheng HM, Reisman D, et al. Transforming growth factor-beta 1 inhibits cyclin D1 expression in intestinal epithelial cells. Oncogene 1995; 10:177–184.
21. Beauchamp RD, Sheng HM, Alam T, et al. Posttranscriptional regulation of albumin and alpha-fetoprotein messenger RNA by transforming growth factor-beta 1 requires de novo RNA and protein synthesis. Mol Endocrinol 1992; 6:1789–1796.
22. Ko TC, Beauchamp RD, Townsend CM Jr., et al. Transforming growth factor-beta inhibits rat intestinal cell growth by regulating cell cycle specific gene expression. Am J Surg 1994; 167:14–19.
23. Matsushime H, Roussel MF, Ashmun RA, Sherr CJ. Colony-stimulating factor 1 regulates novel cyclins during the G1 phase of the cell cycle. Cell 1991; 65:701–713.
24. Sherr CJ. D-type cyclins. Trends Biochem Sci 1995; 20:187–190.
25. Ko TC, Sheng HM, Thompson EA, Beauchamp RD. Effect of fasting and refeeding on cyclin D_3 and CDK4 expression in rat jejunum. Gastroenterology 1995; 108(suppl):A981.
26. Harper JW, Adami GR, Wei N, et al. The p21 Cdk-interacting protein Cip1 is a potent inhibitor of G1 cyclin-dependent kinases. Cell 1993; 75:805–816.
27. Harper JW, Elledge SJ, Khandan K, et al. Inhibition of Cyclin-dependent Kinases by p21. Mol Biol Cell 1995; 6:387–400.

Discussion

DR. WILEY C. SOUBA (Boston, Massachusetts): Thank you, Dr. Thompson and Secretary Copeland. This is a complicated paper, but an excellent paper, and I appreciate Dr. Beauchamp sending me a copy ahead of time. I had to read it three times.

I will just make a couple of comments and then ask Dan three questions. I think the reason the work is important is because it has tremendous implications for the surgeon. What he and his group have shown is that there are three genes, cyclin D1, cyclin-dependent kinase, and p21 gene, which play a very important role in regulating cell growth and cell turnover in the epithelium of the bowel.

These genes are not just altered with growth arrest but are very likely to be changed by a variety of disease states that we as surgeons encounter.

You mentioned that cyclin D1 and Cdk4 mRNA levels really did not change; yet, there was an increase in expression. This implies some regulation at the translational level.

From a more clinical standpoint, is the expression of these proteins altered *in vivo*? If you starve an animal or a patient or if you give an animal glutamine or if you give an animal a growth factor, how does the expression of these proteins change?

I think the regulation of this may have tremendous applications in terms of carcinogenesis in the intestine. I would be interested to know if you see this kind of regulation cellular turnover in other tissues such as the endothelium or the renal epithelium.

Thank you for the privilege of reviewing the work, and I thank the Association for the privilege of the floor.

DR. B. MARK EVERS (Galveston, Texas): Thank you, Dr.

Thompson, Dr. Copeland, Members, and Guests. I, too, would like to commend Dr. Beauchamp and his colleagues for an excellent study that examines specific cellular mechanisms involved in the growth arrest of intestinal cells.

These studies have important and far-reaching implications to our better understanding of both normal gut development and abnormal gut growth, for example, colon cancers. Dr. Beauchamp's present study is a very nice extension of his ongoing careful examination at the molecular level of the various cell cycle proteins that regulate growth of the normal and neoplastic gut. I have three questions for Dr. Beauchamp:

First, this study has examined only one of the cyclin kinase inhibitors, that is, p21. Do you think that other inhibitors such as p27, p15, or p16, may also be playing a role in this process, and have you analyzed some of these other inhibitors?

Second, the retinoblastoma protein (RB) plays a critical role in the progression of growth and subsequent growth arrest. Have you had the opportunity to examine the phosphorylation status of RB in your present model? Specifically, is there an accumulation of the underphosphorylated form with growth arrest?

And, finally, the IEC-6 cell line has been described as a normal intestinal cell line. Have you looked at colon cancer cell lines? Specifically, are the cell cycle mechanisms that you have identified as important for growth arrest of IEC-6 cells absent in colon cancers?

I enjoyed this talk and the manuscript. This work will provide a good foundation for future studies to better define the important cellular mechanisms responsible for gut growth and differentiation. Thank you.

DR. R. DANIEL BEAUCHAMP (Closing Discussion): I would like to thank Dr. Souba and Dr. Evers for their thoughtful comments and their questions. I will answer the questions briefly.

Dr. Souba asked whether I can explain or discuss further the discrepancy between messenger RNA levels and the protein levels of these cyclins and cyclin-dependent kinases. And as I said, the messenger RNA levels remained relatively stable during density arrest, while the protein levels were decreasing. And I think that points out the importance of examining protein levels and not merely relying on messenger RNA levels when we are trying to determine what is happening at the protein level. The protein is the real effector.

Why does this occur? I think that teleologically, this makes sense. If an organism wishes to preserve the ability to replicate or have cells replicate, then you have to have the substrate there for the cells to produce protein. If the substrate is not present, you still would like to have the message there so that these cells are ready to produce this protein when they are provided the substrate. I think that the preservation of the messenger RNA level provides this available message so that it can be translated in response to the growth stimulus.

I think that this does point out an important level of regulation that we have not explored and one that has really not been carefully looked at with regard to these questions, and that is, translational control. You have a message there, but it is not being translated. How does that regulation occur? And I think that is an important question.

The second question was about the expression of these proteins and whether they are changed *in vivo* and what might be the real biological significance of this. I showed you one small piece of data in which we have done a short-term fasting in rats and showed that Cdk4 protein levels are dramatically decreased and then they recover after refeeding. Unfortunately, in these animals in the small intestine, using the reagents that we have available to us, we are not able to detect very readily the cyclin D1 protein levels. We can detect the cyclin mRNA and it does not change much.

We have looked at cyclin D3 under those conditions, and cyclin D3 does not change. So we are still investigating this area. With regard to the role of these proteins in carcinogenesis, cyclin D1 is an oncogene, and it was first discovered as the oncogene called PRAD1, associated with parathyroid adenoma. It is associated with B-cell lymphoma or leukemia. Also, cyclin D1 levels or cyclin D1 gene amplification occurs in a number of different cancers, such as esophageal carcinoma, head and neck carcinoma, and breast cancer. It has been looked for but has not been observed in colorectal cancers. Only 1 of 46 tumor lines examined had amplification of any of the cyclin D's, and that was cyclin D2 in colorectal cancer.

But we have some preliminary data which suggest that increases in cyclin D1 expression occurs at a very early stage in carcinogenesis, and we have done a study on mice with a familial polyposis, the same gene defect that patients have with familial polyposis. We see that in the polyps in these mice that there is an increase in cyclin D1 expression in the polyps as compared with the grossly normal mucosa adjacent to the polyps. And we have also seen in human samples with familial polyposis that there is an increase in cyclin D1 protein in the polyp as compared with the grossly normal mucosa adjacent to the polyps. So I think that that points out some of the biological relevance of these studies.

Now with regard to the cyclin kinase inhibitors, the p16 is an inhibitor that is probably the most frequently associated with malignancies, and p16 deletions have been observed in a number of different cancers, and probably most prominently, melanoma. Therefore, loss of these inhibitors may lead probably to carcinoma.

Dr. Evers asked about these other inhibitors in our cell line. Our cells, interestingly enough, do not seem to express p15 or p16. And we are not sure if that is the result of cells being in culture or whether that actually occurs *in vivo*. But we are investigating this.

p27 probably behaves similarly, at least in our preliminary experiments, to p21. And we have not done the extensive amount of experiments that we have done with p21.

Regarding the retinoblastoma (RB) phosphorylation status in our cells, we have not done as extensive a study as I have shown you here, but RB phosphorylation is decreased in quiescent cells. RB phosphorylation is increased in the cells when they are proliferating. We have not done the full time course that we showed you in these experiments, but that work is ongoing.

I think I have already addressed the last question that Dr. Evers asked about the role of some of these cyclin kinases in colorectal cancers.

Thank you.

EXHIBIT I

Links

☐ 1: AH005371. Homo sapiens p16-...[gi:16753086]

```
LOCUS       HSPCDK1                   340 bp    DNA     linear   PRI 13-DEC-2001
DEFINITION  Homo sapiens p16-INK4 (p16) gene, exon 1.
ACCESSION   U12818
VERSION     U12818.1  GI:533724
KEYWORDS    .
SEGMENT     1 of 3
SOURCE      Homo sapiens (human)
  ORGANISM  Homo sapiens
            Eukaryota; Metazoa; Chordata; Craniata; Vertebrata; Euteleostomi;
            Mammalia; Eutheria; Primates; Catarrhini; Hominidae; Homo.
REFERENCE   1  (bases 1 to 340)
  AUTHORS   Serrano,M., Hannon,G.J. and Beach,D.
  TITLE     A new regulatory motif in cell-cycle control causing specific
            inhibition of cyclin D/CDK4
  JOURNAL   Nature 366 (6456), 704-707 (1993)
  MEDLINE   94081956
   PUBMED   8259215
REFERENCE   2  (bases 1 to 340)
  AUTHORS   Dracopoli,N.C.
  TITLE     Direct Submission
  JOURNAL   Submitted (01-AUG-1994) Nicholas C. Dracopoli, NCHGR, NIH, Building
            49, Room 4A82, 9000 Rockville Pike, Bethesda, MD 20892, USA
REFERENCE   3  (bases 1 to 340)
  AUTHORS   Hussussian,C.J., Struewing,J.P., Goldstein,A.M., Higgins,P.A.,
            Ally,D.S., Sheahan,M.D., Clark,W.H. Jr., Tucker,M.A. and
            Dracopoli,N.C.
  TITLE     Germline p16 mutations in familial melanoma
  JOURNAL   Nat. Genet. 8 (1), 15-21 (1994)
  MEDLINE   95078916
   PUBMED   7987387
FEATURES             Location/Qualifiers
     source          1..340
                     /organism="Homo sapiens"
                     /db_xref="taxon:9606"
                     /chromosome="9"
                     /map="9p21"
                     /cell_line="lymphoblastoid"
     exon            <129..254
                     /gene="p16"
                     /note="CDKN2"
                     /number=1
     conflict        208
                     /gene="p16"
                     /citation=[1]
                     /replace="t"
BASE COUNT       59 a     77 c    165 g     39 t
ORIGIN
```

```
        1 gaagaaagag gaggggctgg ctggtcacca gagggtgggg cggaccgcgt gcgctcggcg
       61 gctgcggaga gggggagagc aggcagcggg cggcggggag cagcatggag ccggcggcgg
      121 ggagcagcat ggagccttcg gctgactggc tggccacggc cgcggcccgg ggtcgggtag
      181 aggaggtgcg ggcgctgctg gaggcggggg cgctgcccaa cgcaccgaat agttacggtc
      241 ggaggccgat ccaggtgggt agagggtctg cagcgggagc aggggatggc gggcgactct
      301 ggaggacgaa gtttgcaggg gaattggaat caggtagcgc
//
LOCUS       HSPCDK2                   585 bp    DNA     linear   PRI 13-DEC-2001
DEFINITION  Homo sapiens p16-INK4 (p16) gene, exon 2.
ACCESSION   U12819
VERSION     U12819.1  GI:533725
KEYWORDS    .
SEGMENT     2 of 3
SOURCE      Homo sapiens (human)
  ORGANISM  Homo sapiens
            Eukaryota; Metazoa; Chordata; Craniata; Vertebrata; Euteleostomi;
            Mammalia; Eutheria; Primates; Catarrhini; Hominidae; Homo.
REFERENCE   1  (bases 1 to 585)
  AUTHORS   Dracopoli,N.C.
  TITLE     Direct Submission
  JOURNAL   Submitted (01-AUG-1994) Nicholas C. Dracopoli, NCHGR, NIH, Building
            49, Room 4A82, 9000 Rockville Pike, Bethesda, MD 20892, USA
REFERENCE   2  (bases 1 to 585)
  AUTHORS   Hussussian,C.J., Struewing,J.P., Goldstein,A.M., Higgins,P.A.,
            Ally,D.S., Sheahan,M.D., Clark,W.H. Jr., Tucker,M.A. and
            Dracopoli,N.C.
  TITLE     Germline p16 mutations in familial melanoma
  JOURNAL   Nat. Genet. 8 (1), 15-21 (1994)
  MEDLINE   95078916
   PUBMED   7987387
FEATURES             Location/Qualifiers
     source          1..585
                     /organism="Homo sapiens"
                     /db_xref="taxon:9606"
                     /chromosome="9"
                     /map="9p21"
                     /cell_line="lymphoblastoid"
     exon            151..457
                     /gene="p16"
                     /note="CDKN2"
                     /number=2
BASE COUNT      100 a    180 c    195 g    110 t
ORIGIN
        1 ggaaattgga aactggaagc aaatgtaggg gtaattagac acctggggct tgtgtggggg
       61 tctgcttggc ggtgaggggg ctctacacaa gcttcctttc cgtcatgccg gcccccaccc
      121 tggctctgac cattctgttc tctctggcag gtcatgatga tgggcagcgc ccgagtggcg
      181 gagctgctgc tgctccacgg cgcggagccc aactgcgccg accccgccac tctcacccga
      241 cccgtgcacg acgctgcccg ggagggcttc ctggacacgc tggtggtgct gcaccgggcc
      301 ggggcgcggc tggacgtgcg cgatgcctgg ggccgtctgc ccgtggacct ggctgaggag
      361 ctgggccatc gcgatgtcgc acggtacctg cgcgcggctg cgggggcac cagaggcagt
      421 aaccatgccc gcatagatgc cgcggaaggt ccctcaggtg aggactgatg atctgagaat
      481 ttgtaccctg agagcttcca aagctcagag cattcatttt ccagcacaga aagttcagcc
      541 cgggagacca gtctccggtc ttgcctcagc tcacgcgcca atcgg
//
LOCUS       HSPCDK3                   422 bp    DNA     linear   PRI 13-DEC-2001
DEFINITION  Homo sapiens p16-INK4 (p16) gene, exon 3 and complete cds.
ACCESSION   U12820
VERSION     U12820.1  GI:533726
KEYWORDS    .
SEGMENT     3 of 3
```

```
SOURCE      Homo sapiens (human)
  ORGANISM  Homo sapiens
            Eukaryota; Metazoa; Chordata; Craniata; Vertebrata; Euteleostomi;
            Mammalia; Eutheria; Primates; Catarrhini; Hominidae; Homo.
REFERENCE   1  (bases 1 to 422)
  AUTHORS   Dracopoli,N.C.
  TITLE     Direct Submission
  JOURNAL   Submitted (01-AUG-1994) Nicholas C. Dracopoli, NCHGR, NIH, Building
            49, Room 4A82, 9000 Rockville Pike, Bethesda, MD 20892, USA
REFERENCE   2  (bases 1 to 422)
  AUTHORS   Hussussian,C.J., Struewing,J.P., Goldstein,A.M., Higgins,P.A.,
            Ally,D.S., Sheahan,M.D., Clark,W.H. Jr., Tucker,M.A. and
            Dracopoli,N.C.
  TITLE     Germline p16 mutations in familial melanoma
  JOURNAL   Nat. Genet. 8 (1), 15-21 (1994)
  MEDLINE   95078916
   PUBMED   7987387
FEATURES             Location/Qualifiers
     source          1..422
                     /organism="Homo sapiens"
                     /db_xref="taxon:9606"
                     /chromosome="9"
                     /map="9p21"
                     /cell_line="lymphoblastoid"
     gene            join(U12818.1:129..340,U12819.1:1..585,1..422)
                     /gene="p16"
     mRNA            join(U12818.1:<129..254,U12819.1:151..457,274..>422)
                     /gene="p16"
                     /product="p16-INK4"
                     /note="CDKN2"
     CDS             join(U12818.1:129..254,U12819.1:151..457,274..287)
                     /gene="p16"
                     /function="cell cycle regulator, tumor suppressor, CDK4
                     inhibitor"
                     /note="CDKN2; MTS1; similar to PIR Accession Number
                     S39359"
                     /codon_start=1
                     /product="p16-INK4"
                     /protein_id="AAB60645.1"
                     /db_xref="GI:533728"
                     /translation="MEPSADWLATAAARGRVEEVRALLEAGALPNAPNSYGRRPIQVM
                     MMGSARVAELLLLHGAEPNCADPATLTRPVHDAAREGFLDTLVVLHRAGARLDVRDAW
                     GRLPVDLAEELGHRDVARYLRAAAGGTRGSNHARIDAAEGPSDIPD"
     exon            274..>422
                     /gene="p16"
                     /note="CDKN2"
                     /number=3
     3'UTR           288..>422
                     /gene="p16"
BASE COUNT       93 a    118 c    123 g     88 t
ORIGIN
        1 ccccggtcgc gctttctctg ccctccgccc gggtggacct ggagcgcttg agcggtcggc
       61 gcgcctggag cagccaggcg ggcagtggac tagctgctgg accagggagg tgtgggagag
      121 cggtggcggc gggtacatgc acgtgaagcc attgcgagaa ctttatccat aagtatttca
      181 atgccggtag ggacggcaag agaggagggc gggatgtgcc acacatcttt gacctcaggt
      241 ttctaacgcc tgttttcttt ctgccctctg cagacatccc cgattgaaag aaccagagag
      301 gctctgagaa acctcgggaa acttagatca tcagtcaccg aaggtcctac agggccacaa
      361 ctgccccccgc cacaacccac cccgctttcg tagttttcat ttagaaaata gagcttttaa
      421 aa
//
```

Revised: July 5, 2002.

Jan 7 2003 17:14:06

1: Nature 1983 Jun 23-29;303(5919):725-8

Related Articles, Links

Entrez PubMed
Overview
Help | FAQ
Tutorial
New/Noteworthy
E-Utilities

PubMed Services
Journals Database
MeSH Browser
Single Citation Matcher
Batch Citation Matcher
Clinical Queries
LinkOut
Cubby

Related Resources
Order Documents
NLM Gateway
TOXNET
Consumer Health
Clinical Alerts
ClinicalTrials.gov
PubMed Central

Privacy Policy

Nucleotide sequence of cloned cDNA of human c-myc oncogene.

Watt R, Stanton LW, Marcu KB, Gallo RC, Croce CM, Rovera G.

Like other transforming genes of retroviruses, the v-myc gene of the avian virus, MC29, has a homologue in the genome of normal eukaryotic cells. The human cellular homologue, c-myc, located on human chromosome 8, region q24 leads to qter (refs 1, 2), is translocated into the immunoglobulin heavy-chain locus on human chromosome 14 (ref. 3) in Burkitt's lymphoma, suggesting that c-myc has a primary role in transformation of some human haematopoietic cells. In addition, c-myc is amplified in the human promyelocytic leukaemia cell line, HL60 (refs 6, 7) which also contains high levels of c-myc mRNA. Recently, Colby et al. reported the nucleotide sequence of the human c-myc DNA isolated from a genomic recombinant DNA library derived from human fetal liver. This 4,053-base pair (bp) sequence includes two exons and one intron of the myc gene, and the authors have suggested the existence of a human c-myc mRNA of 2,291 nucleotides that has a coding capacity for a protein of molecular weight (Mr) 48,812. We have approached the problem of accurately defining the characteristics of the human c-myc mRNA and c-myc protein by determining the sequence of the c-myc cDNA isolated from a cDNA library prepared from mRNA of a clone of the K562 human leukaemic cell line. K562 cells are known to contain c-myc mRNA which is similar in size to the c-myc mRNA of other human cell types. We report here the sequence of 2,121 nucleotides of a human c-myc mRNA and demonstrate that its 5' noncoding sequence does not correspond to the sequence of the reported genomic human sequence. However, our data confirm that the intact human c-myc mRNA can encode a 48,812-Mr protein with a sequence identical to that reported by Colby et al.

PMID: 6304538 [PubMed - indexed for MEDLINE]